

Tummala, R.L. "Section X – Systems"
The Electrical Engineering Handbook
Ed. Richard C. Dorf
Boca Raton: CRC Press LLC, 2000

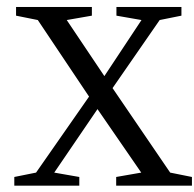


This small robotic rover has been sent to Mars inside the Mars Pathfinder lander which was launched from Kennedy Space Center on December 4, 1996. Known as Sojourner, this compact, semi-autonomous six-wheeler will become the first vehicle to traverse the Martian surface.

The rover weighs just 22 lb (10 kg) and when fully deployed is 11 in. (280 mm) high, 25 in. (630 mm) long, and 19 in. (480 mm) wide. It is equipped with three cameras and an alpha proton x-ray spectrometer which must be in contact with rocks or soil to measure elemental composition. A sensor detects alpha particle scattering and proton and x-ray emissions. Sojourner runs on a solar array, sufficient to power the rover for several hours per day, even in the worst dust storms.

The rover control system features operator designation of targets and autonomous control to reach targets and perform tasks. The instructions will be sent to the rover from a controller on earth. The onboard control system is built around an Intel 80C85 processor, which is an 8-bit processor and runs at about 100,000 instructions per second.

Landers and rovers of the future will share the heritage of Mars Pathfinder designs and technologies first tested during this mission. (Photo courtesy of National Aeronautics and Space Administration.)



Systems

- 100 Control Systems** *W.L. Brogan, G.K.F. Lee, A.P. Sage, B.C. Kuo, C.L. Phillips, R.D. Harbor, R.G. Jacquot, J.E. McInroy, D.P. Atherton, J.S. Bay, W.T. Baumann, M-Y Chow*
Models • Dynamic Response • Frequency Response Methods: Bode Diagram Approach • Root Locus • Compensation • Digital Control Systems • Nonlinear Control Systems • Optimal Control and Estimation • Neural Control
- 101 Robotics** *T.A. Lasky, T.C. Hsia, R.L. Tummala, N.G. Odrey*
Robot Configuration • Dynamics and Control • Applications
- 102 Aerospace Systems** *C.R. Spitzer, D.A. Martinec, C.T. Leondes, A.H. Rana, W. Check*
Avionics Systems • Communications Satellite Systems: Applications
- 103 Command, Control and Communications (C³)** *G. Clapp, D. Swarder*
Scope • Background • The Technologies of C³ • The Dynamics of Encounters • The Role of the Human Decisionmaker in C³
- 104 Industrial Systems** *G.E. Cook, K. Anderson, R.J. Barnett, A.K. Wallace, R. Spée, M. Sznaier, R.S. Sánchez Peña*
Welding and Bonding • Large Drives • Robust Systems
- 105 Man-Machine Systems** *D. McRuer*
Seven Natures of Man • Machine Control—A Catalog of Behavioral Complexities • Full Attention Compensatory Operations—The Crossover Model
- 106 Vehicular Systems** *L.S. Boehmer*
Design Considerations • Land Transportation Classifications • Propulsion • Microprocessor Controls • Monitoring and Diagnostics
- 107 Industrial Illuminating Systems** *K. Chen*
New Concepts in Designing an Industrial Illuminating System • Factors Affecting Industrial Illumination • System Components • Applications • System Energy Efficiency Considerations
- 108 Instruments** *J.L. Schmalzel*
Physical Variables • Transducers • Instrument Elements • Instrumentation System • Modeling Elements of an Instrumentation System • Summary of Noise Reduction Techniques • Personal Computer-Based Instruments • Modeling PC-Based Instruments • The Effects of Sampling • Other Factors
- 109 Navigation Systems** *M. Kayton*
Coordinate Frames • Categories of Navigation • Dead Reckoning • Radio Navigation • Celestial Navigation • Map Matching Navigation • Navigation Software • Design Trade-Offs
- 110 Reliability Engineering** *R. Ramakumar*
Catastrophic Failure Models • The Bathtub Curve • Mean Time To Failure (MTTF) • Average Failure Rate • *A Posteriori* Failure Probability • Units for Failure Rates • Application of the Binomial Distribution • Application of the Poisson Distribution • The Exponential Distribution • The Weibull Distribution • Combinatorial Aspects • Modeling Maintenance • Markov Models • Binary Model for a Repairable Component • Two Dissimilar Repairable Components • Two Identical Repairable Components • Frequency and Duration Techniques • Applications of Markov Process • Some Useful Approximations • Application Aspects • Reliability and Economics

- 111 Environmental Effects** *K. Blades, B. Allenby*
Industrial Ecology • Design for Environment • Environmental Implications for the Electronics Industry • Emerging Technology • Tools and Strategies for Environmental Design
- 112 Computer-Aided Control Systems Design** *C.M. Rimvall, C.P. Jobling*
A Brief History of CACSD • The State of the Art in CACSD • CACSD Block-Diagram Tools

R. Lal Tummala
Michigan State University

FUNDAMENTAL IDEAS, CONCEPTS, AND TOOLS developed in system theory have contributed significantly to the breakthroughs in aerospace, manufacturing, and medicine, to name a few. In 1990, the National Academy of Engineering identified ten outstanding engineering achievements of the preceding 25 years. These feats included five accomplishments made possible by utilizing modern system theory: Apollo lunar landings, satellites, computer-based manufacturing, computer axial tomography, and the jumbo jet. At present, these ideas are being extended to increase the productivity of the manufacturing sector, improve highway safety, increase fuel efficiency of automobiles, and design and produce environmentally friendly products.

This section discusses conceptual approaches and tools of modern system theory and their applications. The key concepts for the analysis and design of linear and non-linear control systems: modeling, dynamic response, frequency response, root locus, compensation, digital control, describing functions, and phase plane are discussed in Chapter 100. Application of these concepts to a variety of systems is discussed in the following chapters. These systems draw their name from their application, for example, vehicular systems. The topic discussed in Chapter 101 is robotics. A robot is a computer-based mechanical manipulator which can be programmed to perform a variety of tasks. The authors review modeling, control, and application of robots. Chapter 102 describes aerospace systems in avionics and their use in communication satellite systems. The next chapter reviews the command, control, and communication systems used to monitor and control military aerospace systems. Chapter 104 describes two key industrial systems: welding and bonding, and large drives. The authors describe modeling, sensor requirements, control system requirements, and implementation for these systems. Chapter 105 discusses man-machine systems and models used to analyze them. The next two chapters review the key characteristics and electronic controls for vehicular systems, and industrial illumination systems. Chapter 108 describes instruments, which are systems consisting of sensors and electronic circuits, usually for measurement applications. Modern approaches to navigation on the land, sea, or in the air are discussed in Chapter 109. Important topics such as reliability (Chapter 110) and environment (Chapter 111) are included to emphasize their importance in the design of modern products and processes. With the advent of computer technology, system theory tools are widely available on the computer and the use of this is widespread and thus deserves special attention. Chapter 112 discusses this software.

Brogan, W.L., Lee, G.K.F., Sage, A.P., Kuo, B.C., Phillips, C.L., Harbor, R.D., Jacquot, R.G., McInroy, J.E., Atherton, D.P., Bay, J.S., Baumann, W.T., Chow, M-Y. "Control Systems"

The Electrical Engineering Handbook

Ed. Richard C. Dorf

Boca Raton: CRC Press LLC, 2000

100

Control Systems

William L. Brogan

University of Nevada, Las Vegas

Gordon K. F. Lee

North Carolina State University

Andrew P. Sage

George Mason University

Benjamin C. Kuo

University of Illinois (Urbana-Champaign)

Charles L. Phillips

Auburn University

Royce D. Harbor

University of West Florida

Raymond G. Jacquot

University of Wyoming

John E. McInroy

University of Wyoming

Derek P. Atherton

University of Sussex

John S. Bay

Virginia Polytechnic Institute and State University

William T. Baumann

Virginia Polytechnic Institute and State University

Mo-Yuen Chow

North Carolina State University

100.1 Models

Classes of Systems to Be Modeled • Two Major Approaches to Modeling • Forms of the Model • Nonuniqueness •

Approximation of Continuous Systems by Discrete Models

100.2 Dynamic Response

Computing the Dynamic System Response • Measures of the Dynamic System Response

100.3 Frequency Response Methods: Bode Diagram Approach

Frequency Response Analysis Using the Bode Diagram • Bode Diagram Design-Series Equalizers • Composite Equalizers • Minor-Loop Design

100.4 Root Locus

Root Locus Properties • Root Loci of Digital Control Systems • Design with Root Locus

100.5 Compensation

Control System Specifications • Design • Modern Control Design • Other Modern Design Procedures

100.6 Digital Control Systems

A Simple Example • Single-Loop Linear Control Laws • Proportional Control • PID Control Algorithm • The Closed-Loop System • A Linear Control Example

100.7 Nonlinear Control Systems

The Describing Function Method • The Sinusoidal Describing Function • Evaluation of the Describing Function • Limit Cycles and Stability • Stability and Accuracy • Compensator Design • Closed-Loop Frequency Response • The Phase Plane Method • Piecewise Linear Characteristics • Discussion

100.8 Optimal Control and Estimation

Linear Quadratic Regulators • Optimal Estimation: The Kalman Filter • Linear-Quadratic-Gaussian (LQG) Control • H_{∞} Control • Example • Other Approaches

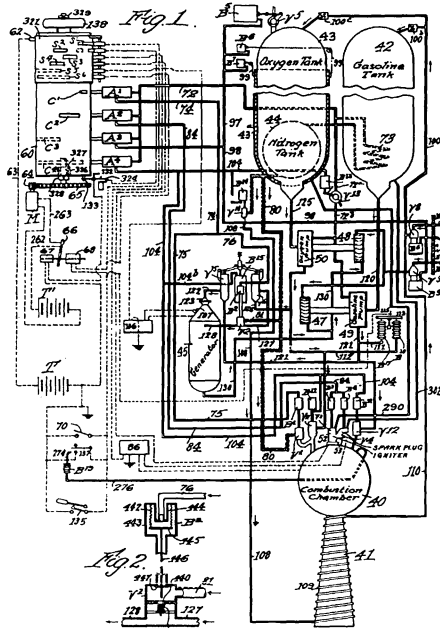
100.9 Neural Control

Brief Introduction to Artificial Neural Networks • Neural Observer • Neural Control • HVAC Illustration • Conclusion

100.1 Models

William L. Brogan

A naive trial-and-error approach to the design of a control system might consist of constructing a controller, installing it into the system to be controlled, performing tests, and then modifying the controller until satisfactory performance is achieved. This approach could be dangerous and uneconomical, if not impossible. A more rational approach to control system design uses mathematical models. A *model* is a mathematical description of system behavior, as influenced by input variables or initial conditions. The model is a stand-in for the actual system during the control system design stage. It is used to predict performance; to carry out stability, sensitivity, and trade-off



CONTROL MECHANISM FOR ROCKET APPARATUS

Robert H. Goddard
Patented April 2, 1946
#2,397,657

An excerpt from Robert Goddard's patent application:

This invention relates to rockets and rocket craft which are propelled by combustion apparatus using liquid fuel and a liquid to support combustion, such as liquid oxygen. Such combustion apparatus is disclosed in my prior application Serial No. 327,257 filed April 1, 1940.

It is the general object of my present invention to provide control mechanism by which the necessary operative steps and adjustments for such mechanism will be affected automatically and in predetermined and orderly sequence.

To the attainment of this object, I provide control mechanism which will automatically discontinue flight in a safe and orderly manner.

Dr. Goddard was instrumental in developing rocket propulsion in this country, both solid-fuel rocket engines and later liquid-fuel rocket motors used in missile and spaceflight applications. Goddard died in 1945, before this pivotal patent (filed June 23, 1941) on automatic control of liquid-fuel rockets was granted. He assigned half the rights to the Guggenheim Foundation in New York. (Copyright © 1995, Dewray Products, Inc. Used with permission.)

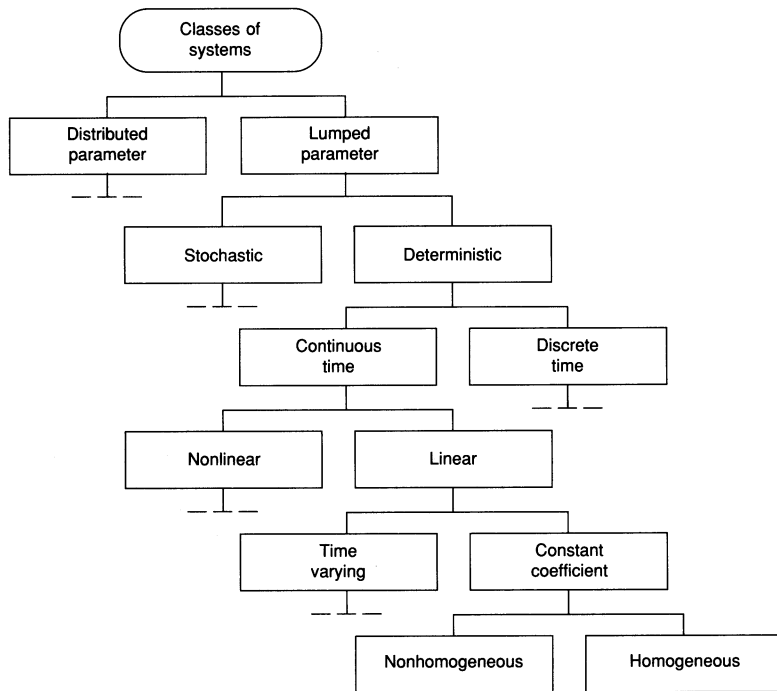


FIGURE 100.1 Major classes of system equations. (Source: W.L. Brogan, *Modern Control Theory*, 3rd ed., Englewood Cliffs, N.J.: Prentice-Hall, 1991, p. 13. With permission.)

studies; and answer various “what-if” questions in a safe and efficient manner. Of course, the validation of the model, and all conclusions derived from it, must ultimately be based upon test results with the physical hardware.

The final form of the mathematical model depends upon the type of physical system, the method used to develop the model, and mathematical manipulations applied to it. These issues are discussed next.

Classes of Systems to Be Modeled

Most control problems are multidisciplinary. The system may consist of electrical, mechanical, thermal, optical, fluidic, or other physical components, as well as economic, biological, or ecological systems. Analogies exist between these various disciplines, based upon the similarity of the equations that describe the phenomena. The discussion of models in this section will be given in mathematical terms and therefore will apply to several disciplines.

Figure 100.1 [Brogan, 1991] shows the classes of systems that might be encountered in control systems modeling. Several branches of this tree diagram are terminated with a dashed line indicating that additional branches have been omitted, similar to those at the same level on other paths.

Distributed parameter systems have variables that are functions of both space and time (such as the voltage along a transmission line or the deflection of a point on an elastic structure). They are described by partial differential equations. These are often approximately modeled as a set of *lumped parameter* systems (described by ordinary differential or difference equations) by using modal expansions, finite element methods, or other approximations [Brogan, 1968]. The lumped parameter continuous-time and discrete-time families are stressed here.

Two Major Approaches to Modeling

In principle, models of a given physical system can be developed by two distinct approaches. Figure 100.2 shows the steps involved in *analytical modeling*. The real-world system is represented by an interconnection of idealized elements. Table 100.1 [Dorf, 1989] shows model elements from several disciplines and their elemental equations. An electrical circuit diagram is a typical result of this physical modeling step (box 3 of Fig. 100.2). Application of the appropriate physical laws (Kirchhoff, Newton, etc.) to the idealized physical model (consisting of point masses, ideal springs, lumped resistors, etc.) leads to a set of mathematical equations. For a circuit these will

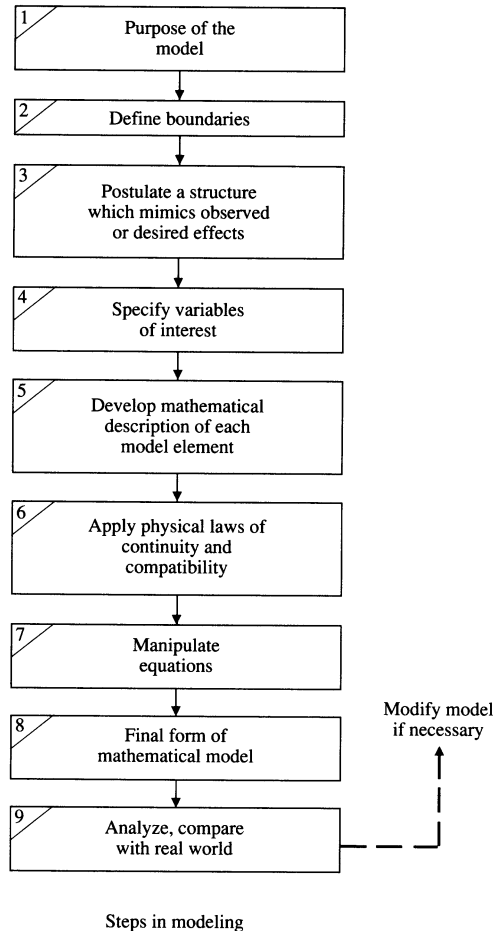


FIGURE 100.2 Modeling considerations. (Source: W.L. Brogan, *Modern Control Theory*, 3rd ed., Englewood Cliffs, N.J.: Prentice-Hall, 1991, p. 5. With permission.)

be mesh or node equations in terms of elemental currents and voltages. Box 6 of Fig. 100.2 suggests a generalization to other disciplines, in terms of continuity and compatibility laws, using through variables (generalization of current that flows through an element) and across variables (generalization of voltage, which has a differential value across an element) [Shearer et al., 1967; Dorf, 1989].

Experimental or empirical modeling typically assumes an *a priori* form for the model equations and then uses available measurements to estimate the coefficient values that cause the assumed form to best fit the data. The assumed form could be based upon physical knowledge or it could be just a credible assumption. Time-series models include autoregressive (AR) models, moving average (MA) models, and the combination, called ARMA models. All are difference equations relating the input variables to the output variables at the discrete measurement times, of the form

$$y(k+1) = a_0y(k) + a_1y(k-1) + a_2y(k-2) + \dots + a_ny(k-n) \\ + b_0u(k+1) + b_1u(k) + \dots + b_pu(k+1-p) + v(k) \quad (100.1)$$

where $v(k)$ is a random noise term. The z-transform transfer function relating u to y is

$$\frac{y(z)}{u(z)} = \frac{b_0 + b_1 z^{-1} + \cdots + b_p z^{-p}}{1 - (a_0 z^{-1} + \cdots + a_{n-1} z^{-n})} = H(z) \quad (100.2)$$

TABLE 100.1 Summary of Describing Differential Equations for Ideal Elements

Type of Element	Physical Element	Describing Equation	Energy E or Power P	Symbol
Inductive storage	Electrical inductance	$v_{21} = L \frac{di}{dt}$	$E = \frac{1}{2} Li^2$	$v_2 \circ \text{---} \overset{L}{\text{---}} i \circ v_1$
	Translational spring	$v_{21} = \frac{1}{K} \frac{dF}{dt}$	$E = \frac{1}{2} \frac{F^2}{K}$	$v_2 \circ \text{---} \overset{K}{\text{---}} \circ v_1 \circ F$
	Rotational spring	$\omega_{21} = \frac{1}{K} \frac{dT}{dt}$	$E = \frac{1}{2} \frac{T^2}{K}$	$\omega_2 \circ \text{---} \overset{K}{\text{---}} \circ \omega_1 \circ T$
Capacitive storage	Fluid inertia	$P_{21} = I \frac{dQ}{dt}$	$E = \frac{1}{2} IQ^2$	$P_2 \circ \text{---} \overset{I}{\text{---}} \circ Q \circ P_1$
	Electrical capacitance	$i = C \frac{dv_{21}}{dt}$	$E = \frac{1}{2} Cv_{21}^2$	$v_2 \circ i \overset{C}{\text{---}} \circ v_1$
	Translational mass	$F = M \frac{dv_2}{dt}$	$E = \frac{1}{2} Mv_2^2$	$F \rightarrow v_2 \boxed{M} \rightarrow v_1 = \text{constant}$
	Rotational mass	$T = J \frac{d\omega_2}{dt}$	$E = \frac{1}{2} J\omega_2^2$	$T \rightarrow \omega_2 \boxed{J} \rightarrow \omega_1 = \text{constant}$
	Fluid capacitance	$Q = C_f \frac{dP_{21}}{dt}$	$E = \frac{1}{2} C_f P_{21}^2$	$Q \rightarrow P_2 \boxed{C_f} \rightarrow P_1$
	Thermal capacitance	$q = C_t \frac{d\tau_2}{dt}$	$E = C_t \tau_2$	$q \rightarrow \tau_2 \boxed{C_t} \rightarrow \tau_1 = \text{constant}$
Energy dissipators	Electrical resistance	$i = \frac{1}{R} v_{21}$	$p = \frac{1}{R} v_{21}^2$	$v_2 \circ \text{---} \overset{R}{\text{---}} i \circ v_1$
	Translational damper	$F = fv_{21}$	$p = fv_{21}^2$	$F \rightarrow v_2 \boxed{f} \rightarrow v_1$
	Rotational damper	$T = f\omega_{21}$	$p = f\omega_{21}^2$	$T \rightarrow \omega_2 \boxed{f} \rightarrow \omega_1$
	Fluid resistance	$Q = \frac{1}{R_f} P_{21}$	$p = \frac{1}{R_f} P_{21}^2$	$P_2 \circ \text{---} \overset{R_f}{\text{---}} \circ Q \circ P_1$
	Thermal resistance	$q = \frac{1}{R_t} \tau_{21}$	$p = \frac{1}{R_t} \tau_{21}$	$\tau_2 \circ \text{---} \overset{R_t}{\text{---}} q \circ \tau_1$

In the MA model all $a_i = 0$. This is alternatively called an all-zero model or a finite impulse response (FIR) model. In the AR model all b_j terms are zero except b_0 . This is called an all-pole model or an infinite impulse response (IIR) model. The ARMA model has both poles and zeros and also is an IIR model [Makhoul, 1975].

Adaptive and learning control systems have an experimental modeling aspect. The data fitting is carried out on-line, in real time, as part of the system operation. The modeling described above is normally done off-line [Astrom and Wittenmark, 1989].

Forms of the Model

Regardless of whether a model is developed from knowledge of the physics of the process or from empirical data fitting, it can be further manipulated into several different but equivalent forms. This manipulation is box 7 in Fig. 100.2. The class that is most widely used in control studies is the deterministic lumped-parameter continuous-time constant-coefficient system. A simple example has one input u and one output y . This might be a circuit composed of one ideal source and an interconnection of ideal resistors, capacitors, and inductors.

The equations for this system might consist of a set of mesh or node equations. These could be reduced to a single n th-order linear ordinary differential equation by eliminating extraneous variables.

$$\frac{d^n y}{dt^n} + a_{n-1} \frac{d^{n-1} y}{dt^{n-1}} + \cdots + a_1 \frac{dy}{dt} + a_0 y = b_0 u + b_1 \frac{du}{dt} + \cdots + b_m \frac{d^m u}{dt^m} \quad (100.3)$$

This n th-order equation can be replaced by an input-output transfer function

$$\frac{Y(s)}{U(s)} = H(s) = \frac{b_m s^m + b_{m-1} s^{m-1} + \cdots + b_1 s + b_0}{s^n + a_{n-1} s^{n-1} + \cdots + a_1 s + a_0} \quad (100.4)$$

The inverse Laplace transform $\mathcal{L}^{-1}\{H(s)\} = h(t)$ is the system impulse response function. Alternatively, by selecting a set of n internal **state variables**, Eq.(100.3) can be written as a coupled set of first-order differential equations plus an algebraic equation relating the states to the original output y . These equations are called state equations, and one possible choice for this example is, assuming $m = n$,

$$\dot{\mathbf{x}}(t) = \begin{bmatrix} -a_{n-1} & 1 & 0 & 0 & \cdots & 0 \\ -a_{n-2} & 0 & 1 & 1 & \cdots & 0 \\ \vdots & \vdots & \vdots & \vdots & \vdots & \vdots \\ -a_1 & 0 & 0 & 0 & \cdots & 1 \\ -a_0 & 0 & 0 & 0 & \cdots & 0 \end{bmatrix} \mathbf{x}(t) + \begin{bmatrix} b_{n-1} - a_{n-1} b_n \\ b_{n-2} - a_{n-2} b_n \\ \vdots \\ b_1 - a_1 b_n \\ b_0 - a_0 b_n \end{bmatrix} u(t)$$

and

$$y(t) = [1 \ 0 \ 0 \ \dots \ 0] \mathbf{x}(t) + b_n u(t) \quad (100.5)$$

In matrix notation these are written more succinctly as

$$\dot{\mathbf{x}} = A\mathbf{x} + Bu \quad \text{and} \quad y = C\mathbf{x} + Du \quad (100.6)$$

Any one of these six possible model forms, or others, might constitute the result of box 8 in Fig. 100.2. Discrete-time system models have similar choices of form, including an n th-order difference equation as given in Eq. (100.1) or a z -transform input-output transfer function as given in Eq. (100.2). A set of n first-order difference equations (state equations) analogous to Eq. (100.5) or (100.6) also can be written.

Extensions to systems with r inputs and m outputs lead to a set of m coupled equations similar to Eq. (100.3), one for each output y_r . These higher-order equations can be reduced to n first-order state differential equations and m algebraic output equations as in Eq. (100.5) or (100.6). The **A** matrix is again of dimension $n \times n$, but **B** is now $n \times r$, **C** is $m \times n$, and **D** is $m \times r$. In all previous discussions, the number of state variables, n , is the order of the model. In transfer function form, an $m \times r$ matrix $H(s)$ of transfer functions will describe the input-output behavior

$$Y(s) = H(s) U(s) \quad (100.7)$$

Other transfer function forms are also applicable, including the left and right forms of the matrix fraction description (MFD) of the transfer functions [Kailath, 1980]

$$H(s) = P(s)^{-1}N(s) \quad \text{or} \quad H(s) = N(s)P(s)^{-1} \quad (100.8)$$

Both \mathbf{P} and \mathbf{N} are matrices whose elements are polynomials in s . Very similar model forms apply to continuous-time and discrete-time systems, with the major difference being whether Laplace transform or z -transform transfer functions are involved.

When time-variable systems are encountered, the option of using high-order differential or difference equations versus sets of first-order state equations is still open. The system coefficients $a_i(t)$, $b_j(t)$ and/or the matrices $\mathbf{A}(t)$, $\mathbf{B}(t)$, $\mathbf{C}(t)$, and $\mathbf{D}(t)$ will now be time-varying. Transfer function approaches lose most of their utility in time-varying cases and are seldom used. With nonlinear systems all the options relating to the order and number of differential or difference equation still apply.

The form of the nonlinear state equations is

$$\begin{aligned}\dot{\mathbf{x}} &= f(\mathbf{x}, \mathbf{u}, t) \\ y &= h(\mathbf{x}, \mathbf{u}, t)\end{aligned}\quad (100.9)$$

where the nonlinear vector-valued functions $f(\mathbf{x}, \mathbf{u}, t)$ and $h(\mathbf{x}, \mathbf{u}, t)$ replace the right-hand sides of Eq. (100.6). The transfer function forms are of no value in nonlinear cases.

Stochastic systems [Maybeck, 1979] are modeled in similar forms, except the coefficients of the model and/or the inputs are described in probabilistic terms.

Nonuniqueness

There is not a unique correct model of a given system for several reasons. The selection of idealized elements to represent the system requires judgment based upon the intended purpose. For example, a satellite might be modeled as a point mass in a study of its gross motion through space. A detailed flexible structure model might be required if the goal is to control vibration of a crucial on-board sensor. In empirical modeling, the assumed starting form, Eq. (100.1), can vary.

There is a trade-off between the complexity of the model form and the fidelity with which it will match the data set. For example, a p th-degree polynomial can exactly fit to $p + 1$ data points, but a straight line might be a better model of the underlying physics. Deviations from the line might be caused by extraneous measurement noise. Issues such as these are addressed in Astrom [1980].

The preceding paragraph addresses nonuniqueness in determining an input-output system description. In addition, state models developed from input-output descriptions are not unique. Suppose the transfer function of a single-input, single-output linear system is known exactly. The state variable model of this system is not unique for at least two reasons. An arbitrarily high-order state variable model can be found that will have this same transfer function. There is, however, a unique minimal or irreducible order n_{\min} from among all state models that have the specified transfer function. A state model of this order will have the desirable properties of **controllability** and **observability**. It is interesting to point out that the minimal order may be less than the actual order of the physical system.

The second aspect of the nonuniqueness issue relates not to order, i.e., the *number* of state variables, but to *choice* of internal variables (state variables). Mathematical and physical methods of selecting state variables are available [Brogan, 1991]. An infinite number of choices exist, and each leads to a different set $\{A, B, C, D\}$, called a realization. Some state variable model forms are more convenient for revealing key system properties such as stability, controllability, observability, **stabilizability**, and **detectability**. Common forms include the controllable canonical form, the observable canonical form, the Jordan canonical form, and the Kalman canonical form.

The reverse process is unique in that every valid realization leads to the same model transfer function

$$H(s) = C\{sI - A\}^{-1}B + D \quad (100.10)$$

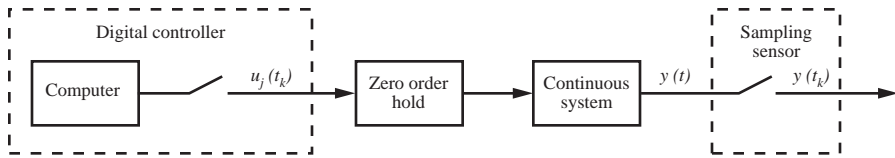


FIGURE 100.3 Digital output provided by modern sensor.

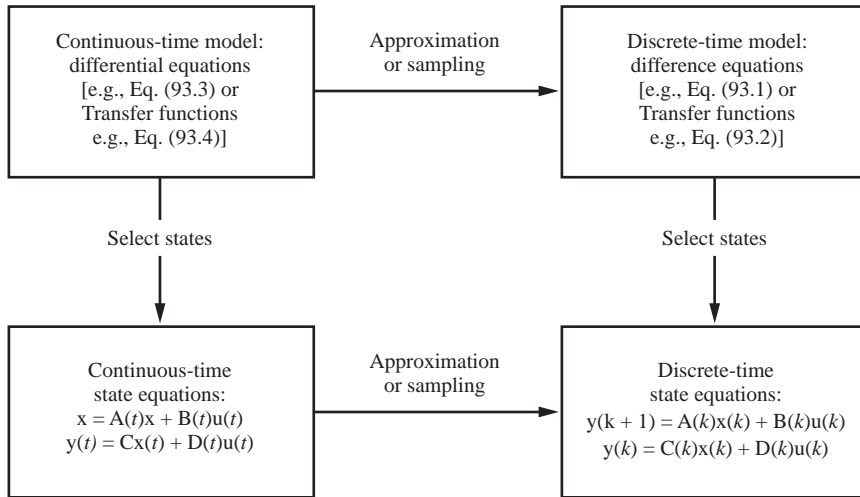


FIGURE 100.4 State variable modeling paradigm.

Approximation of Continuous Systems by Discrete Models

Modern control systems often are implemented digitally, and many modern sensors provide digital output, as shown in Fig. 100.3. In designing or analyzing such systems discrete-time approximate models of continuous-time systems are frequently needed. There are several general ways of proceeding, as shown in Fig. 100.4. Many choices exist for each path on the figure. Alternative choices of states or of approximation methods, such as forward or backward differences, lead to an infinite number of valid models.

Defining Terms

Controllability: A property that in the linear system case depends upon the A, B matrix pair which ensures the existence of some control input that will drive any arbitrary initial state to zero in finite time.

Detectability: A system is detectable if all its unstable modes are observable.

Observability: A property that in the linear system case depends upon the A, C matrix pair which ensures the ability to determine the initial values of all states by observing the system outputs for some finite time interval.

Stabilizable: A system is stabilizable if all its unstable modes are controllable.

State variables: A set of variables that completely summarize the system's status in the following sense. If all states x_i are known at time t_0 , then the values of all states and outputs can be determined uniquely for any time $t_1 > t_0$, provided the inputs are known from t_0 onward. State variables are components in the state vector. State space is a vector space containing the state vectors.

Related Topic

6.1 Definitions and Properties

References

- K.J. Astrom, "Maximum likelihood and prediction error methods," *Automatica*, vol. 16, pp. 551–574, 1980.
- K.J. Astrom and B. Wittenmark, *Adaptive Control*, Reading, Mass.: Addison-Wesley, 1989.
- W.L. Brogan, "Optimal control theory applied to systems described by partial differential equations," in *Advances in Control Systems*, vol. 6, C. T. Leondes (ed.), New York: Academic Press, 1968, chap. 4.
- W.L. Brogan, *Modern Control Theory*, 3rd ed., Englewood Cliffs, N.J.: Prentice-Hall, 1991.
- R.C. Dorf, *Modern Control Systems*, 5th ed., Reading, Mass.: Addison-Wesley, 1989.
- T. Kailath, *Linear Systems*, Englewood Cliffs, N.J.: Prentice-Hall, 1980.
- J. Makhoul, "Linear prediction: A tutorial review," *Proc. IEEE*, vol. 63, no. 4, pp. 561–580, 1975.
- P.S. Maybeck, *Stochastic Models, Estimation and Control*, vol. 1, New York: Academic Press, 1979.
- J.L. Shearer, A.T. Murphy, and H.H. Richardson, *Introduction to Dynamic Systems*, Reading, Mass.: Addison-Wesley, 1967.

Further Information

The monthly *IEEE Control Systems Magazine* frequently contains application articles involving models of interesting physical systems.

The monthly *IEEE Transactions on Automatic Control* is concerned with theoretical aspects of systems. Models as discussed here are often the starting point for these investigations.

Automatica is the source of many related articles. In particular an extended survey on system identification is given by Astrom and Eykhoff in vol. 7, pp. 123–162, 1971.

Early developments of the state variable approach are given by R. E. Kalman in "Mathematical description of linear dynamical systems," *SIAM J. Control Ser.*, vol. A1, no. 2, pp. 152–192, 1963.

100.2 Dynamic Response

Gordon K. F. Lee

Computing the Dynamic System Response

Consider a linear time-invariant dynamic system represented by a differential equation form

$$\begin{aligned} & \frac{d^n y(t)}{dt^n} + a_{n-1} \frac{d^{n-1} y(t)}{dt^{n-1}} + \cdots + a_1 \frac{dy(t)}{dt} + a_0 y(t) \\ &= b_m \frac{d^m f(t)}{dt^m} + \cdots + b_1 \frac{df(t)}{dt} + b_0 f(t) \end{aligned} \quad (100.11)$$

where $y(t)$ and $f(t)$ represent the output and input, respectively, of the system.

Let $p^k(\cdot) = (d^k/dt^k)(\cdot)$ define the differential operator so that (100.11) becomes

$$(p^n + a_{n-1}p^{n-1} + \cdots + a_1p + a_0)y(t) = (b_m p^m + \cdots + b_1p + b_0)f(t) \quad (100.12)$$

The solution to (100.11) is given by

$$y(t) = y_s(t) + y_I(t) \quad (100.13)$$

where $y_s(t)$ is the **zero-input response**, or that part of the response due to the initial conditions (or states) only, and $y_f(t)$ is the **zero-state response**, or that part of the response due to the input $f(t)$ only.

Zero-Input Response: $y_s(t)$

Here $f(t) = 0$, and thus (100.11) becomes

$$(P^n + a_{n-1}P^{n-1} + \dots + a_1P + a_0)y(t) = 0 \quad (100.14)$$

That is,

$$D(p)y(t) = 0$$

The roots of $D(p) = 0$ can be categorized as either distinct or multiple. That is, in general,

$$D(p) = \prod_{i=1}^q (p - \lambda_i)^{k_i} \prod_{i=1}^r (p - \lambda_{\sigma+i})$$

where there are r distinct roots and q sets of multiple roots (each set has multiplicity k_i). Note that $r + \sigma = n$, where $\sigma \triangleq \sum_{i=1}^q k_i$. Each distinct root contributes a term to $y_s(t)$ of the form $c_i e^{\lambda_i t}$, where c_i is a constant, while each set of multiple roots contributes a set of terms to $y_s(t)$ of the form $\sum_{j=0}^{k_i-1} c_{i,j} t^j e^{\lambda_i t}$, where $c_{i,j}$ is some constant. Thus, the zero-input response is given by

$$y_s(t) = \sum_{i=1}^q \sum_{j=0}^{k_i-1} c_{i,j} t^j e^{\lambda_i t} + \sum_{i=1}^r c_{\sigma+i} e^{\lambda_{\sigma+i} t} \quad (100.15)$$

The coefficients $c_{i,j}$ and $c_{\sigma+i}$ are selected to satisfy the initial conditions.

Special Case

If all the roots of $D(p) = 0$ are distinct and the initial conditions for (100.11) are given by

$$\left\{ y(0), \frac{dy(0)}{dt}, \dots, \frac{d^{n-1}y(0)}{dt^{n-1}} \right\}$$

then the coefficients of (100.15) are given by the solution of

$$\begin{bmatrix} y(0) \\ \frac{dy(0)}{dt} \\ \vdots \\ \frac{d^{n-1}y(0)}{dt^{n-1}} \end{bmatrix} = \begin{bmatrix} 1 & 1 & \dots & 1 \\ \lambda_1 & \lambda_2 & \dots & \lambda_n \\ \vdots & \vdots & \ddots & \vdots \\ \lambda_1^{(n-1)} & \lambda_2^{(n-1)} & \dots & \lambda_n^{(n-1)} \end{bmatrix} \begin{bmatrix} c_1 \\ c_2 \\ \vdots \\ c_n \end{bmatrix} \quad (100.16)$$

Zero-State Response: $y_f(t)$

Here the initial conditions are made identically zero. Observing (100.11), let

$$H(p) = \frac{b_m p^m + \dots + b_1 p + b_0}{p^n + a_{n-1} p^{n-1} + \dots + a_1 p + a_0}$$

denote a rational function in the p operator. Consider using partial-fraction expansion on $H(p)$ as

$$H(p) = \sum_{i=1}^q \sum_{j=1}^{k_i} \frac{g_{i,j}}{(p - \lambda_i)^j} + \sum_{i=1}^r \frac{g_{\sigma+i}}{p - \lambda_{q+i}} \quad (100.17)$$

when the first term corresponds to the sets of multiple roots and the second term corresponds to the distinct roots.

Note the constant residuals are computed as

$$g_{\sigma+i} = [(p - \lambda_{q+i})H(p)]_{p=\lambda_{q+i}}$$

and

$$g_{i,j} = \frac{1}{(k_i - j)!} \left. \frac{d^{(k_i-j)}}{dp^{(k_i-j)}} \left\{ (p - \lambda_i)^{k_i} H(p) \right\} \right|_{p=\lambda_i}$$

Then

$$h(t) = \sum_{i=1}^q \sum_{j=1}^{k_i} \frac{g_{i,j}}{(j-1)!} t^{j-1} e^{\lambda_i t} + \sum_{i=1}^r g_{\sigma+i} e^{\lambda_{\sigma+i} t} \quad (100.18)$$

is the **impulse response** of the system (100.11). Then the zero-state response is given by

$$y_I(t) = \int_0^t f(\tau) h(t-\tau) d\tau \quad (100.19)$$

that is, $y_I(t)$ is the time convolution between input $f(t)$ and impulse response $h(t)$. In some instances, it may be easier to find $y_s(t)$ and $y_I(t)$ using Laplace Transform methods.

Measures of the Dynamic System Response

Several measures may be employed to investigate dynamic response performance. These include:

1. Speed of the response—how quickly does the system reach its final value
2. Accuracy—how close is the final response to the desired response
3. Relative stability—how stable is the system or how close is the system to instability
4. Sensitivity—what happens to the system response if the system parameters change

Objectives 3 and 4 may be analyzed by frequency domain methods (Section 100.3). Time-domain measures classically analyze the dynamic response by partitioning the total response into its steady-state (objective 2) and transient (objective 1) components. The **steady-state response** is that part of the response which remains as time approaches infinity; the **transient response** is that part of the response which vanishes as time approaches infinity.

Measures of the Steady-State Response

In the steady state, the accuracy of the time response is an indication of how well the dynamic response follows a desired time trajectory. Usually a test signal (reference signal) is selected to measure accuracy. Consider Fig. 100.5. In this configuration, the objective is to force $y(t)$ to track a reference signal $r(t)$ as close as possible.

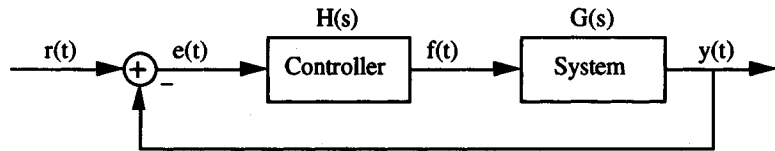


FIGURE 100.5 A tracking controller configuration.

TABLE 100.2 Steady-State Error Constants

r(t) Test Signal	eSS(t)	Error Constant
Ru(t): step function	$\frac{R}{1 + K_p}$	$K_p = \lim_{s \rightarrow 0} sG(s)H(s)$
Rtu(t): ramp function	$\frac{R}{K_v}$	$K_v = \lim_{s \rightarrow 0} sG(s)H(s)$
$\frac{R}{2}t^2u(t)$: parabolic function	$\frac{R}{K_a}$	$K_a = \lim_{s \rightarrow 0} s^2G(s)H(s)$

The **steady-state error** is a measure of the accuracy of the output $y(t)$ in tracking the reference input $r(t)$. Other configurations with different performance measures would result in other definitions of the steady-state error between two signals.

From Fig. 100.5, the error $e(t)$ is

$$e(t) = r(t) - y(t) \quad (100.20)$$

and the steady-state error is

$$e_{ss}(t) = \lim_{t \rightarrow \infty} e(t) = \lim_{s \rightarrow \infty} sE(s) \quad (100.21)$$

assuming the limits exists, where $E(s)$ is the Laplace transform of $e(t)$, and s is the Laplacian operator. With $G(s)$ the transfer function of the system and $H(s)$ the transfer function of the controller, the transfer function between $y(t)$ and $r(t)$ is found to be

$$T(s) = \frac{G(s)H(s)}{1 + G(s)H(s)} \quad (100.22)$$

with

$$E(s) = \frac{R(s)}{1 + G(s)H(s)} \quad (100.23)$$

Direct application of the steady-state error for various inputs yields Table 100.2. Note $u(t)$ is the unit step function. This table can be extended to an m th-order input in a straightforward manner. Note that for $e_{ss}(t)$ to go to zero with a reference signal $Ct^m u(t)$, the term $G(s)H(s)$ must have at least m poles at the origin (a type m system).

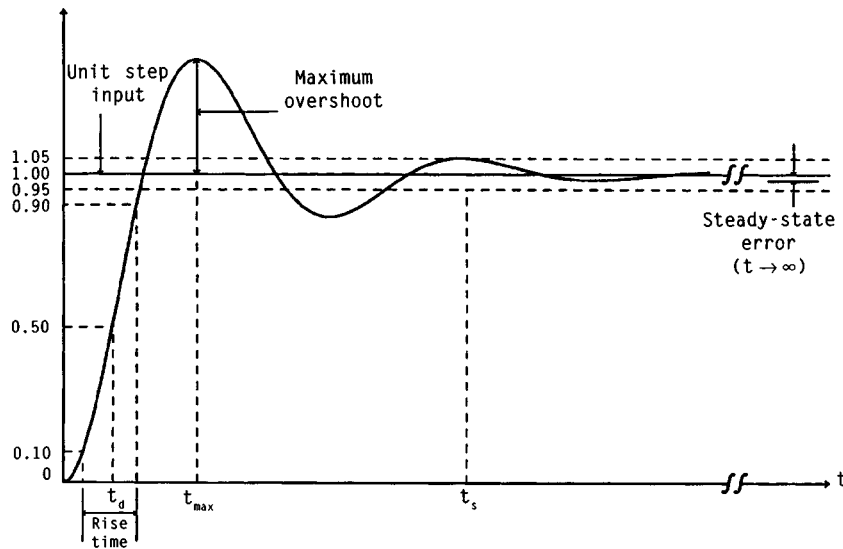


FIGURE 100.6 Step response.

Measures of the Transient Response

In general, analysis of the transient response of a dynamic system to a reference input is difficult. Hence formulating a standard measure of performance becomes complicated. In many cases, the response is dominated by a pair of poles and thus acts like a second-order system.

Consider a reference unit step input to a dynamic system (Fig. 100.6). Critical parameters that measure transient response include:

1. M : maximum overshoot
2. % overshoot = $M/A \times 100\%$, where A is the final value of the time response
3. t_d : delay time—the time required to reach 50% of A
4. t_r : rise time—the time required to go from 10% of A to 90% of A
5. t_s : settling time—the time required for the response to reach and stay within 5% of A

To calculate these measures, consider a second-order system

$$T(s) = \frac{\omega_n^2}{s^2 + 2\xi\omega_n s + \omega_n^2} \quad (100.24)$$

where ξ is the damping coefficient and ω_n is the natural frequency of oscillation.

For the range $0 < \xi < 1$, the system response is *underdamped*, resulting in a damped oscillatory output. For a unit step input, the response is given by

$$y(t) = 1 + \frac{e^{-\xi\omega_n t}}{\sqrt{1 - \xi^2}} \sin \left(\omega_n \sqrt{1 - \xi^2} t - \tan^{-1} \frac{\sqrt{1 - \xi^2}}{-\xi} \right) \quad (0 < \xi < 1) \quad (100.25)$$

The eigenvalues (poles) of the system [roots of the denominator of $T(s)$] provide some measure of the time constants of the system. For the system under study, the eigenvalues are at

$$-\xi\omega_n \pm j\omega_n\sqrt{1 - \xi^2} \quad \text{where} \quad j \triangleq \sqrt{-1}$$

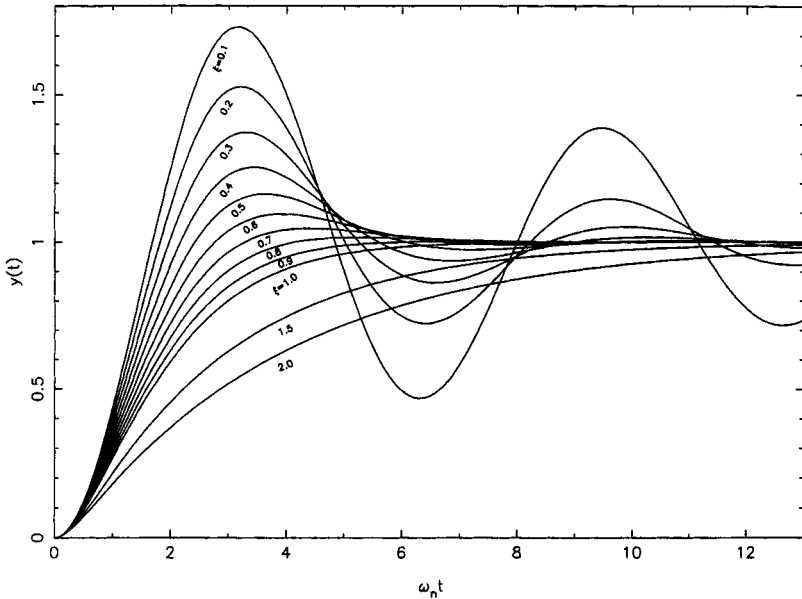


FIGURE 100.7 Effect of the damping coefficient on the dynamic response.

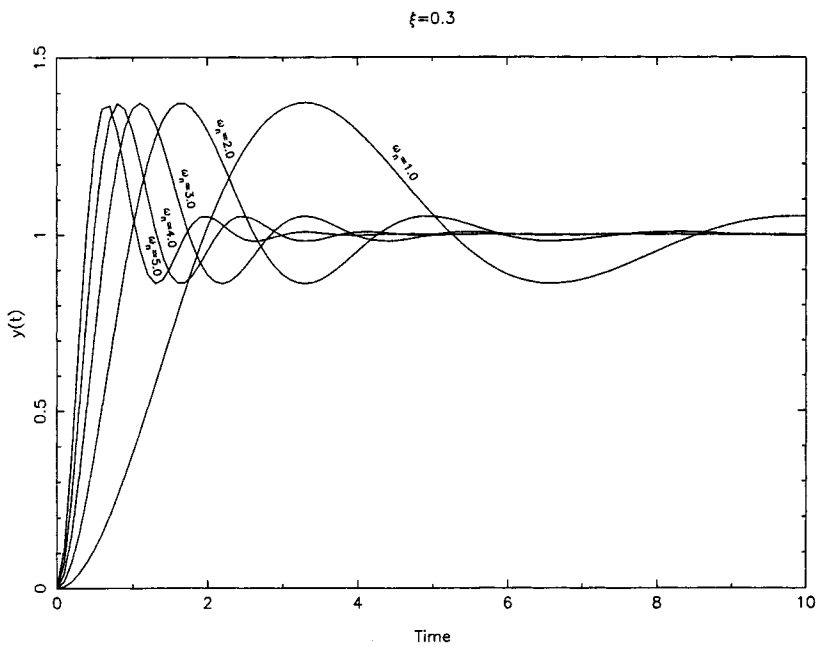


FIGURE 100.8 Effect of the natural frequency of oscillation on the dynamic response.

From the expression of $y(t)$, one sees that the term $\xi\omega_n$ affects the rise time and exponential decay time. The effects of the damping coefficient on the transient response are seen in Fig. 100.7.

The effects of the natural frequency of oscillation ω_n of the transient response can be seen in Fig. 100.8. As ω_n increases, the frequency of oscillation increases.

For the case when $0 < \xi < 1$, the underdamped case, one can analyze the critical transient response parameters.

To measure the peaks of Fig. 100.6, one finds

$$y_{\text{peak}}(t) = 1 + (-1)^{n-1} \exp \frac{-n\pi\xi}{\sqrt{1-\xi^2}} \quad n = 0, 1, \dots \quad (100.26)$$

occurring at

$$t = \frac{n\pi}{\omega_n \sqrt{1-\xi^2}} \quad \begin{array}{l} n: \text{odd (overshoot)} \\ n: \text{even (undershoot)} \end{array} \quad (100.27)$$

Hence

$$y_{\text{max}} = 1 + \exp \frac{-\pi\xi}{\sqrt{1-\xi^2}} \quad (100.28)$$

occurring at

$$t_{\text{max}} = \frac{\pi}{\omega_n \sqrt{1-\xi^2}} \quad (100.29)$$

With these parameters, one finds

$$\begin{aligned} t_d &\approx \frac{1+0.7\xi}{\omega_n} \\ t_r &\approx \frac{1+1.1\xi+1.4\xi^2}{\omega_n} \end{aligned}$$

and

$$t_s \approx \frac{3}{\xi\omega_n}$$

Note that increasing ξ decreases the % overshoot and decreases the settling time but increases t_d and t_r .

When $\xi = 1$, the system has a double pole at $-\omega_n$, resulting in a *critically damped* response. This is the point when the response just changes from oscillatory to exponential in form. For a unit step input, the response is given by

$$y(t) = 1 - e^{-\omega_n t}(1 + \omega_n t) \quad (\xi = 1) \quad (100.30)$$

For the range $\xi > 1$, the system is overdamped due to two real system poles. For a unit step input, the response is given by

$$y(t) = 1 + \frac{1}{c_1 - c_2} \left(\frac{1}{c_1} e^{c_1 \omega_n t} - \frac{1}{c_2} e^{c_2 \omega_n t} \right) \quad (\xi > 1)$$

$$c_1 = -\xi + \sqrt{\xi^2 - 1} \quad c_2 = -\xi - \sqrt{\xi^2 - 1} \quad (100.31)$$

Finally, when $\xi = 0$, the response is purely sinusoidal. For a unit step, the response is given by

$$y(t) = 1 - \cos \omega_n t \quad (\xi = 0) \quad (100.32)$$

Defining Terms

Impulse response: The response of a system when the input is an impulse function.

Steady-state error: The difference between the desired reference signal and the actual signal in steady-state, i.e., when time approaches infinity.

Steady-state response: That part of the response which remains as time approaches infinity.

Transient response: That part of the response which vanishes as time approaches infinity.

Zero-input response: That part of the response due to the initial condition only.

Zero-state response: That part of the response due to the input only.

Related Topics

6.1 Definitions and Properties • 7.1 Introduction • 112.2 A Brief History of CACSD

Further Information

J.J. D'Azzo and C.H. Harpis, *Linear Control System Analysis and Design*, New York: McGraw-Hill, 1981.

R.C. Dorf, *Modern Control Systems*, 5th ed., Reading, Mass.: Addison-Wesley, 1989.

M.E. El-Hawary, *Control Systems Engineering*, Reston, Va.: Reston, 1984.

G.H. Hostetter, C. J. Savant, Jr., and R. T. Stefani, *Design of Feedback Control Systems*, Philadelphia: Saunders, 1989.

B.C. Kuo, *Automatic Control Systems*, Englewood Cliffs, N.J.: Prentice-Hall, 1987.

K. Ogata, *Modern Control Engineering*, Englewood Cliffs, N.J.: Prentice-Hall, 1970.

N.K. Sinha, *Control Systems*, New York: Holt, 1986.

100.3 Frequency Response Methods: Bode Diagram Approach

Andrew P. Sage

Our efforts in this section are concerned with analysis and design of linear control systems by frequency response methods. Design generally involves trial-and-error repetition of analysis until a set of design **specifications** has been met. Thus, analysis methods are most useful in the design process, which is one phase of the **systems engineering** life cycle [Sage, 1992]. We will discuss one design method based on **Bode diagrams**. We will discuss the use of both simple **series equalizers** and composite equalizers as well as the use of minor-loop feedback in systems design.

Figure 100.9 presents a flowchart of the frequency response method design process and indicates the key role of analysis in linear systems control design. The flowchart of Fig. 100.9 is applicable to control system design methods in general. There are several iterative loops, generally calling for trial-and-error efforts, that comprise the suggested design process. An experienced designer will often be able, primarily due to successful prior experience, to select a system structure and generic components such that the design specifications can be met with no or perhaps a very few iterations through the iterative loop involving adjustment of equalizer or compensation parameters to best meet specifications.

If the parameter optimization, or parameter refinement such as to lead to maximum phase margin, approach shows the specifications cannot be met, we are then assured that no **equalizer** of the specific form selected will meet specifications. The next design step, if needed, would consist of modification of the equalizer form or

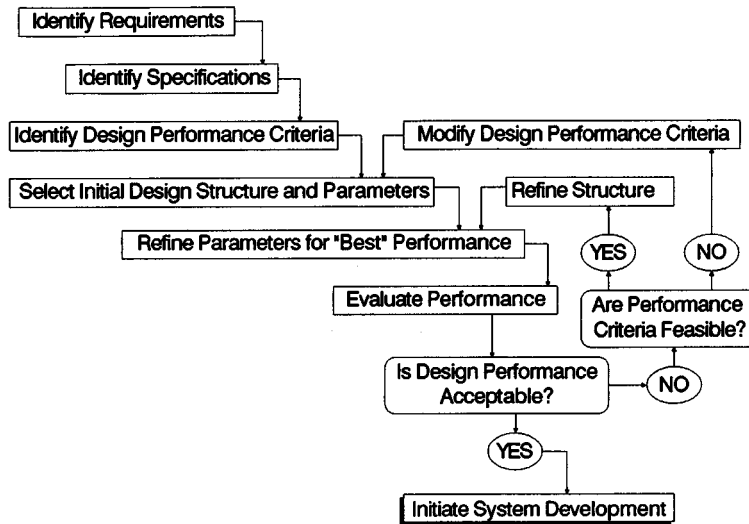


FIGURE 100.9 System design life cycle for frequency-response-based design.

structure and repetition of the analysis process to determine equalizer parameter values to best meet specifications. If specifications still cannot be met, we will usually next modify generic fixed components used in the system. This iterative design and analysis process is again repeated. If no reasonable fixed components can be obtained to meet specifications, then structural changes in the proposed system are next contemplated. If no structure can be found that allows satisfaction of specifications, either the client must be requested to relax the frequency response specifications or the project may be rejected as infeasible using present technology. As we might suspect, economics will play a dominant role in this design process. Changes made due to iteration in the inner loops of Fig. 100.9 normally involve little additional costs, whereas those made due to iterations in the outer loops will often involve major cost changes.

Frequency Response Analysis Using the Bode Diagram

The steady-state response of a stable linear constant-coefficient system has particular significance, as we know from an elementary study of electrical networks and circuits and of dynamics. We consider a stable linear system with input-output transfer function

$$H(s) = \frac{Z(s)}{U(s)}$$

We assume a sinusoidal input $u(t) = \cos \omega t$ so that we have for the Laplace transform of the system output

$$Z(s) = \frac{sH(s)}{s^2 + \omega^2}$$

We expand this ratio of polynomials using the partial-fraction approach and obtain

$$Z(s) = F(s) + \frac{a_1}{s + j\omega} + \frac{a_2}{s - j\omega}$$

In this expression, $F(s)$ contains all the poles of $H(s)$. All of these lie in the left half plane since the system, represented by $H(s)$, is assumed to be stable. The coefficients a_1 and a_2 are easily determined as

$$a_1 = \frac{H(-j\omega)}{2}$$

$$a_2 = \frac{H(j\omega)}{2}$$

We can represent the complex transfer function $H(j\omega)$ in either of two forms,

$$H(j\omega) = B(\omega) + jC(\omega)$$

$$H(-j\omega) = B(\omega) - jC(\omega)$$

The inverse Laplace transform of the system transfer function will result in a transient term due to the inverse transform of $F(s)$, which will decay to zero as time progresses. A steady-state component will remain, and this is, from the inverse transform of the system equation, given by

$$z(t) = a_1 e^{-j\omega t} + a_2 e^{j\omega t}$$

We combine several of these relations and obtain the result

$$z(t) = B(\omega) \left(\frac{e^{j\omega t} + e^{-j\omega t}}{2} \right) - C(\omega) \left(\frac{e^{j\omega t} - e^{-j\omega t}}{2j} \right)$$

This result becomes, using the Euler identity,¹

$$\begin{aligned} z(t) &= B(\omega) \cos\omega t - C(\omega) \sin\omega t \\ &= [B^2(\omega) + C^2(\omega)]^{1/2} \cos(\omega t + \beta) \\ &= |H(j\omega)| \cos(\omega t + \beta) \end{aligned}$$

where $\tan \beta(\omega) = C(\omega)/B(\omega)$.

As we see from this last result, there is a very direct relationship between the transfer function of a linear constant-coefficient system, the time response of a system to any known input, and the sinusoidal steady-state response of the system. We can always determine any of these if we are given any one of them. This is a very important result. This important conclusion justifies a design procedure for linear systems that is based only on sinusoidal steady-state response, as it is possible to determine transient responses, or responses to any given system input, from a knowledge of steady-state sinusoidal responses, at least in theory. In practice, this might be rather difficult computationally without some form of automated assistance.

Bode Diagram Design-Series Equalizers

In this subsection we consider three types of series equalization:

1. Gain adjustment, normally attenuation by a constant at all frequencies
2. Increasing the phase lead, or reducing the phase lag, at the **crossover frequency** by use of a phase **lead network**
3. Attenuation of the gain at middle and high frequencies such that the crossover frequency will be decreased to a lower value where the phase lag is less, by use of a **lag network**

¹The Euler identity is $e^{j\omega t} = \cos \omega t + j\sin \omega t$.

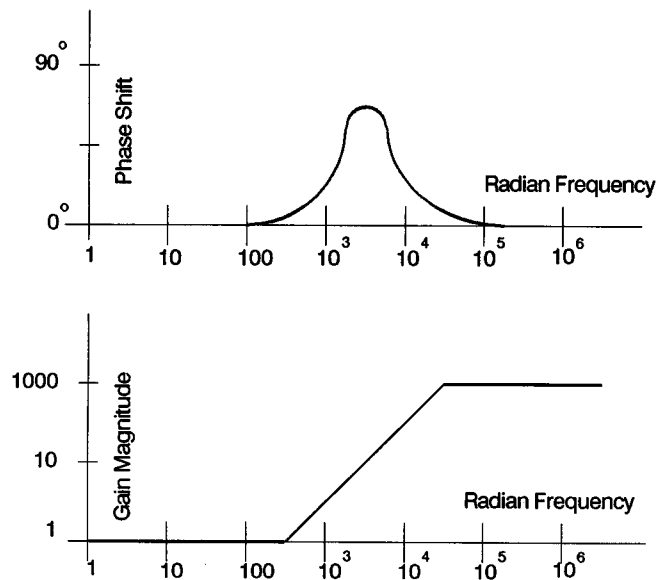


FIGURE 100.10 Phase shift and gain curves for a simple lead network.

In the subsection that follows this, we will first consider use of a composite or **lag-lead network** near crossover to attenuate gain only to reduce the crossover frequency to a value where the phase lag is less. Then we will consider more complex composite equalizers and state some general guidelines for Bode diagram design. Here, we will use Bode diagram frequency domain design techniques to develop a design procedure for each of three elementary types of series equalization.

Gain Reduction

Many linear control systems can be made sufficiently stable merely by reduction of the open-loop system gain to a sufficiently low value. This approach ignores all performance specifications, however, except that of phase margin (PM) and is, therefore, usually not a satisfactory approach. It is a very simple one, however, and serves to illustrate the approach to be taken in more complex cases.

The following steps constitute an appropriate Bode diagram design procedure for compensation by gain adjustment:

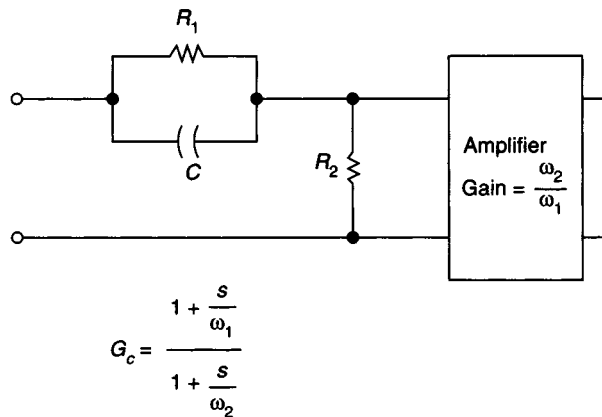
1. Determine the required PM and the corresponding phase shift $\beta_c = -\pi + \text{PM}$.
2. Determine the frequency ω_c at which the phase shift is such as to yield the phase shift at crossover required to give the desired PM.
3. Adjust the gain such that the actual crossover frequency occurs at the value computed in step 2.

Phase-Lead Compensation

In compensation using a phase-lead network, we increase the phase lead at the crossover frequency such that we meet a performance specification concerning phase shift. A phase-lead-compensating network transfer function is

$$G_c(s) = \left(1 + \frac{s}{\omega_1}\right) \Bigg/ \left(1 + \frac{s}{\omega_2}\right) \quad \omega_1 < \omega_2$$

Figure 100.10 illustrates the gain versus frequency and phase versus frequency curves for a simple lead network with the transfer function of the foregoing equation. The maximum phase lead obtainable from a phase-lead network depends upon the ratio ω_2/ω_1 that is used in designing the network. From the expression for the phase shift of the transfer function for this system, which is given by



$$\omega_1 = \frac{1}{R_1 C}, \quad \omega_2 = \left(1 + \frac{R_1}{R_2}\right) \omega_1$$

FIGURE 100.11 A simple electrical lead network.

$$\beta = \tan^{-1} \frac{\omega}{\omega_1} - \tan^{-1} \frac{\omega}{\omega_2}$$

we see that the maximum amount of phase lead occurs at the point where the first derivative with respect to frequency is zero, or

$$\left. \frac{d\beta}{d\omega} \right|_{\omega=\omega_m} = 0$$

or at the frequency where

$$\omega_m = (\omega_1 \omega_2)^{0.5}$$

This frequency is easily seen to be at the center of the two break frequencies for the lead network on a Bode log asymptotic gain plot. It is interesting to note that this is exactly the same frequency that we would obtain using an arctangent approximation² with the assumption that $\omega_1 < \omega < \omega_2$.

There are many ways of realizing a simple phase-lead network. All methods require the use of an active element since the gain of the lead network at high frequencies is greater than 1. A simple electrical network realization is shown in Fig. 100.11.

We now consider a simple design example. Suppose that we have an open-loop system with transfer function

$$G_f(s) = \frac{10^4}{s^2}$$

It turns out that this is often called a type-two system due to the presence of the double integration. This system will have a steady-state error of zero for a constant acceleration input. The crossover frequency, that is to say

²The arctangent approximation is $\tan^{-1}(\omega/\alpha) = \omega/\alpha$ for $\omega < \alpha$ and $\tan^{-1}(\omega/\alpha) = \pi/2 - \alpha/\omega$ for $\omega > \alpha$. This approximation is rather easily obtained through use of a Taylor series approximation.

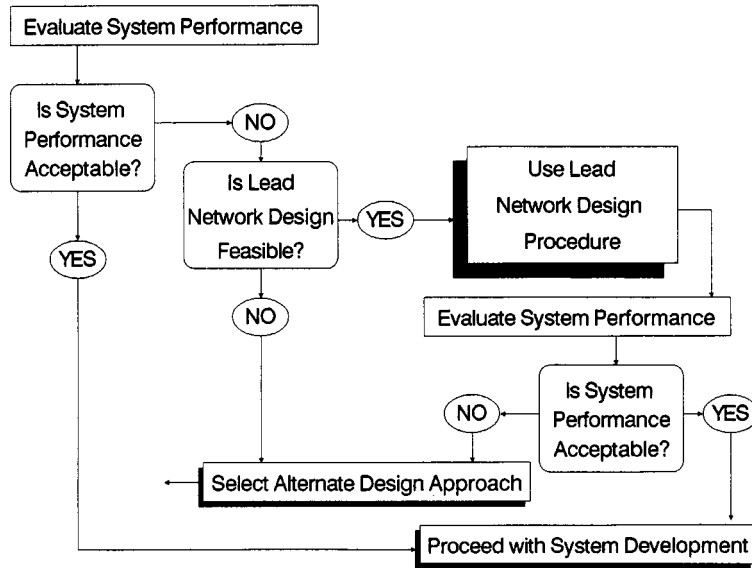


FIGURE 100.12 Life cycle of frequency domain design incorporating lead network compensation.

the frequency where the magnitude of the open-loop gain is 1, is 100 rad/s. The PM for the system without equalization is zero. We will design a simple lead network compensation for this zero PM system. If uncompensated, the closed-loop transfer function will be such that the system is unstable and any disturbance at all will result in a sinusoidally oscillating output.

The asymptotic gain diagram for this example is easily obtained from the open-loop transfer function

$$G_f(s)G_c(s) = \frac{K(1 + s/\omega_1)}{(1 + s/\omega_2)s^2}$$

and we wish to select the break frequencies ω_1 and ω_2 such that the phase shift at crossover is maximum. Further, we want this maximum phase shift to be such that we obtain the specified PM. We use the procedure suggested in Fig. 100.12.

Since the crossover frequency is such that $\omega_1 < \omega_c < \omega_2$, we have for the arctangent approximation to the phase shift in the vicinity of the crossover frequency

$$\begin{aligned} \beta(\omega) &= -\pi + \tan^{-1} \frac{\omega}{\omega_1} - \tan^{-1} \frac{\omega}{\omega_2} \\ &\approx -\frac{\pi}{2} - \frac{\omega_1}{\omega} - \frac{\omega}{\omega_2} \end{aligned}$$

In order to maximize the phase shift at crossover, we set

$$\left. \frac{d\beta}{d\omega} \right|_{\omega=\omega_m} = 0$$

and obtain as a result

$$\omega_m = (\omega_1 \omega_2)^{0.5}$$

We see that the crossover frequency obtained is halfway between the two break frequencies ω_1 and ω_2 on a logarithmic frequency coordinate. The phase shift at this optimum value of crossover frequency becomes

$$\beta_c = \beta(\omega_c) = \frac{-\pi}{2} - 2 \left(\frac{\omega_1}{\omega_2} \right)^{0.5}$$

For a PM of $-3\pi/4$, for example, we have $-3\pi/4 = -\pi/2 - 2(\omega_1/\omega_2)^{0.5}$, and we obtain $\omega_1/\omega_2 = 0.1542$ as the ratio of frequencies. We see that we have need for a lead network with a gain of $\omega_1/\omega_2 = 6.485$. The gain at the crossover frequency is 1, and from the asymptotic gain approximation that is valid for $\omega_1 < \omega < \omega_2$, we have the expressions $|G(j\omega)| = K/\omega\omega_1$ and $|G(j\omega_c)| = 1 = K/\omega_c\omega_1$ which for a known K can be solved for ω_c and ω_1 .

Now that we have illustrated the design computation with a very simple example, we are in a position to state some general results. In the direct approach to design for a specified PM we assume a single lead network equalizer such that the open-loop system to transfer function results. This approach to design results in the following steps that are applicable for Bode diagram design to achieve maximum PM within an experientially determined control system structure that comprises a fixed plant and a compensation network with adjustable parameters:

1. We find an equation for the gain at the crossover frequency in terms of the compensated open-loop system break frequency.
2. We find an equation of the phase shift at crossover.
3. We find the relationship between equalizer parameters and crossover frequency such that the phase shift at crossover is the maximum possible and a minimum of additional gain is needed.
4. We determine all parameter specifications to meet the PM specifications.
5. We check to see that all design specifications have been met. If they have not, we iterate the design process.

Figure 100.12 illustrates the steps involved in implementing this frequency domain design approach.

Phase-Lag Compensation

In the phase-lag-compensation frequency domain design approach, we reduce the gain at low frequencies such that crossover, the frequency where the gain magnitude is 1, occurs before the phase lag has had a chance to become intolerably large. A simple single-stage phase-lag-compensating network transfer function is

$$G_c(s) = \frac{1 + s/\omega_2}{1 + s/\omega_1} \quad \omega_1 < \omega_2$$

Figure 100.13 illustrates the gain and phase versus frequency curves for a simple lag network with this transfer function. The maximum phase lag obtainable from a phase-lag network depends upon the ratio ω_2/ω_1 that is used in designing the network. From the expression for the phase shift of this transfer function,

$$\beta = \tan^{-1} \frac{\omega}{\omega_2} - \tan^{-1} \frac{\omega}{\omega_1}$$

we see that maximum phase lag occurs at that frequency ω_m where $d\beta/d\omega = 0$. We obtain for this value

$$\omega_m = (\omega_1\omega_2)^{0.5}$$

which is at the center of the two break frequencies for the lag network when the frequency response diagram is illustrated on a Bode diagram log-log asymptotic gain plot.

The maximum value of the phase lag obtained at $\omega = \omega_m$ is

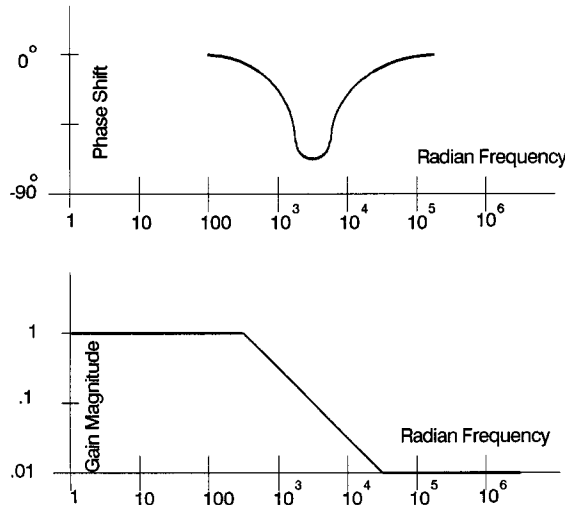


FIGURE 100.13 Phase shift and gain curves for a simple lag network.

$$\begin{aligned}\beta_m(\omega_m) &= \frac{\pi}{2} - 2 \tan^{-1} \left(\frac{\omega_2}{\omega_1} \right)^{0.5} \\ &= \frac{\pi}{2} - 2 \tan^{-1} \left(\frac{\omega_1}{\omega_2} \right)^{0.5}\end{aligned}$$

which can be approximated in a more usable form, using the arctangent approximation, as

$$\beta_m(\omega_m) \approx \frac{\pi}{2} \sqrt{\frac{\omega_2}{\omega_1}}$$

The attenuation of the lag network at the frequency of minimum phase shift, or maximum phase lag, is obtained from the asymptotic approximation as

$$|G_c(\omega_m)| = \left(\frac{\omega_1}{\omega_2} \right)^{0.5}$$

Figure 100.13 presents a curve of attenuation magnitude obtainable at the frequency of maximum phase lag and the amount of the phase lag for various ratios ω_2/ω_1 for this simple lag network.

There are many ways to physically realize a lag network transfer function. Since the network only attenuates at some frequencies, as it never has a gain greater than 1 at any frequency, it can be realized with passive components only. [Figure 100.14](#) presents an electrical realization of the simple lag network. [Figure 100.15](#) presents a flowchart illustrating the design procedure envisioned here for lag network design. This is conceptually very similar to that for a lead network and makes use of the five-step parameter optimization procedure suggested earlier.

The object of lag network design is to reduce the gain at frequencies lower than the original crossover frequency in order to reduce the open-loop gain to unity before the phase shift becomes so excessive that the system PM is too small. A disadvantage of lag network compensation is that the attenuation introduced reduces

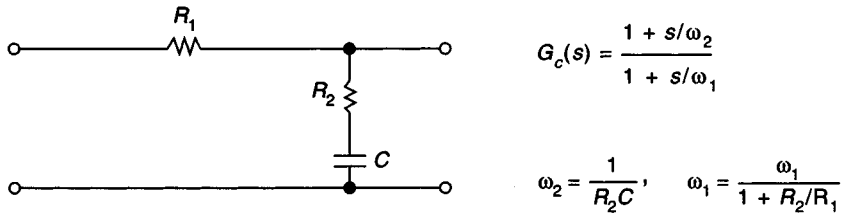


FIGURE 100.14 A simple electrical lag network.

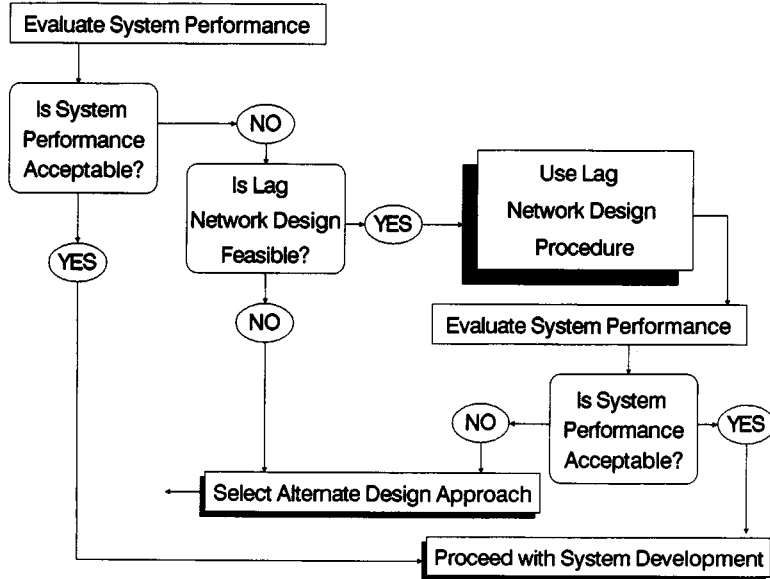


FIGURE 100.15 Life cycle of frequency domain design incorporating lag network compensation.

the crossover frequency and makes the system slower in terms of its transient response. Of course, this would be advantageous if high-frequency noise is present and we wish to reduce its effect. The lag network is an entirely passive device and thus is more economical to instrument than the lead network.

In lead network compensation we actually insert phase lead in the vicinity of the crossover frequency to increase the PM. Thus we realize a specified PM without lowering the medium-frequency system gain. We see that the disadvantages of the lag network are the advantages of the lead network and the advantages of the lag network are the disadvantages of the lead network.

We can attempt to combine the lag network with the lead network into an all-passive structure called a lag-lead network. Generally we obtain better results than we can achieve using either a lead or a lag network. We will consider design using lag-lead networks in our next subsection as well as more complex composite equalization networks.

Composite Equalizers

In the previous subsection we examined the simplest forms of series equalization: gain adjustment, lead network compensation, and lag network compensation. In this subsection we will consider more complex design examples in which composite equalizers will be used for series compensation. The same design principles used earlier in this section will be used here as well.

Lag-Lead Network Design

The prime purpose of a lead network is to add phase lead near the crossover frequency to increase the PM. Accompanied with this phase lead is a gain increase that will increase the crossover frequency. This will sometimes cause difficulties if there is much phase lag in the uncompensated system at high frequencies. There may be situations where use of a phase-lead network to achieve a given PM is not possible due to too many high-frequency poles.

The basic idea behind lag network design is to reduce the gain at “middle” frequencies such as to reduce the crossover frequency to a lower value than for the uncompensated system. If the phase lag is less at this lower frequency, then the PM will be increased by use of the lag network. We have seen that is not possible to use a lag network in situations in which there is not a frequency where an acceptable PM would exist if this frequency were the crossover frequency. Even if use of a lag network is possible, the significantly reduced crossover frequency resulting from its use may make the system so slow and sluggish in response to an input that system performance is unacceptable even though the relative stability of the system is acceptable.

Examination of these characteristics or attributes of lead network and lag network compensation suggests that it might be possible to combine the two approaches to achieve the desirable features of each approach. Thus we will attempt to provide attenuation below the crossover frequency to decrease the phase lag at crossover and phase lead closer to the crossover frequency in order to increase the phase lead of the uncompensated system at the crossover frequency.

The transfer function of the basic lag-lead network is

$$G_c(s) = \frac{(1 + s/\omega_2)(1 + s/\omega_3)}{(1 + s/\omega_1)(1 + s/\omega_4)}$$

where $\omega_4 > \omega_3 > \omega_2 > \omega_1$. Often it is desirable that $\omega_2\omega_3 = \omega_1\omega_4$ such that the high-frequency gain of the equalizer is unity. It is generally not desirable that $\omega_1\omega_4 > \omega_2\omega_3$ as this indicates a high-frequency gain greater than 1, and this will require an active network, or gain, and a passive equalizer. It is a fact that we should always be able to realize a linear minimum phase network using passive components only if the network has a rational transfer function with a gain magnitude that is no greater than 1 at any real frequency.

[Figure 100.16](#) illustrates the gain magnitude and phase shift curves for a single-stage lag-lead network equalizer or compensator transfer function. [Figure 100.17](#) illustrates an electrical network realization of a passive lag-lead network equalizer. Parameter matching can be used to determine the electrical network parameters that yield a specified transfer function. Because the relationships between the break frequencies and the equalizer component values are complex, it may be desirable, particularly in preliminary instrumentation of the control system, to use analog or digital computer programming techniques to construct the equalizer. Traditionally, there has been much analog computer simulation of control systems. The more contemporary approach suggests use of digital computer approaches that require numerical approximation of continuous-time physical systems.

[Figure 100.18](#) presents a flowchart that we may use for lag-lead network design. We see that this flowchart has much in common with the charts and design procedures for lead network and lag network design and that each of these approaches first involves determining or obtaining a set of desired specifications for the control system. Next, the form of a trial compensating network and the number of break frequencies in the network are selected. We must then obtain a number of equations, equal to the number of network break frequencies plus 1. One of these equations shows that the gain magnitude is 1 at the crossover frequency. The second equation will be an equation for the phase shift at crossover. It is generally desirable that there be at least two unspecified compensating network break frequencies such that we may use a third equation, the optimality of the phase shift at crossover equation, in which we set $d\beta/d\omega|_{\omega=\omega_c} = 0$. If other equations are needed to represent the design situation, we obtain these from the design specifications themselves.

General Bode Diagram Design

[Figure 100.19](#) presents a flowchart of a general design procedure for Bode diagram design. As we will see in the next subsection, a minor modification of this flowchart can be used to accomplish design using minor-loop feedback

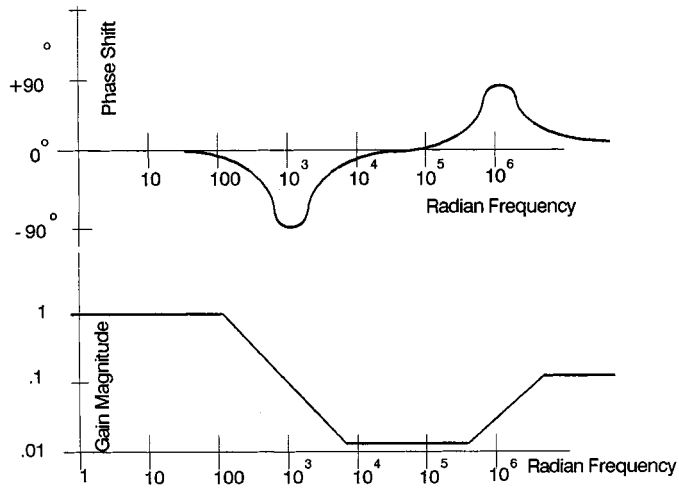
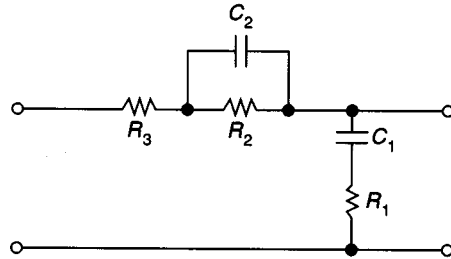


FIGURE 100.16 Phase shift and gain curves for a simple lag-lead network.



$$\begin{aligned}
 G_c(s) &= \frac{(1 + s/\omega_2)(1 + s/\omega_3)}{(1 + s/\omega_1)(1 + s/\omega_4)} \\
 &= \frac{(1 + R_1 C_1 s)(1 + R_2 C_2 s)}{1 + (R_1 C_1 + R_2 C_1 + R_3 C_1 + R_2 C_2)s + (R_1 R_2 C_1 C_2 + R_2 R_3 C_1 C_2)s^2}
 \end{aligned}$$

Special case: $R_3 = 0$

$$\omega_2 = \frac{1}{R_1 C_1}, \quad \omega_3 = \frac{1}{R_2 C_2}, \quad \omega_1 \omega_4 = \omega_2 \omega_3, \quad \omega_1 + \omega_4 = \omega_2 + \omega_3 + \frac{1}{R_1 C_2}$$

FIGURE 100.17 Simple electrical lag-lead network.

or a combination of minor-loop and series equations. These detailed flowcharts for Bode diagram design are, of course, part of the overall design procedure of Fig. 100.9.

Much experience leads to the conclusion that satisfactory linear systems control design using frequency response approaches is such that the crossover frequency occurs on a gain magnitude curve which has a -1 slope at the crossover frequency. In the vicinity of crossover we may approximate any minimum phase transfer function, with crossover on a -1 slope, by

$$G(s) = G_f(s)G_c(s) = \frac{\omega_c \omega_1^{n-1} (1 + s/\omega_1)^{n-1}}{s^n (1 + s/\omega_2)^{m-1}} \quad \text{for } \omega_1 > \omega_c > \omega_2$$

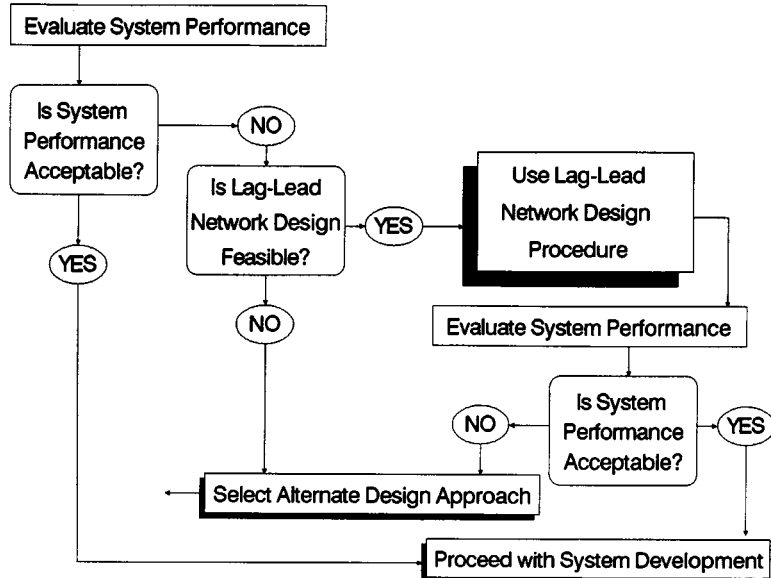


FIGURE 100.18 Life cycle of frequency domain design incorporating lag-lead network compensation.

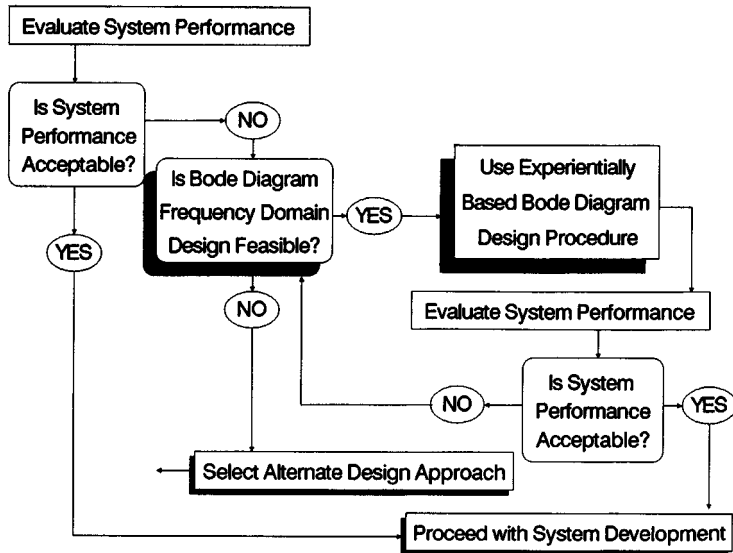


FIGURE 100.19 Life cycle of frequency domain design incorporating general Bode diagram compensation procedure.

Here ω_1 is the break frequency just prior to crossover and ω_2 is the break frequency just after crossover. It is easy to verify that we have $|G(j\omega_c)| = 1$ if $\omega_1 > \omega_c > \omega_2$. Figure 100.20 illustrates this rather general approximation to a compensated system Bode diagram in the vicinity of the crossover frequency. We will conclude this subsection by determining some general design requirements for a system with this transfer function and the associated Bode asymptotic gain magnitude diagram of Fig. 100.20.

There are three unknown frequencies in the foregoing equation. Thus we need three requirements or equations to determine design parameters. We will use the same three requirements used thus far in all our efforts in this section, namely:

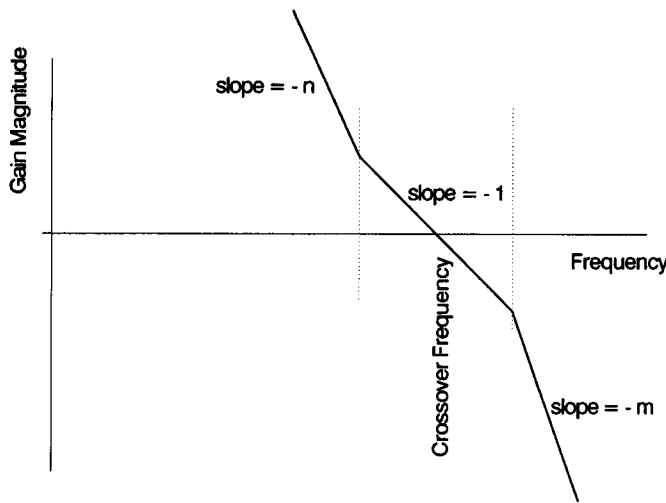


FIGURE 100.20 Illustration of generic gain magnitude in the vicinity of crossover.

1. The gain at crossover is 1.
2. The PM is some specified value.
3. The PM at crossover is the maximum possible for a given ω_2/ω_1 ratio.

We see that the first requirement, that the gain is 1 at the crossover frequency, is satisfied by the foregoing equation if the crossover frequency occurs on the -1 slope portion of the gain curve as assumed in Fig. 100.20. We use the arctangent approximation to obtain the phase shift in the vicinity of crossover as

$$\beta(\omega) = -\frac{n\pi}{2} + (n-1)\left(\frac{\pi}{2} - \frac{\omega_1}{\omega}\right) - (m-1)\frac{\omega}{\omega_2}$$

To satisfy requirement 3 we set

$$\left. \frac{d\beta(\omega)}{d\omega} \right|_{\omega=\omega_c} = 0 = \frac{(n-1)\omega_1}{\omega_c^2} - \frac{m-1}{\omega_2}$$

and obtain

$$\omega_c^2 = \frac{n-1}{m-1} \omega_1 \omega_2$$

as the optimum setting for the crossover frequency. Substitution of the “optimum” frequency given by the foregoing into the phase shift equation results in

$$\beta(\omega_c) = \frac{-\pi}{2} - 2\sqrt{(m-1)(n-1)} \sqrt{\frac{\omega_1}{\omega_2}}$$

We desire a specific PM here, and so the equalizer break frequency locations are specified. There is a single parameter here that is unspecified, and an additional equation must be found in any specific application. Alternately, we could simply assume a nominal crossover frequency of unity or simply normalize frequencies ω_1 and ω_2 in terms of the crossover frequency by use of the normalized frequencies $\omega_1 = W_1\omega_c$ and $\omega_2 = W_2\omega_c$.

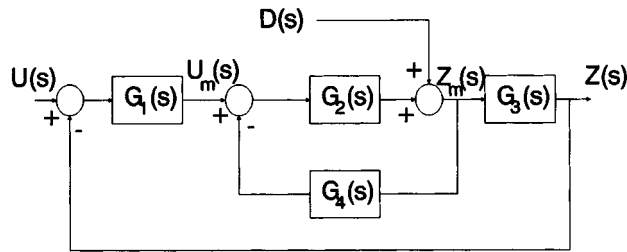


FIGURE 100.21 Feedback control system with a single minor loop and output disturbance.

It is a relatively simple matter to show that for a specified PM expressed in radians, we obtain for the normalized break frequencies

$$W_1 = \frac{\omega_1}{\omega_c} = \frac{PM}{2(n-1)}$$

$$W_2 = \frac{\omega_2}{\omega_c} = \frac{2(m-1)}{PM}$$

It is relatively easy to implement this suggested Bode diagram design procedure which is based upon considering only these break frequencies immediately above and below crossover and which approximate all others. Break frequencies far below crossover are approximated by integrations or differentiations, that is, poles or zeros at $s = 0$, and break frequencies far above the crossover frequency are ignored.

Minor-Loop Design

In our efforts thus far in this section we have assumed that compensating networks would be placed in series with the fixed plant and then a unity feedback ratio loop closed around these elements to yield the closed-loop system. In many applications it may be physically convenient, perhaps due to instrumentation considerations, to use one or more minor loops to obtain a desired compensation of a fixed plant transfer function.

For a single-input-single-output linear system there are no theoretical advantages whatever to any minor-loop compensation to series compensation as the same closed-loop transfer function can be realized by all procedures. However, when there are multiple inputs or outputs, then there may be considerable advantages to minor-loop design as contrasted to series compensation design. Multiple inputs often occur when there is a single-signal input and one or more noise or disturbance inputs present and a task of the system is to pass the signal inputs and reject the noise inputs. Also there may be saturation-type nonlinearities present, and we may be concerned not only with the primary system output but also with keeping the output at the saturation point within bounds such that the system remains linear. Thus there are reasons why minor-loop design may be preferable to series equalization.

We have discussed block diagrams elsewhere in this handbook. It is desirable here to review some concepts that will be of value for our discussion of minor-loop design. Figure 100.21 illustrates a relatively general linear control system with a single minor loop. This block diagram could represent many simple control systems. $G_1(s)$ could represent a discriminator and series compensation and $G_2(s)$ could represent an amplifier and that part of a motor transfer function excluding the final integration to convert velocity to position. $G_3(s)$ might then represent an integrator. $G_4(s)$ would then represent a minor-loop compensation transfer function, such as that of a tachometer.

The closed-loop transfer function for this system is given by

$$\frac{Z(s)}{U(s)} = H(s) = \frac{G_1(s)G_2(s)G_3(s)}{1 + G_2(s)G_4(s) + G_1(s)G_2(s)G_3(s)}$$

It is convenient to define several other transfer functions that are based on the block diagram in Fig. 100.21. First there is the minor-loop gain

$$G_m(s) = G_2(s)G_4(s)$$

which is just the loop gain of the minor loop only. The minor loop has the transfer function

$$\frac{Z_m(s)}{U_m(s)} = H_m(s) = \frac{G_2(s)}{1 + G_2(s)G_4(s)} = \frac{G_2(s)}{1 + G_m(s)}$$

There will usually be a range or ranges of frequency for which the minor-loop gain magnitude is much less than 1, and we then have

$$\frac{Z_m(s)}{U_m(s)} = H_m(s) \approx G_2(s) \quad |G_m(\omega)| \ll 1$$

There will also generally be ranges of frequency for which the minor-loop gain magnitude is much greater than 1, and we then have

$$\frac{Z_m(s)}{U_m(s)} = H_m(s) \approx \frac{1}{G_4(s)} \quad |G_m(\omega)| \gg 1$$

We may use these two relations to considerably simplify our approach to the minor-loop design problem. For illustrative purposes, we will use two major-loop gain functions. First we will consider the major-loop gain with the minor-loop-compensating network removed such that $G_4(s) = 0$. This represents the standard situation we have examined in the last subsection. This uncompensated major-loop transfer function is

$$G_{Mu}(s) = G_1(s)G_2(s)G_3(s)$$

With the minor-loop compensation inserted, the major-loop gain, the input-output transfer function with the unity ratio feedback open, is

$$G_{Mc}(s) = \frac{G_1(s)G_2(s)G_3(s)}{1 + G_m(s)}$$

We may express the complete closed-loop transfer function in the form

$$\frac{Z(s)}{U(s)} = H(s) = \frac{G_{Mc}(s)}{1 + G_{Mc}(s)}$$

A particularly useful relationship may be obtained by combining the last three equations into one equation of the form

$$G_{Mc}(s) = \frac{G_{Mu}(s)}{1 + G_m(s)}$$

We may give this latter equation a particularly simple interpretation. For frequencies where the minor-loop gain $G_m(s)$ is low, the minor-loop-closed major-loop transfer function $G_{Mc}(s)$ is approximately that of the minor-loop-open major-loop transfer function G_{Mu} in that

$$G_{Mc}(s) \approx G_{Mu}(s) \quad |G_m(\omega)| \ll 1$$

For frequencies where the minor-loop gain $G_m(s)$ is high, the minor-loop-closed major-loop transfer function is just

$$G_{Mc}(s) \approx \frac{G_{Mu}(s)}{G_m(s)} \quad |G_m(\omega)| \gg 1$$

This has an especially simple interpretation on the logarithmic frequency plots we use for Bode diagrams for we may simply subtract the minor-loop gain $G_m(s)$ from the minor-loop-open major-loop gain $G_{Mu}(s)$ to obtain the compensated system gain as the transfer function $G_{Mc}(s)$.

The last several equations are the key relations for minor-loop design using this frequency response approach. These relations indicate that some forms of series compensation yield a given major-loop transfer function $G_{Mc}(s)$ which will not be appropriate for realization by minor-loop compensation. In particular, a lead network series compensation cannot be realized by means of equivalent minor-loop compensation. The gain of the fixed plant $G_{Mu}(s)$ is raised at high frequencies due to the use of a lead network compensation. Also, we see that $G_{Mc}(s)$ can only be lowered by use of a minor-loop gain $G_m(s)$.

A lag network used for series compensation will result in a reduction in the fixed plant gain $|G_{Mu}(\omega)|$ at all high frequencies. This can only be achieved if the minor-loop transfer gain $G_m(s)$ is constant for high frequencies. In some cases this may be achievable but often will not be. It is possible to realize the equivalent of lag network series equalization by means of a minor-loop equalization for systems where the low- and high-frequency behavior of $G_{Mu}(s)$, or $G_f(s)$, and $G_{Mc}(s)$ are the same and where the gain magnitude of the compensated system $|G_{Mc}(s)|$ is at no frequency any greater than is the gain magnitude of the fixed plant $|G_f(s)|$ or the minor-loop-open major-loop transfer function $|G_{Mu}(s)|$. Thus we see that lag-lead network series equalization is an ideal type of equalization to realize by means of equivalent minor-loop equalization. Figures 100.9 and 100.19 represent flowcharts of a suggested general design procedure for minor-loop compensator design as well as for the series equalization approaches we examined previously.

In our work thus far we have assumed that parameters were constant and known. Such is seldom the case, and we must naturally be concerned with the effects of parameter variations, disturbances, and nonlinearities upon system performance. Suppose, for example, that we design a system with a certain gain assumed as K_1 . If the system operates open loop and the gain K_1 is in cascade or series with the other input-output components, then the overall transfer function changes by precisely the same factor as K_1 changes. If we have an amplifier with unity ratio feedback around a gain K_1 , the situation is much different. The closed-loop gain would nominally be $K_1/(1 + K_1)$, and a change to $2K_1$ would give a closed-loop gain $2K_1/(1 + 2K_1)$. If K_1 is large, say 10³, then the new gain is 0.99950025, which is a percentage change of less than 0.05% for a change in gain of 100%.

Another advantage of minor-loop feedback occurs when there are output disturbances such as those due to wind gusts on an antenna. We consider the system illustrated in Fig. 100.21. The response due to $D(s)$ alone is

$$\frac{Z(s)}{D(s)} = \frac{1}{1 + G_2(s) G_4(s) + G_1(s) G_2(s)}$$

When we use the relation for the minor-loop gain

$$G_m(s) = G_2(s) G_4(s)$$

and the major-loop gain

$$G_{Mc}(s) = \frac{G_1(s)G_2(s)}{1 + G_2(s)G_4(s)}$$

we can rewrite the response due to $D(s)$ as

$$\frac{Z(s)}{D(s)} = \frac{1}{[1 + G_m(s)]G_{Mc}(s)}$$

Over the range of frequency where $|G_{Mc}(j\omega)| >> 1$, such that the corrected loop gain is large, the attenuation of a load disturbance is proportional to the uncorrected loop gain. This is generally larger over a wider frequency range than the corrected loop gain magnitude $|G_{Mc}(j\omega)|$, which is what the attenuation would be if series compensation were used.

Over the range of frequencies where the minor-loop gain is large but where the corrected loop gain is small, that is, where $|G_m(j\omega)| > 1$ and $|G_{Mc}(j\omega)| < 1$, we obtain for the approximate response due to the disturbance

$$\frac{Z(s)}{D(s)} \approx G_m(s)$$

and the output disturbance is therefore seen to be attenuated by the minor-loop gain rather than unattenuated as would be the case if series compensation had been used. This is, of course, highly desirable.

At frequencies where both the minor-loop gain transfer and the major-loop gain are small we have $Z(s)/D(s) \approx 1$, and over this range of frequencies neither minor-loop compensation nor series equalization is useful in reducing the effect of a load disturbance. Thus, we have shown here that there are quite a number of advantages to minor-loop compensation as compared to series equalization. Of course, there are limitations as well.

Summary

In this section, we have examined the subject of linear system compensation by means of the frequency response method of Bode diagrams. Our approach has been entirely in the frequency domain. We have discussed a variety of compensation networks, including:

1. Gain attenuation
2. Lead networks
3. Lag networks
4. Lag-lead networks and composite equalizers
5. Minor-loop feedback

Despite its age, the frequency domain design approach represents a most useful approach for the design of linear control systems. It has been tested and proven in a great many practical design situations.

Defining Terms

Bode diagram: A graph of the gain magnitude and frequency response of a linear circuit or system, generally plotted on log-log coordinates. A major advantage of Bode diagrams is that the gain magnitude plot will look like straight lines or be asymptotic to straight lines. H.W. Bode, a well-known Bell Telephone Laboratories researcher, published *Network Analysis and Feedback Amplifier Design* in 1945. The approach, first described there, has been refined by a number of other workers over the past half-century.

Crossover frequency: The frequency where the magnitude of the open-loop gain is 1.

Equalizer: A network inserted into a system that has a transfer function or frequency response designed to compensate for undesired amplitude, phase, and frequency characteristics of the initial system. Filter and equalizer are generally synonymous terms.

Lag network: In a simple phase-lag network, the phase angle associated with the input-output transfer function is always negative, or lagging. Figures 100.13 and 100.14 illustrate the essential characteristics of a lag network.

Lag-lead network: The phase shift versus frequency curve in a phase lag-lead network is negative, or lagging, for low frequencies and positive, or leading, for high frequencies. The phase angle associated with the input-output transfer function is always positive, or leading. Figures 100.16 and 100.17 illustrate the essential characteristics of a lag-lead network, or composite equalizer.

Lead network: In a simple phase-lead network, the phase angle associated with the input-output transfer function is always positive, or leading. Figures 100.10 and 100.11 illustrate the essential characteristics of a lead network.

Series equalizer: In a single-loop feedback system, a series equalizer is placed in the single loop, generally at a point along the forward path from input to output where the equalizer itself consumes only a small amount of energy. In Fig. 100.21, $G_1(s)$ could represent a series equalizer. $G_1(s)$ could also be a series equalizer if $G_4(s) = 0$.

Specification: A statement of the design or development requirements to be satisfied by a system or product.

Systems engineering: An approach to the overall life cycle evolution of a product or system. Generally, the systems engineering process comprises a number of phases. There are three essential phases in any systems engineering life cycle: formulation of requirements and specifications, design and development of the system or product, and deployment of the system. Each of these three basic phases may be further expanded into a larger number. For example, deployment generally comprises operational test and evaluation, maintenance over an extended operational life of the system, and modification and retrofit (or replacement) to meet new and evolving user needs.

Related Topic

11.1 Introduction

References

- J.L. Bower and P.M. Schultheiss, *Introduction to the Design of Servomechanisms*, New York: Wiley, 1958.
A.P. Sage, *Linear Systems Control*, Champaign, Ill.: Matrix Press, 1978.
A.P. Sage, *Systems Engineering*, New York: Wiley, 1992.
M.G. Singh, Ed., *Systems and Control Encyclopedia*, Oxford: Pergamon, 1987.

Further Information

Many of the practical design situations used to test the frequency domain design approach are described in the excellent classic text by Bower and Schultheiss [1958]. A rather detailed discussion of the approach may also be found in Sage [1978] on which this discussion is, in part, based. A great variety of control systems design approaches, including frequency domain design approaches, are discussed in a recent definitive control systems encyclopedia [Singh, 1987], and there are a plethora of new introductory control systems textbooks that discuss it as well. As noted earlier, frequency domain design, in particular, and control systems design, in general, constitute one facet of systems engineering effort, such as described in Sage [1992].

100.4 Root Locus

Benjamin C. Kuo

Root locus represents a trajectory of the roots of an algebraic equation with constant coefficients when a parameter varies. The technique is used extensively for the analysis and design of linear time-invariant control

systems. For linear time-invariant control systems the roots of the characteristic equation determine the stability of the system. For a stable continuous-data system the roots must all lie in the left half of the s plane. For a digital control system to be stable, the roots of the characteristic equation must all lie inside the unit circle $|z| = 1$ in the z plane. Thus, in the s plane, the imaginary axis is the stability boundary, whereas in the z plane the stability boundary is the unit circle. The location of the characteristic equation roots with respect to the stability boundary also determine the relative stability, i.e., the degree of stability, of the system.

For a linear time-invariant system with continuous data, the characteristic equation can be written as

$$F(s) = P(s) + KQ(s) = 0 \quad (100.33)$$

where $P(s)$ is an N th-order polynomial of s ,

$$P(s) = s^N + a_1s^{N-1} + \dots + a_{N-1}s + a_N \quad (100.34)$$

and $Q(s)$ is the M th-order polynomial of s ,

$$Q(s) = s^M + b_1s^{M-1} + \dots + b_{M-1}s + b_M \quad (100.35)$$

where N and M are positive integers. The real constant K can vary from $-\infty$ to $+\infty$. The coefficients $a_1, a_2, \dots, a_N, b_1, b_2, \dots, b_M$ are real. As K is varied from $-\infty$ to $+\infty$, the roots of Eq. (100.33) trace out continuous trajectories in the s plane called the *root loci*.

The above development can be extended to digital control systems by replacing s with z in Eqs. (100.33) through (100.35).

Root Locus Properties

The root locus problem can be formulated from Eq. (100.33) by dividing both sides of the equation by the terms that do not contain the variable parameter K . The result is

$$1 + \frac{KQ(s)}{P(s)} = 0 \quad (100.36)$$

For a closed-loop control system with the loop transfer function $KG(s)H(s)$, where the gain factor K has been factored out, the characteristic equation is known to be the zeros of the rational function

$$1 + KG(s)H(s) = 0 \quad (100.37)$$

Since Eqs. (100.36) and (100.37) have the same form, the general root locus problem can be formulated using Eq. (100.36).

Equation (100.37) is written

$$G(s)H(s) = -\frac{1}{K} \quad (100.38)$$

To satisfy the last equation, the following conditions must be met simultaneously:

$$\text{Condition on magnitude: } |G(s)H(s)| = \frac{1}{|K|} \quad (100.39)$$

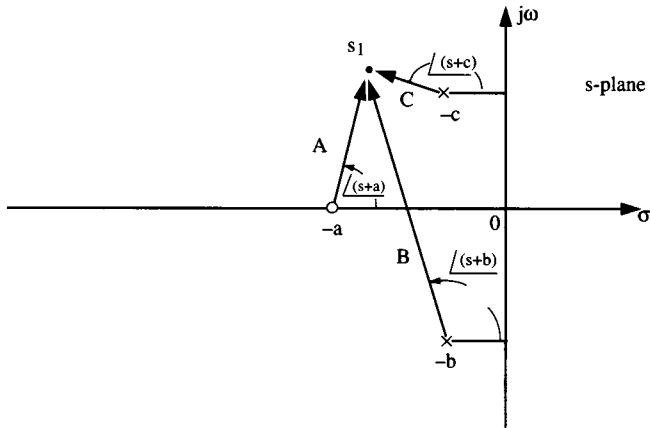


FIGURE 100.22 Graphical interpretation of magnitude and angle conditions of root loci.

where K varies between $-\infty$ and $+\infty$.

$$\begin{aligned} \text{Conditions on angles: } & \angle G(s)H(s) = (2k + 1)\pi \quad K \geq 0 \\ & = \text{odd multiples of } \pi \text{ rad} \end{aligned} \quad (100.40)$$

$$\begin{aligned} \angle G(s)H(s) &= 2k\pi \quad K \leq 0 \\ &= \text{even multiples of } \pi \text{ rad} \end{aligned} \quad (100.41)$$

where $k = 0, \pm 1, \pm 2, \dots, \pm$ any integer.

In general, the conditions on angles in Eqs. (100.40) and (100.41) are used for the construction of the root loci, whereas the condition on magnitude in Eq. (100.39) is used to find the value of K on the loci once the loci are drawn. Let $KG(s)H(s)$ be of the form

$$KG(s)H(s) = \frac{K(s + a)}{(s + b)(s + c)} \quad (100.42)$$

Applying Eqs. (100.40) and (100.41) to the last equation, the angles conditions are

$$\begin{aligned} K \geq 0: \quad & \angle G(s)H(s) = \angle(s + a) - \angle(s + b) - \angle(s + c) \\ & = (2k + 1)\pi \end{aligned} \quad (100.43)$$

$$\begin{aligned} K \leq 0: \quad & \angle G(s)H(s) = \angle(s + a) - \angle(s + b) - \angle(s + c) \\ & = 2k\pi \end{aligned} \quad (100.44)$$

where $k = 0, \pm 1, \pm 2, \dots$. The graphical interpretation of the last two equations is shown in Fig. 100.22. For the point s_1 to be a point on the root locus, the angles of the phasors drawn from the poles and zeros of $G(s)H(s)$ to s_1 must satisfy Eq. (100.43) or (100.44) depending on the sign of K . Applying the magnitude condition of Eq. (100.39) to (100.42), the magnitude of K is expressed as

$$|K| = \frac{|s + b| |s + c|}{|s + a|} = \frac{B \cdot C}{A} \quad (100.45)$$

where A , B , and C are the lengths of the phasors drawn from the poles and zeros of $G(s)H(s)$ to the point s_1 .

The following properties of the root loci are useful for sketching the root loci based on the pole-zero configuration of $G(s)H(s)$. Many computer programs, such as the ROOTLOCI in the ACSP software package [Kuo, 1991b], are available for computing and plotting the root loci. The proofs and derivations of these properties can be carried out from Eqs. (100.39), (100.40), and (100.41) [Kuo, 1991a].

Starting Points (K = 0 Points). The points at which $K = 0$ on the root loci are at the poles of $G(s)H(s)$.

Ending Points (K = $\pm\infty$ Points). The points at which $K = \pm\infty$ on the root loci are at the zeros of $G(s)H(s)$. The poles and zeros referred to above include those at $s = \infty$.

Number of Root Loci. The total number of root loci of Eq. (100.37) equals the higher of the number of poles and zeros of $G(s)H(s)$.

Symmetry of Root Loci. The root loci are symmetrical with respect to the axes of symmetry of the pole-zero configuration of $G(s)H(s)$. In general, the root loci are symmetrical at least to the real axis of the complex s plane.

Asymptotes of the Root Loci. Asymptotes of the root loci refer to the behavior of the root loci at $|s| = \infty$ when the number of poles and zeros of $G(s)H(s)$ is not equal. Let N denote the number of finite poles of $G(s)H(s)$ and M be the number of finite zeros of $G(s)H(s)$. In general, $2|N - M|$ of the loci will approach infinity in the s plane. The properties of the root loci at $|s| = \infty$ are described by the angles and the intersects of the asymptotes. When $N \neq M$, the angles of the asymptotes are given by

$$\phi_k = \begin{cases} \frac{(2k + 1)\pi}{|N - M|} & K \geq 0 \\ \frac{2k\pi}{|N - M|} & K \leq 0 \end{cases} \quad (100.46)$$

where $k = 0, 1, 2, \dots, |N - M| - 1$.

The asymptotes intersect on the real axis at

$$\sigma = \frac{\sum \text{finite poles of } G(s)H(s) - \sum \text{finite zeros of } G(s)H(s)}{N - M} \quad (100.48)$$

Root Loci on the Real Axis. The entire real axis of the s plane is occupied by the root loci. When $K > 0$, root loci are found in sections of the real axis to the right of which the total number of poles and zeros of $G(s)H(s)$ is *odd*. When $K < 0$, root loci are found in sections to the right of which the total number of poles and zeros of $G(s)H(s)$ is *even*.

As a summary of the root locus properties discussed above, the properties of the root loci of the following equation are displayed in Fig. 100.23.

$$s^3 + 2s^2 + 2s + K(s + 3) = 0 \quad (100.49)$$

Dividing both sides of the last equation by the terms that do not contain K we get

$$1 + KG(s)H(s) = 1 + \frac{K(s + 3)}{s(s^2 + 2s + 2)} \quad (100.50)$$

Thus, the poles of $G(s)H(s)$ are at $s = 0$, $s = -1 + j$, and $s = -1 - j$. The zero of $G(s)H(s)$ is at $s = -3$.

As shown in Fig. 100.23, the $K = 0$ points on the root loci are at the poles of $G(s)H(s)$, and the $K = \pm\infty$ points are at the zeros of $G(s)H(s)$. Since $G(s)H(s)$ has two zeros at $s = \infty$, two of the three root loci approach

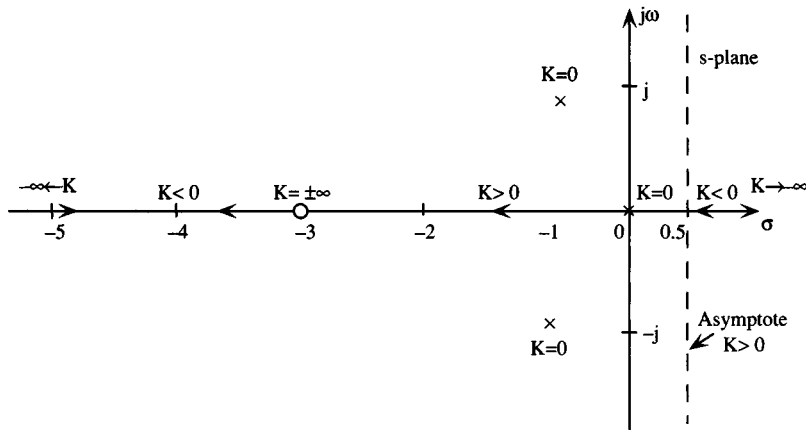


FIGURE 100.23 Some properties of the root loci of $G(s)H(s) = K(s+3)/[s(s^2 + 2s + 2)]$.

infinity in the s plane. The root loci are symmetrical to the real axis of the s plane, since the pole-zero configuration of $G(s)H(s)$ is symmetrical to the axis. The asymptotes of the two root loci that approach infinity are characterized by Eqs. (100.46) through (100.48). The angles of the asymptotes are:

$$K \geq 0: \quad \phi_k = \frac{(2k+1)\pi}{3-1} \quad k = 0, 1 \quad (100.51)$$

$$K \leq 0: \quad \phi_k = \frac{2k\pi}{3-1} \quad k = 0, 1 \quad (100.52)$$

Thus, for $K \geq 0$, the angles of the asymptotes are $\phi_0 = 90^\circ$ and $\phi_1 = 270^\circ$. For $K \leq 0$, $\phi_0 = 0^\circ$ and $\phi_1 = 180^\circ$.

The intersect of the asymptotes is at

$$\sigma = \frac{-1 + j - 1 - j - (-3)}{3-1} = \frac{1}{2} \quad (100.53)$$

The root loci on the real axis are as indicated in Fig. 100.23.

Angles of Departure and Arrival. The slope of the root locus in the vicinity of a pole of $G(s)H(s)$ is measured at the *angle of departure* and that in the vicinity of a zero of $G(s)H(s)$ is measured at the *angle of arrival*.

The angle of departure (arrival) of a root locus at a pole (zero) of $G(s)H(s)$ is determined by assigning a point s_1 to the root locus that is very close to the pole (zero) and applying the angle conditions of Eqs. (100.40) or (100.41). Figure 100.24 illustrates the calculation of the angles of arrival and departure of the root locus at the pole $s = -1 + j$. We assign a point s_1 that is on the locus for $K > 0$ near the pole and draw phasors from all the poles and the zero of $G(s)H(s)$ to this point. The angles made by the phasors with respect to the real axis must satisfy the angle condition in Eq. (100.46). Let the angle of the phasor drawn from $-1 + j$ to s_1 be designated as θ , which is the angle of departure; the angles drawn from the other poles and zero can be approximated by regarding s_1 as being very close to $-1 + j$. Thus, Eq. (100.46) leads to

$$\angle G(s_1)H(s_1) = -\theta - 135^\circ - 90^\circ + 26.6^\circ = -180^\circ \quad (100.54)$$

or $\theta = -18.4^\circ$. For the angle of arrival of the root locus at the pole $s = -1 + j$, we assign a point s_1 on the root loci for $K < 0$ near the pole. Drawing phasors from all the poles and the zero of $G(s)H(s)$ to s_1 and applying the angle condition in Eq. (100.47), we have

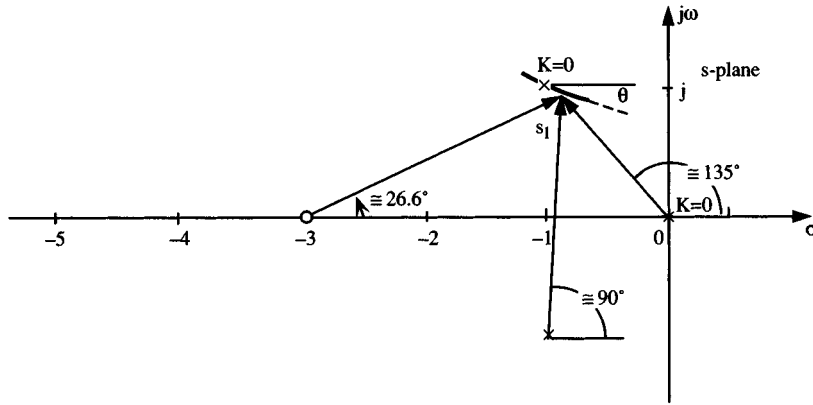


FIGURE 100.24 Angle of arrival and departure calculations.

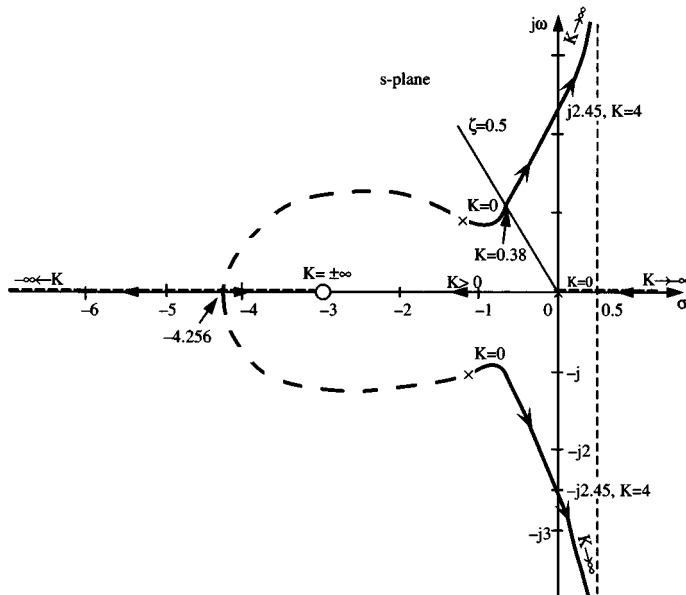


FIGURE 100.25 The complete root loci of $G(s)H(s) = K(s+3)/[s(s^2 + 2s + 2)]$.

$$\angle G(s_1)H(s_1) = -\theta - 135^\circ - 90^\circ + 26.6^\circ = 0^\circ \quad (100.55)$$

Thus, the angle of arrival of the root locus for $K < 0$ is $\theta = 198.4^\circ$. Similarly, we can show that the angles of arrival and departure of the root locus at $s = -3$ are 180° and 0° , respectively.

Intersection of the Root Loci with the Imaginary Axis. The points where the root loci intersect the imaginary axis (if there is any) in the s plane, and the corresponding values of K , may be determined by means of the Routh-Hurwitz stability criterion [Kuo, 1991a]. The root locus program can also be used on a computer to give the intersects.

The complete root loci in Fig. 100.25 show that the root loci intersect the imaginary axis at $s = \pm j2.45$, and the value of K is 4. The system is stable for $0 \leq K < 4$.

Breakaway Points of the Root Loci. Breakaway points on the root loci correspond to multiple-order roots of the equation. At a breakaway point several root loci converge and then break away in different directions. The breakaway point can be real or complex. The latter case must be in complex conjugate pairs.

The breakaway points of the root loci of Eq. (100.37) must satisfy the following condition:

$$\frac{dG(s)H(s)}{ds} = 0 \quad (100.56)$$

On the other hand, not all solutions of Eq. (100.56) are breakaway points. To satisfy as a breakaway point, the point must also lie on the root loci, or satisfy Eq. (100.37). Applying Eq. (100.56) to the function $G(s)H(s)$ given in Eq. (100.50), we have the equation that the breakaway points must satisfy,

$$2s^3 + 11s^2 + 12s + 6 = 0 \quad (100.57)$$

The roots of the last equation are $s = -4.256, -0.622 + j0.564$ and $-0.622 - j0.564$. As shown in Fig. 100.25, only the solution $s = -4.256$ is a breakaway point on the root loci.

Root Loci of Digital Control Systems

The root locus analysis presented in the preceding subsections can be applied to digital control systems without modifying the basic principles. For a linear time-invariant digital control system, the transfer functions are expressed in terms of the z -transform rather than the Laplace transform. The relationship between the z -transform variable z and the Laplace transform variable s is

$$z = e^{Ts} \quad (100.58)$$

where T is the sampling period in seconds. Typically, the characteristic equation roots are solutions of the equation

$$1 + KGH(z) = 0 \quad (100.59)$$

where K is the variable gain parameter. The root loci for a digital control system are constructed in the complex z plane. All the properties of the root loci in the s plane apply readily to the z plane, with the exception that the stability boundary is now the unit circle $|z| = 1$. That is, the system is stable if all the characteristic equation roots lie inside the unit circle.

As an illustration, the open-loop transfer function of a digital control system is given as

$$G(z) = \frac{K(z + 0.1)}{z(z - 1)} \quad (100.60)$$

The characteristic equation of the closed-loop system is

$$z(z - 1) + K(z + 0.1) = 0$$

The root loci of the system are shown in Fig. 100.26. Notice that the system is stable for $0 \leq K < 2.22$. When $K = 2.22$, one root is at $z = -1$, which is on the stability boundary.

Design with Root Locus

The root locus diagram of the characteristic equation of a closed-loop control system can be used for design purposes. The roots of the characteristic equation can be positioned in the s plane (or the z plane for digital control systems) to realize a certain desired relative stability or damping of the system. It should be kept in mind that the zeros of the closed-loop transfer function also affect the relative stability of the system, although the absolute stability is strictly governed by the characteristic equation roots.

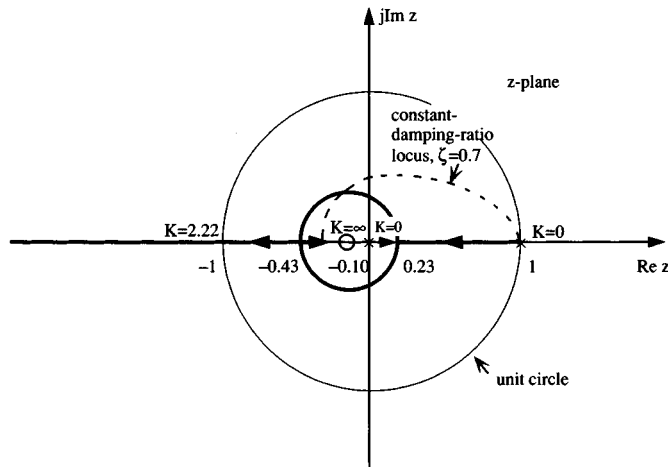


FIGURE 100.26 Root loci in the z plane for a digital control system.

As an illustrative example, the constant-damping ratio line for $\zeta = 0.5$ is shown in Fig. 100.25. The intersect of the $\zeta = 0.5$ line and the root locus corresponds to $K = 0.38$. Let us assume that we want to keep the relative damping at approximately 0.5 but the gain K should be increased tenfold. The following cascade controller is applied to the system [Evans, 1948]:

$$G_c(s) = \frac{1 + 5s}{1 + 50s} \quad (100.61)$$

The open-loop transfer function of the compensated system is now

$$G_c(s)G(s)H(s) = \frac{0.1K(s + 3)(s + 0.2)}{s(s + 0.02)(s^2 + 2s + 2)} \quad (100.62)$$

Figure 100.27 shows the root locus diagram of the compensated system for $K \geq 0$. The shape of the complex root loci is not appreciably affected by the controller, but the value of K that corresponds to a relative damping ratio of 0.5 is now approximately 3.9.

In a similar manner the root loci of digital control systems can be reshaped in the z plane for design. The constant-damping ratio locus in the z plane is shown in Fig. 100.26.

Defining Terms

Angles of departure and arrival: The slope of the root locus in the vicinity of a pole of $G(s)H(s)$ is measured as the angle of departure, and that in the vicinity of a zero of $G(s)H(s)$ is measured as the angle of arrival.

Asymptotes of root loci: The behavior of the root loci at $|s| = \infty$ when the number of poles and zeros of $G(s)H(s)$ is not equal.

Breakaway points of the root loci: Breakaway points on the root loci correspond to multiple-order roots of the equation.

Root locus: The trajectory of the roots of an algebraic equation with constant coefficient when a parameter varies.

Related Topics

6.1 Definitions and Properties • 12.1 Introduction

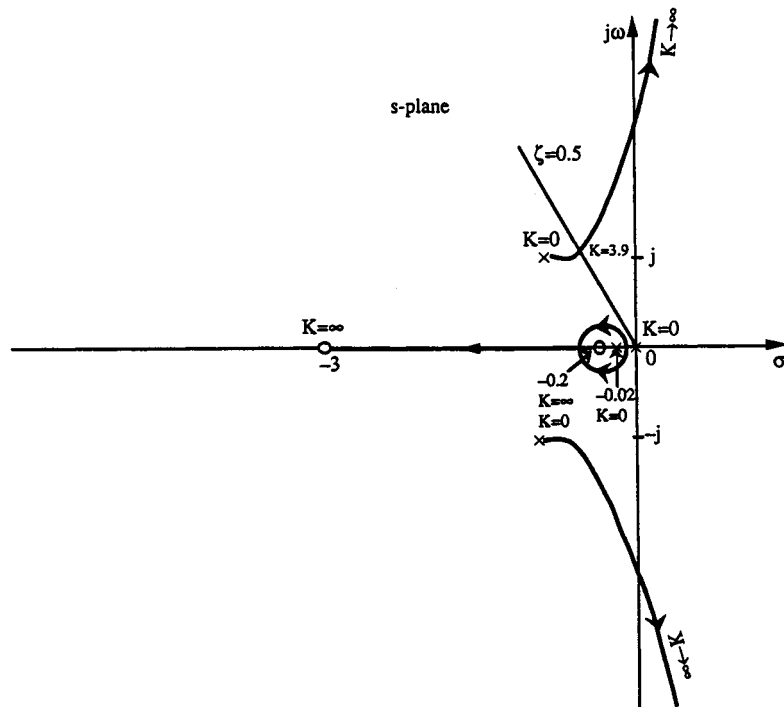


FIGURE 100.27 Root loci of Eq. (100.62).

References and Further Information

- R. C. Dorf, *Modern Control Systems*, 5th ed., Reading, Mass.: Addison-Wesley, 1989.
- W. R. Evans, "Graphical analysis of control systems," *Trans. AIEE*, vol. 67, pp. 547–551, 1948.
- B. C. Kuo, *Automatic Control Systems*, 6th ed., Englewood Cliffs, N.J.: Prentice-Hall, 1991a.
- B. C. Kuo, *ACSP Software and Manual*, Englewood Cliffs, N.J.: Prentice-Hall, 1991b.
- B. C. Kuo, *Digital Control Systems*, 2nd ed., New York: Holt, 1992a.
- B. C. Kuo, *DCSP Software and Manual*, Champaign, Ill.: SRL, Inc., 1992b.

100.5 Compensation

Charles L. Phillips and Royce D. Harbor

Compensation is the process of modifying a closed-loop control system (usually by adding a *compensator* or *controller*) in such a way that the compensated system satisfies a given set of design specifications. This section presents the fundamentals of compensator design; actual techniques are available in the references.

A single-loop control system is shown in Fig. 100.28. This system has the transfer function from input $R(s)$ to output $C(s)$

$$T(s) = \frac{C(s)}{R(s)} = \frac{G_c(s)G_p(s)}{1 + G_c(s)G_p(s)H(s)} \quad (100.63)$$

and the characteristic equation is

$$1 + G_c(s)G_p(s)H(s) = 0 \quad (100.64)$$

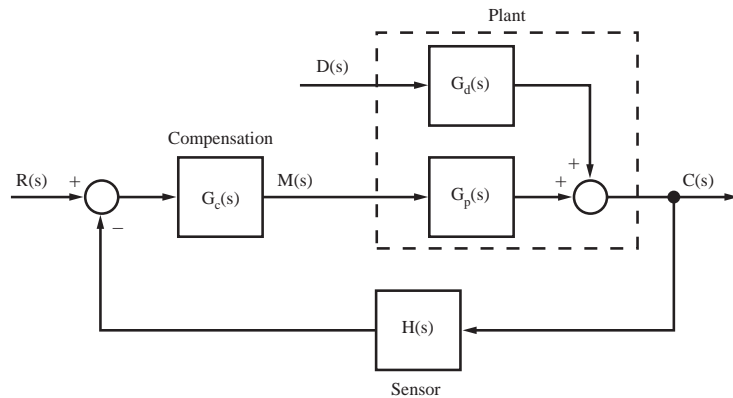


FIGURE 100.28 A closed-loop control system.

where $G_c(s)$ is the *compensator* transfer function, $G_p(s)$ is the *plant* transfer function, and $H(s)$ is the *sensor* transfer function. The transfer function from the disturbance input $D(s)$ to the output is $G_d(s)/[1 + G_c(s)G_p(s)H(s)]$. The function $G_c(s)G_p(s)H(s)$ is called the *open-loop function*.

Control System Specifications

The compensator transfer function $G_c(s)$ is designed to give the closed-loop system certain specified characteristics, which are realized through achieving one or more of the following:

1. Improving the transient response. Increasing the speed of response is generally accomplished by increasing the open-loop gain $G_c(j\omega)G_p(j\omega)H(j\omega)$ at higher frequencies such that the system bandwidth is increased. Reducing overshoot (ringing) in the response generally involves increasing the phase margin ϕ_m of the system, which tends to remove any resonances in the system. The phase margin ϕ_m occurs at the frequency ω_1 and is defined by the relationship

$$|G_c(j\omega_1)G_p(j\omega_1)H(j\omega_1)| = 1$$

with the angle of $G_c(j\omega_1)G_p(j\omega_1)H(j\omega_1)$ equal to $(180^\circ + \phi_m)$.

2. Reducing the steady-state errors. Steady-state errors are decreased by increasing the open-loop gain $G_c(j\omega)G_p(j\omega)H(j\omega)$ in the frequency range of the errors. Low-frequency errors are reduced by increasing the low-frequency open-loop gain and by increasing the type number of the system [the number of poles at the origin in the open-loop function $G_c(s)G_p(s)H(s)$].
3. Reducing the sensitivity to plant parameters. Increasing the open-loop gain $G_c(j\omega)G_p(j\omega)H(j\omega)$ tends to reduce the variations in the system characteristics due to variations in the parameters of the plant.
4. Rejecting disturbances. Increasing the open-loop gain $G_c(j\omega)G_p(j\omega)H(j\omega)$ tends to reduce the effects of disturbances [$D(s)$ in Fig. 100.28] on the system output, provided that the increase in gain does not appear in the direct path from disturbance inputs to the system output.
5. Increasing the relative stability. Increasing the open-loop gain tends to reduce phase and gain margins, which generally increases the overshoot in the system response. Hence, a trade-off exists between the beneficial effects of increasing the open-loop gain and the resulting detrimental effects of reducing the stability margins.

Design

Design procedures for compensators are categorized as either *classical methods* or *modern methods*. Classical methods discussed are:

- Phase-lag frequency response
- Phase-lead frequency response
- Phase-lag root locus
- Phase-lead root locus

Modern methods discussed are:

- Pole placement
- State estimation
- Optimal

Frequency Response Design

Classical design procedures are normally based on the open-loop function of the uncompensated system, $G_p(s)H(s)$. Two compensators are used in classical design; the first is called a *phase-lag compensator*, and the second is called a *phase-lead compensator*.

The general characteristics of phase-lag-compensated systems are as follows:

1. The low-frequency behavior of a system is improved. This improvement appears as reduced errors at low frequencies, improved rejection of low-frequency disturbances, and reduced sensitivity to plant parameters in the low-frequency region.
2. The system bandwidth is reduced, resulting in a slower system time response and better rejection of high-frequency noise in the sensor output signal.

The general characteristics of phase-lead-compensated systems are as follows:

1. The high-frequency behavior of a system is improved. This improvement appears as faster responses to inputs, improved rejection of high-frequency disturbances, and reduced sensitivity to changes in the plant parameters.
2. The system bandwidth is increased, which can increase the response to high-frequency noise in the sensor output signal.

The transfer function of a first-order compensator can be expressed as

$$G_c(s) = \frac{K_c(s/\omega_0 + 1)}{s/\omega_p + 1} \quad (100.65)$$

where $-\omega_0$ is the compensator zero, $-\omega_p$ is its pole, and K_c is its dc gain. If $\omega_p < \omega_0$, the compensator is phase-lag. The Bode diagram of a phase-lag compensator is given in Fig. 100.29 for $K_c = 1$.

It is seen from Fig. 100.29 that the phase-lag compensator reduces the high-frequency gain of the open-loop function relative to the low-frequency gain. This effect allows a higher low-frequency gain, with the advantages listed above. The pole and zero of the compensator must be placed at very low frequencies relative to the compensated-system bandwidth so that the destabilizing effects of the negative phase of the compensator are negligible.

If $\omega_p > \omega_0$ the compensator is phase-lead. The Bode diagram of a phase-lead compensator is given in Fig. 100.30 for $K_c = 1$.

It is seen from Fig. 100.30 that the phase-lead compensator increases the high-frequency gain of the open-loop function relative to its low-frequency gain. Hence, the system has a larger bandwidth, with the advantages listed above. The pole and zero of the compensator are generally difficult to place, since the increased gain of the open-loop function tends to destabilize the system, while the phase lead of the compensator tends to stabilize the system. The pole-zero placement for the phase-lead compensator is much more critical than that of the phase-lag compensator.

A typical Nyquist diagram of an uncompensated system is given in Fig. 100.31. The pole and the zero of a phase-lag compensator are placed in the frequency band labeled A. This placement negates the destabilizing

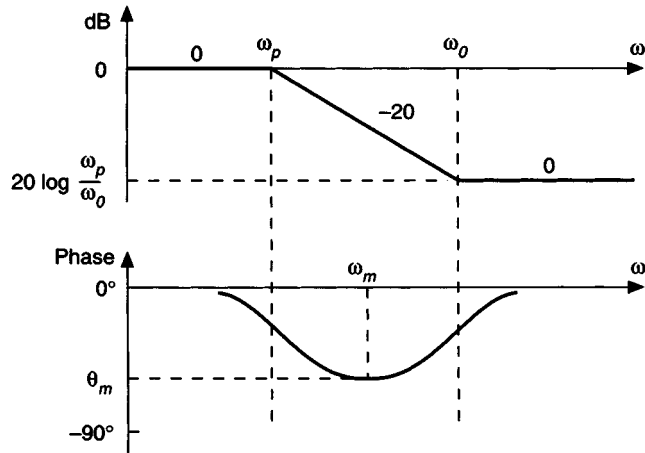


FIGURE 100.29 Bode diagram for a phase-lag compensator.

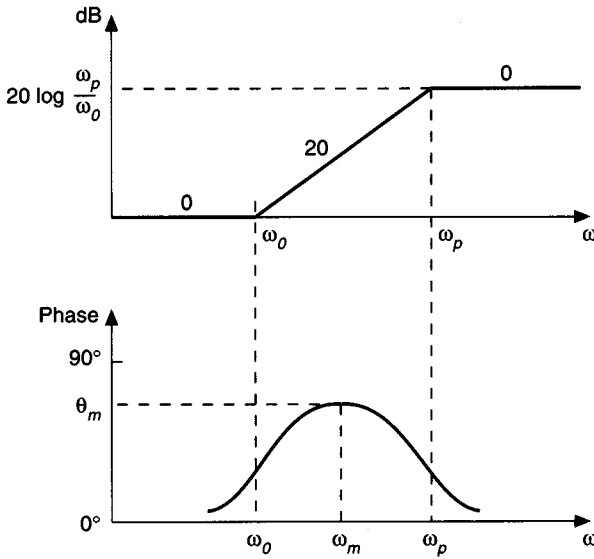


FIGURE 100.30 Bode diagram for a phase-lead compensator.

effect of the negative phase of the compensator. The pole and zero of a phase-lead compensator are placed in the frequency band labeled *B*. This placement utilizes the stabilizing effect of the positive phase of the compensator.

PID Controllers

Proportional-plus-integral-plus-derivative (PID) compensators are probably the most utilized form for compensators. These compensators are essentially equivalent to a phase-lag compensator cascaded with a phase-lead compensator. The transfer function of this compensator is given by

$$G_c(s) = K_p + \frac{K_I}{s} + K_D s \quad (100.66)$$

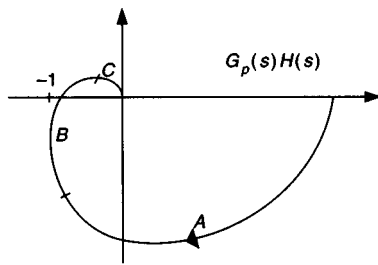


FIGURE 100.31 A typical Nyquist diagram for $G_p(s)H(s)$.

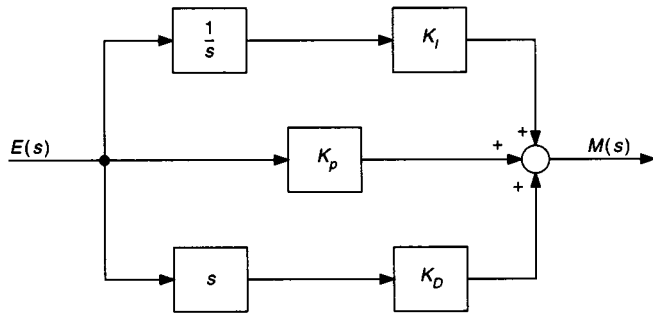


FIGURE 100.32 Block diagram of a PID compensator.

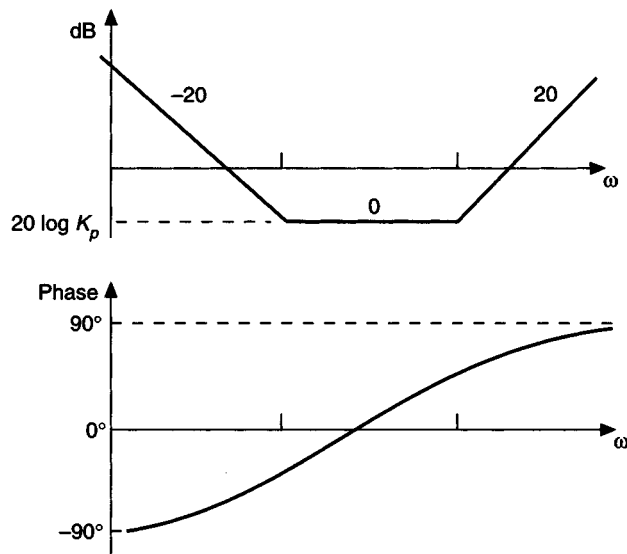


FIGURE 100.33 Bode diagram of a PID compensator.

A block diagram portrayal of the compensator is shown in Fig. 100.32. The integrator in this compensator increases the system type by one, resulting in an improved low-frequency response. The Bode diagram of a PID compensator is given in Fig. 100.33.

With $K_D = 0$, the compensator is phase-lag, with the pole in (100.65) moved to $\omega_p = 0$. As a result the compensator is type one. The zero of the compensator is placed in the low-frequency range to correspond to the zero of the phase-lag compensator discussed above.

With $K_I = 0$, the compensator is phase-lead, with a single zero and the pole moved to infinity. Hence, the gain continues to increase with increasing frequency. If high-frequency noise is a problem, it may be necessary to add one or more poles to the PD or PID compensators. These poles must be placed at high frequencies relative to the phase-margin frequency such that the phase margin (stability characteristics) of the system is not degraded. PD compensators realized using rate sensors minimize noise problems [Phillips and Harbor, 1991].

Root Locus Design

Root locus design procedures generally result in the placement of the two dominant poles of the closed-loop system transfer function. A system has two dominant poles if its behavior approximates that of a second-order system.

The differences in root locus designs and frequency response designs appear only in the interpretation of the control-system specifications. A root locus design that improves the low-frequency characteristics of the system will result in a phase-lag controller; a phase-lead compensator results if the design improves the high-frequency response of the system. If a root locus design is performed, the frequency response characteristics of the system should be investigated. Also, if a frequency response design is performed, the poles of the closed-loop transfer function should be calculated.

Modern Control Design

The classical design procedures above are based on a transfer-function model of a system. Modern design procedures are based on a *state-variable model* of the plant. The plant transfer function is given by

$$\frac{Y(s)}{U(s)} = G_p(s) \quad (100.67)$$

where we use $u(t)$ for the plant input and $y(t)$ for the plant output. If the system model is n th order, the denominator of $G_p(s)$ is an n th-order polynomial.

The state-variable model, or state model, for a single-input-single-output plant is given by

$$\begin{aligned} \frac{d\mathbf{x}(t)}{dt} &= \mathbf{A}\mathbf{x}(t) + \mathbf{B}u(t) \\ y(t) &= \mathbf{C}\mathbf{x}(t) \end{aligned} \quad (100.68)$$

$$y(t) = \mathbf{C}\mathbf{x}(t)$$

where $\mathbf{x}(t)$ is the $n \times 1$ state vector, $u(t)$ is the plant input, $y(t)$ is the plant output, \mathbf{A} is the $n \times n$ *system matrix*, \mathbf{B} is the $n \times 1$ *input matrix*, and \mathbf{C} is the $1 \times n$ *output matrix*. The transfer function of (100.67) is an input-output model; the state model of (100.68) yields the same input-output model and in addition includes an internal model of the system. The state model of (100.68) is readily adaptable to a multiple-input–multiple-output system (*a multivariable system*); for that case, $u(t)$ and $y(t)$ are vectors. We will consider only single-input–single-output systems.

The plant transfer function of (100.67) is related to the state model of (100.68) by

$$G_p(s) = \mathbf{C}(s\mathbf{I} - \mathbf{A})^{-1}\mathbf{B} \quad (100.69)$$

The state model is not unique; many combinations of the matrices \mathbf{A} , \mathbf{B} , and \mathbf{C} can be found to satisfy (100.69) for a given transfer function $G_p(s)$.

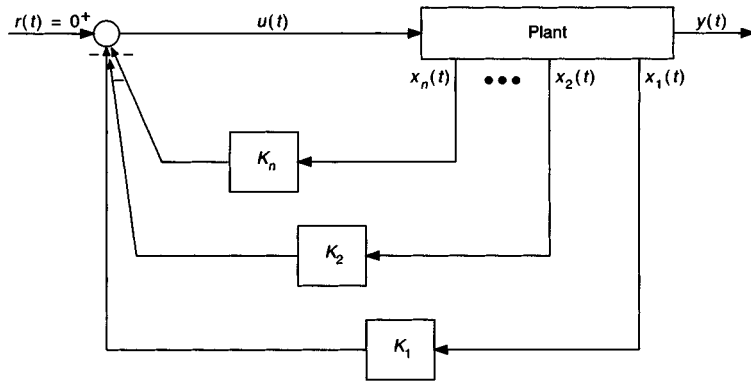


FIGURE 100.34 Implementation of pole-placement design.

Classical compensator design procedures are based on the open-loop function $G_p(s)H(s)$ of Fig. 100.28. It is common to present modern design procedures as being based on only the plant model of (100.68). However, the models of the sensors that measure the signals for feedback must be included in the state model. This problem will become more evident as the modern procedures are presented.

Pole Placement

Probably the simplest modern design procedure is *pole placement*. Recall that root locus design was presented as placing the two dominant poles of the closed-loop transfer function at desired locations. The pole-placement procedure places *all* poles of the closed-loop transfer function, or equivalently, all roots of the closed-loop system characteristic equation, at desirable locations.

The system design specifications are used to generate the desired closed-loop system characteristic equation $\alpha_c(s)$, where

$$\alpha_c(s) = s^n + \alpha_{n-1}s^{n-1} + \dots + \alpha_1s + \alpha_0 = 0 \quad (100.70)$$

for an n th-order plant. This characteristic equation is realized by requiring the plant input to be a linear combination of the plant states, that is,

$$u(t) = -K_1x_1(t) - K_2x_2(t) - \dots - K_nx_n(t) = -\mathbf{K}\mathbf{x}(t) \quad (100.71)$$

where \mathbf{K} is the $1 \times n$ feedback-gain matrix. Hence *all* states must be measured and fed back. This operation is depicted in Fig. 100.34.

The feedback-gain matrix \mathbf{K} is determined from the desired characteristic equation for the closed-loop system of (100.70):

$$\alpha_c(s) = |sI - A + BK| = 0 \quad (100.72)$$

The state feedback gain matrix \mathbf{K} which yields the specified closed-loop characteristic equation $\alpha_c(s)$ is

$$\mathbf{K} = [0 \ 0 \ \dots \ 0 \ 1][\mathbf{B} \ \mathbf{AB} \ \dots \ \mathbf{A}^{n-1}\mathbf{B}]^{-1}\alpha_c(\mathbf{A}) \quad (100.73)$$

where $\alpha_c(\mathbf{A})$ is (100.70) with the scalar s replaced with the matrix \mathbf{A} . A plant is said to be *controllable* if the inverse matrix in (100.73) exists. Calculation of \mathbf{K} completes the design process. A simple computer algorithm is available for solving (100.73) for \mathbf{K} .

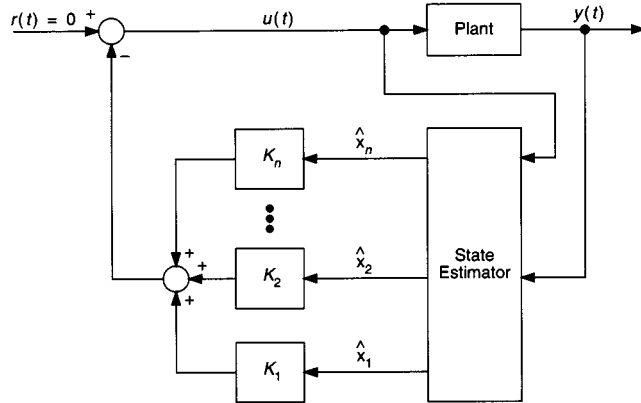


FIGURE 100.35 Implementation of observer-pole-placement design.

State Estimation

In general, modern design procedures require that the state vector $\mathbf{x}(t)$ be fed back, as in (100.71). The measurement of all state variables is difficult to implement for high-order systems. The usual procedure is to estimate the states of the system from the measurement of the output $y(t)$, with the estimated states then fed back.

Let the estimated state vector be $\hat{\mathbf{x}}$. One procedure for estimating the system states is by an *observer*, which is a dynamic system realized by the equations

$$\frac{d\hat{\mathbf{x}}(t)}{dt} = (\mathbf{A} - \mathbf{G}\mathbf{C})\hat{\mathbf{x}}(t) + \mathbf{B}u(t) + \mathbf{G}y(t) \quad (100.74)$$

with the feedback equation of (100.71) now realized by

$$u(t) = -\mathbf{K}\hat{\mathbf{x}}(t) \quad (100.75)$$

The matrix \mathbf{G} in (100.74) is calculated by assuming an n th-order characteristic equation for the observer of the form

$$\alpha_e(s) = |sI - \mathbf{A} + \mathbf{G}\mathbf{C}| = 0 \quad (100.76)$$

The estimator gain matrix \mathbf{G} which yields the specified estimator characteristic equation $\alpha_e(s)$ is

$$\mathbf{G} = \alpha_e(\mathbf{A})[\mathbf{C} \ \mathbf{CA} \ \dots \ \mathbf{CA}^{n-1}]^{-T}[0 \ 0 \ \dots \ 0 \ 1]^T \quad (100.77)$$

where $[\cdot]^T$ denotes the matrix transpose. A plant is said to be *observable* if the inverse matrix in (100.77) exists. An implementation of the closed-loop system is shown in Fig. 100.35. The observer is usually implemented on a digital computer. The plant and the observer in Fig. 100.35 are both n th-order; hence, the closed-loop system is of order $2n$.

The observer-pole-placement system of Fig. 100.35 is equivalent to the system of Fig. 100.36, which is of the form of closed-loop systems designed by classical procedures. The transfer function of the controller-estimator (equivalent compensator) of Fig. 100.36 is given by

$$\mathbf{G}_{ec}(s) = \mathbf{K}[s\mathbf{I} - \mathbf{A} + \mathbf{G}\mathbf{C} + \mathbf{B}\mathbf{K}]^{-1}\mathbf{G} \quad (100.78)$$

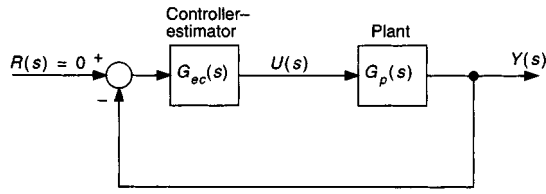


FIGURE 100.36 Equivalent system for pole-placement design.

This compensator is n th-order for an n th-order plant; hence, the total system is of order $2n$. The characteristic equation for the compensated system is given by

$$|s\mathbf{I} - \mathbf{A} + \mathbf{B}\mathbf{K}| |s\mathbf{I} - \mathbf{A} + \mathbf{G}\mathbf{C}| = \alpha_c(s)\alpha_e(s) = 0 \quad (100.79)$$

The roots of this equation are the roots of the pole-placement design plus those of the observer design. For this reason, the roots of the characteristic equation for the observer are usually chosen to be faster than those of the pole-placement design.

Linear Quadratic Optimal Control

We define an optimal control system as one for which some mathematical function is minimized. The function to be minimized is called the *cost function*. For steady-state linear quadratic optimal control the cost function is given by

$$V_\infty = \int_t^\infty [\mathbf{x}^T(\tau)\mathbf{Q}\mathbf{x}(\tau) + R u^2(\tau)] d\tau \quad (100.80)$$

where \mathbf{Q} and R are chosen to satisfy the design criteria. In general, the choices are not straightforward. Minimization of (100.80) requires that the plant input be given by

$$u(t) = -R^{-1}\mathbf{B}^T\mathbf{M}_\infty\mathbf{x}(t) \quad (100.81)$$

where the $n \times n$ matrix \mathbf{M}_∞ is the solution to the *algebraic Riccati equation*

$$\mathbf{M}_\infty\mathbf{A} + \mathbf{A}^T\mathbf{M}_\infty - \mathbf{M}_\infty\mathbf{B}\mathbf{R}^{-1}\mathbf{B}^T\mathbf{M}_\infty + \mathbf{Q} = 0 \quad (100.82)$$

The existence of a solution for this equation is involved [Friedland, 1986] and is not presented here. Optimal control systems can be designed for cost functions other than that of (100.80).

Other Modern Design Procedures

Other modern design procedures exist; for example, *self-tuning control systems* continually estimate certain plant parameters and adjust the compensator based on this estimation. These control systems are a type of *adaptive control systems* and usually require that the control algorithms be implemented using a digital computer. These control systems are beyond the scope of this book (see, for example, Astrom and Wittenmark, 1984).

Defining Term

Compensation: The process of physically altering a closed-loop system such that the system has specified characteristics. This alteration is achieved either by changing certain parameters in the system or by adding a physical system to the closed-loop system; in some cases both methods are used.

Related Topics

100.3 Frequency Response Methods: Bode Diagram Approach • 100.4 Root Locus

References

- K. J. Astrom and B. Wittenmark, *Computer Controlled Systems*, Englewood Cliffs, N.J.: Prentice-Hall, 1984.
- W. L. Brogan, *Modern Control Theory*, Englewood Cliffs, N.J.: Prentice-Hall, 1985.
- R. C. Dorf, *Modern Control Systems*, 7th ed., Reading, Mass.: Addison-Wesley, 1995.
- G. F. Franklin, J. D. Powell, and A. Emami-Naeini, *Feedback Control of Dynamic Systems*, Reading, Mass.: Addison-Wesley, 1986.
- B. Friedland, *Control System Design*, New York: McGraw-Hill, 1986.
- B. C. Kuo, *Automatic Control Systems*, Englewood Cliffs, N.J.: Prentice-Hall, 1987.
- C. L. Phillips and R. D. Harbor, *Feedback Control Systems*, 2nd ed., Englewood Cliffs, N.J.: Prentice-Hall, 1991.

100.6 Digital Control Systems

Raymond G. Jacquot and John E. McInroy

The use of the **digital computer** to control physical processes has been a topic of discussion in the technical literature for over four decades, but the actual use of a digital computer for control of industrial processes was reserved only for massive and slowly varying processes such that the high cost and slow computing speed of available computers could be tolerated. The invention of the integrated circuit microprocessor in the early 1970s radically changed all that; now microprocessors are used in control tasks in automobiles and household appliances, applications where high cost is not justifiable.

When the term *digital control* is used, it usually refers to the process of employing a digital computer to control some process that is characterized by continuous-in-time dynamics. The control can be of the open-loop variety where the control strategy output by the digital computer is dictated without regard to the status of the process variables. An alternative technique is to supply the digital computer with digital data about the process variables to be controlled, and thus the control strategy output by the computer depends on the process variables that are to be controlled. This latter strategy is a **feedback control** strategy wherein the computer, the process, and interface hardware form a closed loop of information flow.

Examples of dynamic systems that are controlled in such a closed-loop digital fashion are flight control of civilian and military aircraft, control of process variables in chemical processing plants, and position and force control in industrial robot manipulators. The simplest form of feedback control strategy provides an on-off control to the controlling variables based on measured values of the process variables. This strategy will be illustrated by a simple example in a following subsection.

In the past decade and a half many excellent textbooks on the subject of digital control systems have been written, and most of them are in their second edition. The texts in the References provide in-depth development of the theory by which such systems are analyzed and designed.

A Simple Example

Such a closed-loop or feedback control situation is illustrated in Fig. 100.37, which illustrates the feedback control of the temperature in a simple environmental chamber that is to be kept at a constant temperature somewhat above room temperature.

Heat is provided by turning on a relay that supplies power to a heater coil. The on-off signal to the relay can be supplied by 1 bit of an output port of the microprocessor (typically the port would be 8 bits wide). A second bit of the port can be used to turn a fan on and off to supply cooling air to the chamber. An analog-to-digital (A/D) converter is employed to convert the amplified thermocouple signal to a digital word that is then supplied to the input port of the microprocessor. The program being executed by the microprocessor reads the temperature data supplied to the input port and compares the binary number representing the temperature to a binary

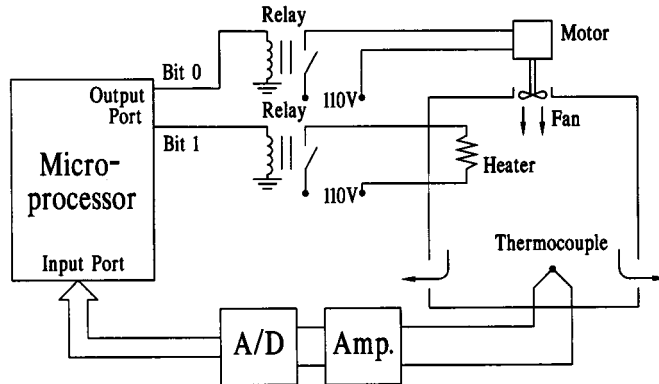


FIGURE 100.37 Microprocessor control of temperature in a simple environmental chamber.

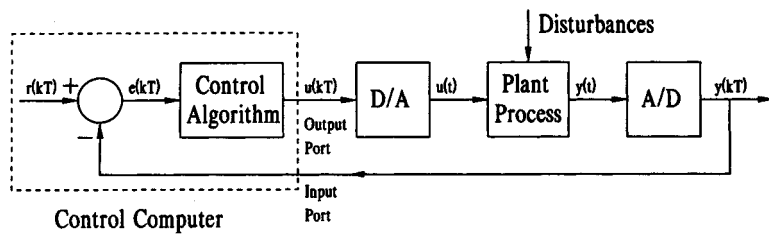


FIGURE 100.38 Closed-loop control of a single process variable.

version of the desired temperature and makes a decision whether or not to turn on the heater or the fan or to do nothing. The program being executed runs in a continuous loop, repeating the operations discussed above.

This simple on-off control strategy is often not the best when extremely precise control of the process variables is required. A more precise control may be obtained if the controlling variable levels can be adjusted to be somewhat larger if the deviation of the process variable from the desired value is larger.

Single-Loop Linear Control Laws

Consider the case where a single variable of the process is to be controlled, as illustrated in Fig. 100.38. The output of the plant $y(t)$ is to be sampled every T seconds by an A/D converter, and this sequence of numbers will be denoted as $y(kT)$, $k = 0, 1, 2, \dots$. The goal is to make the sequence $y(kT)$ follow some desired known sequence [the reference sequence $r(kT)$]. Consequently, the sequence $y(kT)$ is subtracted from $r(kT)$ to obtain the so-called error sequence $e(kT)$. The control computer then acts on the error sequence, using some control algorithms, to produce the control effort sequence $u(kT)$ that is supplied to the digital-to-analog (D/A) converter which then drives the actuating hardware with a signal proportional to $u(kT)$. The output of the D/A converter is then held constant on the current time interval, and the control computer waits for the next sample of the variable to be controlled, the arrival of which repeats the sequence. The most commonly employed control algorithm or control law is a linear difference equation of the form

$$\begin{aligned} u(kT) = & a_n e(kT) + a_{n-1} e((k-1)T) + \dots + a_0 e((k-n)T) \\ & + b_{n-1} u((k-1)T) + \dots + b_0 u((k-n)T) \end{aligned} \quad (100.83)$$

The question remains as to how to select the coefficients a_0, \dots, a_n and b_0, \dots, b_{n-1} in expression (100.83) to give an acceptable degree of control of the plant.

Proportional Control

This is the simplest possible control algorithm for the digital processor wherein the most current control effort is proportional to the current error or using only the first term of relation (100.83)

$$u(kT) = a_n e(kT) \quad (100.84)$$

This algorithm has the advantage that it is simple to program, while, on the other hand, its disadvantage lies in the fact that it has poor disturbance rejection properties in that if a_n is made large enough for good disturbance rejection, the closed-loop system can be unstable (i.e., have transient responses which increase with time). Since the object is to regulate the system output in a known way, these unbounded responses preclude this regulation.

PID Control Algorithm

A common technique employed for decades in chemical process control loops is that of proportional-plus-integral-plus-derivative (PID) control wherein a continuous-time control law would be given by

$$u(t) = K_p e(t) + K_i \int_0^t e(\tau) d\tau + K_d \frac{de}{dt} \quad (100.85)$$

This would have to be implemented by an analog filter.

To implement the design in digital form the proportional term can be carried forward as in relation (100.84); however, the integral can be replaced by trapezoidal integration using the error sequence, while the derivative can be replaced with the backward difference resulting in a computer control law of the form [Jacquot, 1995]

$$\begin{aligned} u(kT) &= u((k-1)T) + \left(K_p + \frac{K_i T}{2} + \frac{K_d}{T} \right) e(kT) \\ &\quad + \left(\frac{K_i T}{2} - K_p - \frac{2K_d}{T} \right) e((k-1)T) + \frac{K_d}{T} e((k-2)T) \end{aligned} \quad (100.86)$$

where T is the duration of the sampling interval. The selection of the coefficients in this algorithm (K_p , K_d , and K_i) is best accomplished by the Ziegler-Nichols tuning process [Franklin et al., 1990].

The Closed-Loop System

When the plant process is linear or may be linearized about an operating point and the control law is linear as in expressions (100.83), (100.84), or (100.86), then an appropriate representation of the complete closed-loop system is by the so-called z -transform. The z -transform plays the role for linear, constant-coefficient difference equations that the Laplace transform plays for linear, constant-coefficient differential equations. This z -domain representation allows the system designer to investigate system time response, frequency response, and stability in a single analytical framework.

If the plant can be represented by an s -domain transfer function $G(s)$, then the discrete-time (z -domain) transfer function of the plant, the analog-to-digital converter, and the driving digital-to-analog converter is

$$G(z) = \left(\frac{z-1}{z} \right) Z \left\{ L^{-1} \left[\frac{G(s)}{s} \right] \right\} \quad (100.87)$$

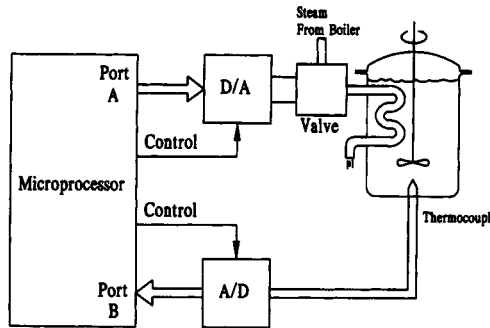


FIGURE 100.39 A computer-controlled thermal mixing tank.

where $Z(\cdot)$ is the z -transform and $L^{-1}(\cdot)$ is the inverse Laplace transform. The transfer function of the control law of (100.83) is

$$D(z) = \frac{U(z)}{E(z)} = \frac{a_n z^n + a_{n-1} z^{n-1} + \dots + a_0}{z^n - b_{n-1} z^{n-1} - \dots - b_0} \quad (100.88)$$

For the closed-loop system of Fig. 100.38 the closed-loop z -domain transfer function is

$$M(z) = \frac{Y(z)}{R(z)} = \frac{G(z)D(z)}{1 + G(z)D(z)} \quad (100.89)$$

where $G(z)$ and $D(z)$ are specified above. The characteristic equation of the closed-loop system is

$$1 + G(z)D(z) = 0 \quad (100.90)$$

The dynamics and stability of the system can be assessed by the locations of the zeros of (100.90) (the closed-loop poles) in the complex z plane. For stability the zeros of (100.90) above must be restricted to the unit circle of the complex z plane.

A Linear Control Example

Consider the temperature control of a chemical mixing tank shown in Fig. 100.39. From a transient power balance the differential equation relating the rate of heat added $q(t)$ to the deviation in temperature from the ambient $\theta(t)$ is given as

$$\frac{d\theta}{dt} + \frac{1}{\tau} \theta = \frac{1}{mc} q(t) \quad (100.91)$$

where τ is the time constant of the process and mc is the heat capacity of the tank. The transfer function of the tank is

$$\frac{\Theta(s)}{Q(s)} = G(s) = \frac{1/mc}{s + 1/\tau} \quad (100.92)$$

The heater is driven by a D/A converter, and the temperature measurement is sampled with an A/D converter. The data converters are assumed to operate synchronously, so the discrete-time transfer function of the tank and the two data converters is from expression (100.87):

$$G(z) = \frac{\Theta(z)}{Q(z)} = \frac{\tau}{mc} \frac{1 - e^{-T/\tau}}{z - e^{-T/\tau}} \quad (100.93)$$

If a proportional control law is chosen, the transfer function associated with the control law is the gain $a_n = K$ or

$$D(z) = K \quad (100.94)$$

The closed-loop characteristic equation is from (100.90):

$$1 + \frac{K\tau}{mc} \frac{1 - e^{-T/\tau}}{z - e^{-T/\tau}} = 0 \quad (100.95)$$

If a common denominator is found, the resulting numerator is

$$z - e^{-T/\tau} + \frac{K\tau}{mc} (1 - e^{-T/\tau}) = 0 \quad (100.96)$$

The root of this equation is

$$z = e^{-T/\tau} + \frac{K\tau}{mc} (e^{-T/\tau} - 1) \quad (100.97)$$

If this root location is investigated as the gain parameter K is varied upward from zero, it is seen that the root starts at $z = e^{-T/\tau}$ for $K = 0$ and moves to the left along the real axis as K increases. Initially it is seen that the system becomes faster, but at some point the responses become damped and oscillatory, and as K is further increased the oscillatory tendency becomes less damped, and finally a value of K is reached where the oscillations are sustained at constant amplitude. A further increase in K will yield oscillations that increase with time. Typical unit step responses for $r(k) = 1$ and $T/\tau = 0.2$ are shown in Fig. 100.40.

It is easy to observe this tendency toward oscillation as K increases, but a problem that is clear from Fig. 100.40 is that in the steady state there is a persistent error between the response and the reference [$r(k) = 1$]. Increasing the gain K will make this error smaller at the expense of more oscillations. As a remedy for this steady-state error problem and control of the dynamics, a control law transfer function $D(z)$ will be sought that inserts integrator action into the loop while simultaneously canceling the pole of the plant. This dictates that the controller have a transfer function of the form

$$D(z) = \frac{U(z)}{E(z)} = \frac{K(z - e^{-T/\tau})}{z - 1} \quad (100.98)$$

Typical unit step responses are illustrated in Fig. 100.41 for several values of the gain parameter. The control law that must be programmed in the digital processor is

$$u(kT) = u((k - 1)T) + K[e(kT) - e^{-T/\tau}e((k - 1)T)] \quad (100.99)$$

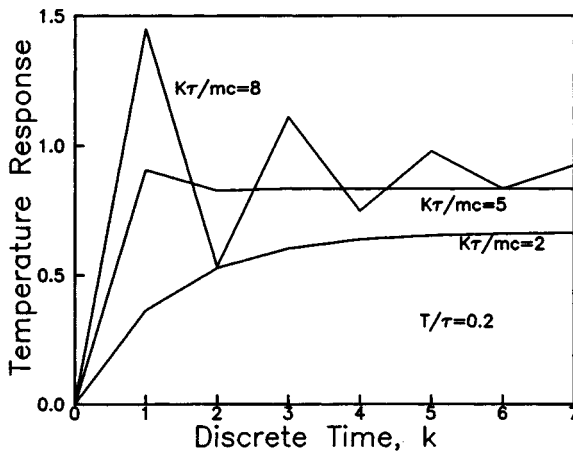


FIGURE 100.40 Step responses of proportionally controlled thermal mixing tank.

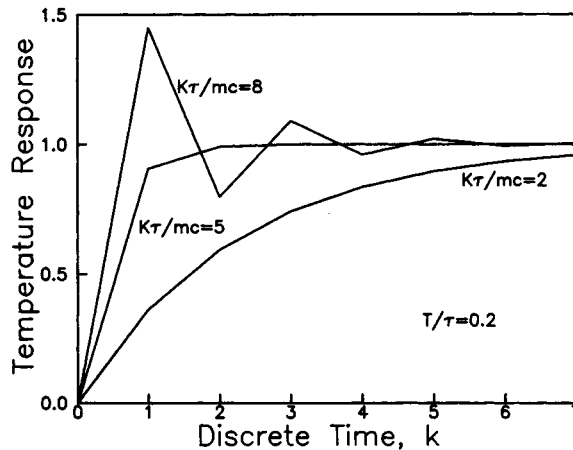


FIGURE 100.41 Step responses of the compensated thermal mixing tank.

The additional effort to program this over that required to program the proportional control law of (100.94) is easily justified since K and $e^{-T/\tau}$ are simply constants.

Defining Terms

Digital computer: A collection of digital devices including an arithmetic logic unit (ALU), read-only memory (ROM), random-access memory (RAM), and control and interface hardware.

Feedback control: The regulation of a response variable of a system in a desired manner using measurements of that variable in the generation of the strategy of manipulation of the controlling variables.

Related Topics

8.1 Introduction • 112.1 Introduction • 112.3 The State of the Art in CACSD

References

K.J. Astrom and B. Wittenmark, *Computer Controlled Systems: Theory and Design*, Englewood Cliffs, N.J.: Prentice-Hall, 1984.

- G.F. Franklin, J.D. Powell, and M.L. Workman, *Digital Control of Dynamic Systems*, 2nd ed., Reading, Mass.: Addison-Wesley, 1990.
- C.H. Houpis and G.B. Lamont, *Digital Control Systems: Theory, Hardware, Software*, 2nd ed., New York: McGraw-Hill, 1992.
- R.G. Jacquot, *Modern Digital Control Systems*, 2nd ed., New York: Marcel Dekker, 1995.
- B.C. Kuo, *Digital Control Systems*, 2nd ed., Orlando, Fla.: Saunders, 1992.
- C.L. Phillips and H.T. Nagle, *Digital Control System Analysis and Design*, 3rd ed., Englewood Cliffs, N.J.: Prentice-Hall, 1995.
- R. J. Vaccaro, *Digital: A State-Space Approach*, New York: McGraw-Hill, 1995.

Further Information

The *IEEE Control Systems Magazine* is a useful information source on control systems in general and digital control in particular. Highly technical articles on the state of the art in digital control may be found in the *IEEE Transactions on Automatic Control*, the *IEEE Transactions on Control Systems Technology*, and the ASME *Journal of Dynamic Systems, Measurement and Control*.

100.7 Nonlinear Control Systems³

Derek P. Atherton

The Describing Function Method

The describing function method, abbreviated as DF, was developed in several countries in the 1940s [Atherton, 1982], to answer the question: “What are the necessary and sufficient conditions for the nonlinear feedback system of Fig. 100.42 to be stable?” The problem still remains unanswered for a system with static nonlinearity, $n(x)$, and linear plant $G(s)$. All of the original investigators found limit cycles in control systems and observed that, in many instances with structures such as Fig. 100.42, the wave form of the oscillation at the input to the nonlinearity was almost sinusoidal. If, for example, the nonlinearity in Fig. 100.42 is an ideal relay, that is has an on-off characteristic, so that an odd symmetrical input wave form will produce a square wave at its output, the output of $G(s)$ will be almost sinusoidal when $G(s)$ is a low pass filter which attenuates the higher harmonics in the square wave much more than the fundamental. It was, therefore, proposed that the nonlinearity should be represented by its gain to a sinusoid and that the conditions for sustaining a sinusoidal limit cycle be evaluated to assess the stability of the feedback loop. Because of the nonlinearity, this gain in response to a sinusoid is a function of the amplitude of the sinusoid and is known as the describing function. Because describing function methods can be used other than for a single sinusoidal input, the technique is referred to as the single sinusoidal DF or sinusoidal DF.

The Sinusoidal Describing Function

For the reasons explained above, if we assume in Fig. 100.42 that $x(t) = a \cos \theta$, where $\theta = \omega t$ and $n(x)$ is a symmetrical odd nonlinearity, then the output $y(t)$ will be given by the Fourier series,

$$y(\theta) = \sum_{n=0}^{\infty} a_n \cos n\theta + b_n \sin n\theta, \quad (100.100)$$

$$\text{where } a_0 = 0, \quad (100.101)$$

³The material in this section was previously published by CRC Press in *The Control Handbook*, William S. Levine, Ed., 1996.

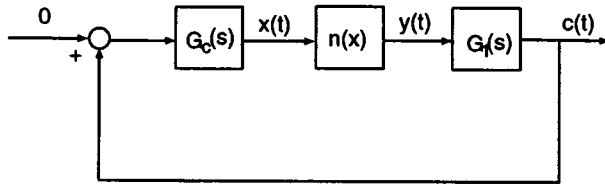


FIGURE 100.42 Block diagram of a nonlinear system.

$$a_1 = (1/\pi) \int_0^{2\pi} y(\theta) \cos \theta d\theta, \quad (100.102)$$

and

$$b_1 = (1/\pi) \int_0^{2\pi} y(\theta) \sin \theta d\theta. \quad (100.103)$$

The fundamental output from the nonlinearity is $a_1 \cos \theta + b_1 \sin \theta$, so that the describing function, DF, defined as the fundamental output divided by the input amplitude, is complex and given by

$$N(a) = (a_1 - jb_1)/a \quad (100.104)$$

which may be written

$$N(a) = N_p(a) + jN_q(a) \quad (100.105)$$

where

$$N_p(a) = a_1/a \text{ and } N_q(a) = -b_1/a. \quad (100.106)$$

Alternatively, in polar coordinates,

$$N(a) = M(a)e^{j\Psi(a)} \quad (100.107)$$

where

$$M(a) = (a_1^2 + b_1^2)^{1/2}/a$$

and

$$\Psi(a) = -\tan^{-1}(b_1/a_1). \quad (100.108)$$

If $n(x)$ is single valued, then $b_1 = 0$ and

$$a_1 = (4/\pi) \int_0^{\pi/2} y(\theta) \cos \theta d\theta \quad (100.109)$$

giving

$$N(a) = a_1/a = (4/a\pi) \int_0^{\pi/2} y(\theta) \cos \theta d\theta \quad (100.110)$$

Although Eqs. (100.102) and (100.103) are an obvious approach to evaluating the fundamental output of a nonlinearity, they are indirect, because one must first determine the output wave form $y(\theta)$ from the known nonlinear characteristic and sinusoidal input wave form. This is avoided if the substitution $\theta = \cos^{-1}(x/a)$ is made. After some simple manipulations,

$$a_1 = (4/a) \int_0^a x n_p(x) p(x) dx \quad (100.111)$$

and

$$b_1 = (4/a\pi) \int_0^a n_q(x) dx. \quad (100.112)$$

The function $p(x)$ is the amplitude probability density function of the input sinusoidal signal given by

$$p(x) = (1/\pi)(a^2 - x^2)^{-1/2}. \quad (100.113)$$

The nonlinear characteristics $n_p(x)$ and $n_q(x)$, called the inphase and quadrature nonlinearities, are defined by

$$n_p(x) = [n_1(x) + n_2(x)]/2 \quad (100.114)$$

and

$$n_q(x) = [n_2(x) - n_1(x)]/2 \quad (100.115)$$

where $n_1(x)$ and $n_2(x)$ are the portions of a double-valued characteristic traversed by the input for $\dot{x} > 0$ and $\dot{x} < 0$, respectively. When the nonlinear characteristic is single-valued, $n_1(x) = n_2(x)$, so $n_p(x) = n(x)$ and $n_q(x) = 0$. Integrating Eq. (100.111) by parts yields

$$a_1 = (4/\pi)n(0^+) + (4/a\pi) \int_0^a n'(x)(a^2 - x^2)^{1/2} dx \quad (100.116)$$

where $n'(x) = dn(x)/dx$ and $n(0^+) = \lim_{\epsilon \rightarrow 0} n(\epsilon)$, a useful alternative expression for evaluating a_1 .

An additional advantage of using Eqs. (100.111) and (100.112) is that they yield proofs of some properties of the DF for symmetrical odd nonlinearities. These include the following:

1. For a double-valued nonlinearity, the quadrature component $N_q(a)$ is proportional to the area of the nonlinearity loop, that is,

$$N_q(a) = -(1/a^2\pi)(\text{area of nonlinearity loop}) \quad (100.117)$$

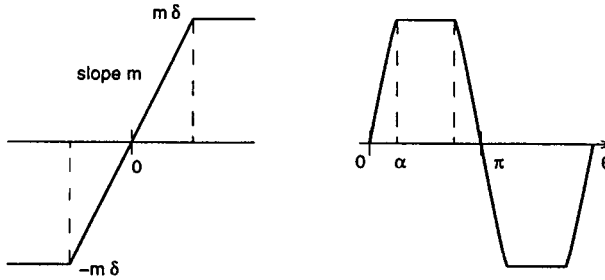


FIGURE 100.43 Saturation nonlinearity.

2. For two single-valued nonlinearities $n_\alpha(x)$ and $n_\beta(x)$, with $n_\alpha(x) < n_\beta(x)$ for all $0 < x < b$, $N_\alpha(a) < N_\beta(a)$ for input amplitudes less than b .
3. For a single-valued nonlinearity with $k_1 x < n(x) < k_2 x$ for all $0 < x < b$, $k_1 < N(a) < k_2$ for input amplitudes less than b . This is the sector property of the DF; a similar result can be obtained for a double-valued nonlinearity [Cook, 1973].

When the nonlinearity is single valued, from the properties of Fourier series, the DF, $N(a)$, may also be defined as:

1. the variable gain, K , having the same sinusoidal input as the nonlinearity, which minimizes the mean squared value of the error between the output from the nonlinearity and that from the variable gain, and
2. the covariance of the input sinusoid and the nonlinearity output divided by the variance of the input.

Evaluation of the Describing Function

To illustrate the evaluation of the DF two simple examples are considered.

Saturation Nonlinearity

To calculate the DF, the input can alternatively be taken as $a \sin \theta$. For an ideal saturation characteristic, the nonlinearity output wave form $y(\theta)$ is as shown in Fig. 100.43. Because of the symmetry of the nonlinearity, the fundamental of the output can be evaluated from the integral over a quarter period so that

$$N(a) = \frac{4}{a\pi} \int_0^{\pi/2} y(\theta) \sin \theta d\theta,$$

which, for $a > \delta$, gives

$$N(a) = \frac{4}{a\pi} \left[\int_0^\alpha ma \sin^2 \theta d\theta + \int_\alpha^{\pi/2} m\delta \sin \theta d\theta \right]$$

where $a = \sin^{-1} \delta/a$. Evaluation of the integrals gives

$$N(a) = (4m/\pi) \left[\frac{\alpha}{2} - \frac{\sin 2\alpha}{4} + \delta \cos \alpha \right]$$

which, on substituting for δ , give the result

$$N(a) = (m/\pi)(2\alpha + \sin 2\alpha). \quad (100.118)$$

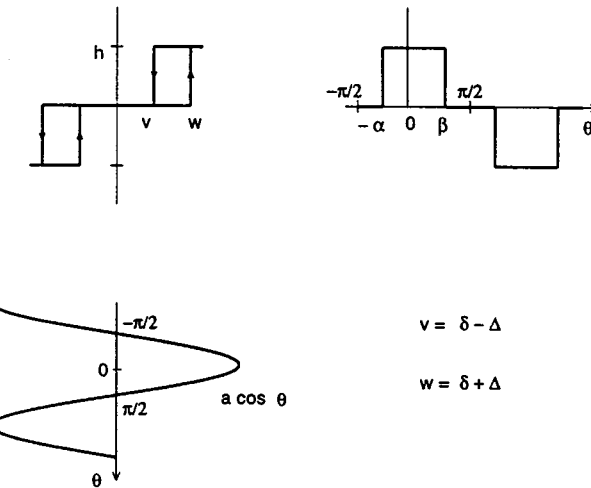


FIGURE 100.44 Relay with dead zone and hysteresis.

Because, for $a < \delta$, the characteristic is linear giving $N(a) = m$, the DF for ideal saturation is $mN_s(\delta/a)$ where

$$N_s(\delta/a) = \begin{cases} 1, & \text{for } a < \delta, \text{ and} \\ (1/\pi)[2\alpha + \sin 2\alpha], & \text{for } a > \delta, \end{cases} \quad (100.119)$$

where $a = \sin^{-1} \delta/a$.

Alternatively, one can evaluate $N(a)$ from Eq. (100.116), yielding

$$N(a) = a_1/a = (4/a^2 \pi) \int_0^\delta m(a^2 - x^2)^{1/2} dx.$$

Using the substitution $x = a \sin \theta$,

$$N(a) = (4m/\pi) \int_0^\alpha \cos^2 \theta d\theta = (m/\pi)(2\alpha + \sin 2\alpha)$$

as before.

Relay with Dead Zone and Hysteresis

The characteristic is shown in Fig. 100.44 together with the corresponding input, assumed equal to $a \cos \theta$, and the corresponding output wave form. Using Eqs. (100.102) and (100.103) over the interval $-\pi/2$ to $\pi/2$ and assuming that the input amplitude a is greater than $\delta + \Delta$,

$$\begin{aligned} a_1 &= \left(2/\pi \int_{-\alpha}^{\beta} h \cos \theta d\theta \right) \\ &= (2h/\pi)(\sin \beta + \sin \alpha), \end{aligned}$$

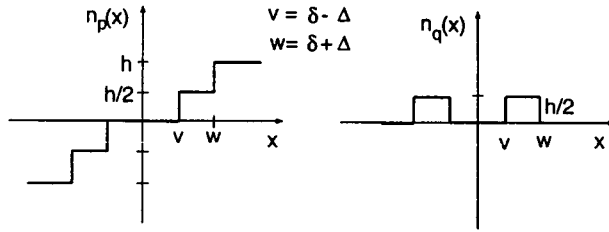


FIGURE 100.45 Function $n_p(x)$ and $n_q(x)$ for the relay of Figure 100.44.

where $\alpha = \cos^{-1}[(\delta - \Delta)/a]$ and $\beta = \cos^{-1}[(\delta + \Delta)/a]$, and

$$\begin{aligned} b_1 &= (2/\pi) \int_{-\alpha}^{\beta} h \sin \theta d\theta \\ &= (-2h/\pi) \left(\frac{(\delta + \Delta)}{a} - \frac{\delta - \Delta}{a} \right) = 4h\Delta/a\pi. \end{aligned}$$

Thus

$$N(a) = \frac{2h}{a^2\pi} \left\{ \left[a^2 - (\delta + \Delta)^2 \right]^{1/2} + \left[a^2 - (\delta - \Delta)^2 \right]^{1/2} \right\} - \frac{j4h\Delta}{a^2\pi}. \quad (100.120)$$

For the alternative approach, one must first obtain the in-phase and quadrature nonlinearities shown in Fig. 100.45. Using Eqs. (100.111) and (100.112),

$$\begin{aligned} a_1 &= (4/a) \int_{\delta-\Delta}^{\delta+\Delta} x(h/2)p(x)dx + \int_{\delta+\Delta}^a xhp(x)dx, \\ &= \frac{2h}{a\pi} \left\{ \left[a^2 - (\delta + \Delta)^2 \right]^{1/2} + \left[a^2 - (\delta - \Delta)^2 \right]^{1/2} \right\}, \end{aligned}$$

and

$$\begin{aligned} b_1 &= (4/a\pi) \int_{\delta-\Delta}^{\delta+\Delta} (h/2 dx) = 4h\Delta/a\pi \\ &= (\text{Area of nonlinearity loop})/a\pi \end{aligned}$$

as before.

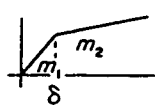
The DF of two nonlinearities in parallel equals the sum of their individual DFs, a result very useful for determining DFs, particularly of linear segmented characteristics with multiple break points. Several procedures [Altherton, 1982] are available for approximating the DF of a given nonlinearity either by numerical integration or by evaluating the DF of an approximating nonlinear characteristic defined, for example, by a quantized characteristic, linear segmented characteristic, or Fourier series. Table 100.3 gives a list of DFs for some commonly used approximations of nonlinear elements. Several of the results are in terms of the DF for an ideal saturation characteristic of unit slope, $N_s(\delta/a)$, defined in Eq. (100.119).

TABLE 100.3 DFs of Single-Valued Nonlinearities

General quantizer	$a < \delta_1$ $\delta_{M+1} > a > \delta_M$	$N_p = 0$ $N_p = \left(4/a^2\pi\right) \sum_{m=1}^M h_m (a^2 - \delta_m^2)^{1/2}$
Uniform quantizer $h_1 = h_2 = \dots = h$ $\delta_m = (2m-1)\delta/2$	$a < \delta$ $(2M+1)\delta > a > (2M-1)\delta$	$N_p = 0$ $N_p = \left(4h/a^2\pi\right) \sum_{m=1}^M (a^2 - n^2\delta^2)^{1/2}$
Relay with dead zone	$n = (2m-1)/2$ $a < \delta$ $a > \delta$	$N_p = 0$ $N_p = 4h(a^2 - \delta^2)^{1/2}/a^2\pi$
Ideal relay		$N_p = 4h/a\pi$
Preload		$N_p = (4h/a\pi) + m$
General piecewise linear	$a < \delta_1$ $\delta_{M+1} > \alpha > \delta_M$	$N_p = (4h/a\pi) + m_1$ $N_p = (4h/a\pi) + m_{M+1}$ $+ \sum_{i=1}^M (m_j - m_{j+1}) N_s(\delta_j/a)$
Ideal saturation		$N_p = m N_s(\delta/a)$
Dead zone		$N_p = m[1 - N_s(\delta/a)]$

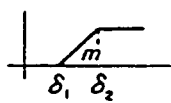
TABLE 100.3 (continued) DFs of Single-Valued Nonlinearities

Gain changing nonlinearity

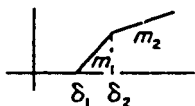


$$N_p = (m_1 - m_2)N_s(\delta/a) + m_2$$

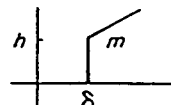
Saturation with dead zone



$$N_p = m[N_s(\delta_2/a) - N_s(\delta_1/a)]$$



$$N_p = -m_1 N_s(\delta_1/a) + (m_1 - m_2)N_s(\delta_2/a) + m_2$$

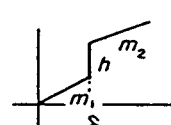


$$a < \delta$$

$$N_p = 0$$

$$a > \delta$$

$$N_p = 4h(a^2 - \delta^2)^{1/2}/a_2\pi + m - mN_s(\delta/a)$$

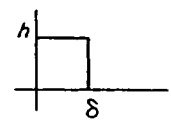


$$a < \delta$$

$$N_p = m_1$$

$$a > \delta$$

$$N_p = (m_1 - m_2)N_s(\delta/a) + m_2 + 4h(a^2 - \delta^2)^{1/2}/a^2\pi$$



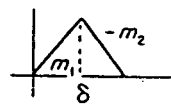
$$a < \delta$$

$$N_p = 4h/a\pi$$

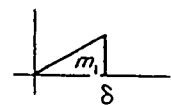
$$a > \delta$$

$$N_p = 4h/[a - (a^2 - \delta^2)^{1/2}]/a^2\pi$$

Limited field of view



$$N_p = (m_1 + m_2)N_s(\delta/a) - m_2N_s[(m_1 + m_2)\delta/m_2a]$$



$$a < \delta$$

$$N_p = m_1$$

$$a > \delta$$

$$N_p = m_1N_s(\delta/a) - 4m_1\delta(a^2 - \delta^2)^{1/2}/a^2\pi$$

$$y = x^m$$

$m > -2$ Γ is the gamma function

$$\begin{aligned} N_p &= \frac{\Gamma(m+1)a^{m-1}}{2^{m-1}\Gamma[(3+m)/2]\Gamma[(1+m)/2]} \\ &= \frac{2}{\sqrt{\pi}} \frac{\Gamma[(m+2)/2]a^{m-1}}{\Gamma[(m+3)/2]} \end{aligned}$$

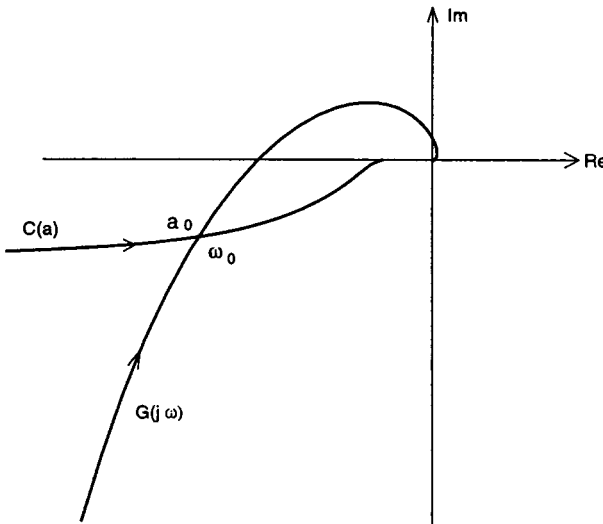


FIGURE 100.46 Nyquist plot showing solution for a limit cycle.

Limit Cycles and Stability

To investigate the possibility of limit cycles in the autonomous closed loop system of Fig. 100.42, the input to the nonlinearity $n(x)$ is assumed to be a sinusoid so that it can be replaced by the amplitude-dependent DF gain $N(a)$. The open loop gain to a sinusoid is thus $N(a)G(j\omega)$ and, therefore, a limit cycle exists if

$$N(a)G(j\omega) = -1 \quad (100.121)$$

where $G(j\omega) = G_c(j\omega)G_1(j\omega)$. As in general, $G(j\omega)$ is a complex function of ω and $N(a)$ is a complex function of a , solving Eq. (100.121) will yield both the frequency ω and amplitude a of a possible limit cycle.

A common procedure to examine solutions of Eq. (100.120) is to use a Nyquist diagram, where the $G(j\omega)$ and $C(a) = -1/N(a)$ loci are plotted as in Fig. 100.46, where they are shown intersecting for $a = a_0$ and $\omega = \omega_0$. The DF method indicates therefore that the system has a limit cycle with the input sinusoid to the nonlinearity, x , equal to $a_0 \sin(\omega_0 t + \phi)$, where ϕ depends on the initial conditions. When the $G(j\omega)$ and $C(a)$ loci do not intersect, the DF method predicts that no limit cycle will exist if the Nyquist stability criterion is satisfied for $G(j\omega)$ with respect to any point on the $C(a)$ locus. Obviously, if the nonlinearity has unit gain for small inputs, the point $(-1, j0)$ will lie on $C(a)$ and may be used as the critical point, analogous to a linear system.

For a stable case, it is possible to use the gain and phase margin to judge the relative stability of the system. However, a gain and phase margin can be found for every amplitude a on the $C(a)$ locus, so it is usually appropriate to use the minimum values of the quantities [Atherton, 1982]. When the nonlinear block includes dynamics so that its response is both amplitude and frequency dependent, that is $N(a, \omega)$, then a limit cycle will exist if

$$G(j\omega) = -1/N(a, \omega) = C(a, \omega). \quad (100.122)$$

To check for possible solutions of this equation, a family of $C(a, \omega)$ loci, usually as functions of a for fixed values of ω , is drawn on the Nyquist diagram.

An additional point of interest is whether when a solution to Eq. (100.120) exists the predicted limit cycle is stable. When there is only one intersection point, the stability of the limit cycle can be found using the Loeb criterion which states that if the Nyquist stability criterion indicates instability (stability) for the point on $C(a)$ with $a < a_0$ and stability (instability) for the point on $C(a)$ with $a > a_0$ the limit cycle is stable (unstable).

When multiple solutions exist, the situation is more complicated and the criterion above is a necessary but not sufficient result for the stability of the limit cycle [Choudhury and Atherton, 1974].

Normally in these cases, the stability of the limit cycle can be ascertained by examining the roots of the characteristic equation

$$1 + N_{iy}(a)G(s) = 0 \quad (100.123)$$

where $N_{iy}(a)$ is known as the incremental describing function (IDF). $N_{iy}(a)$ for a single valued nonlinearity can be evaluated from

$$N_{iy}(a) = \int_{-a}^a n'(x)p(x)dx \quad (100.124)$$

where $n'(x)$ and $p(x)$ are as previously defined. $N_{iy}(a)$ is related to $N(a)$ by the equation

$$N_{iy}(a) = N(a) + (a/2)dN(a)/da. \quad (100.125)$$

Thus, for example, for an ideal relay, making $\delta = \Delta = 0$ in Eq. (100.120) gives $N(a) = 4h/a\pi$, also found directly from Eq. (100.116), and, substituting this value in Eq. (100.125) yields $N_{iy}(a) = 2h/a\pi$. Some examples of feedback system analysis using the DF follow.

Autotuning in Process Control

In 1943 Ziegler and Nichols [1943] suggested a technique for tuning the parameters of a PID controller. Their method was based on testing the plant in a closed loop with the PID controller in the proportional mode. The proportional gain was increased until the loop started to oscillate and then the value of gain and the oscillation frequency were measured. Formulae were given for setting the controller parameters based on the gain named the critical gain, K_c , and the frequency called the critical frequency, ω_c .

Assuming that the plant has a linear transfer function $G_l(s)$, then K_c is its gain margin and ω_c the frequency at which its phase shift is 180° . Performing this test in practice may prove difficult. If the plant has a linear transfer function and the gain is adjusted too quickly, a large amplitude oscillation may start to build up. In 1984 Astrom and Hagglund [1984] suggested replacing the proportional control by a relay element to control the amplitude of the oscillation. Consider therefore the feedback loop of Fig. 100.42 with $n(x)$ an ideal relay, $G_c(s) = 1$, and the plant with a transfer function $G_l(s) = 10/(s + 1)^3$. The $C(a)$ locus, $-1/N(a) = -a\pi/4h$, and the Nyquist locus $G(j\omega)$ in Fig. 100.47 intersect. The values of a and ω at the intersection can be calculated from

$$-a\pi/4h = \frac{10}{(1 + j\omega)^3} \quad (100.126)$$

which can be written

$$\text{Arg}\left(\frac{10}{(1 + j\omega)^3}\right) = 180^\circ, \text{ and} \quad (100.127)$$

$$\frac{a\pi}{4h} = \frac{10}{(1 + \omega^2)^{3/2}}. \quad (100.128)$$

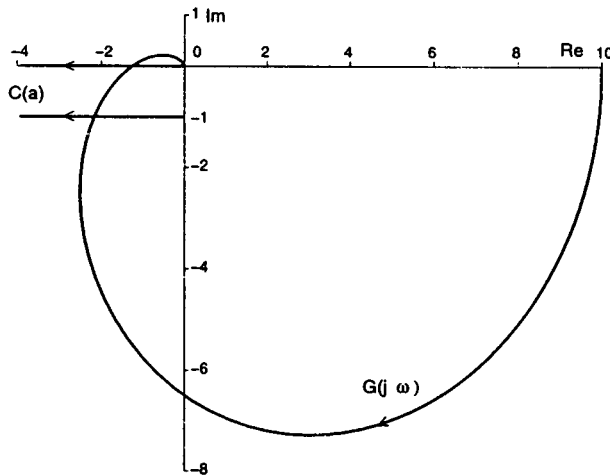


FIGURE 100.47 Nyquist plot $10/(s + 1)^3$ and $C(a)$ loci for $\Delta = 0$ and $4h/\pi$.

The solution for ω_c from Eq. (100.127) is $\tan^{-1} \omega_c = 60^\circ$, giving $\omega_c = \sqrt{3}$. Because the DF solution is approximate, the actual measured frequency of oscillation will differ from this value by an amount which will be smaller the closer the oscillation is to a sinusoid. The exact frequency of oscillation in this case will be 1.708 rads/sec in error by a relatively small amount. For a square wave input to the plant at this frequency, the plant output signal will be distorted by a small percentage. The distortion, d , is defined by

$$d = \left[\frac{\text{M.S. value of signal} - \text{M.S. value of fundamental harmonic}}{\text{M.S. value of fundamental harmonic}} \right]^{1/2} \quad (100.129)$$

Solving Eq. (100.128) gives the amplitude of oscillation a as $5h/\pi$. The gain through the relay is $N(a)$ equal to the critical gain K_c . In the practical situation where a is measured, K_c equal to $4h/a\pi$, should be close to the known value of 0.8 for this transfer function.

If the relay has an hysteresis Δ , then with $\delta = 0$ in Eq. (100.120) gives

$$N(a) = \frac{4h(a^2 - \Delta^2)^{1/2}}{a^2\pi} - j \frac{4h\Delta}{a^2\pi}$$

from which

$$C(a) = \frac{-1}{N(a)} = \frac{-\pi}{4h} \left[(a^2 - \Delta^2)^{1/2} + j\Delta \right].$$

Thus on the Nyquist plot, $C(a)$ is a line parallel to the real axis at a distance $\pi\Delta/4h$ below it, as shown in Fig. 100.47 for $\Delta = 1$ and $h = \pi/4$ giving $C(a) = -(a^2 - 1)^{1/2} - j$. If the same transfer function is used for the plant, then the limit cycle solution is given by

$$-(a^2 - 1)^{1/2} - j = \frac{10}{(1 + j\omega)^3} \quad (100.130)$$

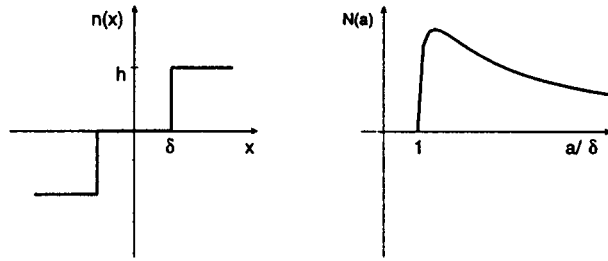


FIGURE 100.48 $N(a)$ for ideal relay with dead zone.

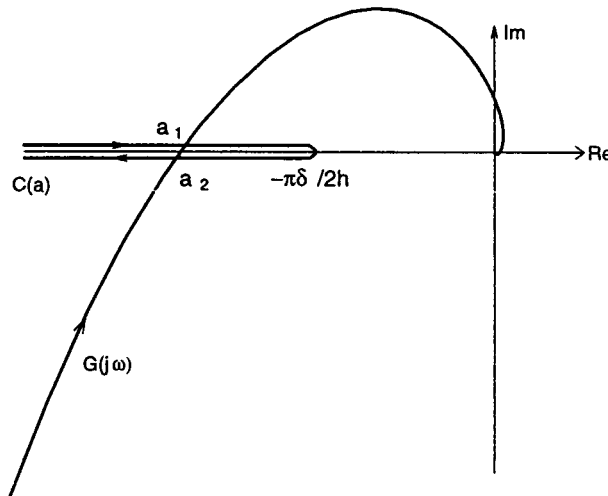


FIGURE 100.49 Two limit cycles: a_1 , unstable; a_2 , stable.

where $\omega = 1.266$, which compares with an exact solution value of 1.254, and $a = 1.91$. For the oscillation with the ideal relay, Eq. (100.123) with $N_{iy}(a) = 2h/\pi a$ shows that the limit cycle is stable. This agrees with the perturbation approach which also shows that the limit cycle is stable when the relay has hysteresis.

Feedback Loop with a Relay with Dead Zone

For this example the feedback loop of Fig. 100.42 is considered with $n(x)$ a relay with dead zone and $G(s) = 2/s(s + 1)^2$. From Equation 19.22 with $\Delta = 0$, the DF for this relay, given by

$$N(a) = 4h(a^2 - \delta^2)^{1/2} / a^2\pi \text{ for } a > \delta. \quad (100.131)$$

is real because the nonlinearity is single valued. A graph of $N(a)$ against a is in Fig. 100.48, and shows that $N(a)$ starts at zero, when $a = \delta$, increases to a maximum, with a value of $2h/\pi\delta$ at $a = \delta\sqrt{2}$, and then decreases toward zero for larger inputs. The $C(a)$ locus, shown in Fig. 100.49, lies on the negative real axis starting at $-\infty$ and returning there after reaching a maximum value of $-\pi\delta/2h$. The given transfer function $G(j\omega)$ crosses the negative real axis, as shown in Fig. 100.49, at a frequency of $\tan^{-1}\omega = 45^\circ$, that is, $\omega = 1$ rad/sec and, therefore, cuts the $C(a)$ locus twice. The two possible limit cycle amplitudes at this frequency can be found by solving

$$\frac{a^2\pi}{4h(a^2 - \delta^2)^{1/2}} = 1$$

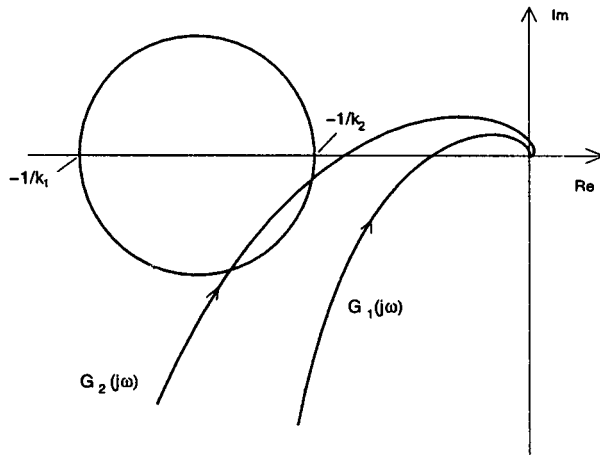


FIGURE 100.50 Circle criterion and stability.

which gives $a = 1.04$ and 3.86 for $\delta = 1$ and $h = \pi$. Using the perturbation method or the IDF criterion, the smallest amplitude limit cycle is unstable and the larger one is stable. If a condition similar to the lower amplitude limit cycle is excited in the system, an oscillation will build up and stabilize at the higher amplitude limit cycle.

Other techniques show that the exact frequencies of the limit cycles for the smaller and larger amplitudes are 0.709 and 0.989 , respectively. Although the transfer function is a good low pass filter, the frequency of the smallest amplitude limit cycle is not predicted accurately because the output from the relay, a wave form with narrow pulses, is highly distorted.

If the transfer function of $G(s)$ is $K/s(s + 1)^2$, then no limit cycle will exist in the feedback loop, and it will be stable if

$$\left. \frac{K}{\omega(1 + \omega^2)} \right|_{\omega=1} < \frac{\pi d}{2h},$$

that is, $K < \pi\delta/h$. If $\delta = 1$ and $h = \pi$, $K < 1$ which may be compared with the exact result for stability of $K < 0.96$.

Stability and Accuracy

Because the DF method is an approximate procedure, it is desirable to judge its accuracy. Predicting that a system will be stable, when in practice it is not, may have unfortunate consequences. Many attempts have been made to solve this problem, but those obtained are difficult to apply or produce too conservative results [Mess and Bergen, 1975].

The problem is illustrated by the system of Fig. 100.42 with a symmetrical odd single-valued nonlinearity confined to a sector between lines of slope k_1 and k_2 , that is, $k_1x < n(x) < k_2x$ for $x > 0$. For absolute stability, the circle criterion requires satisfying the Nyquist criterion for the locus $G(j\omega)$ for all points within a circle having its diameter on the negative real axis of the Nyquist diagram between the points $(-1/k_1, 0)$ and $(-1/k_2, 0)$, as shown in Fig. 100.50. On the other hand, because the DF for this nonlinearity lies within the diameter of the circle, the DF method requires satisfying the Nyquist criterion for $G(j\omega)$ for all points on the circle diameter, if the autonomous system is to be stable.

Therefore, for a limit cycle in the system of Fig. 100.42, errors in the DF method relate to its inability to predict a phase shift, which the fundamental harmonic may experience in passing through the nonlinearity, rather than an incorrect magnitude of the gain. When the input to a single-valued nonlinearity is a sinusoid together with some of its harmonics, the fundamental output is not necessarily in phase with the fundamental

input, that is, the fundamental gain has a phase shift. The actual phase shift varies with the harmonic content of the input signal in a complex manner, because the phase shift depends on the amplitudes and phases of the individual input components.

From an engineering viewpoint one can judge the accuracy of DF results by estimating the distortion, d , in the input to the nonlinearity. This is straightforward when a limit-cycle solution is given by the DF method; the loop may be considered opened at the nonlinearity input, the sinusoidal signal corresponding to the DF solution can be applied to the nonlinearity, and the harmonic content of the signal fed back to the nonlinearity input can be calculated. Experience indicates that the percentage accuracy of the DF method in predicting the fundamental amplitude and frequency of the limit cycle is less than the percentage distortion in the feedback signal. As mentioned previously, the DF method may incorrectly predict stability. To investigate this problem, the procedure above can be used again, by taking, as the nonlinearity input, a sinusoid with amplitude and frequency corresponding to values of those parameters where the phase margin is small. If the calculated feedback distortion is high, say greater than 2% per degree of phase margin, the DF result should not be relied on.

The limit-cycle amplitude predicted by the DF is an approximation to the fundamental harmonic. The accuracy of this prediction cannot be assessed by using the peak value of the limit cycle to estimate an equivalent sinusoid. It is possible to estimate the limit cycle more accurately by balancing more harmonics, as mentioned earlier. Although this is difficult algebraically other than with loops whose nonlinearity is mathematically simply described, for example a cubic, software is available for this purpose [McNamara and Atherton, 1987]. The procedure involves solving sets of nonlinear algebraic equations but good starting guesses can usually be obtained for the magnitudes and phases of the other harmonic components from the wave form feedback to the nonlinearity, assuming its input is the DF solution.

Compensator Design

Although the design specifications for a control system are often in terms of step-response behavior, frequency domain design methods rely on the premise that the correlation between the frequency and a step response yields a less oscillatory step response if the gain and phase margins are increased. Therefore the design of a suitable linear compensator for the system of Fig. 100.42 using the DF method, is usually done by selecting for example a lead network to provide adequate gain and phase margins for all amplitudes. This approach may be used in example 2 of the previous section where a phase lead network could be added to stabilize the system, say for a gain of 1.5, for which it is unstable without compensation. Other approaches are the use of additional feedback signals or modification of the nonlinearity $n(x)$ directly or indirectly [Atherton, 1982; Gelb and van der Velde, 1968].

When the plant is nonlinear, its frequency response also depends on the input sinusoidal amplitude represented as $G(j\omega, a)$. In recent years several approaches [Nanka-Bruce and Atherton, 1990; Taylor and Strobel, 1984] use the DF method to design a nonlinear compensator for the plant, with the objective of closed-loop performance independent of the input amplitude.

Closed-Loop Frequency Response

When the closed-loop system of Fig. 100.42 has a sinusoidal input $r(t) = R \sin(\omega t + \theta)$, it is possible to evaluate the closed-loop frequency response using the DF. If the feedback loop has no limit cycle when $r(t) = 0$ and, in addition, the sinusoidal input $r(t)$ does not induce a limit cycle, then, provided that $G_c(s)G_1(s)$ gives good filtering, $x(t)$, the nonlinearity input, almost equals the sinusoid $a \sin \omega t$. Balancing the components of frequency ω around the loop,

$$\begin{aligned} g_c R \sin(\omega t + \theta - \phi_c) - ag_1 g_c M(a) \\ \sin[\omega t + \phi_1 + \phi_c + \psi(a)] = a \sin \omega t \end{aligned} \quad (100.132)$$

where $G_c(j\omega) = g_c e^{j\phi_c}$ and $G_1(j\omega) = g_1 e^{j\phi_1}$. In principle Eq. (100.132), which can be written as two nonlinear algebraic equations, can be solved for the two unknowns a and θ and the fundamental output signal can then be found from

$$c(t) = aM(a)g_1 \sin[\omega t + \psi(a) + \phi_1] \quad (100.133)$$

to obtain the closed-loop frequency for R and ω .

Various graphical procedures have been proposed for solving the two nonlinear algebraic equations resulting from Eq. (100.132) [Levinson, 1953; Singh, 1965; West and Douce, 1954]. If the system is lightly damped, the nonlinear equations may have more than one solution, indicating that the frequency response of the system has a jump resonance. This phenomenon of a nonlinear system has been studied by many authors, both theoretically and practically [Lamba and Kavanagh, 1971; West et al., 1954].

The Phase Plane Method

The phase plane method was the first method used by control engineers for studying the effects of nonlinearity in feedback systems. The technique which can only be used for systems with second order models was examined and further developed for control engineering purposes for several major reasons,

1. The phase plane approach has been used for several studies of second order nonlinear differential equations arising in fields such as planetary motion, nonlinear mechanics and oscillations in vacuum tube circuits.
2. Many of the control systems of interest, such as servomechanisms, could be approximated by second order nonlinear differential equations.
3. The phase plane was particularly appropriate for dealing with nonlinearities with linear segmented characteristics which were good approximations for the nonlinear phenomena encountered in control systems.

The next section considers the basic aspects of the phase plane approach but later concentration is focused on control engineering applications where the nonlinear effects are approximated by linear segmented nonlinearities.

Background

Early analytical work [Andronov et al., 1966], on second order models assumed the equations

$$\begin{aligned} \dot{x}_1 &= P(x_1, x_2) \\ \dot{x}_2 &= Q(x_1, x_2) \end{aligned} \quad (100.134)$$

for two first-order nonlinear differential equations. Equilibrium, or singular points, occur when

$$\dot{x}_1 = \dot{x}_2 = 0$$

and the slope of any solution curve, or trajectory, in the $x_1 - x_2$ state plane is

$$\frac{dx_2}{dx_1} = \frac{\dot{x}_2}{\dot{x}_1} = \frac{Q(x_1, x_2)}{P(x_1, x_2)} \quad (100.135)$$

A second order nonlinear differential equation representing a control system can be written

$$\ddot{x} + f(x, \dot{x}) = 0 \quad (100.136)$$

If this is rearranged as two first-order equations, choosing the phase variables as the state variables, that is $x_1 = x$, $x_2 = \dot{x}$, then Eq. (100.136) can be written as

$$\dot{x}_1 = \dot{x}_2 \quad \dot{x}_2 = -f(x_1, x_2) \quad (100.137)$$

which is a special case of Eq. (100.135). A variety of procedures has been proposed for sketching state [phase] plane trajectories for Eqs. (100.135) and (100.137). A complete plot showing trajectory motions throughout the entire state (phase) plane is known as a state (phase) portrait. Knowledge of these methods, despite the improvements in computation since they were originally proposed, can be particularly helpful for obtaining an appreciation of the system behavior. When simulation studies are undertaken, phase plane graphs are easily obtained and they are often more helpful for understanding the system behavior than displays of the variables x_1 and x_2 against time.

Many investigations using the phase plane technique were concerned with the possibility of limit cycles in the nonlinear differential equations. When a limit cycle exists, this results in a closed trajectory in the phase plane. Typical of such investigations was the work of Van der Pol, who considered the equation

$$\ddot{x} - \mu(1 - x^2)\dot{x} + x = 0 \quad (100.138)$$

where μ is a positive constant. The phase plane form of this equation can be written as

$$\begin{aligned} \dot{x}_1 &= x_2 \\ \dot{x}_2 &= -f(x_1, x_2) = \mu(1 - x_1^2)x_2 - x_1 \end{aligned} \quad (100.139)$$

The slope of a trajectory in the phase plane is

$$\frac{dx_2}{dx_1} = \frac{\dot{x}_2}{\dot{x}_1} = \frac{\mu(1 - x_1^2)x_2 - x_1}{x_2} \quad (100.140)$$

and this is only singular (that is, at an equilibrium point), when the right hand side of Eq. (100.140) is 0/0, that is $x_1 = x_2 = 0$.

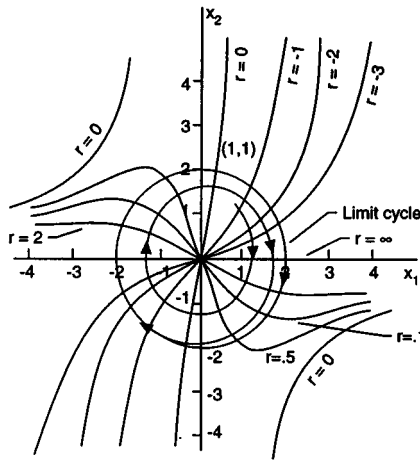
The form of this singular point which is obtained from linearization of the equation at the origin depends upon μ , being an unstable focus for $\mu < 2$ and an unstable node for $\mu > 2$. All phase plane trajectories have a slope of r when they intersect the curve

$$rx_2 = \mu(1 - x_1^2)x_2 - x_1 \quad (100.141)$$

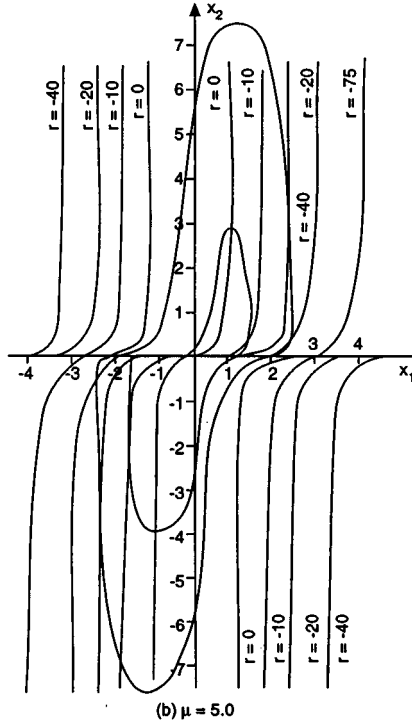
One way of sketching phase plane behavior is to draw a set of curves given for various values of r by Eq. (100.141) and marking the trajectory slope r on the curves. This procedure is known as the method of isoclines and has been used to obtain the limit cycles shown in Fig. 100.51 for the Van der Pol equation with $\mu = 0.2$ and 4.

Piecewise Linear Characteristics

When the nonlinear elements occurring in a second order model can be approximated by linear segmented characteristics then the phase plane approach is usually easy to use because the nonlinearities divide the phase



(a) $\mu = 0.2$



(b) $\mu = 5.0$

FIGURE 100.51 Phase portraits of the Van der Pol equation for different values, of μ .

plane into various regions within which the motion may be described by different linear second-order equations [Atherton, 1982]. The procedure is illustrated by the simple relay system in Fig. 100.52.

The block diagram represents an “ideal” relay position control system with velocity feedback. The plant is a double integrator, ignoring viscous (linear) friction, hysteresis in the relay, or backlash in the gearing. If the system output is denoted by x_1 and its derivative by x_2 , then the relay switches when $-x_1 - x_2 = \pm 1$; the equations of the dotted lines are marked switching lines on Fig. 100.53.

Because the relay output provides constant values of ± 2 and 0 to the double integrator plant, if we denote the constant value by h , then the state equations for the motion are

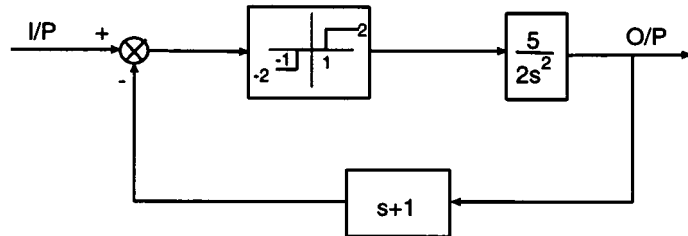


FIGURE 100.52 Relay system.

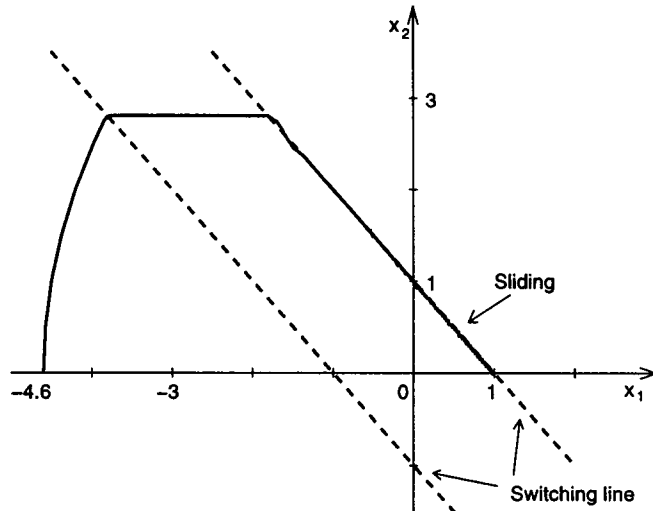


FIGURE 100.53 Phase plane for relay system.

$$\begin{aligned}\dot{x}_1 &= x_2 \\ \dot{x}_2 &= h\end{aligned}\tag{100.142}$$

which can be solved to give the phase plane equation

$$x_2^2 - x_{20}^2 = 2h(x_1 - x_{10})\tag{100.143}$$

which is a parabola for h finite and the straight line $x_2 = x_{20}$ for $h = 0$, where x_{20} and x_{10} are the initial values of x_2 and x_1 . Similarly, more complex equations can be derived for other second-order transfer functions. Using Eq. (100.143) with the appropriate values of h for the three regions in the phase plane, the step response for an input of 4.6 units can be obtained as shown in Fig. 100.53.

In the step response, when the trajectory meets the switching line $x_1 + x_2 = -1$ for the second time, trajectory motions at both sides of the line are directed towards it, resulting in a sliding motion down the switching line. Completing the phase portrait by drawing responses from other initial conditions shows that the autonomous system is stable and also that all responses will finally slide down a switching line to equilibrium at $x_1 = \pm 1$.

An advantage of the phase plane method is that it can be used for systems with more than one nonlinearity and for those situations where parameters change as functions of the phase variables. For example, Fig. 100.54 shows the block diagram of an approximate model of a servomechanism with nonlinear effects due to torque saturation and Coulomb friction.

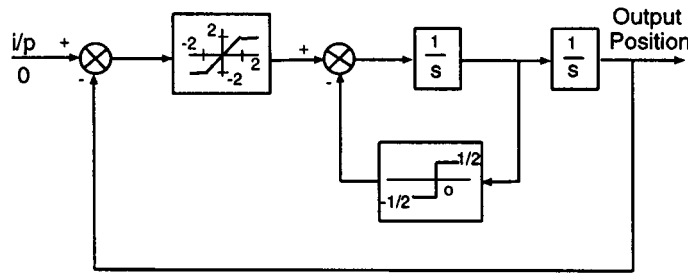


FIGURE 100.54 Block diagram of servomechanism.

The differential equation of motion in phase variable form is

$$\dot{x}_2 = f_s(-x_1) - (1/2) \operatorname{sgn} x_2 \quad (100.144)$$

where f_s denotes the saturation nonlinearity and sgn the signum function, which is +1 for $x_2 > 0$ and -1 for $x_2 < 0$. There are six linear differential equations describing the motion in different regions of the phase plane. For x_2 positive, Eq. (100.144) can be written

$$\dot{x}_1 + f_s(x_1) + 1/2 = 0$$

so that for

- (a) x_2 +ve, $x_1 < -2$, we have $\dot{x}_1 = x_2$, $\dot{x}_2 = 3/2$, a parabola in the phase plane.
- (b) x_2 +ve, $|x_1| < 2$, we have $\dot{x}_1 = x_2$, $\dot{x}_2 + x_1 + 1/2 = 0$.
- (c) x_2 +ve, $x_1 > 2$, we have $\dot{x}_1 = x_2$, $\dot{x}_2 = -5/2$, a parabola in the phase plane. Similarly for x_2 negative,
- (d) x_2 -ve, $x_1 < -2$, we have $\dot{x}_1 = x_2$, $\dot{x}_2 = -5/2$, a parabola in the phase plane.
- (e) x_2 -ve, $|x_2| < 2$, we have $\dot{x}_1 = x_2$, $\dot{x}_2 + x_1 - 1/2 = 0$, a circle in the phase plane.
- (f) x_2 -ve, $x_1 > 2$, we have $\dot{x}_1 = x_2$, $\dot{x}_2 = -3/2$, a parabola in the phase plane.

Because all the phase plane trajectories are described by simple mathematical expressions, it is straightforward to calculate specific phase plane trajectories.

Discussion

The phase plane approach is useful for understanding the effects of nonlinearity in second order systems, particularly if it may be approximated by a linear segmented characteristic. Solutions for the trajectories with other nonlinear characteristics may not be possible analytically so that approximate sketching techniques were used in early work on nonlinear control. These approaches are described in many books, for example, [Blaquiere, 1966; Cosgriff, 1958; Cunningham, 1958; Gibson, 1963; Graham and McRuer, 1961; Hayashi, 1964, Thaler and Pastel, 1962; West, 1960]. Although the trajectories are now easily obtained with modern simulation techniques, knowledge of the topological aspects of the phase plane are still useful for interpreting the responses in different regions of the phase plane and appreciating the system behavior.

Related Topics

5.2 Limiters • 12.1 Introduction • 12.3 Lyapunov Stability Theory

References

A.A. Andronov, A.A. Vitt, and S.E. Khaikin, *Theory of Oscillators*, Reading, Mass.: Addison-Wesley, 1966. (First edition published in Russia in 1937.)

- K.J. Astrom, and T. Haggland, *Automatic tuning of single regulators*, Budapest: Proc IFAC Congress, Vol. 4, 267–272, 1984.
- D.P. Atherton, *Nonlinear Control Engineering, Describing Function Analysis and Design*, London: Van Nostrand Reinhold, 1975.
- D.P. Atherton, *Non Linear Control Engineering*, Student Ed., New York: Van Nostrand Reinhold, 1982.
- A. Blaquiere, *Nonlinear Systems Analysis*, New York: Academic Press, 1966.
- S.K. Choudhury, and D.P. Atherton, “Limit cycles in high order nonlinear systems,” *Proc. Inst. Electr. Eng.*, 121, 717–724, 1974.
- P.A. Cook, “Describing function for a sector nonlinearity,” *Proc. Inst. Electr. Eng.*, 120, 143–144, 1973.
- R. Cosgriff, *Nonlinear Control Systems*, New York: McGraw-Hill, 1958.
- W.J. Cunningham, *Introduction to Nonlinear Analysis*, New York: McGraw-Hill, 1958.
- A. Gelb and W.E. van der Velde, *Multiple Input Describing Functions and Nonlinear Systems Design*, New York: McGraw-Hill, 1968.
- J.E. Gibson, *Nonlinear Automatic Control*, New York: McGraw-Hill, 1963.
- D. Graham and D. McRuer, *Analysis of Nonlinear Control Systems*, New York: John Wiley & Sons, 1961.
- C. Hayashi, *Nonlinear Oscillations in Physical Systems*, New York, McGraw-Hill, 1964.
- S.S. Lamba and R.J. Kavanagh, “The phenomenon of isolated jump resonance and its application,” *Proc. Inst. Electr. Eng.*, 118, 1047–1050, 1971.
- E. Levinson, “Some saturation phenomena in servomechanisms with emphasis on the tachometer stabilised system,” *Trans. Am. Inst. Electr. Eng.*, Part 2, 72, 1–9, 1953.
- O.P. McNamara, and D.P. Atherton, “Limit cycle prediction in free structured nonlinear systems,” *IFAC Congress*, Munich, 8, 23–28, July 1987.
- A.I. Mees and A.R. Bergen, “Describing function revisited,” *IEEE Trans. Autom. Control*, 20, 473–478, 1975.
- O. Nanka-Bruce and D.P. Atherton, “Design of nonlinear controllers for nonlinear plants,” *IFAC Congress*, Tallinn, 6, 75–80, 1990.
- T.P. Singh, “Graphical method for finding the closed loop frequency response of nonlinear feedback control systems,” *Proc. Inst. Electr. Eng.*, 112, 2167–2170, 1965.
- J.H. Taylor and K.L. Strobel, “Applications of a nonlinear controller design approach based on the quasilinear system models,” *Prof ACC*, San Diego, 817–824, 1984.
- G.J. Thaler and M.P. Pastel, *Analysis and Design of Nonlinear Feedback Control Systems*, New York: McGraw-Hill, 1962.
- J.C. West, *Analytical Techniques of Nonlinear Control Systems*, London: E.U.P., 1960.
- J.C. West and J.L. Douce, “The frequency response of a certain class of nonlinear feedback systems,” *Br. J. Appl. Phys.*, 5, 201–210, 1954.
- J.C. West, B.W. Jayawant, and D.P. Rea, “Transition characteristics of the jump phenomenon in nonlinear resonant circuits,” *Proc. Inst. Electr. Eng.*, 114, 381–392, 1967.
- J.G. Ziegler and N.B. Nichols, “Optimal setting for automatic controllers,” *Trans. ASME*, 65, 433–444, 1943.

Further Information

Many control engineering text books contain material on nonlinear systems where the describing function is discussed. The coverage, however, is usually restricted to the basic sinusoidal DF for determining limit cycles in feedback systems. The basic DF method, which is one of quasilinearisation, can be extended to cover other signals, such as random signals, and also to cover multiple input signals to nonlinearities and feedback system analysis. The two books with the most comprehensive coverage of this are Gelb and Van der Velde [1968] and Atherton [1975]. More specialized books on nonlinear feedback systems usually cover the phase plane method and the DF together with other topics such as absolute stability, exact linearization, etc.

100.8 Optimal Control and Estimation

John S. Bay and William T. Baumann

Consider the closed-loop feedback control of linear time-invariant, multi-input/multi-output (MIMO) state-space systems of the form:

$$\begin{aligned}\dot{x}(t) &= Ax(t) + Bu(t) \\ y(t) &= Cx(t) + Du(t)\end{aligned}\tag{100.145}$$

In this form, the vector $x \in \mathbb{R}^n$ represents the internal state, $u \in \mathbb{R}^p$ represents the input, and $y \in \mathbb{R}^q$ represents the measured outputs. It is well known that if the system in Eq. (100.145) is *stabilizable* (i.e., its unstable part is **controllable**), then it can be asymptotically stabilized with static state feedback. If it is **detectable** (i.e., its unstable part is **observable**), then a state estimator can be found, whose state variables asymptotically approach the true state variables in Eq. (100.145). However, merely determining the state feedback gain or observer gain leaves considerable design freedom for satisfying criteria other than stabilization and asymptotic observation. In this chapter section, we will provide results of some basic techniques of optimal control and estimation, which provide a mechanism to find *optimal* feedback and **observer (estimator)** gains according to selected optimality criteria.

Linear Quadratic Regulators

The linear quadratic regulator (LQR) problem is to find an *optimal* control input $u^*(t)$ that minimizes the performance criterion

$$J(x, u) = \frac{1}{2} x^T(t_f) S x(t_f) + \frac{1}{2} \int_{t_0}^{t_f} [x(t)^T Q x(t) + u^T(t)^T R u(t)] dt\tag{100.146}$$

where S and Q are symmetric, **positive-semidefinite** weighting matrices; and R is a symmetric, **positive-definite** weighting matrix. In this criterion, the term $\frac{1}{2} x^T(t_f) S x(t_f)$ represents a penalty for the state at the final time t_f being different from zero. The term inside the integral, $x^T(t) Q x(t)$, represents a penalty on the transient response of the state vector. The term $u^T(t)^T R u(t)$ represents a penalty on the size of the control input $u(t)$. We allow S and Q to be positive-semidefinite because we can generally tolerate unbounded state variables, provided they are not observed at the output. However, by forcing R to be positive-definite, we can guarantee that the process of minimizing Eq. (100.146) gives a bounded input. Minimization of this control energy is one of the primary reasons for using optimal control.

The optimal control $u^*(t)$ can be found via a number of techniques, including dynamic programming [Bay, 1999] and variational techniques [Kirk, 1970]. The result of any of these methods is that the optimal control $u^*(t)$ is a linear function of the state vector (linear state feedback) of the form:

$$u^*(t) = -R^{-1}B^T P(t)x(t)\tag{100.147}$$

where the $n \times n$ matrix function $P(t)$ satisfies the following equation:

$$\dot{P} = PBR^{-1}B^T P - Q - PA - A^T P\tag{100.148}$$

Equation (100.148) is known as the differential matrix Riccati equation, and it is solved in backward time, with the end-time condition $P(t_f) = S$.

It may be noted that a reasonable optimization criterion may have no finite final time t_f . Instead, it may be desired that the controller be continually active, implying $t_f \rightarrow \infty$ and eliminating the possibility of the final state term in Eq. (100.146). In this case, the optimization criterion is more properly written as

$$J(x, u) = \frac{1}{2} \int_{t_0}^{\infty} [x^T(t) Q x(t) + u^T(t) R u(t)] dt \quad (100.149)$$

Fortunately, this criterion simplifies the optimal control solution to the steady-state solution of the finite-time problem. That is, for the criterion of Eq. (100.149), the optimal control is

$$u^*(t) = -R^{-1}B^T P x(t) \quad (100.150)$$

where in this case P is the matrix solution to the following algebraic Riccati equation:

$$0 = PBR^{-1}B^T P - Q - PA - A^T P \quad (100.151)$$

Such a steady-state optimal solution exists whenever the system (A, B) is stabilizable. Furthermore, this constant P is the unique positive-definite solution of Eq. (100.151) if and only if the pair (A, T) is detectable, where T is defined as the square-root of Q , $Q = T^T T$. **Stabilizability** of (A, B) ensures convergence of the cost criterion integral Eq. (100.149), and detectability of (A, T) guarantees that no unstable part of $x(t)$ escapes integration as part of the integrand of Eq. (100.149).

We should point out also that for the corresponding discrete-time system:

$$\begin{aligned} x(k+1) &= Ax(k) + Bu(k) \\ y(k) &= Cx(k) + Du(k) \end{aligned} \quad (100.152)$$

minimization of the cost criterion:

$$J = \frac{1}{2} \sum_{k=k_0}^{\infty} [x^T(k) Q x(k) + u^T(k) R u(k)] \quad (100.153)$$

over all inputs $u(k)$ results in the optimal control

$$u^*(k) = -[R + B^T S B]^{-1} B^T S A x(k) \quad (100.154)$$

where S is the solution to the corresponding discrete-time algebraic Riccati equation:

$$S = A^T S A - A^T S B [R + B^T S B]^{-1} B^T S A + Q \quad (100.155)$$

Note that in both the continuous- and the discrete-time infinite-horizon cases, the optimal control is actually static state feedback of the form $u = Kx$.

Optimal Estimation: The Kalman Filter

It was noted above that the optimal controller for the linear quadratic cost criterion takes the form of full-state feedback. However, it is often the case that the full state is not physically available for feedback. Rather, it is usually the *output* that is measurable, so that we prefer a technique that uses $y(t)$ (and possibly $u(t)$) to construct the control signal instead of the state $x(t)$.

The simple solution to this problem is to design an *observer (or estimator)*, which produces an *estimated* state vector $\hat{x}(t)$. If this estimate asymptotically approaches the true state $x(t)$, then we can simply combine the observer and the state feedback to produce a feedback control $u(t) = K\hat{x}(t)$. That we can simply substitute the observed value $\hat{x}(t)$ for $x(t)$ in the feedback function is a fortunate property called the separation principle, which ensures that our controller calculations and observer calculations do not interfere with one another.

Just as we have improved static state feedback by introducing the optimal LQR above, we can take the principles of observer design and extend them with some guarantees of optimality. Such an optimal estimator is the Kalman filter.

The Kalman filter is derived assuming the system model:

$$\begin{aligned}\dot{\hat{x}}(t) &= Ax(t) + Bu(t) + Gv(t) \\ y(t) &= Cx(t) + w(t)\end{aligned}\tag{100.156}$$

where $v(t)$ and $w(t)$ are two white, Gaussian, zero-mean, mutually uncorrelated noise signals with $E[w(t)v^T(\tau)] = 0$ and

$$E[v(t)] = 0, \quad E[v(t)v^T(\tau)] = V\delta(t - \tau)\tag{100.157}$$

and

$$E[w(t)] = 0, \quad E[w(t)w^T(\tau)] = W\delta(t - \tau)\tag{100.158}$$

where $\delta(t)$ is the Dirac delta. Noise $v(t)$ is called the *plant noise*, and $w(t)$ is the *measurement noise*, often representing sensor noise. (By assuming these signals are first passed through auxiliary filters with specified dynamics, these noises can be made to resemble harmonic or narrow-band disturbances.)

The goal is now to design a system that produces an estimated state $\hat{x}(t)$ for Eq. (100.156) while rejecting the influence of the signals $v(t)$ and $w(t)$. To do this, we need the further assumptions that the system's initial state is guessed to be $x(t_0) = x_0$ and that this guess is uncorrelated with the plant and measurement noise:

$$E[x_0 v^T(\tau)] = 0 \quad E[x_0 w^T(\tau)] = 0\tag{100.159}$$

The covariance of the initial guess is defined as

$$E\left\{ [x_0 - E(x_0)][x_0 - E(x_0)]^T \right\} \triangleq P_0\tag{100.160}$$

The Kalman filter is the system that performs this estimation, rejecting the influence of the noise. The filter itself is given by the equation:

$$\dot{\hat{x}}(t) = A\hat{x}(t) + Bu(t) + L(t)[y(t) - C\hat{x}(t)]\tag{100.161}$$

which can be seen to resemble the standard full-order observer [Bay, 1999]. However, rather than choosing an observer gain L in Eq. (100.161) to simply stabilize the error dynamics of the observer, the *Kalman gain* $L(t)$ is

$$L(t) = P(t)C^T W^{-1} \quad (100.162)$$

where $P(t)$ is the solution to the following differential Riccati equation:

$$\dot{P}(t) = AP(t) + P(t)A^T - P(t)C^T W^{-1} C P(t) + G V G^T \quad (100.163)$$

whose initial condition is $P(t_0) = P_0$.

For the discrete-time system

$$\begin{aligned} x(k+1) &= Ax(k) + Bu(k) + Gv(k) \\ y(k) &= Cx(k) + w(k) \end{aligned} \quad (100.164)$$

with assumptions analogous to Eq. (100.157) through (100.158) for plant noise $v(k)$ and measurement noise $w(t)$, and with $E[(x_0 - E(x_0))(x_0 - E(x_0))^T] \triangleq S_0$, the Kalman filter is given by the two-stage estimator

$$\bar{x}(k+1) = A\hat{x}(k) + Bu(k) \quad (100.165)$$

$$\hat{x}(k+1) = \bar{x}(k+1) + L(k+1)[y(k+1) - C\bar{x}(k+1)] \quad (100.166)$$

where the Kalman gain $L(k+1)$ is computed from the equation

$$L(k+1) = [AS(k)A^T + GVG^T]C^T \left\{ C[AS(k)A^T + GVG^T]C^T + W \right\}^{-1} \quad (100.167)$$

In Eq. (100.167), the term $S(k)$ is determined from the Riccati equation:

$$\begin{aligned} S(k+1) &= [I - L(k+1)C][AS(k)A^T + GVG^T][I - L(k+1)C]^T \\ &\quad + L(k+1)WL^T(k+1) \end{aligned} \quad (100.168)$$

with initial condition $S(k_0) = S_0$. (Note that these equations can be combined and rearranged to produce a number of alternate formulations.)

Equation (100.165) is often referred to as the *time update* equation. It represents the estimate of the state vector that results from knowledge of the system dynamics. Equation (100.166) is sometimes called the *measurement* update equation because it revises the time update with a so-called *innovations* term $L(y - \bar{y})$ that adjusts this time update according to the error between the output expected from the time update, $y(k+1)$, and the actual, measured output, $\bar{y}(k+1)$.

The matrices $P(t)$ in the continuous-time filter, and $S(k)$ in the discrete-time filter are the error covariance matrices for the state estimate. That is,

$$S(k) \triangleq E[e(k)e^T(k)] \quad \text{and} \quad P(t) \triangleq E[e(t)e^T(t)] \quad (100.169)$$

where $e(k) \triangleq x(k) - \hat{x}(k)$ and $e(t) \triangleq x(t) - \hat{x}(t)$. Thus, the size of these matrices is an indicator of the error variance in various components in the estimates, and it can be seen in Eq. (100.161) and (100.167) that as these covariances decrease, the estimators rely less and less on the innovations term and more on the system dynamics for an accurate estimate. Early in the estimation process, the situation is usually reversed, with the innovations having the larger effect.

Linear-Quadratic-Gaussian (LQG) Control

It can be shown that the Kalman filter is the *optimal* estimator for the state of system Eq. (100.156) or (100.164) in the sense that it minimizes the squared error due to the noise input terms. Therefore, it becomes a likely candidate for combination with the LQR of the previous section. Together, the combination of LQR and Kalman filter is known as the LQG (linear-quadratic-Gaussian) controller, and is a useful controller in many situations. This controller is optimal in the sense that it minimizes the expected root-mean-square value of the optimization criterion

$$\lim_{T \rightarrow \infty} E \left\{ \frac{1}{T} \int_0^T x^T(t) Q x(t) + u^T(t) R u(t) dt \right\}^{1/2} \quad (100.170)$$

when the noise inputs are unit variance white noise. In the frequency domain, this is equivalent to minimizing the H_2 -norm

$$\|G\|_2 = \left\{ \frac{1}{2\pi} \int_{-\infty}^{\infty} \text{trace}(G^*(j\omega) G(j\omega)) d\omega \right\}^{1/2} \quad (100.171)$$

of the transfer function G from the white noise inputs $\begin{bmatrix} v \\ w \end{bmatrix}$ to the output $z = \begin{bmatrix} Tx \\ R^{1/2}u \end{bmatrix}$ where $Q = T^T T$, as before.

We should point out that the so-called H_2 controller is equivalent to the LQG controller but provides a unified framework for control and observation that explains the striking similarity between the LQ controller equations and the Kalman filter equations (for example, in the Riccati equations of (100.148) and (100.63)). See Zhou and Doyle [1998] for further information.

H_∞ Control

The standard H_∞ control problem considers a system of the form

$$\begin{aligned} \dot{x} &= Ax + B_1 w + B_2 u \\ z &= C_1 x + D_{12} u \\ y &= C_2 x + D_{21} w \end{aligned} \quad (100.172)$$

where w is a deterministic disturbance input vector, y is the measured output vector, and z is a vector of variables to be controlled. The objective of H_∞ control is to minimize the H_∞ norm

$$\|G\|_\infty = \sup_{\omega} \bar{\sigma}[G(j\omega)] \quad (100.173)$$

(where $\bar{\sigma}$ denotes the maximum **singular value** of a matrix, and sup denotes “supremum,” or least upper bound of the transfer function G from the disturbance input w to the output z . In the time domain, the square of this

norm corresponds to the maximum possible energy magnification between the input and the output, where energy is defined as the integral of the square of a signal; for example, $\int_0^\infty w^T(t)w(t)dt$.

One of the major reasons for the development of H_∞ control is that many performance and robustness criteria for MIMO systems involve the maximum **singular value** of certain system transfer functions. To optimize the performance or robustness of these systems requires the minimization of the maximum singular value of these transfer functions, which is exactly the objective of H_∞ control.

From a disturbance rejection point of view, the H_∞ controller can be used to minimize the root-mean-square value of the controlled variable z due to the worst-case unit-energy disturbance w . This is to be contrasted with LQG (or H_2) controller, which minimizes the average response to a unit-variance random disturbance.

In practice, it is common to solve the suboptimal H_∞ problem where it is desired to find an output feedback controller such that $\|G\|_\infty < \gamma$, where γ is specified by the designer. For large values of γ , there will always be a solution to the problem. In fact, as γ approaches infinity in the equations below, the central H_∞ controller will approach the LQG controller. By decreasing the value of γ until just before a solution to the problem ceases to exist, the designer can get as close to the optimal H_∞ controller as desired. To ensure that a solution for some value of γ exists, the following standard assumptions on the system are made [Green and Limebeer, 1995]:

1. The pair (A, B_2) is stabilizable and the pair (A, C_2) is detectable
2. $D_{12}^T D_{12} = I$ and $D_{21} D_{21}^T = I$
3. Rank $\begin{bmatrix} A - j\omega I & B_2 \\ C_1 & D_{12} \end{bmatrix} = n + m$ for all real ω
4. Rank $\begin{bmatrix} A - j\omega I & B_1 \\ C_2 & D_{21} \end{bmatrix} = n + q$ for all real ω

where n is the dimension of x , m is the dimension of u , and q is the dimension of y .

Under these assumptions, it can be shown that there exists a stabilizing, measurement feedback solution to the suboptimal H_∞ control problem if and only if the following three conditions are met.

1. The algebraic Riccati equation $X_\infty \tilde{A} + \tilde{A}^T X_\infty + \tilde{C}^T \tilde{C} - X_\infty (B_2 B_2^T - \gamma^2 B_1 B_1^T) X_\infty = 0$ has a positive semi-definite solution such that $\tilde{A} - (B_2 B_2^T - \gamma^2 B_1 B_1^T) X_\infty$ is stable, where $\tilde{A} = A - B_2 D_{12}^T C_1$ and $\tilde{C}^T \tilde{C} = C_1^T (I - D_{12} D_{12}^T) C_1$.
2. The algebraic Riccati equation $\bar{A} Y_\infty + Y_\infty \bar{A}^T + \bar{B} \bar{B}^T - Y_\infty (C_2^T C_2 - \gamma^2 C_1^T C_1) Y_\infty = 0$ has a positive semi-definite solution such that $\bar{A} - Y_\infty (C_2^T C_2 - \gamma^2 C_1^T C_1)$ is stable, where $\bar{A} = A - B_1 D_{12}^T C_2$ and $\bar{B} \bar{B}^T = B_1 (I - D_{21}^T D_{12}) B_1^T$.
3. $\rho(X_\infty Y_\infty) < \gamma^2$, where $\rho(\cdot)$ denotes the maximum of the absolute values of the matrix's eigenvalues.

The so-called central controller that solves the suboptimal H_∞ problem can be written in a form that closely resembles the state-estimate feedback form of the LQG controller:

$$\begin{aligned} \dot{\hat{x}} &= A\hat{x} + B_1 \hat{w}^* + B_2 u + \left[B_1 D_{21}^T + Z_\infty C_{2z}^T \right] \left(y - C_2 \hat{x} - D_{21} \hat{w}^* \right) \\ u &= -F_\infty \hat{x} \\ \hat{w}^* &= \gamma^{-2} B_1^T X_\infty \hat{x} \end{aligned} \tag{100.174}$$

where $C_{2z} = C_2 + \gamma^{-2} D_{21} B_1^T X_\infty$, $F_\infty = D_{12}^T C_1 + B_2^T X_\infty$, and $Z_\infty = Y_\infty (I - \gamma^{-2} X_\infty Y_\infty)^{-1}$. The dynamic part of the above compensator can be interpreted as an estimate of the state assuming that the worst-case disturbance w^* is present. The control signal is a linear feedback of the estimated state, just as in the LQG case. Although the controller formulas above look more complicated than in the LQG case, this is largely due to the fact that the controlled variable z has a more general form in the H_∞ problem statement above. It should be noted, however, that unlike the LQG case, the solution of the Riccati equations is coupled in the H_∞ case due to condition 3 above.

Example

Consider the following state-space system, which represents a plant with two lightly damped modes at approximately $\omega_1 \approx 1$ and $\omega_2 \approx 3.2$:

$$\begin{aligned}\dot{x}(t) &= \begin{bmatrix} 0 & 1 & 0 & 0 \\ -1 & -1 & 0 & 0 \\ 0 & 0 & 0 & 1 \\ 0 & 0 & -10 & -1 \end{bmatrix}x(t) + \begin{bmatrix} 0 & 0 \\ 1 & 0 \\ 0 & 0 \\ .2 & 0 \end{bmatrix}d(t) + \begin{bmatrix} 0 \\ 1 \\ 0 \\ -1 \end{bmatrix}u(t) \\ y(t) &= [1 \quad 0 \quad .5 \quad 0]x(t) + [0 \quad .01]d(t)\end{aligned}\quad (100.175)$$

Here, the term $d(t) = [d_1(t) \quad d_2(t)]^T$ is a vector whose first term represents the plant disturbance, and whose second term represents the measurement disturbance (deterministic). To pose the LQG control problem, we can propose minimizing the cost function

$$\int_0^\infty (x^T T^T T x + r u^2) dt = \int_0^\infty z^T z dt \quad (100.176)$$

where

$$z \triangleq \begin{bmatrix} T \\ 0 \end{bmatrix}x + \begin{bmatrix} 0 \\ r \end{bmatrix}u \quad (100.177)$$

and $T = [.5 \quad 0 \quad -1 \quad 0]$. However, Eq. (100.175) and (100.177) are also in the form of Eq. (100.172), facilitating an H_∞ design that minimizes the H_∞ norm of the transfer function from the disturbance d to the controlled variable z . We can compare this design to an H_2 controller design that minimizes the H_2 norm (Eq. (100.176)). The two controllers will therefore minimize different norms of the same transfer function.

The results of this comparison are shown in the curves of Fig. 100.55. The distinguishing feature of this comparison is the flattening effect of the H_∞ controller. Although this is a plot of a frequency response magnitude and not the maximum singular value, it is apparent that the H_∞ controller is reducing the peak response, while the H_2 controller is reducing the average response and providing faster roll-off in the frequency domain.

Other Approaches

Although the LQG and H_∞ design methodologies are probably the most commonly used techniques for linear MIMO controller design, there are many other optimization-based techniques available. A well-developed theory exists for L_1 control, which minimizes the maximum magnification of the peak of the input signal using a linear programming algorithm [Dahleh and Diaz-Bobillo, 1995]. This approach departs from traditional controller design methodologies that have attempted to arrive at a set of formulas for the optimal controller. But with the advent of powerful computers, it makes sense to consider a problem solved if it can be reduced to a problem that can be efficiently solved using a computer algorithm. This is also the premise underlying the design methodology of *linear matrix inequalities*, in which the control design problem is reduced to a convex programming problem [Boyd et al., 1994].

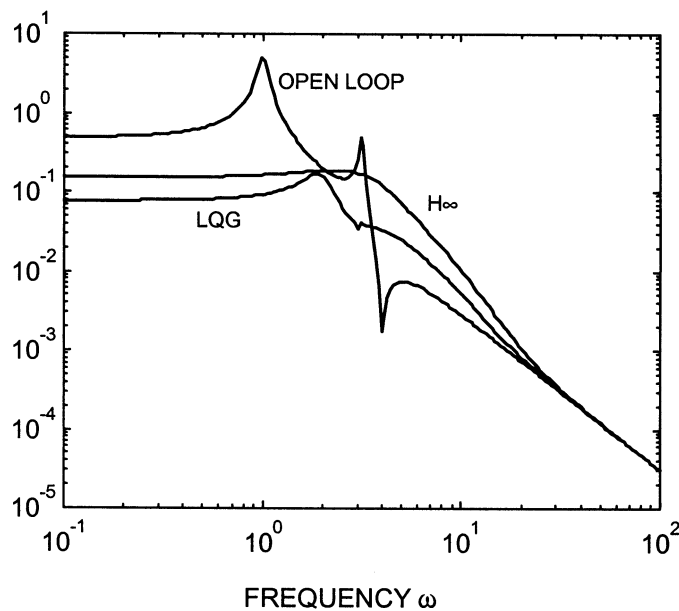


FIGURE 100.55 Frequency response of the closed-loop transfer function from d_1 to Tx , comparing the H_2 (LQG) and H_∞ control designs, using $r = 0.1$.

Defining Terms

Controllability: A linear system is said to be controllable if a control input exists that will drive a system with an arbitrary initial condition to a desired final state in a finite time.

Stabilizability: A linear system is said to be stabilizable if its unstable part is controllable.

Observability: A linear system is said to be observable if its state vector can be reconstructed from finite-length observations of its input and output.

Detectability: A linear system is said to be detectable if its unstable part is observable.

Positive-(semi)definite: A positive-(semi)definite matrix is a symmetric matrix A such that for any nonzero vector x , the quadratic form $x^T Ax$ is positive (non-negative).

Observer (or estimator): A linear system whose state output approximates the state vector of a different system, rejecting noise and disturbances in the process.

Singular value: Singular values are non-negative real numbers that measure the magnification effect of an operator in the different basis directions of the operator's space.

References

- B. D. O. Anderson and J. B. Moore, *Optimal Filtering*, Prentice-Hall, 1979.
- J. S. Bay, *Fundamentals of Linear State Space Systems*, WCB/McGraw-Hill, 1999.
- S. Boyd et al., *Linear Matrix Inequalities in System and Control Theory*, Society for Industrial and Applied Mathematics, 1994.
- A. E. Bryson, Jr. and Y. C. Ho, *Applied Optimal Control*, Hemisphere Publishing, 1975.
- M. Dahleh and I. J. Diaz-Bobillo, *Control of Uncertain Systems: A Linear Programming Approach*, Prentice-Hall, 1995.
- J. C. Doyle, K. Glover, P. P. Khargonekar, and B. A. Francis, State-space solutions to standard H_2 and H_∞ control problems, *IEEE Trans. on Automatic Control*, AC-34, 831–847, 1988.

- B. A. Francis, *A Course in H_∞ Control Theory*, Lecture Notes in Control and Information Sciences, Vol. 88, Springer-Verlag, 1987.
- M. Green and D. J. N. Limebeer, *Linear Robust Control*, Prentice-Hall, 1995.
- R. E. Kalman, A new approach to linear filtering and prediction problems, *Transactions of the ASME, Journal of Basic Engineering*, 82, 35–45, 1960.
- D. E. Kirk, *Optimal Control Theory*, Prentice-Hall, 1970.
- K. Zhou and J. C. Doyle, *Essentials of Robust Control*, Prentice-Hall, 1998.

Further Information

Optimal control and estimation is an actively growing field of control systems research. Classic texts in the area include [Kirk, 1970] and [Bryson and Ho, 1975] for optimal control systems, and [Anderson and Moore, 1979] for Kalman filtering, with the original source being [Kalman, 1960]. Further information on H_2 and H_∞ theory can be found in [Doyle, et al., 1989], [Zhou and Doyle, 1998], [Green and Limebeer, 1995], and [Francis, 1987].

100.9 Neural Control

Mo-Yuen Chow

Artificial intelligence had strong ties with automatic control during its early development stages several decades ago. Typical examples of these ties are the development of cybernetics, robotics, and early learning systems. Recent efforts to incorporate aspects of artificial intelligence into the design and operation of automatic control systems have focused on using techniques such as artificial neural networks, fuzzy logic, and expert systems. The application of one or more of these techniques in the design of control systems has come to be known as *intelligent control* [Antsaklis et al., 1994], a term questioned by some for its implications. Whether or not such systems should be classified as intelligent, they represent significant contributions to the field of automatic control, as evidenced by the rapidly growing wealth of literature devoted to the successful application of such systems to complex control problems [Chow and Menozzi, 1994a; 1994b; Chow and Teeter, 1997; Chow and Yee, 1991; Hunt et al., 1992; Miller et al., 1990; Nguyen and Widrow, 1990; Psaltis et al., 1988; Werbos, 1990].

The nonlinear functional mapping properties of Artificial Neural Networks (ANNs) are central to their use in system identification and control [Narendra and Parthasarathy, 1990]. Although a number of key theoretical problems remain, results pertaining to the approximation capabilities of neural networks demonstrate that they have great promise in the modeling and control of nonlinear systems. The artificial neural network technology has become increasingly popular as a tool for performing tasks such as automatic control, system identification, pattern recognition, and time series prediction. Most of the *conventional methods*, such as PI control, are based on mathematical and statistical procedures for the modeling of the system and the estimation of the optimal controller parameters. In practice, the plant to be controlled is often highly nonlinear and a mathematical model may be difficult to derive. In such cases, conventional techniques may prove to be suboptimal and may lack robustness in the face of modeling error, because they are only as accurate as the model that was used to design them. With the advancement of technology, however, sophisticated control using artificial neural network techniques has been developed and used successfully to improve the control of systems that cannot be easily handled by conventional control, thus giving rise to terminology such as *neural control* and *intelligent control*.

Usually, a human operator is responsible for adjusting the controller's parameters in order to use his/her own idea of good performance. Indirectly, the operator is performing a minimization of a cost function based on his/her knowledge. More generally, when confronted with a problem situation, humans execute a mapping between a set of events and the set of corresponding appropriate actions. The appropriateness of these actions is due to some basic acquired knowledge, or even instinct, that guides the initial stages of the mapping. Then, through experience and a set of implicit guidelines, the human learns to perform a better mapping. This is an ongoing process throughout a person's life. Similarly, an ANN, if given initial guidance, can learn to improve its performance through a set of guidelines, (e.g., minimize a cost function). In fact, a properly structured ANN can learn any arbitrarily complicated mapping [Cybenko, 1989; Rumelhart and McClelland, 1986; Werbos, 1974].

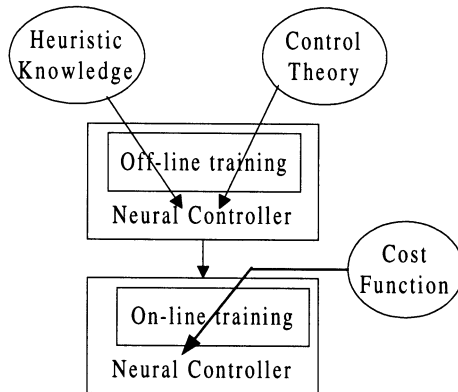


FIGURE 100.56 A two-step training process for a neural controller.

Successful adaptation of online neural controllers in many cases requires careful and substantial design effort. One of the common practices is to pre-train a neural controller offline, based on some simplified design methods, in the same way that a PI controller is designed based on *approximated* system models that can provide reasonable control performance, before putting the neural controller for online fine-tuning [Chow and Menozzi, 1993; Chow and Teeter, 1995; Teeter et al., 1996]. This approach, as shown in Fig. 100.56, can speed up the neural controller online adaptation process and increase the closed-loop online adaptation stability because the initial weights of the neural controller are much closer to the optimal final weights (if they exist) after the pre-training process. By learning online, the ANN controller can adapt to changing operating environments.

This chapter section briefly describes the feedforward net paradigm to facilitate the discussion of the *neural observer* and *neural controller* concepts in later sections. An example of using neural control for an HVAC system will then be provided to demonstrate its effectiveness for solving real-world problems.

Brief Introduction to Artificial Neural Networks

Increasing interest in studying the mechanisms and structure of the brain has led to the development of new computational models for solving problems such as pattern recognition, fast information processing, and adaptation. In the 1940s, McCulloch and Pitts studied the potential and capabilities of the interconnection of components based on a model of a biological neuron. Since then, many different models and architectures have been developed and analyzed for a variety of applications [Zurada, 1992]. One of the most common neuron models is shown in Fig. 100.57.

The inputs x to the neuron model are scaled by connection weights w and summed. An additional input b , often referred to as a *bias*, is added to this sum and the result becomes the input to a function $f(\cdot)$, called the *activation function*, which computes the output of the neuron. The bias can be considered as a connection weight for a constant input of +1. The terms *neuron model* and *neuron* are used interchangeably in this chapter section.

The individual neurons are not very powerful in terms of computation or representation, but the interconnection of neurons to form an *artificial neural network* (ANN) can provide a means of encoding complex relationships between input and output variables. Of the many ANN architectures that have been proposed, the *multilayer feedforward artificial neural network* (MFANN) shown in Fig. 100.58 is one of the most popular.

Bias terms have been omitted in Fig. 100.58 for simplicity. The layers between the input and output layers of an MFANN are usually referred to as *hidden layers* because their inputs and outputs are not measurable at the inputs or outputs of the network. It has been shown that an MFANN with a single hidden layer can approximate any continuous function to an arbitrary degree of accuracy [Cybenko, 1989; Werbos, 1974]. The process of adjusting ANN connection weights in an effort to obtain a desired input/output mapping is usually referred to as *training*. Training represents an optimization problem for which the solution is a set of weights that minimizes some measure of approximation error. The choices of activation functions, number of neurons, error measures, and optimization methods can significantly affect training results.

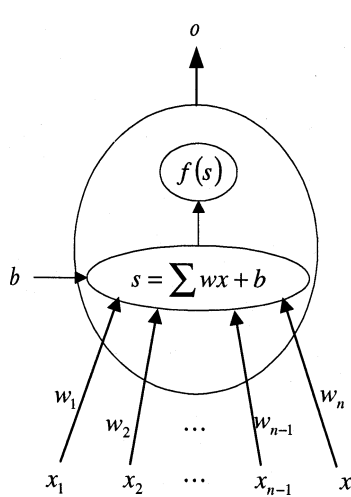


FIGURE 100.57 Computational model of a biological neuron.

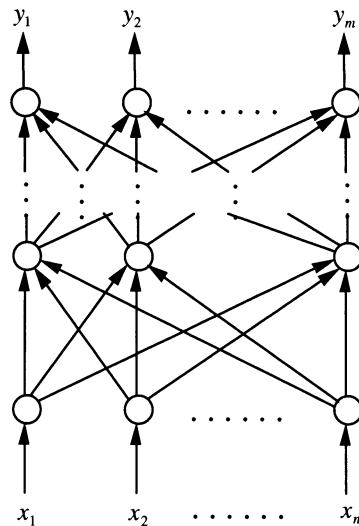


FIGURE 100.58 A multilayer feedforward ANN.

When the desired mapping is described by a set of input/output data, weights are usually modified after the presentation of each input/output pattern. This method is referred to as *pattern update* and represents an approximation of true gradient descent that is generally valid when a sufficiently small stepsize is used. *Batch update*, for which weight changes are accumulated over one sweep of the set of training patterns before being applied, is sometimes used in an effort to more closely mimic true gradient descent. Variants of back-propagation and other training methods can be found in [Zurada, 1992].

Neural Observer

The nonlinear functional mapping properties of *neural networks* are central to their use in identification and control [Chow and Teeter, 1995; Hunt et al., 1992; Poggio and Girosi, 1990; Teeter and Chow, 1998; Teeter et al. 1994]. Although a number of key theoretical problems remain, results pertaining to the approximation capabilities of neural networks demonstrate that they have great promise in the modeling of nonlinear systems. An important question in system identification is whether a system under study can be adequately represented within a given model structure [Hunt et al., 1992]. In the absence of such concrete theoretical results for neural networks, it is usually assumed that the system under consideration belongs to the class of systems that the chosen network is able to represent. Two system identification techniques are now introduced: *forward modeling* and *inverse modeling*.

The procedure of training a neural network to represent the forward dynamics of a system is often referred to as the *forward system identification* approach [Hunt et al., 1992]. A schematic diagram of this process is shown in Fig. 100.59.

The neural network is placed in parallel with the system, and the error, e , between the system outputs, y , and network outputs, \hat{y} , is used to train the network. This represents a classical *supervised learning* problem for which the teacher (i.e., the system) provides target values (i.e., system outputs) directly in the output coordinate system of the learner (i.e., the network model) [Jordan and Rumelhart, 1991].

In an *inverse system identification* approach, a network is trained in an effort to model the inverse of the plant mapping [Hunt et al., 1992]. One of the simplest approaches, known as *direct inverse system identification*, is shown schematically in Fig. 100.60.

A synthetic training signal, s , is introduced to the system, and the system output, y , is used as the input to the network. The network output is compared to the training signal and this error is used to train the network.

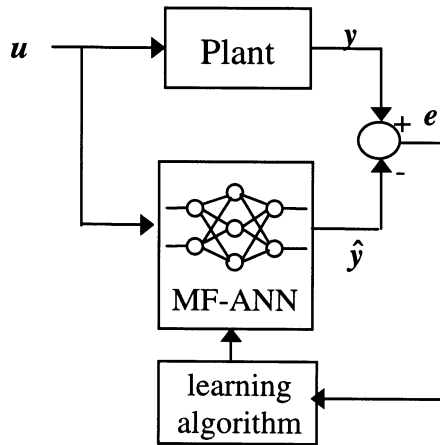


FIGURE 100.59 Forward system identification approach.

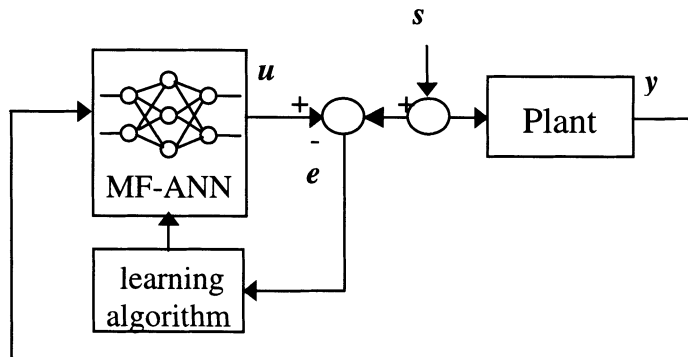


FIGURE 100.60 Direct inverse system identification approach.

The inverse modeling structure shown in Fig. 100.60 tends to force the network to represent the inverse of the plant, but there are potential drawbacks to this approach. The training signal must be chosen to sample over a wide range of system inputs, and the actual operational inputs may be difficult to define *a priori* [Jordan and Rumelhart, 1991]. This point is strongly related to the concept of persistent excitation discussed in adaptive control literature. A second drawback is that an incorrect inverse model can be obtained if the nonlinear system mapping is not one-to-one. An approach called *specialized inverse modeling* has been proposed in an effort to overcome these problems. The details of this approach can be found in [Psaltis et al., 1988]. The neural network identification models can be used in the adaptive control of unknown nonlinear plants.

Neural Control

A method of *direct adaptive control* is depicted in Fig. 100.61.

Methods for directly adjusting control parameters based on the output error e , are generally not available. This is because the unknown nonlinear plant in Fig. 100.61 lies between the controller and the output error. Until such methods are developed, adaptive control of nonlinear plants must be performed using *indirect* methods [Narendra and Parthasarathy, 1990]. Figure 100.62 depicts a general method of indirect adaptive control using artificial neural networks.

Tapped delay lines (TDL) provide delayed inputs and outputs of the plant to the neural controller and neural observer. Error e_i is used to adapt the neural observer, while the parameters of the neural observer along with

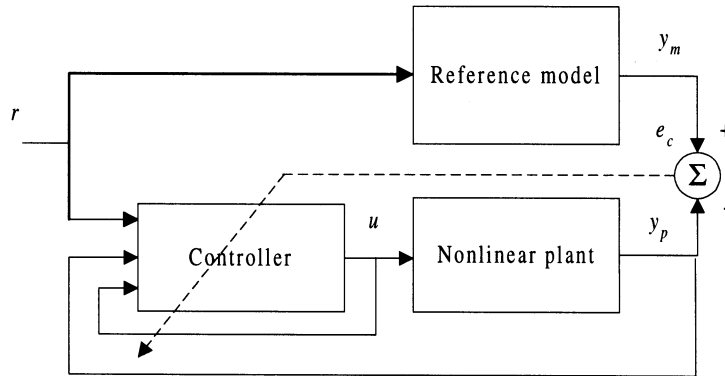


FIGURE 100.61 Direct adaptive control.

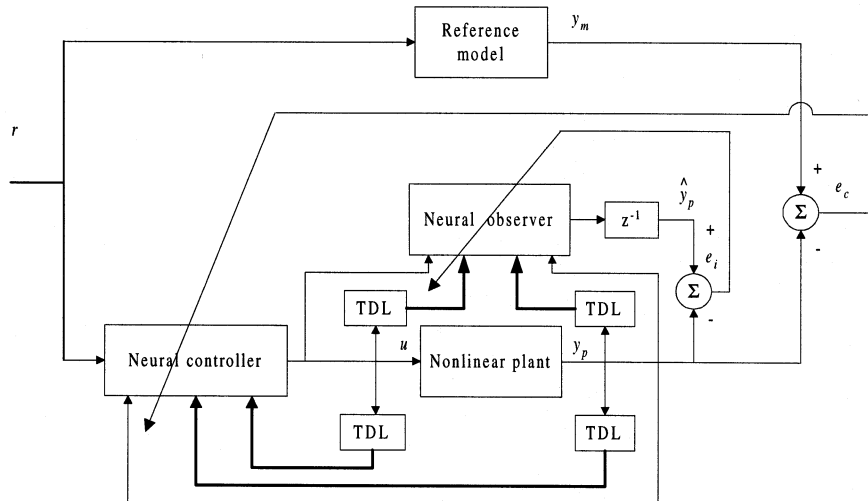


FIGURE 100.62 A method of indirect adaptive control using neural networks.

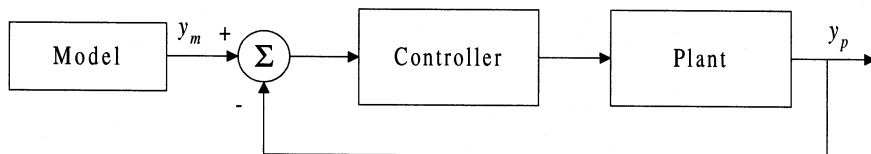


FIGURE 100.63 Explicit model-following.

error e_c are used to adapt the neural controller. The model reference approach depicted in Fig. 100.62 is commonly referred to as *implicit model-following* in adaptive control literature [Narendra and Annaswamy, 1989]. This type of model-following is performed when the dynamics of the closed-loop system are forced to asymptotically match the dynamics of the reference model. The method of *explicit model-following* is depicted in Fig. 100.63. In this case, the reference model acts as a prefilter, and the value of the system output is forced to asymptotically track the value of the reference model output [Narendra and Annaswamy, 1989].

A neural control and identification scheme can be described as the following: at each time step, the plant states are measured and a neural network controller computes the plant inputs. Controller parameters are then

adjusted between samples so that the system approaches optimal performance with respect to a given cost index. The general form of the cost index used to adapt the neural controller is:

$$J_k = \sum_{i=k+1}^N L(\mathbf{x}(i), \mathbf{u}(i)) \quad (100.178)$$

where L is the cost function as a function of system state \mathbf{x} and control \mathbf{u} . Thus, at each time step, the goal is to minimize J_k subject to system dynamics and control constraints, with k denoting the current time step and N the prediction horizon.

The back-propagation training algorithm can be used to adapt neural networks for the identification and control of nonlinear plants [Teeter and Chow, 1998; Werbos, 1990]. For system identification, a network can be trained offline using plant input/output data obtained from simulation of a mathematical model or from observation of the physical system. When the network is used for adaptive identification, training can be performed using *batch update* with a window of sampled data, or with the *pattern update* method in which training patterns consist of past inputs and outputs measured at each sample time.

In order to adaptively train a neural *controller* using gradient descent, the partial derivatives of a cost index, J_k , with respect to the network weights, \mathbf{w} , must be obtained [Chow and Yee, 1991]. Let J_k have the form $J_k = L(\mathbf{y}(k+1), \mathbf{u}(k+1)) + L(\mathbf{y}(k+2), \mathbf{u}(k+2)) + \dots + L(\mathbf{y}(k+n), \mathbf{u}(k+n))$ where k is the current sample. For simplicity of notation, let $L(\mathbf{y}(k+i), \mathbf{u}(k+i))$ be denoted by $L(k+i)$. Application of the chain rule yields

$$\frac{\partial L(k+i)}{\partial \mathbf{w}} = \frac{\partial L(k+i)}{\partial \mathbf{u}(k)} \frac{\partial \mathbf{u}(k)}{\partial \mathbf{w}} = \left[\frac{\partial L(k+i)}{\partial \mathbf{y}(k+i)} \frac{\partial \mathbf{y}(k+i)}{\partial \mathbf{u}(k)} + \frac{\partial L(k+i)}{\partial \mathbf{u}(k+i)} \frac{\partial \mathbf{u}(k+i)}{\partial \mathbf{u}(k)} \right] \frac{\partial \mathbf{u}(k)}{\partial \mathbf{w}} \quad (100.179)$$

The $\partial \mathbf{u}(k)/\partial \mathbf{w}$ term can be calculated using the backpropagation approach since the controller is a neural network. The $\partial \mathbf{y}(k+i)/\partial \mathbf{u}(k)$ and $\partial \mathbf{u}(k+i)/\partial \mathbf{u}(k)$ terms are obtained using the neural controller and identifiers. First, future inputs and outputs of the plant are predicted. The partial derivatives are then obtained by recursively computing the input/output sensitivities of the plant and controller through i samples. This approach is often referred to as *back-propagation through time* [Chow and Yee, 1991; Werbos, 1990].

The training algorithm resembles methods used by Nguyen and Widrow [1990] and others for training a neural controller to achieve an end goal. In this case, however, the output *trajectory* is of interest and the training is performed in realtime (i.e., output values must be repeatedly predicted rather than observed over several trials). A flowchart of the control methodology is shown in Fig. 100.64.

After controller outputs are computed, the weights of the controller are adjusted N times before the next sample time. The value of N can be selected based on time constraints or convergence properties of the neural controller and observers. If N is large, the neural observers are inaccurate; and if a large prediction horizon is used, the adaptation of controller parameters may cause performance to deteriorate.

HVAC Illustration

In order to demonstrate the ability of the neural identification and control schemes to handle disturbances and changes in nonlinear plant dynamics, a Heat, Ventilation, and Air-Conditioning (HVAC) system where a thermal load is added and the actual output vs. the commanded output of each actuator is modified. The neural observers are adapted at each time step in one simulation, while adaptation of the observers is stopped at time step $k = 200$ in another simulation. Both simulations are performed for 1000 time steps. The reference trajectory is plotted in Fig. 100.65, along with the output of the system that uses nonadaptive identifiers after time step $k = 200$. Tracking errors for both simulations are plotted in Fig. 100.66, where T_3 is the temperature to be controlled and r is the reference signal to be tracked.

The performance of the system with nonadaptive observers deteriorates due to the disturbance and the changes in plant dynamics. In this case, adapting the neural observers enables them to more accurately predict

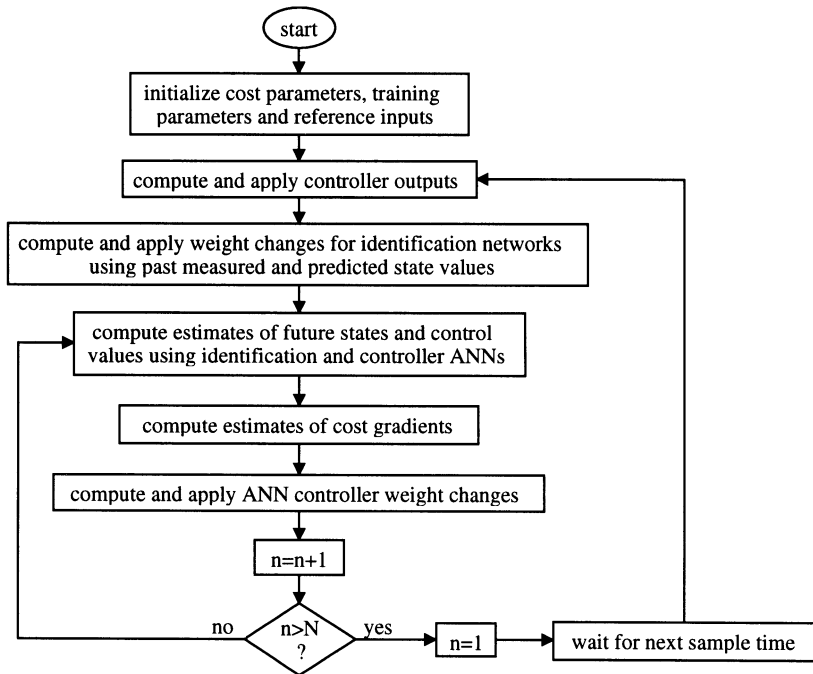


FIGURE 100.64 Flowchart of the neural control training methodology.

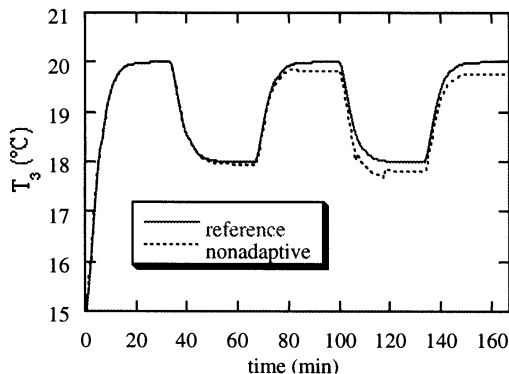


FIGURE 100.65 Reference and output trajectories using nonadaptive neural identifiers.

future states and inputs, and results in better tracking. It is important to select appropriate adaptation stepsizes for the observers because only one training pattern, consisting of the most recent set of plant inputs and states, is available for training. In order to compare the neural identification and control methodology with another potential control methodology, a PI-type controller has been designed for the HVAC system. Typical responses of the system with PI-type controller are shown in Fig. 100.67.

The simple PI-type controller satisfies the conservative performance specifications for the cases tested, but does not always use its resources efficiently. For example, if the outside air temperature of the HVAC system is close to the steady-state reference temperature, it may be more efficient to increase the room volumetric flow rate for a period of time in order to reduce the amount of heating or cooling performed by the heat exchanger. The neural and PI-type control schemes are tested using initial conditions $T_3(0) = 15^\circ\text{C}$, a constant outside temperature of 22°C , and a steady-state reference value of 20°C . The tracking errors and heat exchanger outputs for both methods are shown in Figs. 100.68 and 100.69, respectively.

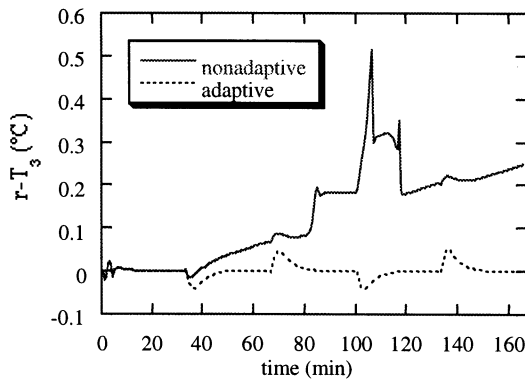


FIGURE 100.66 Tracking errors for the system using adaptive and nonadaptive neural identifiers.

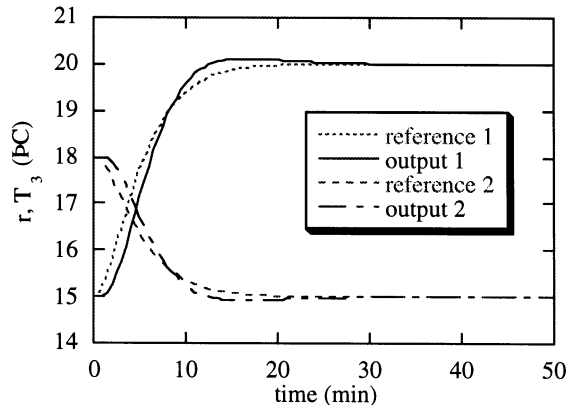


FIGURE 100.67 Typical responses of the system with PI-type controller.

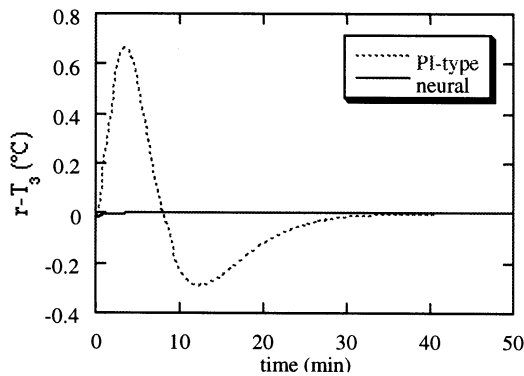


FIGURE 100.68 Tracking errors of the PI-type and neural control systems.

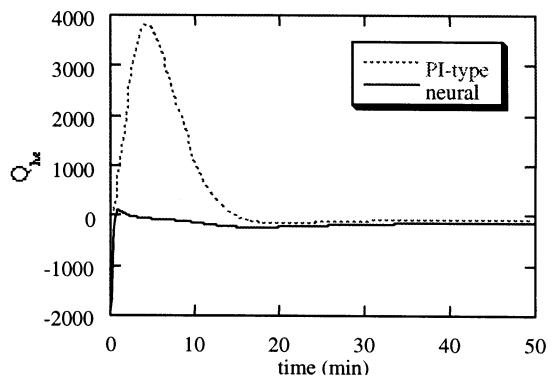


FIGURE 100.69 Heat exchanger outputs for the PI-type and neural control systems.

Conclusion

The use of neural networks for system identification and control provides a means of adapting a controller online in an effort to minimize a given cost index. The cost index includes typical measures associated with system performance and can be modified without significantly increasing the computational complexity of the adaptation process. For nonlinear systems, the identification networks demonstrate the capacity to learn changes in the plant dynamics. The performance of the neural control and identification methodology compares favorably with many types of conventional approaches.

References

- Antsaklis, P. J., Albus, S., Lemmon, M. D., Mystel, A., Passino, K. M., Saridis, G. N., and Werbos, P. (1994). Defining intelligent control, *IEEE Control Systems*, 4, 5, 58–66.
- Chow, M.-Y. and Menozzi, A. (1993). Design Methodology of an Intelligent Controller Using Artificial Neural Networks, *IECON'93*, Maui, Hawaii.
- Chow, M.-Y. and Menozzi, A. (1994). A Self-Organized CMAC Controller for Robot Arm Movements, *IEEE International Conference on Industrial Technology*, Guangzhou, China.
- Chow, M.-Y. and Menozzi, A. (1994). Using a Cerebellar Model for FES Control of the Upper Limb, *16th Annual International IEEE Engineering in Medicine and Biology Society Conference*, Baltimore, MD.

- Chow, M.-Y. and Teeter, J. (1995). A knowledge-based approach for improved neural network control of a servomotor system with nonlinear friction characteristics, *Mechatronics*, 5(8), 949–962.
- Chow, M.-Y. and Teeter, J. (1997). Reduced-Order Functional Link Neural Network for HVAC Thermal System Identification and Modeling, *1997 International Conference on Neural Networks*, Houston, TX.
- Chow, M.-Y. and Yee, S. O. (1991). An adaptive backpropagation through time training algorithm for a neural controller, *1991 IEEE International Symposium on Intelligent Control*, Arlington, VA, 170–175.
- Cybenko, G. (1989). Approximation by superpositions of a sigmoidal function, *Mathematics of Control, Signals, and Systems*, 2, 303–314.
- Hunt, K. J., Sbarbaro, D., Zbikowski, R., and Gawthrop, P. J. (1992). Neural networks for control systems — a survey, *Automatica*, 28(6), 1083–1112.
- Jordan, M. I. and Rumelhart, D. E. (1991). Forward models: supervised learning with a distal teacher. *Occasional Paper No. 40*, Center for Cognitive Science, MIT.
- Miller, III, W. Thomas, Sutton, Richard S., Werbos, Paul J. (1990). *Neural Networks for Control*, The MIT Press, Cambridge, MA.
- Narendra, K. S. and Annaswamy, A. M. (1989). *Stable Adaptive Systems*, Prentice-Hall, Englewood Cliffs, NJ.
- Narendra, K. S. and Parthasarathy, K. (1990). Identification and control of dynamical systems using neural networks, *IEEE Transactions on Neural Networks*, 1(1), 4–27.
- Nguyen, D. and Widrow, B. (1990). The truck backer-upper: an example of self-learning in neural networks, *Neural Networks for Control*, The MIT Press, Cambridge, MA, 287–299.
- Poggio, T. and Girosi, F. (1990). Networks for approximation and learning, *Proceedings of the IEEE*, 78(9), 1481–1497.
- Psaltis, D., Sideris, A., and Yamamura, A. A. (1988). A multilayered neural network controller, *IEEE Control Systems Magazine*, 17–21.
- Rumelhart, D. E. and McClelland, J. L. (1986). *Parallel Distributed Processing: Explorations in the Microstructure of Cognition*, The MIT Press, Cambridge, MA.
- Teeter, J. and Chow, M.-Y. (1998). Application of functional link neural network to HVAC thermal dynamic system identification, *IEEE Transactions on Industrial Electronics*, 45(1), 170–176.
- Teeter, J., Chow, M.-Y., and Brickley, J. J. Jr. Use of a Fuzzy Gain Tuner for Improved Control of a DC Motor System with Nonlinearities, *IEEE International Conference on Industrial Technology*, Guangzhou, China.
- Teeter, J. T., Chow, M.-Y., and Brickley, J. J. Jr.(1996). A novel fuzzy friction compensation approach to improve the performance of a dc motor control system, *IEEE Transactions on Industrial Electronics*, 43(1), 113–120.
- Werbos, P. J. (1974). *Beyond Regression: New Tools for Prediction and Analysis in Behavioral Science*, Harvard University Press, Cambridge, MA.
- Werbos, P. J. (1990). Backpropagation through time: What it does and how to do it, *Proceedings of the IEEE*, 78(10), 1550–1560.
- Zurada, J. M. (1992). *Introduction to Artificial Neural Systems*, West Publishing Company, St. Paul, MN.

Lasky, T.A., Hsia, T.C., Tummala, R.L., Odrey, N.G. "Robotics"
The Electrical Engineering Handbook
Ed. Richard C. Dorf
Boca Raton: CRC Press LLC, 2000

101

Robotics

Ty A. Lasky
University of California, Davis

Tien C. Hsia
University of California, Davis

R. Lal Tummala
Michigan State University

Nicholas G. Odrey
Lehigh University

- 101.1 **Robot Configuration**
Cartesian Configuration • Cylindrical Configuration • Spherical Configuration • Articulated Configuration • SCARA Configuration • Gantry Configuration • Additional Information
- 101.2 **Dynamics and Control**
Independent Joint Control of the Robot • Dynamic Models • Computed Torque Methods • Adaptive Control • Resolved Motion Control • Compliant Motion • Flexible Manipulators
- 101.3 **Applications**
Justification • Implementation Strategies • Applications in Manufacturing • Emerging Issues

101.1 Robot Configuration

Ty A. Lasky and Tien C. Hsia

Configuration is a fundamental classification for industrial robots. Configuration refers to the geometry of the robot manipulator, i.e., the manner in which the links of the manipulator are connected at each joint. The Robotic Industries Association (RIA) defines a robot as *a manipulator designed to move material, parts, tools, or specialized devices, through variable programmed motions for the performance of a variety of tasks*. With this definition, attention here is focused on industrial manipulator arms, typically mounted on a fixed pedestal base. Mobile robots and hard automation [e.g., Computer Numerical Control (CNC) machines] are excluded. The emphasis here is on serial-chain manipulator arms, which consist of a serial chain of linkages, where each link is connected to exactly two other links, with the exception of the first and last, which are connected to only one other link. Additionally, the first three links, called the major linkages, are focused on, with only a brief mention of the last three links, or wrist joints, also called the minor linkages.

Robot configuration is an important consideration in the selection of a manipulator. Configuration refers to the way the manipulator links are connected at each joint. Each link will be connected to the subsequent link by either a linear (sliding or prismatic) joint, which can be abbreviated with a P, or a revolute (or rotary) joint, abbreviated with an R. Using this notation, a robot with three revolute joints would be abbreviated as RRR, while one with a rotary joint followed by two linear (prismatic) joints would be denoted RPP. Each configuration type is well suited to certain types of tasks and ill suited to others. Some configurations are more versatile than others. In addition to the geometrical considerations, robot configuration affects the structural stiffness of the robot, which may be an important consideration. Also, configuration impacts the complexity of the forward and inverse **kinematics**, which are the mappings between the robot actuator (joint) space, and the Cartesian position and orientation of the robot end-effector, or tool.

There are six major robot configurations commonly used in industry. Details for each configuration are presented in subsequent subsections. The simplest configuration is the Cartesian robot, which consists of three orthogonal, linear joints (PPP), so that the robot moves in the x, y, and z directions in the joint space. The

cylindrical configuration consists of one revolute and two linear joints (RPP), so that the robot joints correspond to a cylindrical coordinate system. The spherical configuration consists of two revolute joints and one linear joint (RRP), so that the robot moves in a spherical, or polar, coordinate system. The articulated (arm-and-elbow) configuration consists of three revolute joints (RRR), giving the robot a somewhat human-like range of motion. The SCARA (Selectively Compliant Assembly Robot Arm) configuration consists of two revolute joints and one linear joint (RRP), arranged in a different fashion than the spherical configuration. It may also be equipped with a revolute joint on the final sliding link. The gantry configuration is essentially a Cartesian configuration, with the robot mounted on an overhead track system. One can also mount other robot configurations on an overhead gantry system to give the robot an extended workspace, as well as free up valuable factory floor space. The percentage usage of the first five configuration types is listed in Table 101.1. This table does not include gantry robots, which are assumed to be included in the Cartesian category. Additionally, this information is from 1988, and does not accurately represent current usage.

In general, robots with a rotary base have a speed advantage. However, they have more variation in resolution and dynamics compared to Cartesian robots. This can lead to inferior performance if a fixed controller is used over the robot's entire workspace.

Cartesian Configuration

The Cartesian configuration consists of three orthogonal, linear axes, abbreviated as PPP, as shown in Fig. 101.1. Thus, the joint space of the robot corresponds directly with the standard right-handed Cartesian xyz -coordinate system, yielding the simplest possible kinematic equations. The work envelope of the Cartesian robot is shown in Fig. 101.2. The work envelope encloses all the points that can be reached by the robot arm or the mounting point for the end-effector or tool. The area reachable by an end effector or tool is not considered part of the work envelope. All interaction with other machines, parts, or processes must take place within this volume [Critchlow, 1985]. Here, the workspace of a robot is assumed to be equivalent to the work envelope.

There are several advantages to this configuration. As noted above, the robot is kinematically simple, since motion on each Cartesian axis corresponds to motion of a single actuator. This eases the programming of linear motions. In particular, it is easy to do a straight vertical motion, the most common motion in assembly tasks. The Cartesian geometry also yields a constant arm resolution throughout the workspace; i.e., for any configuration, the resolution for each axis corresponds directly to the resolution for that joint. The simple geometry of the Cartesian robot leads to correspondingly simple manipulator dynamics.

The disadvantages of this configuration include inability to reach objects on the floor or points invisible from the base of the robot, and slow speed of operation in the horizontal plane compared to robots with a rotary base. Additionally, the Cartesian configuration requires a large operating volume for a relatively small workspace.

Cartesian robots are used for several applications. As noted above, they are well suited for assembly operations, as they easily perform vertical straight-line insertions. Because of the ease of straight-line motions, they are also well suited to machine loading and unloading. They are also used in clean room tasks.

TABLE 101.1 Robot Arm Geometry Usage

Arm Geometry	Percent of Use
Cartesian	18
Cylindrical	15
Spherical	10
Articulated	42
SCARA	15

Source: V. D. Hunt, *Robotics Sourcebook*, New York: Elsevier, 1988. With permission.

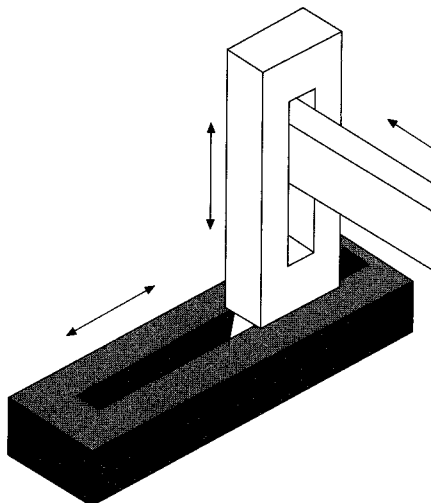


FIGURE 101.1 The Cartesian configuration. (Source: T. Owen, *Assembly with Robots*, Englewood Cliffs, N.J.: Prentice-Hall, 1985. With permission.)

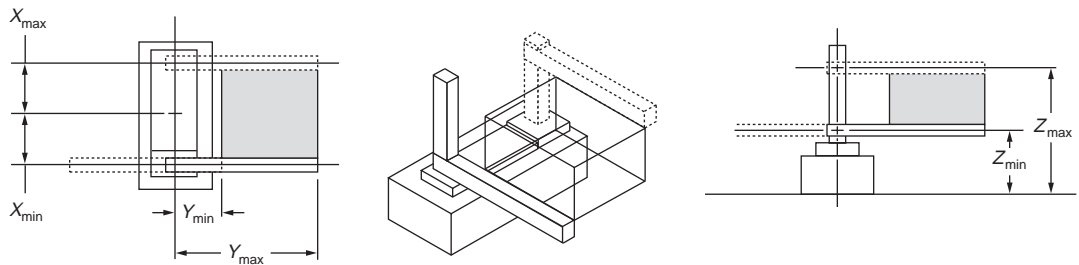


FIGURE 101.2 Cartesian robot work envelope.

Cylindrical Configuration

The cylindrical configuration consists of one vertical revolute joint and two orthogonal linear joints (RPP), as shown in Fig. 101.3. The resulting work envelope of the robot is a cylindrical annulus, as shown in Fig. 101.4. This configuration corresponds with the cylindrical coordinate system.

As with the Cartesian robot, the cylindrical robot is well suited for straight-line vertical and horizontal motions, so it is useful for assembly and machine loading operations. It is capable of higher speeds in the horizontal plane due to the rotary base. However, general horizontal straight-line motion is more complex and correspondingly more difficult to coordinate. Additionally, the end-point resolution of the cylindrical robot is not constant but depends on the extension of the horizontal linkage. A cylindrical robot cannot reach around obstacles. Additionally, if a monomast construction is used on the horizontal linkage, then there can be clearance problems behind the robot.

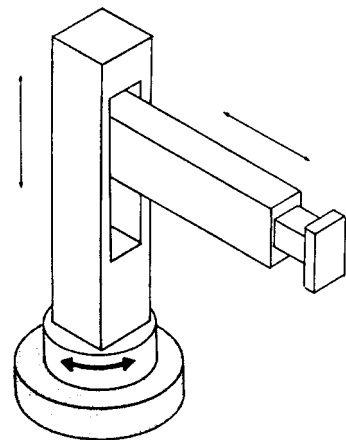


FIGURE 101.3 The cylindrical configuration. (Source: T. Owen, *Assembly with Robots*, Englewood Cliffs, N.J.: Prentice-Hall, 1985. With permission.)

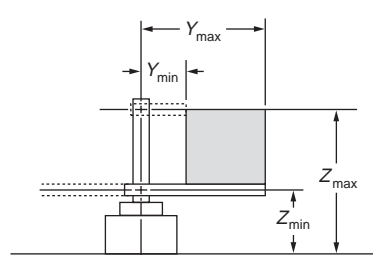
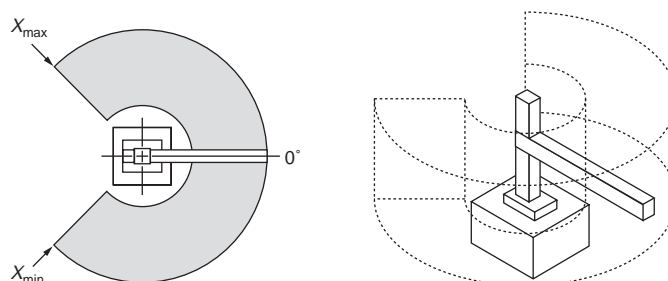


FIGURE 101.4 Cylindrical robot work envelope.

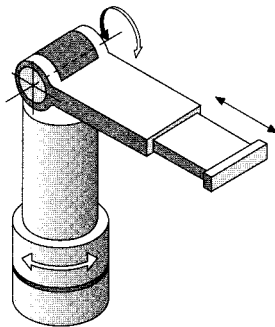


FIGURE 101.5 The spherical configuration. (Source: T. Owen, *Assembly with Robots*, Englewood Cliffs, N.J.: Prentice-Hall, 1985. With permission.)

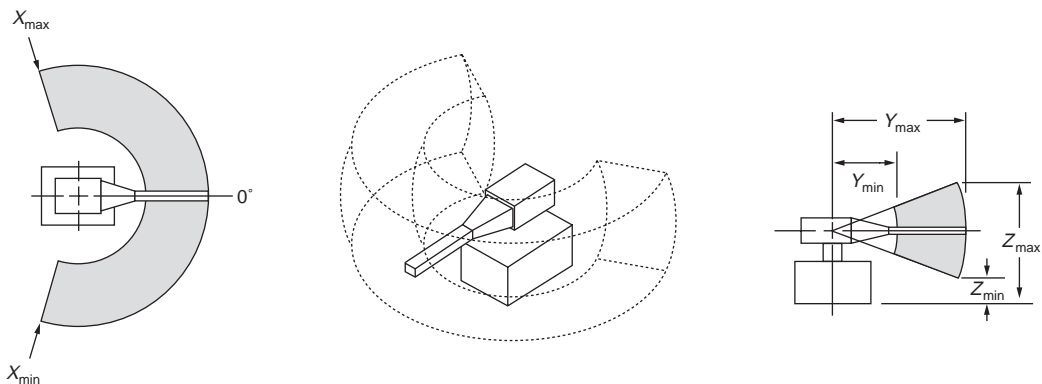


FIGURE 101.6 Spherical robot work envelope.

Spherical robots are typically heavy-duty robots. They have the advantages of high speed due to the rotary base, and a large work volume, but are more kinematically complex than either Cartesian or cylindrical robots. Generally, they are used for heavy-duty tasks in, for example, automobile manufacturing. They do not have the dexterity to reach around obstacles in the workspace. Spherical robots also do not have fixed resolution throughout the workspace.

Articulated Configuration

The articulated (or anthropomorphic, jointed, arm-and-elbow) configuration consists of three revolute joints (RRR), as shown in Fig. 101.7. The resulting joint coordinates do not directly match any standard coordinate system. A slice of a typical work envelope for an articulated robot is shown in Fig. 101.8.

The articulated robot is currently the most commonly used in research. It has several advantages over other configurations. It is closest to duplicating the motions of a human assembler, so there should be less need to redesign an existing workstation to utilize an articulated robot. It has a very large, dexterous work envelope; i.e., it can reach most points in its work envelope from a variety of orientations. Thus, it can more easily reach around or over obstacles in the workspace or into parts or machines. Because all the joints are revolute, high

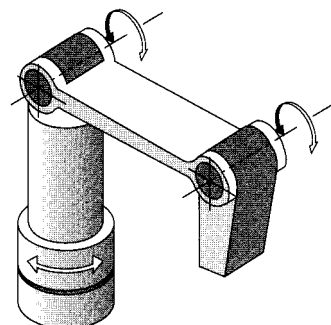


FIGURE 101.7 The articulated configuration. (Source: T. Owen, *Assembly with Robots*, Englewood Cliffs, N.J.: Prentice-Hall, 1985. With permission.)

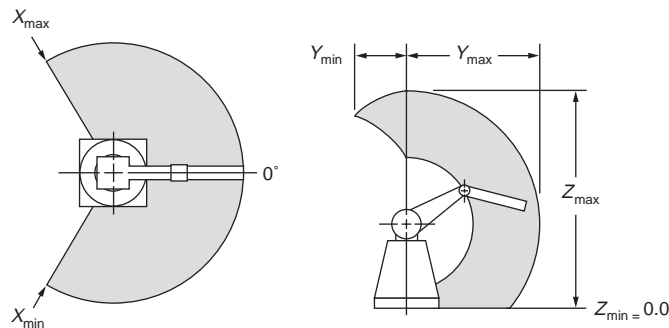


FIGURE 101.8 Articulated robot work envelope.

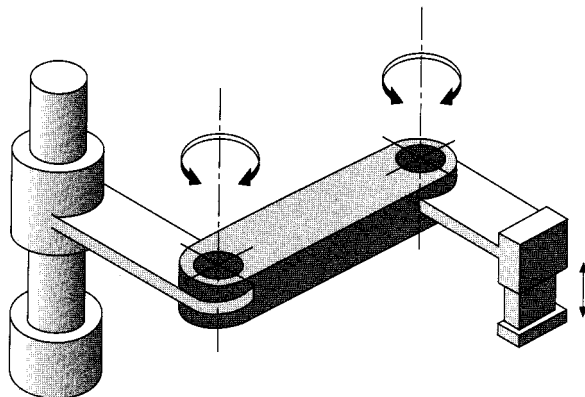


FIGURE 101.9 The SCARA configuration. (Source: T. Owen, *Assembly with Robots*, Englewood Cliffs, N.J.: Prentice-Hall, 1985. With permission.)

speeds are possible. The articulated arm is good for tasks involving multiple insertions, complex motions, and varied tool orientations. The versatility of this configuration makes it applicable to a variety of tasks, so the user has fewer limitations on the use of the robot. However, the same features that give this robot its advantages lead to certain disadvantages. The geometry is complex, and the resulting kinematic equations are quite intricate. Straight-line motion is difficult to coordinate. Control is generally more difficult than for other geometries, with associated increase in cost. Here again, arm resolution is not fixed throughout the workspace. Additionally, the dynamics of an articulated arm vary widely throughout the workspace, so that performance will vary over the workspace for a fixed controller. In spite of these disadvantages, the articulated arm has been applied to a wide variety of research and industrial tasks, including spray painting, clean room tasks, machine loading, and parts-finishing tasks.

SCARA Configuration

The SCARA (Selectively Compliant Assembly Robot Arm) configuration consists of two revolute joints and a linear joint (RRP), as shown in Fig. 101.9. This configuration is significantly different from the spherical configuration, since the axes for all joints are always vertical. In addition to the first three **degrees of freedom** (DOF), the SCARA robot will often include an additional rotation about the last vertical link to aid in orientation of parts. The work envelope of the SCARA robot is illustrated in Fig. 101.10. The SCARA configuration is the newest of the configurations discussed here, and was developed by Professor Hiroshi Makino of Yamanashi University, Japan.

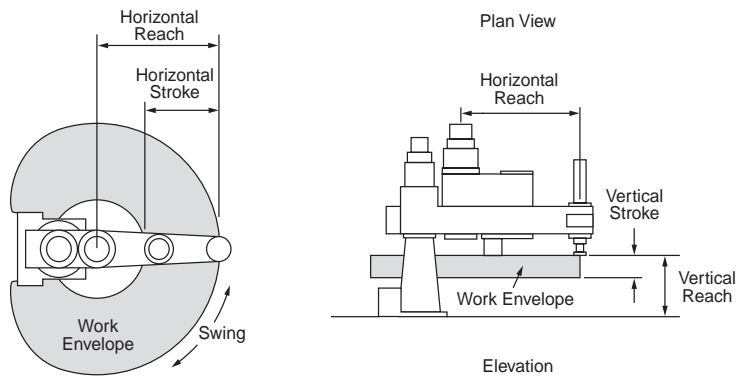


FIGURE 101.10 SCARA robot work envelope.

This configuration has many advantages and is quite popular in industry. The configuration was designed specifically for assembly tasks [Truman, 1990], so has distinct advantages when applied in this area. Because of the vertical orientation of the joints, gravity does not affect the dynamics of the first two joints. In fact, for these joints, the actuators can be shut off and the arm will not fall, even without the application of brakes. As the name SCARA implies, this allows compliance in the horizontal directions to be selectively varied; therefore, the robot can comply to horizontal forces. Horizontal compliance is important for vertical assembly operations. Because of the vertical linear joint, straight-line vertical motions are simple. Also, SCARA robots typically have high positional repeatability. The revolute joints allow high-speed motion. On the negative side, the resolution of the arm is not constant throughout the workspace, and the kinematic equations are relatively complex. In addition, the vertical motion of the SCARA configuration is typically quite limited. While the SCARA robot can reach around objects, it cannot reach over them in the same manner as an articulated arm.

Gantry Configuration

The gantry configuration is geometrically equivalent to the Cartesian configuration, but is suspended from an overhead crane and typically can be moved over a large workspace. It consists of three linear joints (PPP), and is illustrated in Fig. 101.11. In terms of work envelope, it will have a rectangular volume that sweeps out most of the inner area of the gantry system, with a height limited by the length of the vertical mast, and the headroom above the gantry system. One consideration in the selection of a gantry robot is the type of vertical linkage employed in the z axis. A monomast design is more rigid, yielding tighter tolerances for repeatability and accuracy, but requires significant headroom above the gantry to have a large range of z axis motion. On the other hand, a telescoping linkage will require significantly less headroom but is less rigid, with corresponding reduction in repeatability and accuracy. Other robot configurations can be mounted on gantry systems, thus gaining many of the advantages of this geometry.

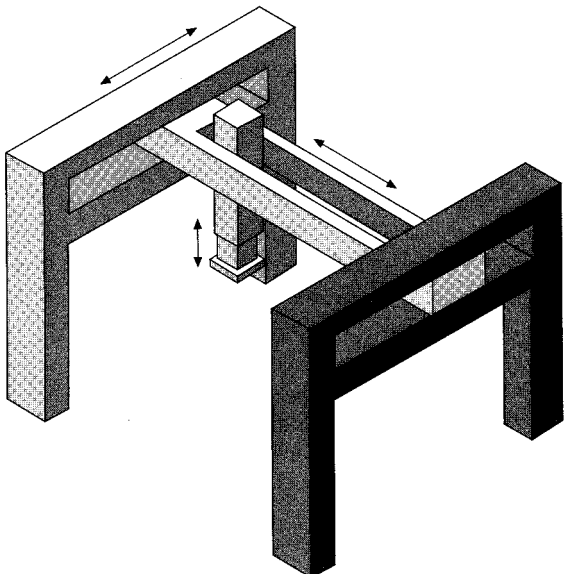


FIGURE 101.11 The gantry configuration. (Source: T. Owen, *Assembly with Robots*, Englewood Cliffs, N.J.: Prentice-Hall, 1985. With permission.)

Gantry robots have many advantageous properties. They are geometrically simple, like the Cartesian robot, with the corresponding kinematic and dynamic simplicity. For the same reasons, the gantry robot has a constant arm resolution throughout the workspace. The gantry robot has better dynamics than the pedestal-mounted Cartesian robot, as its links are not cantilevered. One major advantage over revolute-base robots is that its dynamics vary much less over the workspace. This leads to less vibration and more even performance than typical pedestal-mounted robots in full extension. Gantry robots are much stiffer than other robot configurations, although they are still much less stiff than Numerical Control (NC) machines. The gantry robot can straddle a workstation, or several workstations for a large system, so that one gantry robot can perform the work of several pedestal-mounted robots. As with the Cartesian robot, the gantry robot's simple geometry is similar to that of an NC machine, so technicians will be more familiar with the system and require less training time. Also, there is no need for special path or trajectory computations. A gantry robot can be programmed directly from a Computer-Aided Design (CAD) system with the appropriate interface, and straight-line motions are particularly simple to program. Large gantry robots have a very high payload capacity. Small, table-top systems can achieve linear speeds of up to 40 in./s (1.025 m/s), with a payload capacity of 5.0 lb (2.26 kg), making them suitable for assembly operations. However, most gantry robot systems are not as precise as other configurations, such as the SCARA configuration. Additionally, it is sometimes more difficult to apply a gantry robot to an existing workstation, as the workpieces must be brought into the gantry's work envelope, which may be harder to do than for a pedestal-mounted manipulator.

Gantry robots can be applied in many areas. They are used in the nuclear power industry to load and unload reactor fuel rods. Gantry robots are also applied to materials-handling tasks, such as parts transfer, machine loading, palletizing, materials transport, and some assembly applications. In addition, gantry robots are used for process applications such as welding, painting, drilling, routing, cutting, milling, inspection, and nondestructive testing.

The gantry robot configuration is the fastest-growing segment of the robotics industry. While gantry robots accounted for less than 5% of the units shipped in 1985, they are projected to account for about 30% of the robots by the end of the 1990s. One reason for this is summed up in Long [1990], which contains much more information on gantry robots in general:

Currently gantry robot cells are being set up which allow manufacturers to place a sheet of material in the gantry's work envelope and begin automatic cutting, trimming, drilling, milling, assembly and finishing operations which completely manufacture a part or subassembly using quick-change tools and programmed subroutines.

Additional Information

The above six configurations are the main types currently used in industry. However, there are other configurations used in either research or specialized applications. Some of these configurations have found limited application in industry and may become more prevalent in the future.

All the above configurations are serial-chain manipulators. An alternative to this common approach is the parallel configuration, known as the Stewart platform [Waldron, 1990]. This manipulator consists of two platforms connected by three prismatic linkages. This arrangement yields the full six DOF motion (three position, three orientation) that can be achieved with a six-axis serial configuration but has a comparably very high stiffness. It is used as a motion simulator for pilot training and virtual reality applications. The negative aspects of this configuration are its relatively restricted motion capability and geometric complexity.

The above configurations are restricted to a single manipulator arm. There are tasks that are either difficult or impossible to perform with a single arm. With this realization, there has been significant interest in the use of multiple arms to perform coordinated tasks [Bonitz and Hsia, 1996]. Possible applications include carrying loads that exceed the capacity of a single robot, and assembling objects without special fixturing. Multiple arms are particularly useful in zero-gravity environments. While there are significant advantages to the use of multiple robots, the complexity, in terms of kinematics, dynamics, and control, is quite high. However, the use of multiple robots is opening new areas of application for robots.

Typical industrial robots have six or fewer DOF. With six DOF, the robot can, within its work envelope, reach arbitrary positions and orientations. At the edge of the work envelope, a six-DOF robot can attain only one orientation. To increase the geometric dexterity of the manipulator, it is useful to consider robots with more than six DOF, i.e., redundant robots. These robots are highly dexterous and can use the extra DOF in many ways: avoidance obstacle, joint torque minimization, kinematic **singularity** (points where the manipulator cannot move in certain directions) avoidance, bracing strategies where part of the arm is braced against a structure, which raises the lowest structural resonant frequency of the arm, etc. While the **redundant manipulator** configuration has many desirable properties, the geometric complexity has limited their application in industry.

For any of the six standard robot configurations, the orientation capability of the major linkages is severely limited. Thus, it is critical to provide additional joints, known as the minor linkages, to provide the capability of varied orientations for a given position. Most robots include a three-DOF revolute joint wrist that is connected to the last link of the major linkages. The three revolute axes will be orthogonal and will usually intersect in a common point, known as the wrist center point. Then, the kinematic equations of the manipulator can be partitioned into locating the Cartesian position of the wrist center point and then determining the orientation of a Cartesian frame fixed to the wrist axes.

Conclusions

Each of the six standard configurations has specific advantages and disadvantages. When choosing a manipulator for a task, the properties of the manipulator geometry are one of the most important considerations. If the manipulator will be used for a wide variety of tasks, one may need to trade off performance for any given task for the flexibility that will allow the manipulator to work for the various tasks. In such a case, a more flexible geometry should be considered. The future of robotics will be interesting. With the steady increase in computational capabilities, the more complex geometries, including redundant and multiple robots, are beginning to see increased applications in industry.

Defining Terms

Degrees of freedom: The number of degrees of freedom (DOF) of a manipulator is the number of independent position variables that must be specified in order to locate all parts of the manipulator. For a typical industrial manipulator, the number of joints equals the number of DOF.

Kinematics: The kinematics of the manipulator refers to the geometric properties of the manipulator. *Forward kinematics* is the computation of the Cartesian position and orientation of the robot end-effector given the set of joint coordinates. *Inverse kinematics* is the computation of the joint coordinates given the Cartesian position and orientation of the end-effector. The inverse kinematic computation may not be possible in closed form, may have no solution, or may have multiple solutions.

Redundant manipulator: A redundant manipulator contains more than six DOF.

Singularity: A *singularity* is a location in the workspace of the manipulator at which the robot loses one or more DOF in Cartesian space, i.e., there is some direction (or directions) in Cartesian space along which it is impossible to move the robot end-effector no matter which robot joints are moved.

Related Topic

101.2 Dynamics and Control

References

- R.G. Bonitz and T.C. Hsia, "Internal force-based impedance control for cooperating manipulators," *IEEE Transactions on Robotics and Automation*, Feb. 1996.
- J.J. Craig, *Introduction to Robotics: Mechanics and Control*, Reading, Mass.: Addison-Wesley, 1986.
- A. J. Critchlow, *Introduction to Robotics*, New York: Macmillan, 1985.

- E. Long, "Gantry robots," in *Concise International Encyclopedia of Robotics*, R. C. Dorf, Ed., New York: Wiley-Interscience, 1990.
- R. Truman, "Component assembly onto printed circuit boards," in *Concise International Encyclopedia of Robotics*, R. C. Dorf, Ed., New York: Wiley-Interscience, 1990.
- K. J. Waldron, "Arm design," in *Concise International Encyclopedia of Robotics*, R. C. Dorf, Ed., New York: Wiley-Interscience, 1990.

Further Information

The journal *IEEE Transactions on Robotics and Automation* is a valuable source for a wide variety of robotics research topics, occasionally including new robot configurations. Additionally, IEEE's *Control Systems Magazine* occasionally publishes an issue devoted to robotic systems. The home page for the IEEE Robotics and Automation Society can be found at "<http://www.acim.usi.edu/RAS/>".

Another journal that often has robotics-related articles is the ASME *Journal of Dynamic Systems, Measurement and Control*.

An additional source of robotics information is *The Proceedings of the IEEE International Conference on Robotics and Automation*. This conference is held annually.

Useful sources on the World Wide Web include the *Robotics Internet Resources* page, located at "<http://piglet.cs.umass.edu:4321/robotics.html>", and *Robotics Resources*, located at "<http://www.eg.bucknell.edu/~robotics/rirc.html>". Consult your system administrator for information on this web access.

101.2 Dynamics and Control

R. Lal Tummala

The primary purpose of the robot control system is to issue commands to joint actuators to faithfully execute a planned trajectory in the **tool space**. This may involve position control when the manipulator is following a trajectory through free space or a combination of position and force control if the manipulator is to react continuously to contact forces at the tool or end-effector.

Control systems can operate either in open loop or closed loop. In open-loop systems, the output has no effect on the input. On the other hand, closed-loop systems continuously sense the output and make appropriate adjustments to the input in order to keep the output at the desired level.

The majority of the current industrial robots use the **independent joint control** method and close the loop around the joints of the robot. The desired joint positions corresponding to a tool trajectory are either taught by using a *teach box* or generated by solving an inverse kinematics problem. The independent joint control method, however, is effective only at low speeds. As the speeds increase, the coupling effects between the joints increase and warrant the inclusion of these effects in the controller development. Advanced controller development and implementation based on full dynamics is one of the active areas of current research. New advances in sensor technology, faster computers, advanced robots such as direct drive arms and industrial competition provide new opportunities and motivation for accelerating the development and implementation of advanced controllers for robots in the near future.

Independent Joint Control of the Robot

The independent joint control method assumes that a single joint of a robot is moving while all the other joints are fixed. A typical joint position control system is shown in Fig. 101.12, where the actuator used is a dc servomotor [Luh, 1983]. In general, any one or a combination of electric motors and hydraulic or pneumatic pistons can be used to move the joint through the desired positions. These motors may be connected directly to the joint or indirectly through gears, chains, cables, or lead screws. The desired joint positions that are inputs to the position loops are obtained from the trajectory planner. The actual position of the joint is obtained by using a position sensor, such as a potentiometer or an optical encoder. An amplifier is used for increasing the system gain, denoted by K_a . The velocity feedback K_v is used to reinforce the effect of back emf for controlling

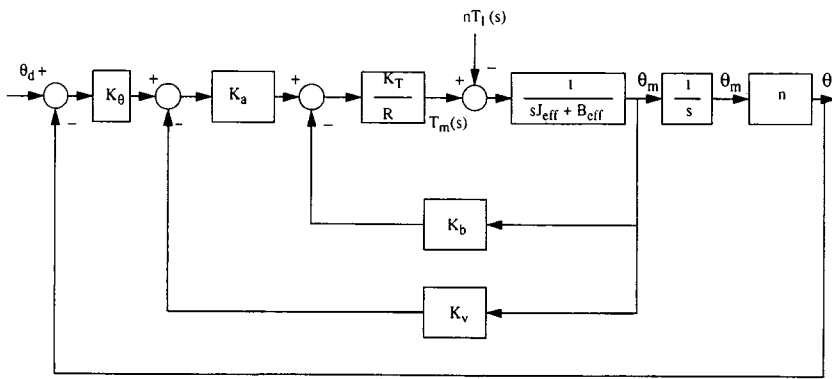


FIGURE 101.12 Closed-loop control of a robot joint. (Source: Adapted from J. Y. S. Luh, “Conventional controller design for industrial robots: A tutorial,” *IEEE Trans. Systems, Man, Cybernetics*, vol. SMC-13, no. 3, June 1983. © 1983 IEEE.)

the damping of the system. This can be done either using a tachometer or computing the difference in angular displacements of the actuator shaft over a fixed time interval.

The design of the control system involves fixing the values of K_a and K_v to achieve the desired response. Consider the closed-loop transfer function of the system shown in Fig. 101.12 (assuming $nT_l = 0$),

$$\frac{\theta_l(s)}{\theta_d(s)} = \frac{nK_a K_T K_\theta}{s^2 R J_{\text{eff}} + s(RB_{\text{eff}} + K_T K_b + K_a K_T K_v) + nK_T K_a K_\theta} \quad (101.1)$$

where K_a = gain of the amplifier, K_T = torque constant of the motor, K_b = back emf constant, K_θ = position sensor constant (volts/rad), R = resistance of the motor winding (ohms), and n = gear ratio. θ_L = link position (rad) and θ_m = angular displacement at the actuator side (rad).

The effective inertia, J_{eff} , and damping, B_{eff} are defined as

$$J_{\text{eff}} = J_m + n^2 J_L \quad (101.2)$$

and

$$B_{\text{eff}} = B_m + n^2 B_L \quad (101.3)$$

where J_m = total inertia on the motor side, B_m = damping coefficient at the motor side, J_L = inertia of the robot link, and B_L = damping coefficient at the load side.

This is a second-order system and stable for all values of K_a and K_v . The values of K_a and K_v are selected to achieve a desired transient response by fixing the damping ratio and the natural frequency of the system and are described below.

The characteristic equation for the above system is

$$s^2 + s \frac{RB_{\text{eff}} + K_T K_b + K_a K_T K_v}{R J_{\text{eff}}} + \frac{nK_T K_a K_\theta}{R J_{\text{eff}}} = 0 \quad (101.4)$$

This can be conveniently written as

$$s^2 + 2\zeta\omega_n s + \omega_n^2 = 0 \quad (101.5)$$

where the natural frequency ω_n and the damping ratio ζ of the system are given as

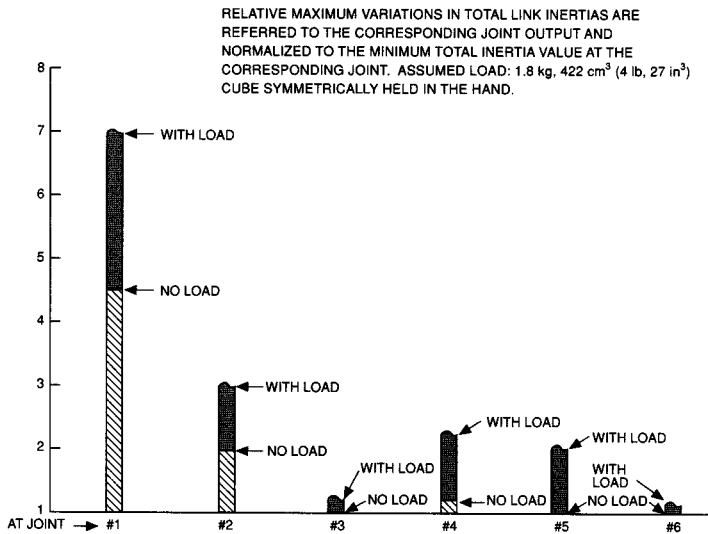


FIGURE 101.13 Variations of link inertias for JPL-Stanford manipulator. (Source: A.K. Bejczy, Jet Propulsion Lab, Pasadena, Calif., American Automatic Control Conference Tutorial Workshop, Washington, D.C., June 18, 1982.)

$$\omega_n = \sqrt{\frac{nK_a K_T K_\theta}{RJ_{\text{eff}}}} > 0 \quad (101.6)$$

$$\zeta = \frac{RB_{\text{eff}} + K_T K_b + K_a K_T K_v}{2\sqrt{nK_a K_T R J_{\text{eff}} K_\theta}} \quad (101.7)$$

These systems are designed to operate with critical damping ($\zeta = 1$) because an underdamped system ($\zeta < 1$) has fast response but results in an overshoot, whereas an overdamped system ($\zeta > 1$) is too slow. However, this is not always possible, because the damping ratio given by Eq. (101.7) depends on B_{eff} and J_{eff} which vary during the actual operation of the manipulator. B_{eff} changes with age or repeated use of the manipulator. J_{eff} varies with the payload. For example, the variation of J_{eff} for the Stanford manipulator under various loading conditions is shown in Fig. 101.13. J_{eff} also varies with the configuration of the manipulator during the actual operation. So a compromise solution will be to design the controller such that $\zeta \geq 1$ throughout the intended operation.

The undamped natural frequency ω_n is selected to be no more than half the resonance frequency of the robot to avoid any structural damage to the robot [Paul, 1981]. These resonances are possible due to the flexibilities associated with the links of the robot and the shafts within the drive system, to name a few. These are called *unmodeled* resonances because they are not explicitly included in the model. In our case, if K_{eff} and J_{eff} are the effective stiffness and the inertias of the joint, respectively, then the resonance frequency ω_r is given by

$$\omega_r = \sqrt{\frac{K_{\text{eff}}}{J_{\text{eff}}}} \quad (101.8)$$

Since K_{eff} is difficult to estimate but constant for a given joint, we can experimentally determine the resonance frequencies for a known inertia and use this information for fixing the gain. Suppose ω is the resonance frequency for a given value of effective inertia J , then

$$\omega = \sqrt{\frac{K_{\text{eff}}}{J}} \quad (101.9)$$

To minimize the effects of unmodeled resonances, we use

$$\omega_n \leq \frac{\omega_r}{2} = \frac{\omega}{2} \sqrt{\frac{J}{J_{\text{eff}}}} \quad (101.10)$$

The selection of K_a and K_v depends on selecting ζ and ω_n . Using Eqs. (101.6) and (101.10), we can find an upper bound on K_a given by

$$K_a \leq \frac{J\omega^2 R}{4nK_T K_\theta} \quad (101.11)$$

The upper bound on K_v is obtained by setting $\zeta \geq 1$. Using Eq. (101.7),

$$RB_{\text{eff}} + K_T K_b + K_a K_T K_v \geq 2\sqrt{nK_a K_T R J_{\text{eff}} K_\theta} \quad (101.12)$$

Substituting the upper bound for K_a from Eq. (101.11), we get

$$K_v \geq \left(\omega R \sqrt{J J_{\text{eff}}} - RB_{\text{eff}} - K_T K_b \right) \frac{4nK_\theta}{J\omega^2 R} \quad (101.13)$$

The steady-state errors to step position commands for the system shown in Fig. 101.12 are zero. However, in the presence of disturbances such as external load torques or **gravitational torques**, the system will have steady-state errors. For example, if T_L is the load torque as shown in Fig. 101.12, the available torque for the joint motion is given by

$$(J_{\text{eff}} s^2 + B_{\text{eff}} s) \Theta_m(s) = T_m(s) - nT_L(s) \quad (101.14)$$

Using the superposition property, we get

$$\Theta_L(s) = F_1(s)\Theta_d(s) + F_2(s)T_L(s) \quad (101.15)$$

where

$$\begin{aligned} F_1(s) &= \frac{nK_a K_T K_\theta}{\Omega(s)} \\ F_2(s) &= -\frac{n^2 R}{\Omega(s)} \end{aligned} \quad (101.16)$$

$$\Omega(s) = RJ_{\text{eff}} s^2 + (RB_{\text{eff}} + K_b K_T + K_v K_a K_T) s + nK_a K_T K_\theta$$

Now if $T_L(s) = C_L/s$ and $\Theta_d(s) = C_\theta/s$, then the steady-state error is

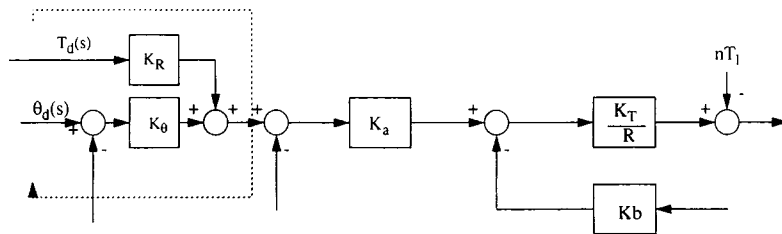


FIGURE 101.14 Feedback compensation method for disturbances. (Source: Adapted from J. Y. S. Luh, “Conventional controller design for industrial robots: A tutorial,” *IEEE Trans. Systems, Man, Cybernetics*, vol. SMC-13, no. 3, June 1983. ©1983 IEEE.)

$$e_{ss} = \frac{nC_L R}{K_a K_T K_\theta} \quad (101.17)$$

Since the value of K_a has an upper bound, this error cannot be made arbitrarily small. A possible way to reduce this error is to add a feedforward term, as shown in Fig. 101.14 [Luh, 1983]. The feedforward signal $T_d(s)$ is chosen such that the steady-state error is zero. In this case,

$$T_d(s) = \frac{R}{K_T K_a K_R} n\hat{T}_L(s) \quad (101.18)$$

Similar considerations apply for other disturbances such as frictional torques and gravitational torques. Notice from Eq. (101.18) that the feedforward signal is a function of the estimated torque. The burden of determining these torques should not be underestimated. The other factor that was not mentioned earlier is the centrifugal torque, a nonlinear function of velocity. In the case of positioning applications, the velocity tends to zero as $t \rightarrow \infty$. However, if the robot is required to follow a conveyor with constant speed, then the input is a velocity. In this case, the centrifugal contribution will affect the steady-state velocity error. A feed-forward compensation can be used in this case as well. Another method of compensating for the steady-state errors caused by gravitational and load torque disturbances is by adding an integral feedback (PID control), which of course increases the order of the system. The system is no longer stable for all values of the gains and thus adds another constraint in the selection of K_a and K_θ .

So far we have considered the control of one joint of the robot while the other joints are fixed. Implementation of this control by successively positioning each joint while the other joints are fixed slows the robot operation and can also result in awkward hand motions, which is undesirable especially when the robot is supposed to follow a continuous path. Simultaneous fast motion of the joints, on the other hand, requires the inclusion of dynamic interactions between the joints. The controllers designed without considering these dynamic interactions tend to make the arm move slower and can potentially cause overshoots, oscillations, and path errors. To estimate the dynamic effects, one needs to obtain the equations of motion (dynamic models) of the robot. These equations are, in general, complex and take the form of coupled nonlinear differential equations.

Dynamic Models

Two of the most popular methods used to obtain dynamic models of the robot are the *Newton-Euler method* and the *Lagrange-Euler method*. The equations obtained using Lagrangian formulation are more suitable for the application of modern control theory than the recursive equations obtained using the Newton-Euler method. In the Lagrangian formulation, the dynamic models are obtained using kinetic and potential energies associated with the rigid bodies in motion. The derivation is systematic and conceptually simple. This method yields closed-form dynamic equations that explicitly express joint variables in terms of joint torques. To arrive

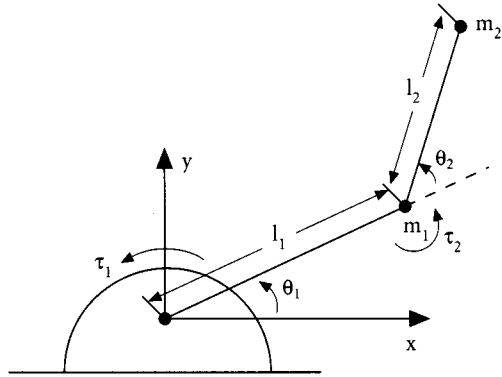


FIGURE 101.15 Two-degree-of-freedom planar manipulator.

at these equations, one starts with a set of generalized coordinates q_i , $i = 1, 2, 3, \dots, n$, that completely locate the dynamic system and finds the total kinetic energy K and potential energy P of the system [Paul, 1981]. Then the equations of motion are given by

$$\frac{d}{dt} \frac{\partial L}{\partial \dot{q}_i} - \frac{\partial L}{\partial q_i} = T_i \quad \text{for } i = 1, 2, 3, \dots, n \quad (101.19)$$

where T_i is the generalized force and $L(q, \dot{q}) = K - P$ is the Lagrangian. A simple example is given next to illustrate these ideas.

Example. Consider a planar arm with two degrees of freedom, shown in Fig. 101.15. For simplicity, we assume that the masses m_1 and m_2 of the links are represented by point masses at the end of the links. The link lengths are l_1 and l_2 , respectively. The variables θ_1 and θ_2 are the joint angles. We know that the kinetic energy of a mass m moving at a linear velocity v is given by $1/2 mv^2$ and the potential energy associated with a mass m located at a height h in a gravitational field is given by mgh , where g is the gravitational constant.

The kinetic energy K_1 for mass m_1 is found by observing that

$$\begin{aligned} x_1 &= l_1 \cos \theta_1 \\ y_1 &= l_1 \sin \theta_1 \\ v_1^2 &= \dot{x}_1^2 + \dot{y}_1^2 \\ K_1 &= \frac{1}{2} m_1 l_1^2 \dot{\theta}_1^2 \end{aligned} \quad (101.20)$$

Similarly, the kinetic energy K_2 for mass m_2 is given by

$$\begin{aligned} K_2 &= \frac{1}{2} m_2 v_2^2 \\ v_2^2 &= \dot{x}_2^2 + \dot{y}_2^2 \end{aligned} \quad (101.21)$$

From Fig. 101.15, we have

$$\begin{aligned} x_2 &= l_1 \cos \theta_1 + l_2 \cos(\theta_1 + \theta_2) \\ y_2 &= l_1 \sin \theta_1 + l_2 \sin(\theta_1 + \theta_2) \\ v_2^2 &= l_1^2 \dot{\theta}_1^2 + l_2^2 (\dot{\theta}_1 + \dot{\theta}_2)^2 + 2l_1 l_2 \cos \theta_2 (\dot{\theta}_1^2 + \dot{\theta}_1 \dot{\theta}_2) \end{aligned} \quad (101.22)$$

The potential energies for the masses m_i , $i = 1, 2$, are given by

$$\begin{aligned} P_1 &= m_1 g l_1 \sin \theta_1 \\ P_2 &= m_2 g [l_1 \sin \theta_1 + l_2 \sin(\theta_1 + \theta_2)] \end{aligned} \quad (101.23)$$

The next step is to form the Lagrangian,

$$L = \sum_{i=1}^2 K_i - P_i$$

The dynamic model of the robot is obtained by using Eq. (101.19),

$$\tau_1 = \frac{d}{dt} \left[\frac{\partial L}{\partial \dot{\theta}_1} \right] - \frac{\partial L}{\partial \theta_1} \quad (101.24)$$

$$\tau_2 = \frac{d}{dt} \left[\frac{\partial L}{\partial \dot{\theta}_2} \right] - \frac{\partial L}{\partial \theta_2} \quad (101.25)$$

where τ_i , $i = 1, 2$, are the joint torques.

The equations for a general n -degrees-of-freedom robot can be derived by following the same procedure and are compactly written in the generalized coordinates q as

$$D(q)\ddot{q} + H(q, \dot{q}) + V\dot{q} + G(q) = \tau \quad (101.26)$$

where $D(q)$ is the $n \times n$ inertia matrix, $H(\cdot)$ is an $n \times 1$ vector describing the centripetal and Coriolis terms, V is the coefficient of friction and $G(q)$ is an $n \times 1$ vector describing gravitational torques. For the above example, $q_1 = \theta_1$ and $q_2 = \theta_2$. Thus,

$$D(\theta) = \begin{bmatrix} l_2^2 m_2 + 2l_1 l_2 m_2 \cos \theta_2 + l_1^2 (m_1 + m_2) & l_2^2 m_2 + l_1 l_2 m_2 \cos \theta_2 \\ l_2^2 m_2 + l_1 l_2 m_2 \cos \theta_2 & l_2^2 m_2 \end{bmatrix} \quad (101.27)$$

$$H(\theta, \dot{\theta}) = \begin{bmatrix} -m_2 l_1 l_2 \sin \theta_2 \dot{\theta}_2^2 - 2m_2 l_1 l_2 \sin \theta_2 (\dot{\theta}_1 \dot{\theta}_2) \\ (m_2 l_1 l_2 \sin \theta_2) \dot{\theta}_1^2 \end{bmatrix} \quad (101.28)$$

$$G(\theta) = \begin{bmatrix} m_2 l_2^2 g \cos(\theta_1 + \theta_2) + (m_1 + m_2) l_1 g \cos \theta_1 \\ m_2 l_2 g \cos(\theta_1 + \theta_2) \end{bmatrix} \quad (101.29)$$

where

$$\theta = \begin{bmatrix} \theta_1 \\ \theta_2 \end{bmatrix} \quad \dot{\theta} = \begin{bmatrix} \dot{\theta}_1 \\ \dot{\theta}_2 \end{bmatrix} \quad \ddot{\theta} = \begin{bmatrix} \ddot{\theta}_1 \\ \ddot{\theta}_2 \end{bmatrix} \quad (101.30)$$

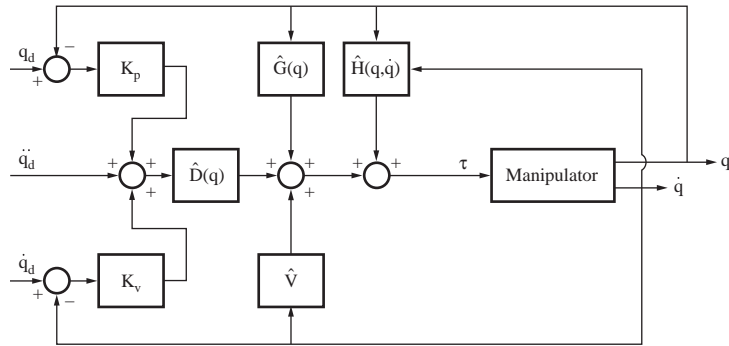


FIGURE 101.16 Computed torque method.

Notice that the inertia matrix $D(\theta)$ is a function of only the position θ . In general, the inertia matrix is symmetric and positive definite and thus invertible. The diagonal elements of this matrix represent the effective inertias at the respective joints, while the off-diagonal elements represent the coupling inertias. For example, the term $m_2 l_2$ represents the effective inertia at the joint 2, and the term $l_2 m_2 + l_1 l_2 m_2 \cos \theta_2$ represents the coupling inertia between joints 1 and 2, i.e., the effect of acceleration of joint 1 on joint 2.

The terms in the matrix $H(\cdot)$ contain all the terms associated with the **centripetal** and **Coriolis forces**. The terms that depend upon the square of the joint velocity are *centripetal forces*. The terms that contain the product of joint velocities are *Coriolis forces*. In our example, the term $-(m_2 l_1 l_2 \sin \theta_2) \dot{\theta}_2^2$ represents the centripetal force acting at joint 1 due to the velocity at joint 2. Similarly, the term $(m_2 l_1 l_2 \sin \theta_2) \dot{\theta}_1^2$ represents the centripetal force acting at joint 2 due to the velocity at joint 1. The term $-(2m_2 l_1 l_2 \sin \theta_2) \dot{\theta}_1 \dot{\theta}_2$ is the Coriolis force acting at joint 2 due to the velocities at joints 1 and 2.

The term $G(\theta)$ contains all the terms involving gravitational constant g . Note that these terms depend only on the position of the arm in the gravitational field. If the arm is operating in the gravity-free environment, then these terms become zero. The term $V\theta$ reflects the frictional forces present in the robot system. In our example, these terms are assumed to be zero. However, in practical robots a substantial amount of friction stiction can be present that if not considered will overestimate the torque available for accelerating the joints.

The above example illustrates that the existence of significant coupling between the joints, if ignored, can cause positioning and tracking errors when the joints are moving simultaneously. However, all these coupling terms become small at low speeds. In this case, independent joint control with appropriate compensations as discussed earlier may be quite adequate. As the operational speeds increase, one needs to take into consideration the full dynamics in the development of control algorithms.

Computed Torque Methods

Several control algorithms that incorporate dynamics have been developed. Many of these are variations of the computed torque method, which is similar to the feedback linearization method used for the control of nonlinear systems [Spong and Vidyasagar, 1989]. In the computed torque method shown in Fig. 101.16, the required input forces or torques are computed as follows:

$$\tau = \hat{D}(q) [\ddot{q}_d + K_v(\dot{q}_d - \dot{q}) + K_p(q_d - q)] + \hat{H}(q, \dot{q}) + \hat{V}\dot{q} + \hat{G}(q) \quad (101.31)$$

where K_v and K_p are diagonal matrices with diagonal elements representing velocity and position gains. If this torque is chosen as the input in Eq. (101.26), and assuming that the model is accurate, i.e., $\hat{D}(q) = D(q)$, $\hat{H}(q, \dot{q}) = H(q, \dot{q})$ etc., we get

$$D(q) [\ddot{q}_d - \ddot{q} + K_v(\dot{q}_d - \dot{q}) + K_p(q_d - q)] = 0 \quad (101.32)$$

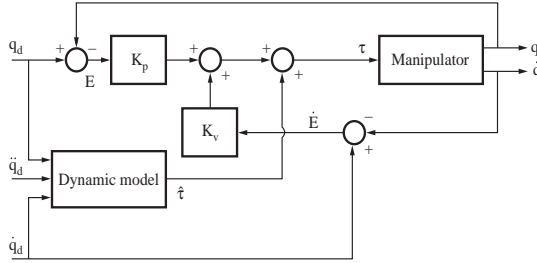


FIGURE 101.17 Dynamic model outside the feedback loop.

Since the inertia matrix, $D(q)$ is nonsingular, we get

$$\ddot{E} + K_v \dot{E} + K_p E = 0 \quad (101.33)$$

which represents a set of decoupled equations where the error $E = q_d - q$. If we select the values of K_v and K_p such that the characteristic roots of Eq. (101.33) have negative real parts, then E approaches zero asymptotically. Effectiveness of this algorithm depends heavily on two factors: (1) the accuracy of the model and (2) the ability to compute the coefficient matrices of the equations of motion in real time.

If the model is not an exact representation of the system, Eq. (101.33) becomes

$$\ddot{E} + K_v \dot{E} + K_p E = R(\ddot{q}, \dot{q}, q) \quad (101.34)$$

where R is the mismatch between the model and the actual dynamics of the robot. This is given by

$$R(\ddot{q}, \dot{q}, q) = \hat{D}^{-1}(q)[(D(q) - \hat{D}(q))\ddot{q} + (H(q, \dot{q}) - \hat{H}(q, \dot{q})) + G(q) - \hat{G}(q)] \quad (101.35)$$

Observe that if the model is an exact match, Eq. (101.34) leads to Eq. (101.33) and the convergence of q to q_d can be guaranteed.

Even if the model is accurate, the ability to compute the dynamics at sample rate (60 to 100 Hz is typical) is still a problem. It is estimated that the Stanford manipulator requires 2000 floating-point additions and 1500 multiplications to compute all joint torques. A way to overcome this problem is to use the control scheme where the model is outside the feedback loop shown in Fig. 101.17, [Craig, 1989]. In this case, the desired torques are calculated *a priori* using the model given in Eq. (101.26) as follows:

$$\hat{\tau} = \hat{D}(q_d)\ddot{q}_d + \hat{H}(q_d, \dot{q}_d) + \hat{V}\dot{q}_d + \hat{G}(q_d) \quad (101.36)$$

Then from Fig. 101.17, we get

$$D\ddot{q} + H(q, \dot{q}) + V\dot{q} + G(q) = \hat{\tau} + K_v(\dot{q}_d - \dot{q}) + K_p(q_d - q) \quad (101.37)$$

If the mismatch between the model and the robot is small, then we get

$$D(\ddot{q}_d - \ddot{q}) + K_v(\dot{q}_d - \dot{q}) + K_p(q_d - q) = 0 \quad (101.38)$$

Since the inertia matrix is nonsingular, we can rewrite the above equation as

$$\ddot{E} + D^{-1}K_v \dot{E} + D^{-1}K_p E = 0 \quad (101.39)$$

where $E = q_d - q$ and can be made to go to zero asymptotically by selecting the gains K_v and K_p appropriately. This method has a definite advantage over the earlier method because the model need not be evaluated in real time. However, it does not provide complete decoupling because the inertia matrix is not diagonal. Furthermore, since the gains are continuously modified by the inertia matrix, the response is a function of the configuration and the payload. A way to circumvent this problem is to continuously modify the gains K_v and K_p . This obviously suggests an adaptive control approach.

Adaptive Control

In an attempt to reduce the errors caused by the mismatch of the model with the real system, several adaptive control schemes have been investigated. Model reference adaptive control (MRAC) is one such approach. Dubowsky and DesForges [1979] were the first to use this method for manipulator control. This method is illustrated in Fig. 101.18. They have chosen a linear second-order system with desired ζ and ω_n as a reference model for each joint. Their scheme works as long as the manipulator changes configuration slowly relative to the adaptation rate. Since then several researchers have extended the concepts well developed for linear systems to manipulator control. Two aspects that are central to all these methods are identification of the plant or its parameters and use of this new information to update the control law. An extensive review of recent work in this area is given by Craig [1988] and Hsia [1986]. In spite of many approaches suggested for this problem, no attempt has been made to implement these methods by the robot industry.

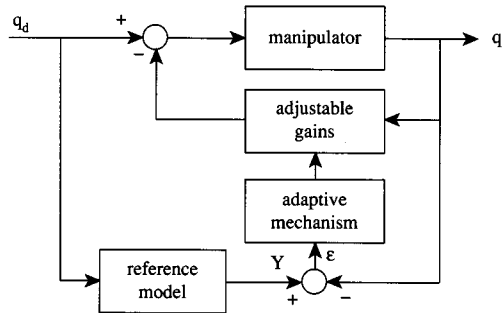


FIGURE 101.18 Model reference adaptive control.

Resolved Motion Control

So far we have discussed the methods to achieve desired joint motion. In practice, the desired motion is specified in terms of hand motions. Resolved motion control methods such as *resolved motion rate control* (RMRC) and *resolved motion acceleration control* have been suggested [papers by Whitney and Luh et al. in Brady et al., 1982]. In these methods, the joint motions are coordinated to achieve coordinated hand motion along any world coordinate axis. Given the relationship between the position and orientation of the hand, $x(t)$, and the joint coordinates $q(t)$ as

$$x(t) = f(q(t)) \quad (101.40)$$

then RMRC transforms the linear and angular velocity of the hand (end effector) to joint velocities using the relationship

$$\dot{q} = J^{-1}(q(t))\dot{x} \quad (101.41)$$

where $J(q(t))$ is the **Jacobian** matrix. Using the above equation, the combination of the joint rates for a given hand motion can be obtained. However, special consideration must be given when the inverse of the Jacobian matrix does not exist. This occurs when the dimension of $x(t)$ and $q(t)$ are not the same (robots with redundant

degrees of freedom) or when a nonredundant robot loses one or more degrees of freedom in its workspace (singular configurations).

Resolved motion acceleration control extends the concepts of RMRC by including desired acceleration of the hand as well. Differentiating Eq. (101.41) twice with respect to time, we get

$$\ddot{x} = J(q)\ddot{q} + \dot{J}(q, \dot{q})\dot{q}(t) \quad (101.42)$$

where \ddot{x} is the acceleration of the hand and \ddot{q} is the joint acceleration. To reduce the position and orientation errors of the hand to zero,

$$\ddot{x}(t) = \ddot{x}_d(t) + K_v[\dot{x}_d(t) - \dot{x}(t)] + K_p[x_d(t) - x(t)] \quad (101.43)$$

By selecting the gains K_p and K_v we can force the error $e(t) = x_d(t) - x(t)$ to zero as before. The desired joint acceleration can be obtained from Eqs. (101.41) and (101.42), and is given as follows:

$$\ddot{q}(t) = J^{-1}(q) \begin{bmatrix} \dot{x}_d(t) + K_v(\dot{x}_d(t) - \dot{x}(t)) \\ + K_p(x_d(t) - x(t) - \dot{J}(q, \dot{q})\dot{q}(t)) \end{bmatrix} \quad (101.44)$$

Since the inverse of the Jacobian is involved, this method suffers from drawbacks similar to the RMRC method.

Compliant Motion

The position control methods described above are not sufficient when the robot has to react continuously to contact forces at the end effector. Consider, for example, a simple operation of sliding a block of wood on a table along a desired path. Pure position control will not work because any small errors orthogonal to the table may result in the block either losing contact with the surface of the table or forcing the block through the table, which can either damage the table or the end effector. To perform this task, we need to control the position in the plane of the table and control force normal to the table. This is called *compliant motion control* and is required whenever the robot is in contact with its “environment.” To perform the above task, for example, a coordinate system called a *compliance frame* or *constraint frame* is defined such that at each instant and along each axis the task can be expressed as a pure position control or pure force control. Suppose we associate a coordinate system with the z -axis normal to the table surface. Then to perform this task, we need to control the position along the x and y directions and force control in the z direction to maintain continuous contact with the table surface. In this case, the position along the z direction is not controlled because one cannot control both position and force in the same direction, just as we cannot control both voltage and current across a resistor. Hence, this framework will provide a natural separation between the axes that need to be position controlled and the axes that need to be force-controlled. This is the idea behind the hybrid position/force control developed by Raibert and Craig [1981]. Another approach for compliant motion control is the impedance control [Hogan, 1985]. Impedance control does not control the end-point position or force directly, rather a desired dynamic relationship between position and force (mechanical impedance). For a good comparison between these two approaches, the reader is referred to Asada and Slotine [1986].

In general, compliance motion control is very important whenever the robot is required to make contact with its “environment.” This is true for many assembly tasks. Apart from the active methods of control discussed above, passive methods can be used to introduce the desired compliance. One such passive scheme is the use of a *remote center compliance* (RCC) device developed at Draper Laboratories. The RCC is a purely mechanical device consisting of a spring with six degrees of freedom that is inserted between the wrist and the end effector. By adjusting the stiffness of the springs, various levels of compliance can be obtained. However, passive methods suffer from lack of programmability achieved through active methods. Active control methods, however, require

sensing of contact forces and torques at the end effector. *Joint torque sensors*, *wrist sensors*, *fingertip tactile sensors*, and *force pedestals* can be used for this purpose.

Joint torque sensors, as the name implies, are placed at the joints of the manipulator. If \mathbf{F} represent the vector of forces at the end effector, then the corresponding vector of joint torques is obtained by using $\boldsymbol{\tau} = [\mathbf{J}(q)]^T \mathbf{F}$, where $\mathbf{J}(q)$ is the Jacobian and q are the generalized joint coordinates. Joint torque sensing has some drawbacks. First, to obtain the endpoint forces \mathbf{F} , the Jacobian which changes with the configuration has to be inverted in real time. Second, the sensors at the joints not only measure the forces and torques applied at the hand but also those applied at the other points of the manipulator. *Wrist sensors* are better at reducing this uncertainty because they are placed close to the end effector and below the last powered joint of the manipulator. Several wrist sensors are available commercially with necessary electronics to obtain force/torque measurements at high speeds suitable for real-time force control. Another method for providing information about the gripping forces is by mounting *tactile sensors* at the fingertips. However, these may not be suitable in situations where high gripping forces are required. *Force pedestals* are employed when a common platform is used for many tasks. In this case, the platform is instrumented to measure interacting forces and torques.

Flexible Manipulators

The discussion so far assumed that the links of the robot are rigid. These are designed intentionally to minimize the vibrations. Most of the present-day industrial robots fall into this category. These robots, however, cannot handle objects heavier than about 5% their weight. In contrast, lightweight flexible arms consume less energy, achieve faster speeds, and can potentially perform precision assembly tasks. However, it is not possible to move these arms quickly without the onset of structural vibrations due to inadequate structural damping. Efforts have been underway to increase the damping without substantial increase in weight by using composite materials or actively controlling the vibrations, or both.

Defining Terms

Centripetal forces: Forces that are present during the robot motion. They depend upon the square of the joint velocities of the robot and tend to reduce the power available from the actuators.

Compliant motion: Motion of the manipulator (robot) when it is in contact with its “environment,” such as writing on a chalkboard or assembling parts.

Coriolis forces: Forces/torques that depend upon the product of joint velocities.

Gravitational torques: Torques that depend upon the position of the robot in the gravitational field.

Independent joint control: A method where each joint is controlled as a single input/single output system. The coupling effects due to motion of other joints are either ignored or treated as disturbances.

Inverse kinematics: A model that maps end-effector positions and orientations to joint variables.

Jacobian of the manipulator: A matrix that maps the joint velocities into end effector velocities.

Tool space: Space of a 6×1 vector representing the positions and orientations of the tool or end effector of the robot.

Related Topics

100.2 Dynamic Response • 101.1 Robot Configuration

References

- H. Asada and J. J. E. Slotine, *Robot Analysis and Control*, New York: John Wiley & Sons, 1986.
M. Brady, J.M. Hollerbach, T.L. Johnson, T. Lozano-Perez, and M.T. Mason, *Robot Motion: Planning and Control*, Cambridge, Mass.: The MIT Press, 1982.
J. J. Craig, *Adaptive Control of Mechanical Manipulators*, Reading, Mass.: Addison-Wesley, 1988.
J. J. Craig, *Introduction to Robotics*, Reading, Mass.: Addison-Wesley, 1989.
S. Dubowsky and D.T. DesForges, “The application of model-referenced adaptive control of robotic manipulators,” *ASME J. Dyn. Syst. Meas. Control*, 1979.

- K. Fu, R. Gonzalez, and C.S.G. Lee, *Robotics: Control, Sensing, Vision, and Intelligence*, New York: McGraw-Hill, 1987.
- T.C. Hsia, "Adaptive control of robot manipulators—a review," IEEE Conference on Robotics and Automation, San Francisco, 1986.
- N. Hogan, "Impedance control: An approach to Manipulation, Part I, II, and III" *ASME J. Dyn. Sys. Meas. Control*, vol. 107, Mar. 1985.
- A. Koivo, *Control of Robotic Manipulators*, New York: John Wiley & Sons, 1989.
- J.Y.S. Luh, "Conventional controller design for industrial robots—a tutorial," *IEEE Trans. Syst., Man and Cybern.*, vol. SMC-13, no. 3, June 1983.
- R.P. Paul, *Robot Manipulators: Mathematics, Programming and Control*, Cambridge, Mass.: The MIT Press, 1981.
- M. Raibert and J. Craig, "Hybrid position/force control of manipulators," *ASME J. Dyn. Syst. Meas. Control*, June 1981.
- M. W. Spong and M. Vidyasagar, *Robot Dynamics and Control*, New York: Wiley, 1989.

Further Information

More information about this subject can be obtained by referring to many of the textbooks available on this subject. These are given in the References. Readers who are interested in current research may refer to several journals published by the Institute of Electrical and Electronics Engineers. In particular, *IEEE Transactions on Robotics and Automation*, *IEEE Transactions on Automatic Control*, and *IEEE Transactions on Systems, Man and Cybernetics* along with the conference proceedings published by the respective societies are useful in this regard.

101.3 Applications

Nicholas G. Odrey

An important utilization of robotics has traditionally been in manufacturing operations. By their very design and reprogrammable features, robots have enhanced the capabilities for flexibility in automation. Robot applications initially focused on replacing repetitive, boring, and hazardous manual tasks. Such initial applications required minimal control, programming, or sensory capability and have evolved to applications that use enhanced controller designs and sophisticated sensory capability. The first recorded commercial application of an industrial robot was at the Ford Motor Company in 1961 that used a Unimate robot to unload a die-casting machine. Since then, robots have been used in various manufacturing processes, fabrication, and assembly operations. Current issues relate to the degree of integration with the total manufacturing system and to the degree of autonomy and/or complexity one wishes to implement for a robotic system. In potential applications, it is necessary to determine the degree of sophistication that one wishes to implement coupled with a detailed economic analysis. The focus in this section is to present a practical implementation strategy for robots within a manufacturing environment, to review particular applications, and to discuss issues relevant to enhancing robot applications on the manufacturing shop floor. Such issues include sensors and their integration within an intelligent control system, the development of grippers for enhanced dexterity, and integration topics within a flexible **cellular manufacturing** system.

Justification

Reprogrammable automated devices such as robots provide the flexible automation capability for modern production systems. To evaluate a potential robotic application within a manufacturing environment, both technical and economic issues must be addressed. Typical technical issues include the choice of the number of **degrees of freedom** to perform a task, the level of controller and programming complexity, end effector and sensor choices, and degree of integration within the overall production system. Economic issues have typically been addressed from a traditional point of view, but it is important to note that other criteria should also be evaluated before a final decision is made to implement a robotic system. Such criteria may be both quantitative and qualitative.

Traditional economic approaches analyze investments and costs to compare alternative projects. Three methods are commonly used: (1) payback period method, (2) equivalent uniform annual costs (EUAC) method, and (3) return on investment (ROI). The payback method balances initial investment cost against net annual cash flow during the life of the project to determine the time required to recoup the investment. Many corporations today require relatively short (1- to 3-year) payback periods to justify an investment. In the current environment with the drive toward shortened product life cycles, it is not unusual to see payback period requirements of no greater than 1 year. The payback technique does not consider the time value of money and should be considered only as a first part attempt at justification.

The EUAC and ROI methods consider the time value of money (continuous or discrete compounding) and convert all investments, cash flows, salvage values, and any other revenues and costs into their equivalent uniform annual cash flow over the anticipated life of the project. In the EUAC method, the interest rate is known and set at a minimal acceptable rate of return, whereas the ROI method has the objective to determine the interest rate earned on the investment. Details to such techniques are presented in various engineering economy texts such as those by White et al. [1977] and Thuesen and Fabrycky [1989].

Various more sophisticated approaches have been taken to justify robotic and automated system implementation. Estimates of indirect factors such as taxes, capital gain or losses, variability consideration, and associated expected value analysis along with **decision tree analysis** and Markovian decision analysis [Michel, 1986] are but a few methods to justify such systems. Other factors to be recognized in robotic justification are that robots are reusable from one project to the next and there is a difference in production rates for a robotic implementation over a manual process. A changeover from a manual method to a robotic implementation would have the potential to affect revenues for any project. Many companies have also developed standard investment analysis forms for an economic evaluation of a proposed robot project. These forms are helpful in displaying costs and savings for a project. Groover et al. [1986] presents one such proposed form and gives several references to examples of forms specifically designed for projects devoted to robotics and related automation areas.

The aforementioned techniques are important in performing an economic justification for a proposed robotic installation. Still, in general, there are other issues that should be included in the overall analysis. These issues are of particular importance if one is considering installing a more comprehensive system such as a flexible manufacturing system that may include many robots and automated systems. As noted by Proth and Hillion [1990], these issues give rise to criteria that are both quantitative and qualitative. Quantitative criteria include not only reduced throughput time and work-in-process inventory but also criteria related to increased productivity coupled with fewer resources. Another measurable criterion is the reduction in management and monitoring staff as a result of smaller quantities and automatic monitoring by sensors. Quality improvement can also be measured both quantitatively and qualitatively. Qualitative benefits from quality improvement can include increased customer satisfaction, increased competitiveness, simplified production management, and other factors. It should be noted that any benefits and cost reductions for installation of an automated system are difficult to evaluate and reflect a long-term commitment of the corporation.

Strategic factors should be incorporated in the overall economic justification process, but they are difficult to access and incorporate due to their inherent complexity. Verk [1990] proposes a general framework that attempts to integrate both qualitative and quantitative factors in an economic justification process. The approach taken is being tested at Cincinnati Milacron and the Mazak Corporation.

Implementation Strategies

A logical approach is a prerequisite to robotic implementation within a manufacturing firm. The following steps have been proposed by Groover et al. [1986] to implement a robotic system:

1. Initial familiarization with the technology.
2. Plant survey to identify potential applications.
3. Selection of an application(s).
4. Selection of a robot(s) for the application(s).
5. Detailed economic analysis and capital authorization.
6. Plan and engineer the installation.
7. Installation.

It should be noted that a particular company may have nuances that could modify the above steps. Also of note is that the underlying issue is systems integration and any robotic application should consider total system impact as well as include the equipment, controllers, sensors, software, and other necessary hardware to have a fully functional and integrated system. Another good source of information on robot implementation is the text by Asfahl [1992].

Critical factors for the introduction of robotics technology within a corporation are management support and production personnel acceptance of the technology. Companies such as General Electric have developed checklists to determine the degree of workforce acceptance. Given that the above two factors are met, a plant survey is conducted to determine suitability for automation or robotic implementation. Two general categories of robot applications may be distinguished: (1) a project for a new plant, or (2) placing a robot project in an existing facility. We focus here on the latter category.

General considerations for a robot installation include hazardous, repetitive, or uncomfortable working conditions, difficult handling jobs, or multishift operations. High- and medium-volume production typically has many examples of repetitive operations. It can prove useful to investigate injury (particularly muscular) reports with medical personnel and ergonomics experts to identify potential manual operations that may be alleviated with the aid of robotics or automation. Multishift operations associated with high demand for a product are likely candidates for robot applications. As compared to manual work that typically has a high variable labor cost, a robot substitution would have a high fixed cost which can be distributed over the number of shifts plus a low variable cost. The overall effect of a robot application would then be to reduce the total operating cost.

Once potential robot applications are identified, one typically must determine which application is the best to pursue. Economic and technical criteria must both be considered. Usually, a simple application that is easy to integrate into the overall system is a good initial choice. A fundamental rule is to implement any straightforward application to minimize the risk of failure. The General Electric Company has been successful in choosing robot applications by considering the following technical criteria:

- Operation is simple and repetitive.
- Cycle time for the operation is greater than five seconds.
- Parts can be delivered with the proper POSE (position and orientation).
- Part weight is suitable (typical upper weight limit is 1100 lb).
- No inspection is required for the operation.
- One to two workers can be replaced in a 24-hour period.
- Setups and changeovers are infrequent.

A choice of a robot for a selected application can be a very difficult decision. Vendor information, expert opinion, and various sources such as the *Robotics Product Database* [Flora, 1989] can aid in the selection. Selection needs to consider the appropriate combination of parameters suitable for the application. These parameters or technical features include the degrees of freedom, the type of drive and control system, sensory capability, programming features, accuracy and precision requirements, and load capacity of the selected robot. Various point or weighing schemes can be applied to rate different robot models.

The planning and engineering of a robot installation must address many issues, including the operational methods to be employed, workcell design and its control, the choice or design of end effectors and other fixturing and tooling requirements, and sensory and programming requirements. In addition, one needs to focus on safety considerations for the workcell as well as overall systems integration. Computer-aided design (CAD) is very helpful to study potential **machine interference** and various layout problems as well as estimating various performance parameters. Various commercial CAD software packages exist to analyze such problems. One such example is McAuto's PLACE System. The study at this stage should consider the basic purpose and function of the planned workcell. Consideration needs to be given to analyzing the cycle time that is basic to determining the production rate. An approach developed by Nof and Lechtman [1982], called Robot Time and Motion (RTM), is useful for analyzing the cycle time of robots.

Applications in Manufacturing

Robots have proven to be beneficial in many industrial and nonindustrial environments. Here, we focus on applications within a traditional manufacturing (shop floor) setting and, in particular, on applications which fall into the following three broad categories:

1. Material handling and machine loading/unloading
2. Processing
3. Assembly and inspection

The discussion that follows is not all-inclusive but rather is intended to present (1) an overview of such applications and (2) a few of the more current topics which are impacting the shop floor, particularly as related to flexible manufacturing systems. In the latter case, such issues include developments in **sensor integration**, mobility, sensory interactive grippers/hands, and issues pertaining to intelligent machines and robots. An important reference for many if not all robotic topics is the *International Encyclopedia of Robotics* edited by Dorf [1988].

Material Handling and Machine Loading/Unloading

Applications in this category pertain to the grasping and movement of a workpart or item from one location to another. General considerations for such applications pertain to the gripper design, distances moved, robot weight capacity, the POSE, and robot-dependent issues pertaining to the configuration, degrees of freedom, accuracy and precision, the controller, and programming features. POSE information is particularly important if there are no sensors (e.g. vision) to provide such information prior to pick-up. Specialized grippers have been designed for various applications in all three of the listed categories [Engelberger, 1980]. Quick-change wrists enabling the robot to change grippers (or tools in processing applications) during the production cycle have also become more common since their introduction [Vranich, 1984], as have multiple grippers mounted turret-like at the end of a robotic arm. Various factors need to be considered in the selection and design of grippers. One such checklist of factors can be found in Groover et al. [1986]. It should be noted that certain applications may require a high degree of accuracy and precision whereas others do not. Higher requirements result in more sophisticated drive mechanisms and controllers with associated increased costs.

Material handling applications are typically unsophisticated with minimal control requirements. Two- to four-degrees-of-freedom robots may be sufficient in many tasks. More sophisticated operations such as palletizing may require up to six degrees of freedom with stricter control requirements and more programming features. Various criteria that have proved to contribute to the success of material handling and machine load/unload applications can be found in Groover et al. [1986]. In addition, excellent examples and case studies on robotic loading/unloading are given in the text by Asfahl [1992].

Processing

Robotic processing applications are considered here to be those applications in which a robot actually performs work on a part and requires that the end effector is a tool. Examples include spot welding electrodes, arc welding, and spray-painting nozzles. The most common robotic applications in manufacturing processes are listed in [Table 101.2](#) [Odrey, 1992a]. Many more processing applications are possible.

Spot welding and arc welding represent two major applications of industrial robots. It has been noted that industrial robot usage in welding tasks may be as high as 40% [Ross, 1984]. Spot welding robots have found wide use in automotive assembly lines and have been found to improve weld quality and provide more consistent welds and better repeatability of weld locations. Continuous arc welding is a more difficult application than spot welding. Welding of dissimilar materials, variations in weld joints, dimensional variations from part to part, irregular edges, and gap variations are some of the difficulties encountered in the continuous arc welding processes. Typical arc welding processes include gas metal arc welding (GMAW), shielding metal arc welding (SMAW), i.e., the commonly known “stick” welding, and submerged arc welding (SAW). The most heavily employed

TABLE 101.2 Most Common Robotic Applications in Manufacturing Processes

Spot welding	Grinding
Continuous arc welding	Deburring
Spray coating	Polishing
Drilling	Wire brushing
Routing	Riveting
Waterjet cutting	Laser machining

robotic welding process is GMAW in which a current is passed through a consumable electrode and into a base metal, and a shielding gas (typically CO₂, argon, or helium) minimizes contamination during melting and solidification.

In welding, a worker can compensate automatically by varying welding parameters such as travel speed, deposition rate by current adjustment, weave patterns, and multiple welds where required. Duplicating human welding ability and skill requires that industrial robots have sensor capability and complex programming capability. A wide variety of sensors for robotic arc welding are commercially available and are designed to track the welding seam and provide feedback information for the purpose of guiding the welding path.

Two basic categories of sensors exist to provide feedback information: noncontact sensors and contact sensors. Noncontact sensors include arc-sensing systems and machine vision systems. The former, also referred to as a *through-the-arc* system, uses feedback measurements via the arc itself. Specifically, measurements for feedback may be the current (constant-voltage welding) or the voltage (constant-current welding) obtained by programming the robot to perform a weave pattern. The motion results in measurements that are interpreted as vertical and cross-seam position. Adaptive positioning is possible by regulating the arc length (constant-current systems) as irregularities in gaps or edge variations are encountered.

Vision systems track the weld seam, and any deviations from the programmed seam path are detected and fed back to the controller for automatic tracking. Single-pass systems detect variations and make corrections in one welding pass. Double-pass systems first do a high-speed scan of the joint to record in memory deviations from the programmed seam path, with actual welding corrections occurring on the second "arc-on" pass. Single-pass systems give the advantages of reduced cycle time and of being able to compensate for thermal distortions during the welding operation. One recent example of a microcomputer-based single-pass system using a welding torch and laser-ranging sensor on a six-axis robot is given by Nayak and Ray [1990]. Their system, dubbed ARTIST for adaptive, real-time, intelligent, seam tracker, has a two-level integrated control system in which the high level contains rule-based heuristics and model-based reasoning to arrive at real-time decisions, whereas the low level enables tracking of a three-dimensional welding seam.

It should be noted that arc welding, like many manufacturing processes, is not well enough understood physically that one can formulate an exact mathematical model to describe the process. Attempts to optimize welding schedules for any arc welding process have led to expert systems for such processes [Tonkay and Knott, 1989]. Other examples of such work can be found in publications of the *Welding Journal* [e.g., Lucas, 1987; Fellers, 1987].

A robotic arc welding cell provides several advantages over manual welding operations. These advantages include higher productivity as measured by "arc-on" time, elimination of worker fatigue, decreased idle time, and improved safety. It is also important to correct upstream production operations to reduce variations. This is best accomplished during the design and installation phase of a robotic welding cell. During this phase, issues to consider include delivery of materials to the cell, fixtures and welding positioners, methods required for the processes, and any production and inventory control problems related to the efficient utilization and operation of the cell.

Other processing applications for robot use include spray coating and various machining or cutting operations. Spray coating is a major application in the automotive industry where robots have proven suitable in overcoming various hazards such as fumes, mist, nozzle noise, fire, and possible carcinogenic ingredients. The advantages of robotic spray coating are lower energy consumption, improved consistency of finish, and reduced paint quantities used. To install a robotic painting application, one needs to consider certain manual requirements. These include continuous-path control to emulate the motion of a human operator, a hydraulic drive system to minimize electrical spark hazards, and manual lead-through programming with multiple program storage capability [Groover, et al., 1986]. Newer schemes have considered geometric modeling, painting mechanics, and robot dynamics to output an optimal trajectory based on CAD data describing the objects [Suh et al., 1991]. The objective of such work is to plan an optimal robot trajectory that gives uniform coating thickness and minimizes coating time.

Machining operations utilizing robots typically employ end effectors that are powered spindles attached to the robot wrist. A tool is attached to the spindle to perform the processing operation. Examples of tools would be wire brushes or a grinding wheel. It should be noted that such applications are inherently flexible and have

the disadvantage that such operations would be less accurate than a regular machine tool. Finishing operations, such as deburring, have provided excellent opportunities for robotic application. Force control systems have proven particularly useful in regulating the contact force between the tool and the edge of the work to be deburred. One such example for robotic deburring is given by Stepien et al. [1987]. In general, force-torque sensors mounted at the robot wrist have proven extremely useful in many applications in processing and assembly operations. The Lord Corporation and JR3 are two manufacturers of such commercial sensors.

Assembly Applications

Automated assembly has become a major application for robotics. Assembly applications consider two basic categories: parts mating and parts joining. Parts mating refers to peg-in-hole or hole-on-peg operations, whereas joining operations are concerned not only with mating but also a fastening procedure for the parts. Typical fastening procedures could include powered screwdrivers with self-tapping screws, glues, or similar adhesives.

In parts-mating applications, remote center compliance (RCC) devices have proven to be an excellent solution. In general, compliance is necessary for avoiding or minimizing impact forces, for correcting positioning error, and for allowing relaxation of part tolerances. In choosing an RCC device, the following parameters need to be determined prior to an application:

- Remote center distance (center of compliance). This is the point about which the active forces are at a minimum. The distance is chosen by considering the length of the part and the gripper.
- Axial force capacity. Maximum designed axial force to function properly.
- Compressive stiffness. Should be high enough to withstand any press fitting requirements.
- Lateral stiffness. Refers to force required to deflect RCC perpendicular to direction of insertion.
- Angular stiffness. Relates to forces that rotate the part about the compliant center (also called the cocking stiffness).
- Torsional stiffness. Relates to moments required to rotate a part about the axis of insertion.

Other parameters also include the maximum allowable lateral and angular errors as determined by the size of the part and by its design. These errors must be large enough to compensate for errors due to parts, robots, and fixturing. Passive and instrumented (IRCC) devices have been developed for assembly applications. One such device that combines a passive compliance with active control is described by Xu and Paul [1992]. In addition, the SCARA (Selective Compliance Articulated Robot for Assembly) class of robots is stiff vertically but relatively compliant laterally.

Many opportunities exist for flexible assembly systems. Many of the issues for such systems have been addressed by Soni [1991]. The reader is also referred to the *Design for Robotic Assembly Handbook* [Boothroyd and Dewhurst, 1985] for quantitative methods to evaluate a product's ease of assembly by robots. Carter [1990] presents a method for determining robot assembly task time as derived from tests and industrial experience. Carter also addresses the relationship between product design and robotic assembly cycle time. Some of the current trends in automated assembly include coordinating multiple robots to increase the flexibility and reliability of an assembly cell [Coupes et al., 1989; Zheng and Sias, 1986], interaction with CAD databases to automatically generate assembly plans [Wolter, 1989; Nnaji, 1989] and the application of sensors to automatic assembly systems [Cook, 1991]. Meijer and Jonker [1991] consider an architecture for an intelligent assembly cell and its subsequent implementation. An article by Jarneteg [1990] considers the strategies necessary for developing adaptive assembly systems.

Inspection

Inspection involves checking of parts, products, and assemblies as a verification of conformation to the specification of the engineering design. With the emphasis on product quality, there is a growing emphasis for 100% inspection. Machine vision systems, robot-manipulated active sensing for inspection, and automatic test equipment are being integrated into total inspection systems. Robot application of vision systems include part location, part identification, and bin picking. Machine vision systems for inspection typically perform tasks which include dimensional accuracy checks, flaw detection, and correctness and completeness of an assembled product. Current vision inspection systems are predominantly two-dimensional systems capable of extracting

feature information, analyzing such information, and comparing to known patterns previously trained into the system. As documented by Nurre and Hall [1989], various techniques for three-dimensional measurements have also been developed by many researchers. Primary factors to be considered in the design or application of a vision system include the resolution and field of view of the camera, the type of camera, lighting requirements, and the required throughput of the vision system.

Machine vision application can be considered to have three levels of difficulty, namely, that (1) the object can be controlled in both appearance and position, (2) it can be controlled in either appearance or position, or (3) neither can be controlled. The ability to control both position and appearance requires advanced, potentially three-dimensional vision capabilities. The objective in an industrial setting is to lower the level of difficulty involved. It should be noted that inspection is but one category of robotic applications of machine vision. Two other broad categories are identification and visual servoing and navigation. In the latter case, the purpose of the vision system is to direct the motion of the robot based on visual input. The reader is directed to Groover et al. [1986] for further details.

Emerging Issues

Robotics, by definition, is a highly multidisciplinary field. Applications are broad, and even those applications focused on the manufacturing shop floor are too numerous to cover in full here. The reader is referred to the various journals published by the IEEE and other societies and publishers, a few of which have been listed in the references. Still, it is worthwhile to note a few issues relevant to manufacturing shop-floor applications that could have an impact over the next decade. These issues include gripper development, mobility, and intelligent robots. The objective of this work is the overall integration of a flexible manufacturing system.

In a manufacturing process or assembly operation, the actions required of a gripper will vary with the task. Much work has been done in developing multifigured hands such as the Utah-MIT hand, the Salisbury hand, and others with an increasing interest of adding tactile sensory input for dexterous manipulation [Allen et al., 1989]. As noted by Allen and his colleagues, robotic systems need to process multiple source data and be easily programmable for grasping and manipulation tasks. One study focused on capturing a machinist's skill in working with parts and tools and codifying this knowledge in a grip taxonomy has been done by Cutkosky and Wright [1986]. Their study suggests some general principles for the design, construction, and control of hands in a manufacturing (particularly machining) environment. The reader is also referred to the work of Feddema and Ahmad [1986] for the development of an algorithm for a static robot grasp for automated assembly and the work of Cutkosky [1991] on robotic grasping and manipulation. This latter work considers dynamic contact and the application of dynamic tactile sensors in manipulation tasks. An application to identify and locate circuit board fixtures within a robotic workcell that integrates a vision system with a tactile probe is given by DeMeter and Deisenroth [1987].

Automated guided vehicles (AGVs) currently dominate the movement of parts through a flexible manufacturing system (FMS). AGVs typically restrict the path to predetermined routes and subsequently decrease the "flexibility" of the system. Work is being done on mobile robots to address this issue. Research by Arkin and Murphy [1990] focuses on intelligent mobility within a manufacturing environment. The reader is also referred to the research of Wiens and Black [1992] who address a mobile robot system within a manufacturing cell as a means to increase the flexibility, capability, and capacity of a robot-based manufacturing cell.

The issues involved with intelligent robots have been surveyed by Nitzan [1985], where he notes that future proliferation of robotic applications will depend strongly on machine (robotic) intelligence. Such applications will lead to a greater diversity of applications and will not be just manufacturing oriented. The reader is also referred to work on intelligent machines by Weisbin [1986]. It should be noted that particular interest has been directed toward integration of multiple sensors as a means to enhance robot intelligence [Luo and Lin, 1989; Pin et al., 1991]. The text by Klafter et al. [1989] categorizes the major sensory needs for robotic tasks and gives valuable insights to current and future robotics applications. **Intelligent control** systems, particularly hierarchical control systems, are being developed by many organizations and research institutes [Odrey, 1992b]. Such systems are expected to have an impact both at the shop-floor level and the management levels of production facilities well into the next century.

ROBOTIC TOOLS

Robotics and Automation Corporation, Minneapolis, Minnesota, manufactures equipment for robotic systems, in particular a variety of tools known as "end effectors", devices attached to the end of a robot arm for picking up, grasping, manipulating, and transferring objects.

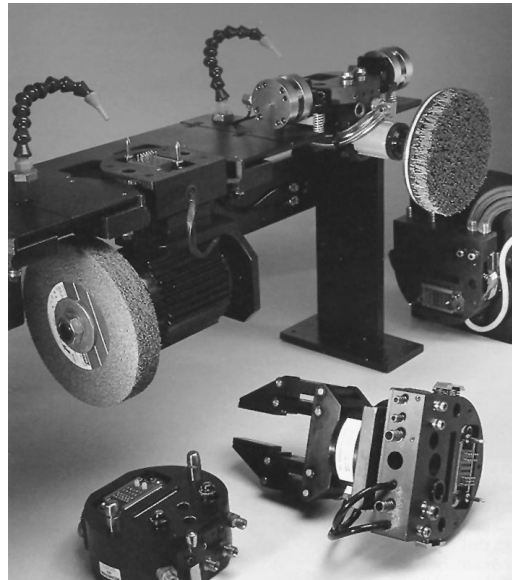
Among the company's newer products is the Automatic Robotics Tool-change System (ARTS), a system designed to meet the growing demand for multiple task work cells for welding and plasma spray functions that require grinding and finishing; deburring, deflashing, routing, hole drilling or parts replacement; and multiple tool disk operations.

The ARTS systems were designed to work with the company's CFD (Constant/controlled Force Device) product line, a series of end effectors and bench mounted devices for controlling the constant pressure of abrasive tools used to deburr, grind, polish, and finish products fabricated by welding, casting, molding, forging, or machining.

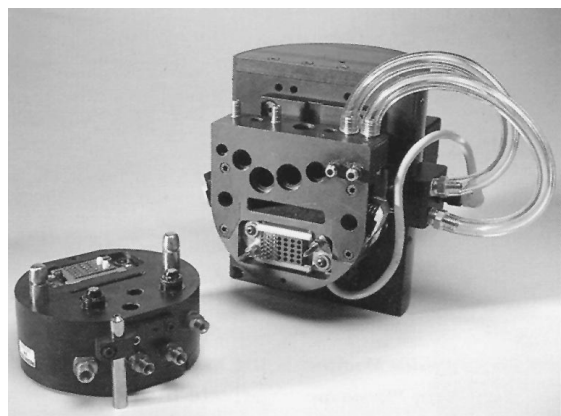
Robotics and Automation Corporation's CFD line includes three end-of-arm devices and two bench-mounted devices. They do not require that the robot apply and control the force, only that it move along a normal programmed path over the work piece; the CFD applies and maintains the required processing pressure.

When the surface to be finished is very rough and course, several different grades of finishing media may be needed, as well as different speeds and power as the surface finish is transformed. To accommodate this multi-step process within a single work cell, and with a single robot, Robotics and Automation Corporation developed the automated tool-change system.

The ARTS-I is being used in industrial applications with six tool positions ranging from coarse sanding disks and abrasive wheels to cloth polishing wheels with motors of various horsepower. The ARTS-II allows a robot to exchange a welding torch for a CFD end effector to finish a welded assembly with a welding robot; using a second tool-changer (ARTS-I) enables finishing the surface conditioning process. (Courtesy of National Aeronautics and Space Administration.)



The tool rack of the Automatic Robotics Tool-Change System includes a two-finger gripper; a grinder, a coated abrasive brush, and a welding torch. (Photo courtesy of National Aeronautics and Space Administration.)



The quick disconnect system allows changing tools with hydraulic, pneumatic, or electric power. (Photo courtesy of National Aeronautics and Space Administration.)

Defining Terms

Cellular manufacturing: Grouping of parts by design and/or processing similarities such that the group (family) is manufactured on a subset of machines which constitute a cell necessary for the group's production.

Decision tree analysis: Decomposing a problem into alternatives represented by branches where nodes (branch intersections) represent a decision point or chance event having probabilistic outcome. Analysis consists of calculating expected values associated with the chain of events leading to the various outcomes.

Degrees of freedom: The total number of individual motions typically associated with a machine tool or robot.

Intelligent control: A sensory-interactive control structure incorporating cognitive characteristics that can include artificial intelligence techniques and contain knowledge-based constructs to emulate learning behavior with an overall capacity for performance and/or parameter adaptation.

Machine interference: The idle time experienced by any one machine in a multiple-machine system that is being serviced by an operator (or robot) and is typically measured as a percentage of the total idle time of all the machines in the system to the operator (or robot) cycle time.

Sensor fusion: Combining of multiple sources of sensory information into one representational format.

Sensor integration: The synergistic use of multiple sources of sensory information to assist in the accomplishment of a task.

Related Topic

112.1 Introduction

References

- P.K. Allen, P. Michelman, and K.S. Roberts, "An integrated system for dexterous manipulation," *IEEE International Conference on Robotics and Automation*, 1989, pp. 612–616.
- R.C. Arkin and R.R. Murphy, "Autonomous navigation in a manufacturing environment," *IEEE Trans. Robotics Autom.*, vol. 6, no. 4, pp. 445–454, 1990.
- C.R. Asfahl, *Robots and Manufacturing Automation*, New York: Wiley, 1992.
- G. Boothroyd and P. Dewhurst, "Design for Robotic Assembly," Department of Industrial and Manufacturing Engineering, University of Rhode Island, Kingston, 1985.
- P.W. Carter, "Estimating cycle time in design for robotic assembly," *J. Manu. Syst.*, vol. 9, no. 1, pp. 1–12, 1990.
- J.W. Cook, "Applying sensors to automatic assembly systems," *IEEE Trans. Ind. Appl.*, vol. 27, no. 2, pp. 282–285, 1991.
- D. Coupes, A. Delchambre, and P. Gaspart, "The supervision and management of a two robots flexible assembly cell," Proceedings of IEEE Conference on Robotics and Automation, 1989, pp. 540–550.
- M.R. Cutkosky, "Robotic grasping and manipulation," *Proceedings of NSF Design and Manufacturing Systems Conference*, Dearborn, Mich.: Society of Manufacturing Engineers, 1991, pp. 423–430.
- M.R. Cutkosky and P.K. Wright, "Modeling manufacturing grips and correlations with the design of robotic hands," IEEE International Conference on Robotics and Automation, San Francisco, Calif., April 7–10, 1986, pp. 1533–1539.
- E.C. DeMeter and M.P. Deisenroth, "The integration of visual and tactile sensing for the definition of regions within a robot workcell," Robots 11/17th ISIR, Chicago, Ill., April 26–30, 1987, pp. 10-51 to 10-61.
- R.C. Dorf, Ed., *International Encyclopedia of Robotics*, vols. 1–3, New York: Wiley, 1988.
- J.F. Engelberger, "Robotics in practice," AMA COM: A Division of American Management Associations, 1980.
- J.T. Feddema and S. Ahmad, "Determining a static robot grasp for automated assembly," IEEE International Conference on Robotics and Automation, San Francisco, Calif., April 7–10, 1986, pp. 918–924.
- K.G. Fellers, "A PC approach to welding variables," *Weld. J.*, vol. 66, pp. 31–40, 1987.
- P.C. Flora, Ed., *Robotics Product Database*, 6th ed., Orlando, Fla.: TecSpec, 1989.
- M.P. Groover, M. Weiss, R.N. Nagel, and N.G. Odrey, *Industrial Robotics: Technology, Programming, and Applications*, New York: McGraw-Hill, 1986.

- B.G. Jarneteg, "FAS control strategies for adaptive assembly systems," 21st CIRP International Seminar on Manufacturing Systems, Stockholm, Sweden, 1990.
- R.D. Klafter, T.A. Chmielewski, and M. Negin, *Robotic Engineering: An Integrated Approach*, Englewood Cliffs, N.J.: Prentice-Hall, 1989.
- W. Lucas, "Microcomputer systems, software and expert systems for welding engineering," *Weld. J.*, vol. 66, pp. 19–30, 1987.
- R.C. Luo and M.-H. Lin, "Intelligent robot multi-sensor data fusion for flexible manufacturing systems," Proceedings of NSF 15th Conference on Production Research and Technology, University of California-Berkeley, Jan. 9–13, 1989, pp. 73–85.
- B.R. Meijer and P.P. Jonker, "The architecture and philosophy of the DIAC (Delft Intelligent Assembly Cell)," IEEE Conference on Robotics and Automation, Sacramento, Calif., 1991, pp. 2218–2223.
- M. Michel, "Justification models for flexible manufacturing," *Robots' 10 Conference Proceedings*, Dearborn, Mich.: Society of Manufacturing Engineers, 1986, pp. 2-55 to 2-81.
- N. Nayak and A. Ray, "An integrated system for intelligent seam tracking in robotic welding: part 1—conceptual and analytical development; part 2—design and implementation," IEEE International Conference on Robotics and Automation, 1990.
- D. Nitzan, "Development of intelligent robots: achievements and issues," *IEEE J. Robotics Autom.* vol. RA-1, no. 1, pp. 3–13, 1985.
- B.O. Nnaji, "RALPH: An automatic robot assembly language programmer: an overview," Proceedings of Robots 13 Conference, Gaithersburg, Md., May 7–11, 1989, pp. 16-41 to 16-63.
- S.Y. Nof and H. Lechtman, "The RTM method of analyzing robot work," *Ind. Eng.*, April 1982, pp. 38–48.
- J.H. Nurre and E.L. Hall, "Three dimensional vision for automated inspection," Proceedings of Robots 13 Conference, Gaithersburg, Md., May 7–11, 1989, pp. 16-1 to 16-11.
- N.G. Odrey, "Robotics and automation," *Maynard's Industrial Engineering Handbook*, 4th ed., W.K. Hodson, Ed., New York: McGraw-Hill, 1992a.
- N.G. Odrey, "Control systems," *1992 McGraw-Hill Yearbook of Science and Technology*, New York: McGraw-Hill, 1992b, pp. 87–90.
- F.G. Pin et al., "Robotic learning from distributed sensory sources," *IEEE Trans. Syst. Man and Cybern.*, vol. 21, no. 5, pp. 1216–1223, 1991.
- J.M. Proth and H.P. Hillion, *Mathematical Tools in Production Management*, New York: Plenum Press, 1990.
- B. Ross, "Machines that can see: here comes a new generation," *Bus. Week.*, January 1984, p. 118.
- A.H. Soni, "Flexible assembly systems: Opportunities and challenges," Proceedings of the 1991 NSF Design and Manufacturing Systems Conference, University of Texas at Austin, Jan. 9–11, 1991, pp. 367–373.
- T.M. Stepien, L.M. Sweet, M.C. Good, and M. Tomizuka, "Control of tool/workpiece contact force with application of robotic deburring," *IEEE J. Robotics Autom.*, vol. RA-3, no. 1, pp. 7–18, 1987.
- S.-H. Suh, I.-K. Woo, and S.-K. Noh, "Automatic trajectory planning system (ATPS) for spray painting robots," *J. Manu. Syst.*, vol. 10, no. 5, pp. 396–406, 1991.
- G.J. Thuesen and W.J. Fabrycky, *Engineering Economy*, 7th ed., Englewood Cliffs, N.J.: Prentice-Hall, 1989.
- G.L. Tonkay and K. Knott, "Intelligent process specification for robotic arc welding," Proceedings of World Conference on Robotics Research: The Next Five Years and Beyond. Robotics International of the Society of Manufacturing Engineers, Gaithersburg, Md., May 11–17, 1989.
- S. Verk, "Strategic optimization cycle as a competitive tool for economic justification of advanced manufacturing systems," *J. Manu. Syst.*, vol. 9, no. 3, pp. 194–205, 1990.
- J.M. Vranich, "Quick change system for robots," SME Paper MS84-418, Conference on Robotics Research—The Next Five Years and Beyond, Lehigh University, Bethlehem, 1984.
- C.R. Weisbin, "CESAR research in intelligent machines," SME Paper MS586-772, Robotics Research Conference, Scottsdale, Ariz., Aug. 18–21, 1986.
- J.A. White, M.H. Agee, and K.E. Case, *Principles of Engineering Economic Analysis*, New York: John Wiley & Sons, 1977.
- G.J. Wiens and J.T. Black, "Design for mobility within a manufacturing cell," Proceedings of the NSF Design and Manufacturing Systems Conference, Georgia Institute of Technology, Jan. 8–10, 1992, pp. 1147–1150.

- J.D. Wolter, "On the automatic generation of assembly plans," Proceedings of the 1989 IEEE Conference on Robotics and Automation, 1989, pp. 62–68.
- Y. Xu and R.P. Paul, "Robotic instrumented compliant wrist," *ASME J. Eng. for Ind.*, vol. 114, pp. 120–123, 1992.
- Y.F. Zheng and F.R. Sias, Jr., "Two robot arms in assembly," IEEE Conference on Robotics and Automation, San Francisco, Calif., April 7–10, 1986, pp. 1230–1235.

Further Information

Various journals publish on topics pertaining to robots. Sources include the bimonthly *IEEE Journal of Robotics and Automation*, the quarterly journal *Robotics and Computer-Integrated Manufacturing* (published by Pergamon Press), *Robotics* (published by Cambridge University Press since 1983), and the *Journal of Robotic Systems* (published by Wiley).

IEEE has sponsored since 1984 the annual "International Conference on Robotics and Automation." IEEE conference proceedings and journals are available from the IEEE Service Center, Piscataway, N.J.

The Society of Manufacturing Engineers (SME) is another source for robot publications that are concerned with both research issues and applications. Robots 1 through 13 (1989) conference proceedings are available as well as the Robot Research conference proceedings (three to date) of Robotics International (RI) of SME. A directory of robot research laboratories is also available. Contact SME, Dearborn, Mich.

The three-volume *International Encyclopedia of Robotics: Applications and Automation* (R.C. Dorf, ed.), published by Wiley (1988), brings together the various interrelated fields constituting robotics and provides a comprehensive reference.

Spitzer, C.R., Martinec, D.A., Leondes, C.T., Rana, A.H., Check, W. "Aerospace Systems"

The Electrical Engineering Handbook

Ed. Richard C. Dorf

Boca Raton: CRC Press LLC, 2000

102

Aerospace Systems

Cary R. Spitzer

AvioniCon Inc.

Daniel A. Martinec

Aeronautical Radio, Inc.

Cornelius T. Leondes

University of California, San Diego

Abdul Hamid Rana

GE LogistiCom

William Check

GE Spacenet

102.1 Avionics Systems

A Modern Example System • Data Buses • Displays • Power • Software in Avionics • CNS/ATM • Navigation Equipment • Emphasis on Communications • Impact of “Free Flight” • Avionics in the Cabin • Avionics Standards

102.2 Communications Satellite Systems: Applications

Satellite Launch • Spacecraft and Systems • Earth Stations • VSAT Communication System • Video • Audio • Second-Generation Systems

102.1 Avionics Systems

Cary R. Spitzer, Daniel A. Martinec, and Cornelius T. Leondes

Avionics (aviation electronics) systems perform many functions: (1) for both military and civil aircraft, avionics are used for flight controls, guidance, navigation, communications, and surveillance; and (2) for military aircraft, avionics also may be used for electronic warfare, reconnaissance, fire control, and weapons guidance and control. These functions are achieved by the application of the principles presented in other chapters of this handbook, e.g., signal processing, electromagnetic, communications, etc. The reader is directed to these chapters for additional information on these topics. This section focuses on the system concepts and issues unique to avionics that provide the traditional functions listed in (1) above.

Development of an avionics system follows the traditional systems engineering flow from definition and analysis of the requirements and constraints at increasing level of detail, through detailed design, construction, validation, installation, and maintenance. Like some of the other aerospace electronic systems, avionics operate in real time and perform mission- and life-critical functions. These two aspects combine to make avionics system design and verification especially challenging.

Although avionics systems perform many functions, there are three elements common to most systems: data buses, displays, and power. Data buses are the signal interfaces that lead to the high degree of integration found today in many modern avionics systems. Displays are the primary form of crew interface with the aircraft and, in an indirect sense, through the display of synoptic information also aid in the integration of systems. Power, of course, is the life blood of all electronics.

The generic processes in a typical avionics system are signal detection and preprocessing, signal fusion, computation, control/display information generation and transmission, and feedback of the response to the control/display information. (Of course, not every system will perform all of these functions.)

A Modern Example System

The B-777 Airplane Information Management System (AIMS) is the first civil transport aircraft application of the integrated, modular avionics concept, similar to that being used in the U.S. Air Force F-22. Figure 102.1 shows the AIMS cabinet with eight modules installed and three spaces for additional modules to be added as the AIMS functions are expanded. Figure 102.2 shows the AIMS architecture.

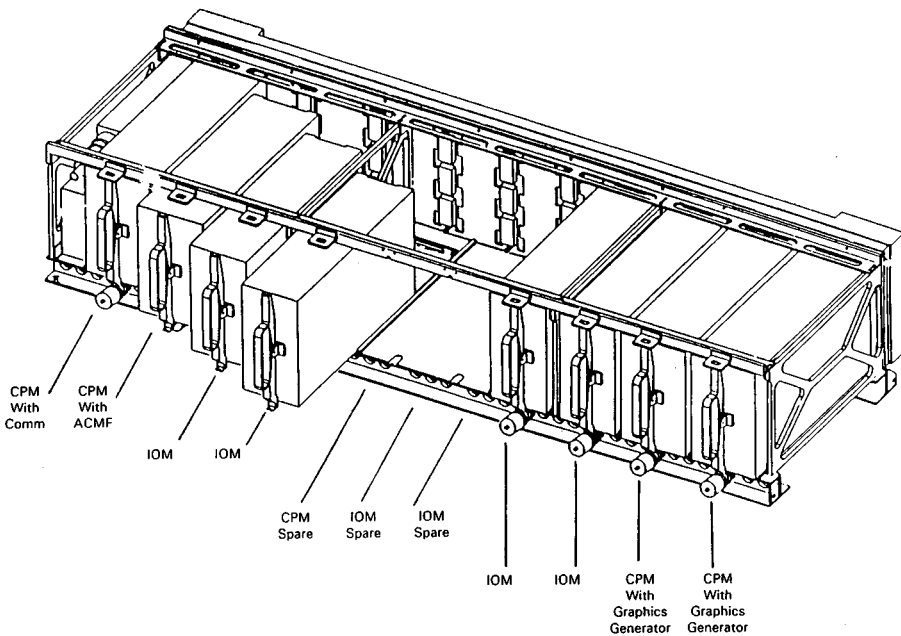


FIGURE 102.1 Cabinet assembly outline and installation (typical installation). (Courtesy of Honeywell, Inc.)

AIMS functions performed in both cabinets include flight management, electronic flight instrument system (EFIS) and engine indicating and crew alerting system (EICAS) displays management, central maintenance, airplane condition monitoring, communications management, data conversion and gateway (ARINC 429 and ARINC 629), and engine data interface. AIMS does not control the engines nor flight controls, nor operate any internal or external voice or data link communications hardware but does select the data link path as part of the communications management function. Subsequent generations of AIMS may include some of these latter functions.

In each cabinet the line replaceable modules (LRMs) are interconnected by dual ARINC 659 backplane data buses. The cabinets are connected to the quadraplex (not shown) or triplex redundant ARINC 629 system and fly-by-wire data buses and are also connected via the system buses to the three multifunction control display units (MCDU) used by flight crew and maintenance personnel to interact with AIMS. The cabinets transmit merged and processed data over quadruple redundant custom designed 100 Mhz buses to the EFIS and EICAS displays.

In the AIMS the high degree of function integration requires levels of system availability and integrity not found in traditional distributed, federated architectures. These extraordinary levels of availability and integrity are achieved by the extensive use of **fault-tolerant** hardware and software maintenance diagnostics and promise to reduce the chronic problem of unconfirmed removals and low mean time between unscheduled removals (MTBUR).

Figure 102.3 is a top-level view of the U.S. Air Force F-22 Advanced Tactical Fighter avionics. Like many other aircraft, the F-22 architecture is hybrid, part federated and part integrated. The left side of the figure is the highly integrated portion, dominated by the two Common Integrated Processors (CIPs) that process, fuse, and distribute signals received from the various sensors on the far left. The keys to this portion of the architecture are the Processor Interconnect (PI) buses within the CIPs and the High Speed Data Buses (HSDBs). (There are provisions for a third CIP as the F-22 avionics grow in capability.) The right side of the figure shows the federated systems including the Inertial Reference, Stores Management, Integrated Flight and Propulsion Control, and Vehicle Management systems and the interface of the latter two to the Integrated Vehicle System Control. The keys to this portion of the architecture are the triple or quadruple redundant AS 15531 (formerly MIL-STD-1553) command/response two-way data buses.

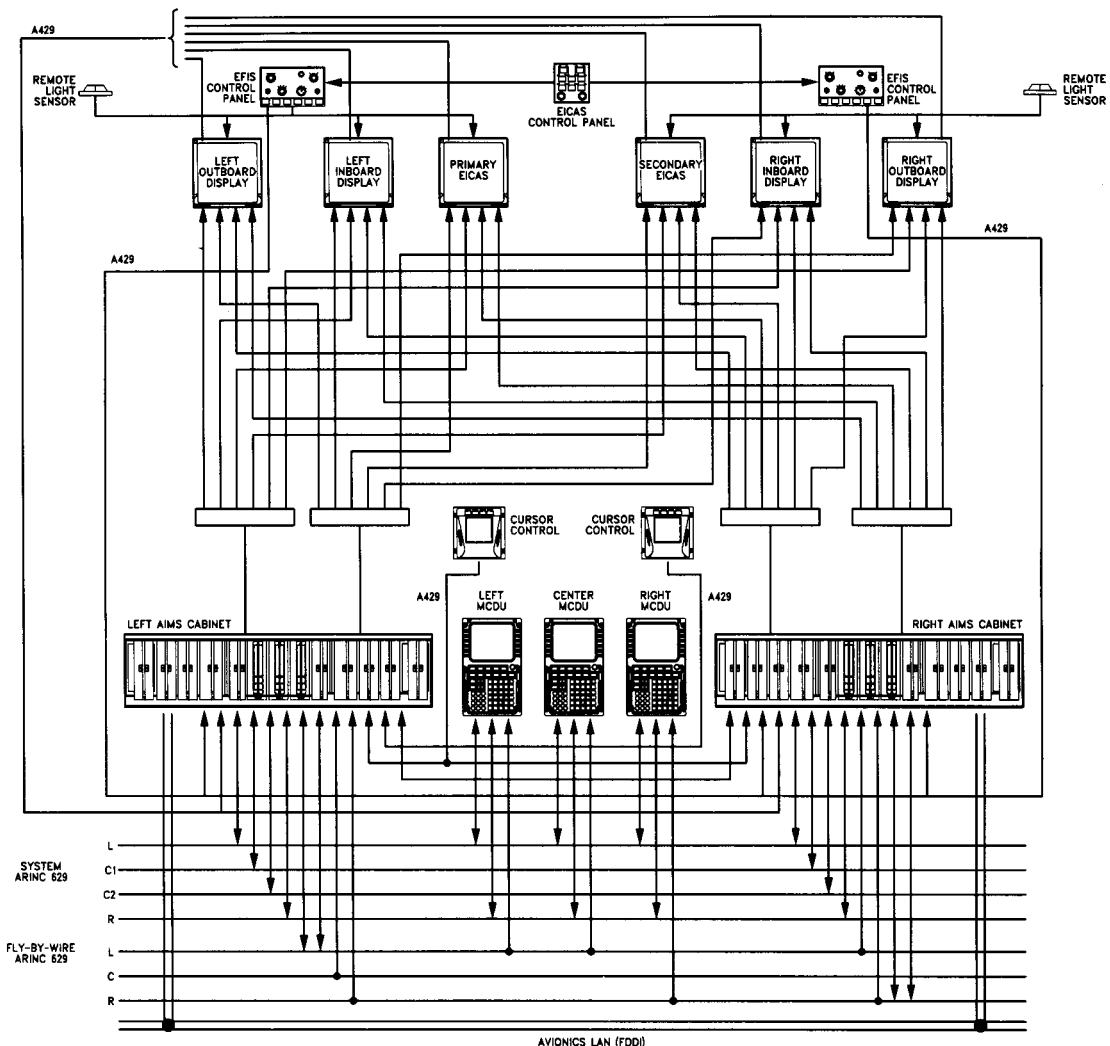


FIGURE 102.2 Architecture for AIMSbaseline configuration. (Courtesy of Honeywell, Inc.)

Data Buses

As noted earlier, data buses are the key to the emerging integrated avionics architectures. Table 102.1 summarizes the major features of the most commonly used system buses. MIL-STD-1553 and ARINC 429 were the first data buses to be used for general aircraft data communications. These are used today widely in military and civil avionics, respectively, and have demonstrated the significant potential of data buses. The others listed in the table build on their success.

Displays

All modern avionics systems use electronic displays, either CRTs or flat-panel LCDs that offer exceptional flexibility in display format and significantly higher reliability than electromechanical displays. Because of the very bright ambient sunlight at flight altitudes the principal challenge for an electronic display is adequate brightness. CRTs achieve the required brightness through the use of a shadow mask design coupled with narrow bandpass optical filters. Flat-panel LCDs also use narrow bandpass optical filters and a bright backlight to achieve the necessary brightness.

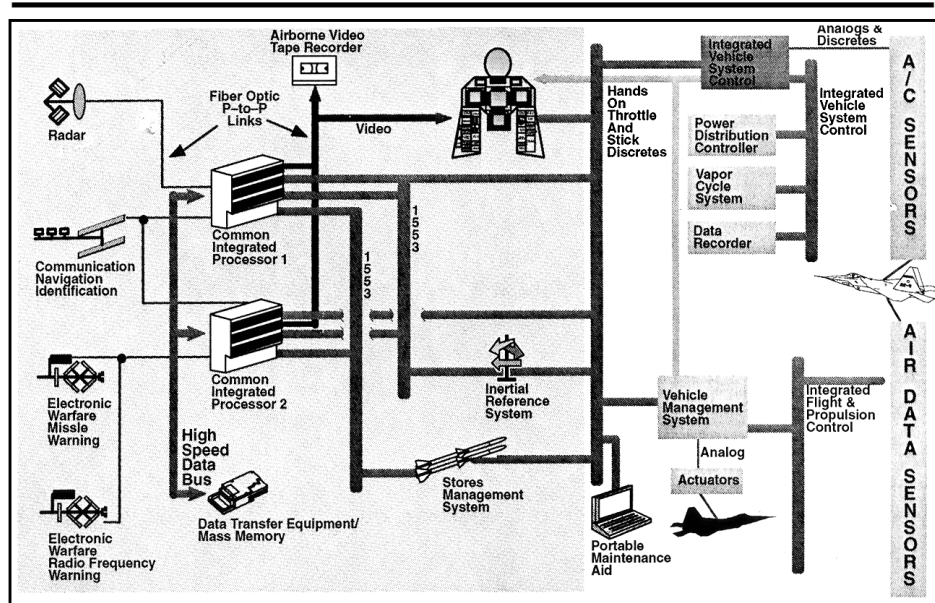


FIGURE 102.3 F-22 EMD Architecture.

TABLE 102.1 Characteristics of Common Avionics Buses

Bus Name	Word Length	Bit Rate	Transmission Media
MIL-STD-1553	20 bits	1 Mb/s	Wire
DOD-STD-1773	20 bits	TBS	Fiber optic
High-speed data bus	32 bits	50 Mb/s	Wire or fiber optic
ARINC 429	32 bits	14.5/100 kb/s	Wire
ARINC 629	20 bits	2 Mb/s	Wire or fiber optic
ARINC 659	32 bits	100 MB/s	Wire

Because of the intrinsic flexibility of electronic displays, a major issue is the design of display formats. Care must be taken not to place too much information in the display and to ensure that the information is comprehensible in high workload (aircraft emergency or combat) situations.

Power

Aircraft power is generally of two types: 28 vdc, and 115 vac, 400 Hz. Some 270 vdc is also used on military aircraft. Aircraft power is of poor quality when compared to power for most other electronics. Under normal conditions, there can be transients of up to 100% of the supply voltage and power interruptions of up to 1 second. This poor quality places severe design requirements on the avionics power supply, especially where the avionics are performing a full-time, flight-critical function. Back-up power sources include ram air turbines and batteries, although batteries require very rigorous maintenance practices to guarantee long-term reliable performance.

Software in Avionics

Most avionics currently being delivered are microprocessor controlled and are software intensive. The “power” achieved from software programs hosted on a sophisticated processor results in very complex avionics with many functions and a wide variety of options. The combination of sophistication and flexibility has resulted

WEATHER INFORMATION SYSTEMS

Weather is a critical factor in aircraft operations. It is the largest single contributor to flight delays and a major cause of aircraft accidents.

A study conducted for NASA by Ohio State University reported that the principal difficulties in making proper flight decisions are the timeliness and clarity of weather data dissemination.

To advance the technology of in-flight weather reporting, Langley Research Center developed in the early 1990's a cockpit weather information system known as CWIN (Cockpit Weather Information). The system draws on several commercial data sensors to create radar maps of storms and lightning, together with reports of surface observations.

Shown above is a CWIN display in the simulation cockpit of Langley's Transport Systems Research Vehicle, a modified jetliner used to test advanced technologies. The CWIN display is the lower right screen among the four center panel screens. By pushing a button, the pilot may select from a menu of several displays, such as a ceiling and visibility map, radar storm map, or lightning strike map. (Courtesy of National Aeronautics and Space Administration.)



in lengthy procedures for validation and certification. The **brickwalling** of software modules in a system during the initial development process to ensure isolation between critical and noncritical modules has been helpful in easing the certification process.

There are no standard software programs or standard software certification procedures. RTCA has prepared Document DO-178 to provide guidance (as opposed to strict rules) regarding development and certification of avionics civil software. The techniques for developing, categorizing, and documenting avionics civil software in DO-178 are widely used.

For military avionics software, the principal document is DOD-STD-498. This standard defines a set of activities and documentation suitable for the development of both weapon systems and automated information systems. Many software languages have been used in the past in avionics applications; however, today there is a strong trend for both military and avionics civil software to use Ada wherever reasonably possible.

The evolving definition of a standards for Applications Exchange (APEX) software promises to provide a common software platform whereby the specialized requirements of varying hardware (processor) requirements are minimized. APEX software is a hardware interface that provides a common link with the functional software within an avionics system. The ultimate benefit is the development of software independent of the hardware platform and the ability to reuse software in systems with advanced hardware while maintaining most, if not all, of the original software design.

CNS/ATM

The last decade of this century has seen much attention focused on Communication/Navigation/Surveillance for Air Traffic Management (CNS/ATM), a satellite-based concept developed by the Future Air Navigation System (FANS) Committees of the International Civil Aviation Organization (ICAO), a special agency of the United Nations. Many studies have predicted enormous economic rewards of CNS/ATM for both aircraft operators and air traffic services providers.

The new CNS/ATM system should provide for:

- Global communications, navigation, and surveillance coverage at all altitudes and embrace remote, off-shore, and oceanic areas.
- Digital data exchange between air-ground systems (voice backup).
- Navigation/approach service for runways and other landing areas which need not be equipped with precision landing aids.

Navigation Equipment

A large portion of the avionics on an aircraft are dedicated to navigation. The following types of navigation and related sensors are commonly found on aircraft:

- Flight control computer (FCC)
- Flight management computer (FMC)
- Inertial navigation system (INS)
- Attitude heading and reference system (AHRS)
- Air data computer (ADC)
- Low range radio altimeter (LRRA)
- Radar
- Distance Measuring Equipment (DME)
- Instrument Landing System (ILS)
- Microwave Landing System (MLS)
- VHF OmniRange (VOR) Receiver
- Global Navigation Satellite System (GNSS)

Emphasis on Communications

An ever-increasing portion of avionics is dedicated to communications. Much of the increase comes in the form of digital communications for either data transfer or digitized voice. Military aircraft typically use digital communications for security. Civil aircraft use digital communications to transfer data for improved efficiency of operations and RF spectrum utilization. Both types of aircraft are focusing more on enhanced communications to fulfill the requirements for better operational capability.

Various types of communications equipment are used on aircraft. The following list tabulates typical communications equipment:

- VHF transceiver (118–136 MHz)
- UHF transceiver (225–328 MHz/335–400 MHz for military)
- HF transceiver (2.8–24 MHz)
- Satellite (1530–1559/1626.5–1660.5 MHz, various frequencies for military)
- Aircraft Communications Addressing and Reporting (ACARS)
- Joint Tactical Information Distribution System (JTIDS)

In the military environment the need for communicating aircraft status and for aircraft reception of crucial information regarding mission objectives are primary drivers behind improved avionics. In the civil environment

HIGH SPEED RESEARCH



This McDonnell Douglas conceptual design for a Mach 2.4 supersonic transport is sized to carry about 300 passengers over a distance of 5,000 nautical miles. A NASA/industry high speed civil transport research effort is a first step toward determining whether such a plane can be economically viable and environmentally acceptable. (Photo Courtesy of National Aeronautics and Space Administration.)

Aircraft manufacturers of several nations are developing technology for the next plateau of international aviation: the long-range, environmentally acceptable, second generation supersonic passenger transport, which could be flying by 2010.

NASA's High Speed Research (HSR) program is intended to demonstrate the technical feasibility of a high speed civil transport (HSCT) vehicle. The program is being conducted as a national team effort with shared government/industry funding and responsibilities.

The team has established a baseline design concept that serves as a common configuration for investigations. A full-scale craft of this design would have a maximum cruise speed of Mach 2.4, only marginally faster than the Anglo-French Concorde supersonic transport. However, the HSCT would have double the capacity of the Concorde, and it would operate at an affordable ticket price.

Phase I of the HSR program, which began in 1990, focused on environmental challenges: engine emission effects on the atmosphere, airport noise, and sonic boom. Phase II, initiated in 1994, focuses on the technology advances needed for economic viability, principally weight reductions in every aspect of the baseline configuration. In materials, the HSR team is developing, analyzing, and verifying the technology for trimming the baseline airframe by 30 to 40%. In aerodynamics, a major goal is to minimize air drag to enable a substantial increase in range. Phase II also includes computational and wind tunnel analyses of the baseline HSCT and alternative designs. Additional research involves ground and flight simulations aimed at development of advanced control systems, flight deck instrumentation, and displays. (Courtesy of National Aeronautics and Space Administration.)

(particularly commercial transport), the desire for improved passenger services, more efficient aircraft routing and operation, safe operations, and reduced time for aircraft maintenance are the primary drivers for improving the communications capacity of the avionics.

The requirements for digital communications for civil aircraft have grown so significantly that the industry as a whole embarked on a virtually total upgrade of the communications system elements. The goal is to achieve a high level of flexibility in processing varying types of information as well as attaining compatibility between a wide variety of communication devices. The approach bases both ground system and avionics design on the ISO Open System Interconnect (OSI) model. This seven-layer model separates the various factors of communications into clearly definable elements of physical media, protocols, addressing, and information identification.

The implementation of the OSI model requires a much higher level of complexity in the avionics as compared to avionics designed for simple dedicated point-to-point communications. The avionics interface to the physical

medium will generally possess a higher bandwidth. The bandwidth is required to accommodate the overhead of the additional information on the communications link for the purpose of system management. The higher bandwidths pose a special problem for aircraft designers due to weight and electromagnetic interference (EMI) considerations. Additional avionics are required to perform the buffering and distribution of the information received by the aircraft. Generally a single unit, commonly identified as the communications management unit (CMU), will perform this function.

The CMU can receive information via RF transceivers operating in conjunction with terrestrial, airborne, or space-based transceivers. The capability also exists for transceiver pairs employing direct wire connections or very short-range optical links to the aircraft. The CMU also provides the routing function between the avionics, when applicable. Large on-board databases, such as an electronic library, may be accessed and provide information to other avionics via the CMU.

The increasing demand on data communication system capacity and flexibility is dictating the development of a system without the numerous limitations of current systems. Current communication systems require rather rigid protocols, message formatting, and addressing. The need for a more flexible and capable system has led to the initial work to develop an Aeronautical Telecommunications Network (ATN). The characteristics envisaged for the ATN are the initiation, transport, and application of virtually any type of digital message in an apparently seamless method between virtually any two end systems. The ATN is expected to be a continually evolving system.

Impact of “Free Flight”

“Free Flight” is a term describing an airspace navigation system in which the “normal” air traffic controls are replaced by the regular transmission of position information from the airplane to the ground. The ground system, by projecting the aircraft position and time, can determine if the intended tracks of two aircraft would result in a cohabitation of the same point in the airspace. This is commonly called “conflict probe”. If a potential conflict occurs, then a message is transmitted to one or more of the aircraft involved to make a change to course and/or speed.

“Free Flight” dictates special requirements for the avionics suite. A highly accurate navigation system with high integrity is required. The communications and surveillance functions must exhibit an extremely high level of availability.

GNSS Avionics performing the position determination functions will require augmentation to achieve the necessary accuracy. The augmentation will be provided by a data communications system and will be in the form of positional information correction. A data communications system will also be required to provide the frequent broadcast of position information to the ground. A modified Mode S transponder squitter is expected to provide that function.

The free flight concept will require the equipage of virtually all aircraft operating within the designated free-flight airspace with a commensurate level of avionics capability. The early stages of the concept development uncovered the need to upgrade virtually all aircraft with enhanced CNS/ATM avionics. The air transport industry resolved this problem on older airplanes by developing improved and new avionics for retrofit applications. The new avionics design addresses the issues of increased accuracy of position and enhancement of navigation management in the form of the GNSS Navigation and Landing Unit (GNLU) housed in a single unit and designed to be a physical and functional replacement for the ILS and/or MLS receivers. A built-in navigator provides enhanced navigation functionality for the airplane. The GNSS can provide ILS lookalike signals and perform landing guidance functions equivalent to Category I.

Avionics in the Cabin

Historically, the majority of avionics have been located in the electronics bay and the cockpit of commercial air transport airplanes. Cabin electronics had generally been limited to the cabin interphone and public address system, the sound and central video system, and the lighting control system. More recently the cabin has been updated with passenger telephones using both terrestrial and satellite systems. The terrestrial telephone system operates in the 900-MHz band in the United States and will operate near 1.6 GHz in Europe. The satellite

system, when completely operational, will also operate near 1.6 GHz. Additional services available to the passengers are the ability to send facsimiles (FAXes) and to view virtually real-time in-flight position reporting via connection of the video system with the flight system. Private displays at each seat will allow personal viewing of various forms of entertainment including movies, games, casual reading, news programming, etc.

Avionics Standards

Standards play an important role in avionics. Military avionics are controlled by the various standards (MIL-STDs, DOD-STDs, etc.) for packaging, environmental performance, operating characteristics, electrical and data interfaces, and other design-related parameters. General aviation avionics are governed by fewer and less stringent standards. Technical Standard Orders (TSOs) released by the Federal Aviation Administration (FAA) are used as guidelines to ensure airworthiness of the avionics. TSOs are derived from and, in most cases, reference RTCA documents characterized as Minimum Operational Performance Standards and Minimum Avionics System Performance Standards. EUROCAE is the European counterpart of RTCA.

The commercial air transport industry adheres to multiple standards at various levels. The International Civil Aviation Organization (ICAO) is commissioned by the United Nations to govern aviation systems including but not limited to Data Communications Systems, On-Board Recorders, Instrument Landing Systems, Microwave Landing Systems, VHF OmniRange Systems, and Distance Measuring Equipment. The ICAO Standards and Recommended Practices (SARPS) control system performance, availability requirements, frequency utilization, etc. at the international level. The SARPS in general maintain alignment between the national avionics standards such as those published by EUROCAE and RTCA.

The commercial air transport industry also uses voluntary standards created by the Airlines Electronic Engineering Committee and published by Aeronautical Radio Inc. (ARINC). The ARINC "characteristics" define form, fit, and function of airline avionics.

Defining Terms

ACARS: A digital communications link using the VHF spectrum for two-way transmission of data between an aircraft and ground. It is used primarily in civil aviation applications.

Brickwalling: Generally used in software design in critical applications to ensure that changes in one area of software will not impact other areas of software or alter their desired function.

Distance measuring equipment: The combination of a receiver and a transponder for determining aircraft distance from a remote transmitter. The calculated distance is based on the time required for the return of an interrogating pulse set initiated by the aircraft transponder.

Fault tolerance: The built-in capability of a system to provide continued correct execution in the presence of a limited number of hardware or software faults.

JTIDS: Joint Tactical Information Distribution System using spread spectrum techniques for secure digital communication. It is used for military applications.

Validation: The process of evaluating a product at the end of the development process to ensure compliance with requirements.

Verification: (1) The process of determining whether the products of a given phase of the software development cycle fulfill the requirements established during the previous phase. (2) Formal proof of program correctness. (3) The act of reviewing, inspecting, testing, checking, auditing, or otherwise establishing and documenting whether items, processes, services, or documents conform to specified requirements (IEEE).

Related Topic

78.1 Introduction

References

Airlines Electronic Engineering Committee Archives, Aeronautical Radio Inc.
FANS Manual, International Air Transport Association, Montreal, Version 1.1, May 1995.

- Federal Radionavigation Plan, DOT-VNTSC-RSPA-90-3/DOD4650.4, Departments of Transportation and Defense, 1990.
- M.J. Morgan, "Integrated modular avionics for next generation commercial airplanes," *IEEE/AES Systems Magazine*, pp. 9–12, August 1991.
- C.R. Spitzer, *Digital Avionics Systems*, 2nd ed., New York: McGraw-Hill, 1992.

Further Information

- K. Feher, *Digital Communications*, Englewood Cliffs, N.J.: Prentice Hall, 1981.
- J.L. Farrell, *Integrated Aircraft Navigation*, New York: Academic Press, 1976.
- L.E. Tannas, Jr., *Flat Panel Displays and CRTs*, New York: Van Nostrand Reinhold, 1985.
- M. Kayton and W.R. Fried, *Avionics Navigation Systems*, New York: John Wiley and Sons, 1969.

102.2 Communications Satellite Systems: Applications

Abdul Hamid Rana and William Check

The history of satellites began in 1957 when the Soviet Union launched Sputnik I, the world's first satellite. In the 1960s the commercial sector became actively involved in satellite communications with the launch of Telstar I by the Bell System followed by the use of a **geosynchronous orbit**. With this type of an orbit, an object 22,753 miles above the earth will orbit the earth once every 24 hours above the equator, and from the earth's surface appear to be stationary. The first geostationary orbit was achieved by NASA using a SYNCOM in 1963. The Communications Satellite Act was signed by the United States Congress in 1962 and created the Communications Satellite Corporation (COMSAT). This was followed by the formation of INTELSAT, an organization that is composed of over 120 countries and provides global satellite communication services. In the 1970s, multiple companies in the private sector in the United States began to operate their own domestic satellite systems. Today there are numerous companies providing this service in the United States: e.g., GE Americom, Hughes, Loral, COMSAT, and American Mobile Satellite Corporation. Other nations such as Canada, Australia, Indonesia, Japan, etc. have their own satellite systems. Several international and regional satellite systems have also been formed. Examples of these are INTELSAT, EUTELSAT, Intersputnik, ARABSAT, AsiaSat, etc. [Pritchard and Sciulli, 1986].

The satellite-based communications systems have significantly evolved over a three-decade period. In the 1960s, satellite communications for commercial use became a viable alternative because of the demand for reliable communications (telephony and voice). In the 1970s, technical innovations made larger, more powerful and more versatile satellites possible. Advanced modulation and multiple-access schemes resulted in smaller, less expensive **earth stations** and better service offerings that were lower cost and higher quality. In the 1980s **very small aperture terminals (VSATs)** emerged and the Ku-band frequency spectrum became widely used. In the 1990's satellites support data, voice, and video communications applications. The VSAT industry has given an overall boost to the entire satellite communication industry.

As new satellites are launched, they will have long-term applications which have expanded opportunities. These include private long-haul networks for internal communications, cable TV, pay TV, business voice and data, satellite news gathering, direct broadcast to the home, integrated VSATs, private international satellite service, high-definition TV, mobile service, personal communications, and ISDN. Disaster recovery planning increasingly includes satellites in order to overcome the coverage limitations of existing terrestrial networks. With the allocation of frequencies for personal communications, the promise of global communications and the reality of a personal phone will soon push satellite communications to a new age.

This section describes satellite communications from the application point-of-view. Since VSATs initiated the growth in satellite communication, a significant portion of the section is devoted to this topic. After a review of the satellites' launch and their characteristics, VSAT networks are discussed in detail. Video/audio applications are described next, along with the equipment necessary for these applications. The section is concluded with a summary of next-generation trends.

Satellite Launch

Launching a communications satellite into orbit is a complex and expensive process. This first stage in a satellite's airborne life may cost several million dollars. The cost for launching is primarily a function of the satellite's weight and size. Traditional geosynchronous communications satellites tend to be large and more costly to launch, although the more compact digital communications payloads and longer satellite life will reduce life cycle costs. Low earth orbit communications satellites tend to be smaller and more economical to launch, but will have shorter in orbit life.

A shortage of launch vehicles influenced the economics of the launch industry following the 1986 U.S. Space Shuttle *Challenger* disaster. The shortage has now given way to other launch alternatives. The dominant player in the satellite launch business is the French company Arianespace. Major U.S. players in the satellite launch business are Lockheed Martin, McDonnell Douglas, and Orbital Sciences Corporation. China and Russia have also begun providing launch services.

The launch of a satellite payload into the geosynchronous orbit involves many complex steps. Using the launch vehicle, the payload is first placed in a parking orbit. This is a nearly circular orbit which places the satellite approximately 300 km above the earth's surface. After reaching this orbit, the next step is to fire a motor known as the payload assist module (PAM) to place the payload in a transfer orbit. The PAM motor is discarded afterwards. The transfer orbit is an elliptical orbit whose perigee matches the parking orbit and whose apogee matches the geostationary orbit. Perigee is defined as the point in the orbit closest to the earth, while apogee is the point in the orbit furthest from the earth. The payload itself consists of the satellite with an apogee kick motor (AKM). Once in a transfer orbit, the AKM is fired at the point when the satellite has reached apogee. This firing will place the satellite in a nearly circular orbit. Final positioning of the satellite in geosynchronous orbit can then take place [Pritchard and Sciulli, 1986].

Spacecraft and Systems

A satellite spacecraft employs several major subsystems. These are propulsion, electrical, tracking, telemetry command and control, and the communications subsystem. [Figure 102.4](#) is a diagram of a typical commercial satellite. The propulsion subsystem consists of thrusters oriented in north-south and east-west directions and is used to maintain the spacecraft in the proper orbit and orientation. An electrical subsystem is used to generate electricity in the spacecraft by means of solar cells. Backup batteries are used during periods of equinoxes. The solar cells are also used to charge the batteries. The tracking, telemetry, and command subsystem is used to receive commands from the controlling ground station, as well as to allow the ground station to monitor on-board systems.

The spacecraft requires some form of stabilization to prevent it from tumbling in space. There are two types of stabilization techniques: spin stabilization and three-axis stabilization. Spin stabilization uses an outside cylinder to spin, creating the effect of a gyroscope providing spacecraft stabilization. An internal platform is decoupled from the cylinder, whose orientation is fixed towards the earth. Three-axis stabilization uses internal gyros which sense movement of the spacecraft. Any movement in the axes is detected and can be compensated by firing thruster jets.

The communications subsystem consists of receiver and transmitter sections. The receiver system consists of wideband redundant units. The transmitter subsystem consists of separate amplifiers (transponders) for each channel utilized. Satellite systems make use of orthogonal polarized signals in order to transmit two signals simultaneously on the same frequency, a technique known as "frequency reuse." Two different polarization methods for signals are used: horizontal and vertical linear polarization, or clockwise and counterclockwise circular polarization.

[Figure 102.5](#) shows a simplified block diagram of a typical satellite. A matrix-type switching arrangement is provided on the input and output of the transmitter subsystem for switching to backup transponders. This satellite is three-axis stabilized and operates at Ku-band. There are 16 operational transponders with a bandwidth of 54 MHz each. The employment of frequency reuse provides nearly 1000 MHz of usable bandwidth. Fourteen of the 16 operational transponders use 20-W traveling wave tube amplifiers (TWTA) to provide ground-commandable east or west regional coverage, for 48-state (CONUS) coverage. The remaining two transponders provide 50-state coverage using 27-W TWTAAs. For the 50-state channels, one spare 27-W TWTA provides

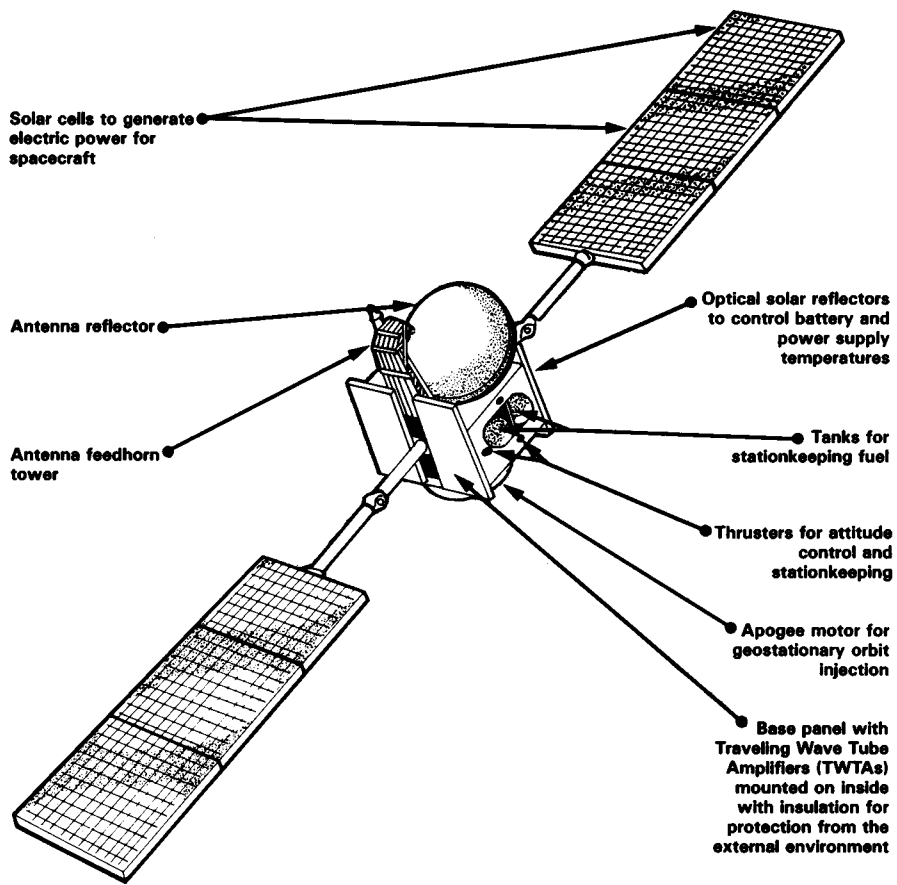


FIGURE 102.4 Simplified block diagram of a communications satellite.

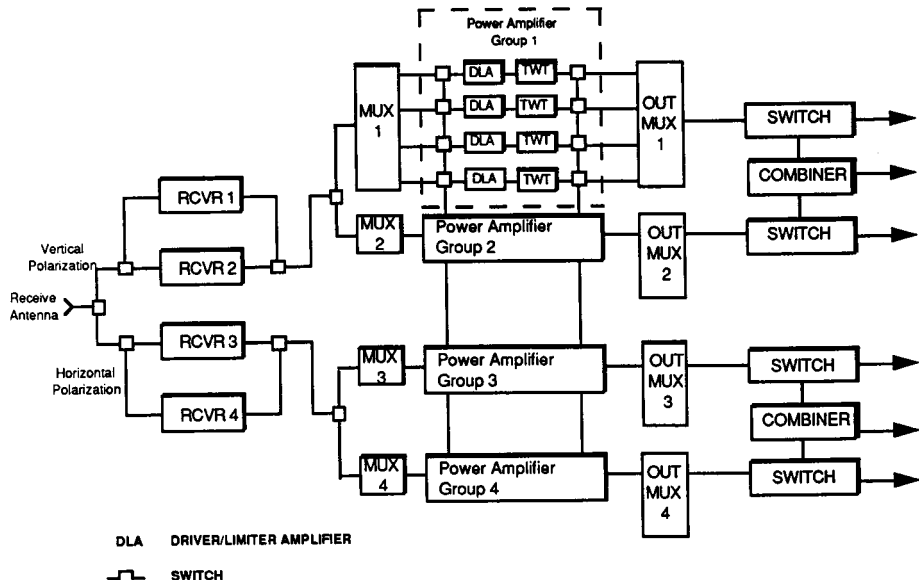


FIGURE 102.5 Simplified block diagram of GSTAR satellite.

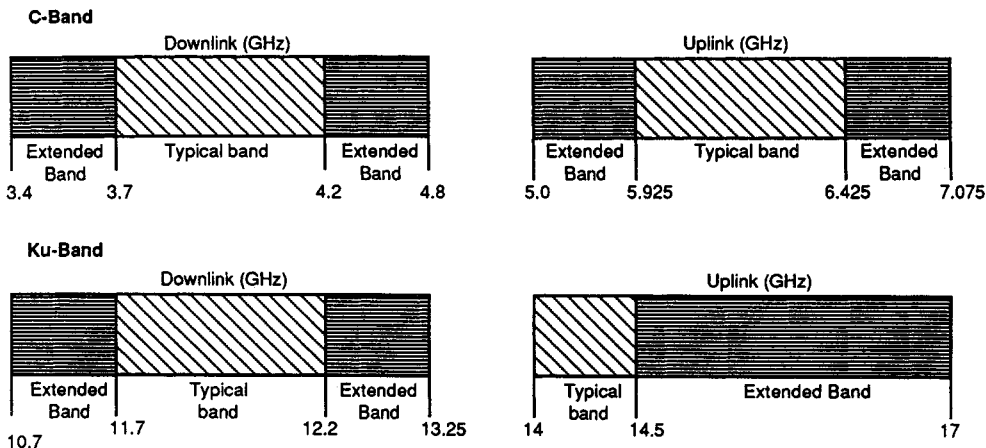


FIGURE 102.6 Ku- and C-band frequency allocation chart.

protection for the two operating TWTAs (3-for-2 redundancy). For the remaining transponder channels, 5 spare 20-W TWTAs provide protection for 14 operating TWTAs (19-for-14 redundancy). Redundant communications receivers are provided on a 4-for-2 basis.

The power radiated from a satellite is described as its effective radiated isotopic power (EIRP) and is the radiated power of the satellite in decibels referenced to one watt of power. The units are in dBW. The strength of the signal received on the ground is a function of the spacecraft location and that of the ground station and will vary depending upon location. A map of the signal strength contours is called the satellite's "footprint."

Geosynchronous Satellites

There are over 500 Ku-band and C-band satellites in geosynchronous orbit. These satellites are typically spaced anywhere between 1 to 3 degrees apart. Older satellites no longer in active service may be spaced less than one degree in an inclined orbit.

The frequency plan for C- and Ku-band satellite services is shown in Fig. 102.6. The typical transmit frequency band used for fixed satellite services in the Ku-band is 14.0–14.5 GHz. Receive frequency is 11.7–12.2 GHz. Some satellites also use the extended band. For C-band satellites, the typical operating transmit frequency is 5.925–6.425 GHz and the receive frequency is 3.7–4.2 GHz. The operating band was extended at WARC '79 to 7.075 GHz to be assigned to individual countries for domestic satellite systems. Ka-band satellites have down-links in the frequency range 17–23 GHz and uplinks in the range 27–31 GHz. Some European and Japanese satellites operate in this range [Long, 1991].

The satellite performance data indicate a wide range of variation in the specifications among the various satellites. Most satellites have a design lifetime of 10 years. The newer GEO satellites tend to have an extended life of 12–15 years. Most domestic U.S. satellites have 24 transponders. The older generation of Asian satellites have very few transponders per satellite. Some planned satellites will have a large number of transponders. Nominal transponder bandwidths include 36, 54, and 72 MHz.

Satellite power is increasing in the newer generation of satellites. Lower-power satellites have an EIRP in the 20–35 dBW range. There are a significantly large number of medium-power satellites in the 35–45 dBW range. Newer high-power satellites tend to have power in the 50–60 dBW range. Direct broadcast satellites are planned for transponder power in the 60–120 W range. The power generally varies with polarization, frequency, and beam. Table 102.2 is a profile of typical satellite performance characteristics.

Mobile Satellite Systems

Mobile satellite systems encompass communications on land, in the air, or over the oceans ideally allowing a person to communicate with anyone anywhere [Long, 1991]. The Inmarsat system is a mobile communications system providing global coverage through a variety of communication paths. In the United States, the FCC has authorized American Mobile Satellite Corporation (AMSC) to provide domestic mobile satellite services. AMSC makes use of geostationary satellites to provide a domestic offering similar to the international offering of Inmarsat.

TABLE 102.2 Typical Satellite Performance

Satellite Operator	System Name	Configuration	EIRP in dBW at Edge	Comments
GE Americom	GSTAR series	Ku-band	38–48	Domestic coverage
	Spacenet series	C- and Ku-band	C-band: 34–36 Ku-band: 39	
Hughes Comm	Galaxy Series	C- and Ku-band	C-band: 34–38 Ku-band: 45–49.5	Domestic coverage
Intelsat	Intelsat VA (IBS)	C- and Ku-band	C-band: 20–26 Ku-band: 38–41	International service, worldwide
	Intelsat VI	C- and Ku-band	C-band: 20–26 Ku-band: 38–41	
	Intelsat VII	C- and Ku-band	C-band: 26–36 Ku-band: 41–46	
Eutelsat	Eutelsat I series	Ku-band	35–43.5	Covers all of Europe
	Eutelsat II	Ku-band	42–47	
NASDA-NTT (Japan)	Sakura 2	C- and Ka-band	C-band: 30 Ka-band: 37	CS-4a, CS-4b in the Sakura series is scheduled for launch during 1992–94

Over the past two decades, there has been active work in the area of low earth orbit (LEO) satellite systems. In general, LEOs are designed to provide a full range of communication services, both voice and data. Proposed systems are designed to complement existing cellular communications technology. Several companies have proposed LEO systems and have made application to the FCC for a “Pioneer’s Preference” license. This license allows the use of new and innovative technology. Motorola’s Iridium system is potentially the largest, using 66 satellites to provide coverage over the entire globe.

Because of the low altitude of the orbit, LEO systems use multiple satellites to provide coverage over a regional area or over the entire globe. Satellites operating at a low orbit are less costly due to the reduced launch costs and reduced weight. However, a low orbit requires the use of multiple satellites since the low altitude of the system provides smaller beam coverage. Since these satellites are not geostationary, ground stations must track an LEO satellite as it passes overhead.

Due to potential growth of mobile satellite communications, several systems are proposed to be in operation in the 1990s. Examples of these systems are the Iridium, Globalstar, ICO, Orbcomm, Starsys, Odyssey, and Teledisc.

Direct Broadcast Satellites

The direct broadcast satellites (DBS) concept is to transmit programming directly to homes using a small receive-only antenna via high-powered satellites. Through the use of a high-powered satellite, a small receive-only satellite antenna may be used for home reception, with the ultimate goal to offer antennas less than one foot in diameter. High-powered DBS satellites use high-powered transponders, i.e., 60–120 W. To prevent interference into the small receive antennas at these high power levels, the DBS satellites will be spaced further apart in geosynchronous orbit.

The first efforts in DBS began in the early 1980s when COMSAT built several DBS satellites, but did not launch them. Internationally, many countries currently have DBS services. Several European countries have high-powered DBS satellites; many others use medium-powered satellites. The DBS industry in the United States is being revitalized by advances in digital video compression technology and the announcement of new players such as Hughes, Primestar, Echostar, etc. to offer DBS services. Hughes Communications and United States Satellite Broadcasting (USSB) system using a high-powered DBS satellite is in operation. As an alternative to the launch of a high-powered satellite, medium-powered DBS systems make use of existing satellites in orbit. However, larger home antennas are required, approximately 2 feet or greater in diameter. A medium-powered DBS in the U.S. is Primestar. Digital video compression techniques using the MPEG-2 standard are used to allow multiple video channels in a transponder. DIRECTV® service, launched in the summer of 1994 by Hughes Electronics, is an example of the direct satellite system.

Earth Stations

Earth stations are the interface point for communications to and from the satellite [Ha, 1986]. An earth station can be divided into two subsystems, the transmit chain and the receive chain. A common element between the transmit and receive chain is the antenna. Because of the large signal attenuation at RF frequencies, the earth station antenna must have high signal gain and be highly directional to focus the power to and from the satellite. A parabolic-shaped reflector antenna is used by earth stations since it can provide these characteristics.

The transmit chain consists of several major components: baseband equipment, modulators, frequency upconverters, high-power amplifiers (HPA), and combiner circuitry used to switch the output of the HPAs to the antenna. The receive chain uses a low-noise amplifier to receive the satellite signals, frequency downconverters, demodulator, and baseband equipment.

In the transit chain the signals are modulated, combined, and frequency-shifted with an upconverter to the desired satellite transmit frequency. After upconversion, the signals are amplified by HPAs. In a large earth station, there may be many HPAs which feed to a single antenna. These signals must be switched and combined appropriately. At microwave frequencies, waveguide combiners are used to route the output of the HPAs to the antenna.

In the receive chain, the counterpart to the HPA is the low-noise amplifier (LNA), which is used to amplify the signals received from the antenna. This amplifier must be designed for maximum gain with a very small noise contribution. The noise generated in this unit contributes significantly to the overall performance of the receive side of the earth station. Gallium arsenide (GaAs) FETs are commonly used in the amplifier section of the LNA because of their low-noise characteristics. The LNA feeds the signal to the frequency downconverter, which converts it to IF frequency suitable for demodulator.

A hub monitoring and control (M&C) system provides the monitoring and control of the RF equipment and baseband equipment. Redundant RF equipment is common at a hub, and the M&C system is used to monitor the components and provide automatic switchover in the event of equipment failure. Switchover between equipment can occur either by operator initiation or automatically by the M&C upon sensing an equipment failure.

Technical characteristics of *large earth stations* have been established for use with the INTELSAT system. INTELSAT categorizes two types of earth stations: multipurpose and special purpose. A multipurpose earth station can be used with any service, while a special-purpose earth station is restricted. Multipurpose standard A, B, and C earth stations have antenna diameters from 11 to 33 meters. Special-purpose standard D, E, and F earth stations have antenna diameters between 3.5 to 11 meters.

In addition to fixed earth stations, "portable" earth stations, called *transportables*, have been manufactured which can be taken to locations originating the programming. These transportables are usually mounted on a truck or trailer and include all the components necessary for an earth station. In the case of the transportable, the antenna size is selected to be as small as 4 meters in diameter. A transportable earth station is designed to be upgraded with "building blocks" to handle heavy, medium, and thin route traffic. Transportable earth stations are designed to meet the requirements for various applications such as temporary business communications, temporary carrier service, backup during the retrofit of an existing earth station, and disaster recovery.

Another type of earth station is the *flyaway*. This is a small remote satellite terminal which can be packed into suitcases for shipment on an airline for delivery anywhere in the world. These systems consist of a small antenna, RF unit, and baseband equipment to provide a complete satellite communications station. An example is an L-band version which provides audio communications via the Inmarsat system. Fitting into a small suitcase, it contains a telephone handset, RF electronics, and antenna that can be assembled to provide audio communications anywhere in the world. Mobile satellite terminals are even smaller, suitable to be carried as handheld or briefcase units.

VSAT Communication System

Advances in technology have revolutionized the satellite communications industry by deployment of very small aperture terminal (VSAT) networks for data, voice, and video communication. Since the mid-1980s, VSAT networks have become widely used in the oil, lodging, financial, auto, retail, and manufacturing industries. By the 1990s, VSATs were operating in C and Ku-bands. Also by the mid-1990s, over 70% of the VSAT market

TABLE 102.3 Typical VSAT Systems Features

Feature	Interactive	Point-to-point	Broadcast
Topology Communication	Star Between hub and VSATs, VSAT to VSAT through hub	Point-to-point, mesh VSAT to VSAT	Point-to-multipoint Hub to VSATs
Frequency	Ku-, C-band	Ku-, C-band	Ku-, C-band
Hub antenna	3–11 m	—	3–11 m
VSAT antenna	0.9–2.4 m	1.8, 2.4 m	0.5–2.4 m
Hub to remote access	TDM, SCPC, spread spectrum	SCPC	SCPC, spread spectrum, FM ²
Remote to hub access	ALOHA, reservation stream, CDMA	SCPC	—
Outbound data rate (Kbps)	56–512	9.6–2048	9.6–2048
Inbound data rate (Kbps)	9.6–256	9.6–2048	—
Modulation	BPSK, QPSK, DPSK	BPSK, QPSK	BPSK, QPSK, FM ²
FEC	Rate 1/2, convolutional or block	Rate 1/2, convolutional	Rate 1/2, convolutional or block
Protocols	SDLC, Bisync, Async, X.25, TCP/IP Burroughs and others	Clear channel	Clear channel, synchronous, HDLC format

was accounted for by the retail, automotive, and financial industries. VSATs are making private networks a viable alternative for many companies, for applications such as point-of-sale, reservation systems, remote monitoring and control, branch office administration, financial transactions, etc. A VSAT is a small earth station suitable for installation at a customer's premises. A VSAT typically consists of antenna less than 2.4 m, an outdoor unit to receive and transmit signals, and an indoor unit containing the satellite and terrestrial interface units [Rana et al., 1990].

VSAT networks fall into three general categories: broadcast networks, point-to-point networks, and interactive networks. In a broadcast network, a centralized hub station broadcasts data, audio, and/or video to a group of receive-only VSATs. Low-cost receive-only VSATs can receive news, weather services, and financial information. Music distribution and video broadcast via broadcast networks is widely used. Point-to-point networks provide direct communication between two locations without the requirement of a large hub for data, voice, and image transmission. Variations of these networks include point-to-multipoint dedicated circuits or demand-assigned mesh topologies. Interactive networks are used for two-way communications services between a central hub station and a large number of VSATs in a star topology. Table 102.3 is a summary of the salient features of VSAT networks. VSATs are available for both C- and Ku-band frequency. Most VSAT systems use BPSK modulation with Rate 1/2 FEC. For interactive networks, the inbound channel is shared on contention basis to conserve space segment. More advanced systems use concatenated codes to improve performance. Recently, hybrid VSATs have been introduced to use terrestrial networks on the return channel. An example is the Hugh's Direct PC which uses a high speed satellite receive channel, and a low speed terrestrial return channel.

A critical element of VSAT networks is the network availability. The VSAT system availability is affected by three major components: effects of rain attenuation, equipment availability, and software availability. The effects of rain attenuation for Ku-band networks are significant. While link availability is usually specified at 99.5%, link performance can be optimized to nearly any desired value through the use of energy dispersion techniques or large antenna sizes. The network hardware must be highly reliable. Hub hardware should provide for optional redundancy and the ability to achieve better than 99.9% availability. The use of hub diversity and uplink power control can also be used to improve the network availability. The VSAT hardware availability is less catastrophic; the loss of one VSAT does not constitute network failure but may require a service call to rectify the problem. Hence, it is common to use nonredundant but highly reliable VSAT units. Software availability needs to be improved since software failures dominate the overall availability of interactive networks in existing VSAT products.

Interactive networks have been by far the most popular for data communication and audio/video overlays. The remaining portion of this section is devoted to these networks. An interactive VSAT system consists of a

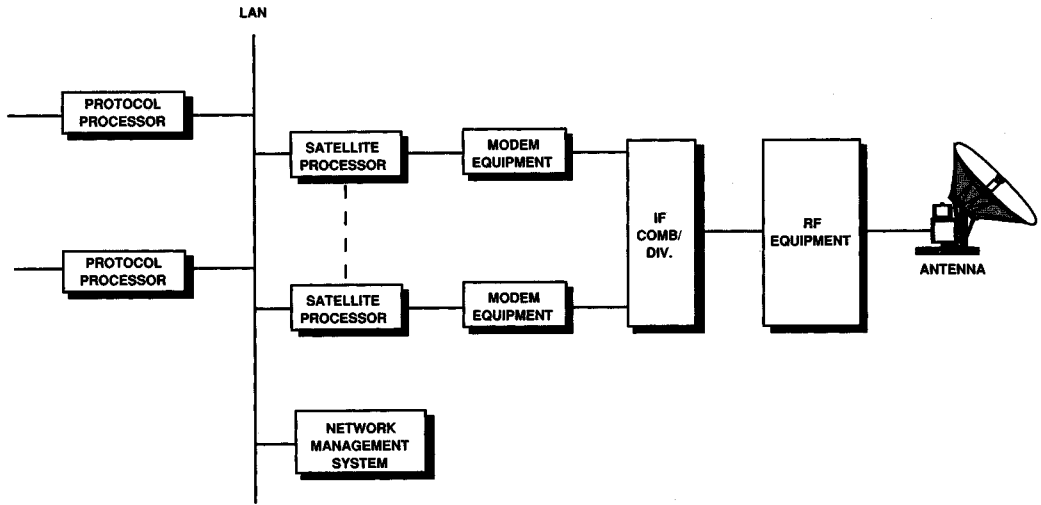


FIGURE 102.7 Block diagram of a hub.

hub, VSAT, network management system, and associated transmission and processing subsystems. These subsystems along with sophisticated **satellite access protocols** and terrestrial protocol interfaces make interactive networks a flexible and powerful communication medium.

Hub

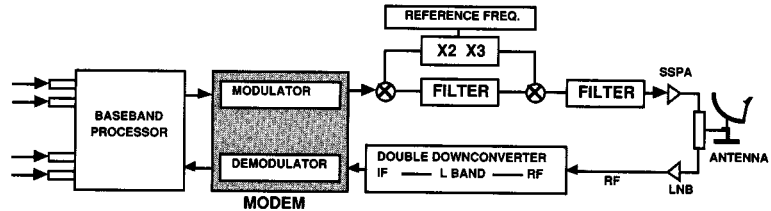
The hub performs all functions that are necessary to establish and maintain virtual connections between the central location and VSATs. In private dedicated networks, the hub is co-located with the user's data processing facility. In shared hub networks, the hub is connected to the user equipment via terrestrial backhaul circuits. Since the hub is a single point for failure in a star network, it is typically configured with 1:1 or 1: N redundancy. The hub consists of antenna, RF, and baseband equipment (Fig. 102.7). It will handle multiple channels of inbound and outbound data and often one or more channels of audio or video broadcast.

The hub antenna consists of a parabolic reflector and associated electrical and mechanical support equipment. The RF subsystem converts the modulated carrier to RF frequency, provides the necessary signal amplification, and transmits the resulting RF carrier to the antenna subsystem. It also receives RF signals from the antenna subsystem, provides low-noise amplification, RF/IF conversion, and passes the resulting IF carriers to the baseband equipment subsystem. The hub baseband equipment consists of the modem equipment and the processing equipment. The hub modems employ continuous modulators and burst demodulators. The processing equipment interfaces to the modem equipment and provides the satellite access processing and protocol processing for interface to the customer host.

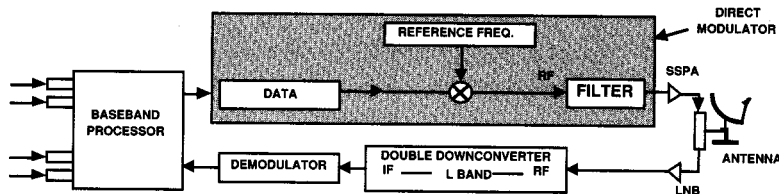
VSAT

The VSAT consists of an antenna, outdoor unit (ODU), interfacility link (IFL), and indoor unit (IDU). The IFL connects the IDU and ODU subsystems, providing the transmit and receive lines, monitor and control signals, and dc power for the ODU electronics. A single-cable IFL, in which all signals are multiplexed on the same cable, is usually used to reduce the cost of IFL. VSATs nominally use a 1.2- or 1.8-m offset feed parabolic antenna. Smaller antenna sizes are preferable to reduce the installation cost. Options for small antennas include the use of either a submeter parabolic reflector or a flat-plate antenna. The choice of antenna is a tradeoff among performance, installation cost, and aesthetic considerations.

The ODU consists of a solid-state power amplifier (SSPA), a low-noise amplifier, upconverter, and a down-converter. VSAT SSPA modules are usually between 1.0 to 3.0 W. The ODU cost can be significantly lowered by utilization of a low-power SSPA (0.1 to 0.5 W) consistent with obtaining the required output power. The VSAT receive side front end can be economically configured using an LNB. Low-cost HEMT LNBs are currently available with 50–60 dB gain and noise figures lower than 1.3 dB.



(a) Conventional VSAT



(b) VSAT using direct modulation.

FIGURE 102.8 Simplified VSAT block diagram.

Direct modulation of the RF carrier may lower the cost of the VSAT IF and RF electronics while consolidating modulation and upconversion functions. Direct modulation allows the design of a VSAT with fewer parts, smaller size, and lower weight than with traditional outdoor units. Figure 102.8 is a block diagram showing a conventional VSAT and a VSAT using direct modulation. An L-band receive interface between the ODU and IDU is preferable in order to receive audio and video overlays.

The IDU is located near the user terminal equipment. Major IDU functions include outbound carrier signal acquisition, tracking, demodulation, bit synchronization, burst modulation, and protocol processing. It also controls the operation of the ODU, monitors VSAT health, and responds to hub commands. The baseband processing system performs satellite channel access and protocol and customer interface processing functions. A video/audio port can be provided with an RF splitter at the IDU to separate the received audio/video signal for the optional video/ audio receiver.

Network Management System

The network management system (NMS) is a critical element of a VSAT network. Through the NMS, the user can have full control of his network, which is usually not possible in the case of terrestrial network facilities. The NMS generally provides a centralized management tool for hub and VSAT equipment configuration control, assignment of inbound and outbound satellite channels, network monitor and control, switchover to back-up equipment, network statistics collection, downline loading of new software, and report generation. In the shared hub environment, the hub operator controls the allocation of resources among various users and controls the RF transmission facility. The user must have the ability to manage his portion of the network transparent to other users. In the case of a dedicated hub, a single management entity can exert full control over the network, including RF transmission facilities.

The network management system standards community has defined five functional areas as requirements for network management systems. These areas are fault management, accounting management, configuration management, performance management, and security management. The VSAT network management system should be capable of interfacing with other network management systems by supporting a standard network management protocol. The protocol standard most widely accepted is the Simple Network Management Protocol (SNMP).

Transmission System

Most VSAT systems employ BPSK or QPSK modulation with rate $R = 1/2$, $K = 7$ convolutional coding and soft-decision Viterbi decoding on both the inbound and outbound channels. Differential phase shift keying (DPSK) modulation may be used to reduce the demodulator complexity and cost. DPSK is relatively insensitive

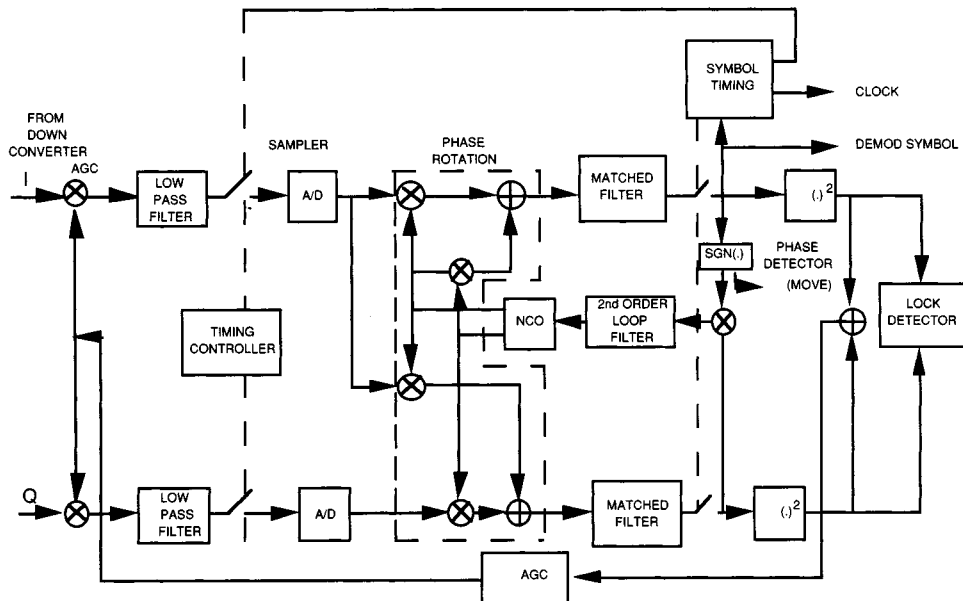


FIGURE 102.9 DSP demodulator functional diagram.

to phase noise and frequency offset, thus allowing the use of lower-cost LNBs in the VSAT terminals. However, as compared to BPSK, convolutionally encoded DPSK requires about 2 dB greater E_b/N_0 at a BER of 10^{-5} . In addition, if operation is required below 10 dB, some form of low-level interleaving may be required.

In lieu of performing the VSAT demodulation function via the traditional analog circuit techniques, an all-digital implementation using digital signal processing (DSP) techniques may be considered. The merits of DSP include the development of a more testable, producible, maintainable, configurable, and cost-effective demodulator. Figure 102.9 presents an illustration of the DSP demodulator functions to be implemented using the DSP processor(s). The functions of the major blocks are as follows: phase locked loop (PLL) for carrier acquisition, narrowband Costas loop for data detection, external automatic gain control (AGC), dynamically advance/retard sampling to achieve optimum data sampling, and A/D converters for signal analog-to-digital conversion.

A VSAT system must employ frequency agility in the remote terminal to use an assigned block of frequencies within a transponder. Within the assigned frequency band, one or more outbound carriers and a number of inbound carriers are precisely located. On the VSAT receive or outbound side, the LNB output can be demodulated directly using a synthesizer-controlled local oscillator, or further downconversion can be used under synthesizer control to obtain the demodulator input signal at a standard IF frequency such as 70 or 140 MHz. In the inbound direction, channel selection can be accomplished by two methods. First, the carrier frequency of the modulator can be shifted to select the appropriate channel and a fixed upconverter may be used to obtain the RF signal. Second, the synthesizer output frequency may be multiplied up to RF to obtain the carrier, which may then be modulated directly with the data as described in Cannistraro and McCarter [1990].

Satellite Access Protocols

The multiple satellite access protocol is one of the most critical elements to the performance of a VSAT network. VSAT systems tend to be used in applications where message delay is critical and this protocol is the controlling element to the delay-throughput performance of the system. During the past 15 years, there have been numerous multiple-access protocols developed and simulated in the context of satellite packet communications [Raychaudhuri and Joseph, 1988]. Table 102.4 provides a comparison of throughput vs. delay for various satellite access protocols.

In the outbound or hub-to-VSAT direction, a TDM channel is employed. This channel may be regarded as a point-to-multipoint or broadcast channel with node selectivity being achieved by the use of addressing

TABLE 102.4 Random Multi-Access Protocols Comparison

	Throughput	Comments
Pure ALOHA	0.13–0.18	Low cost, good for variable-length messages
Slotted ALOHA	0.25–0.37	Good for fixed-length messages
Selective reject ALOHA	0.20–0.30	Variation of pure ALOHA with a modified algorithm
Tree CRA	0.40–0.49	Sensing capability for collision resolution, good for fixed-length messages
Announced retransmission random access (ARRA)	0.50–0.60	Uses modified algorithm of slotted ALOHA by announcement of transmission
Random access with notification	0.45–0.55	Uses partition for new and retransmitted message
CDMA	0.10–0.40	Used in spread spectrum systems, low delay

information embedded in the modulated data stream. The delay performance of this channel is essentially controlled by the queuing behavior of the hub. In the VSAT-to-hub direction, a large number of VSATs share the channel to conserve space segment. Most VSAT networks utilize a combination of slotted ALOHA protocol for the interactive component of the inbound traffic and a reservation TDMA scheme for any bulk data transfers. Most protocols are adaptive in the sense that as the channel traffic increases, they automatically evolve into reservation TDMA systems. Code division multiple access (CDMA) has been used in VSATs operating at C-band. CDMA permits more than one signal to simultaneously utilize the channel bandwidth in a noninterfering manner. This makes it possible to significantly increase the utilization and throughput of the channel.

Interface Capabilities

Most VSAT systems support common data communications protocols such as SDLC, X.25, Async, Bisync, TCP/IP, etc. Coexistence of different protocols is allowed in a network. A VSAT supports multiple ports with common interfaces such as RS232C, RS422, V.35, etc. VSAT networks typically must provide **protocol spoofing** to provide acceptable delay and throughput performance to the end-user application. To minimize the effect of satellite delay, the host computer front-end processor is emulated at the VSAT location, and multiple cluster controllers are emulated at the hub location. The polling associated with the front-end processor to cluster controller communication is not carried on the satellite link, but is instead emulated locally.

Video

Satellites are an excellent medium for video transmission since they can provide a broadcast capability with wide bandwidth. Video on satellites is ideal for applications such as videoconferencing, business TV, distance learning, satellite news gathering, etc.

Video Teleconferencing

Satellite communications provides a cost-effective and flexible means of interactive videoconferencing. Technological improvement in videocompression has resulted in low-cost codecs at data rates less than T1, and good quality videoconferencing is possible at data rates as low as 56 Kbps. Low-cost satellite terminals coupled with low-cost codecs are making videoconferencing via satellite affordable and practical for many organizations. Applications include all types of business meetings and technical information exchange such as management and staff meetings, new product introductions and updates, sales meetings, training, and market presentations. Videoconferencing allows people at different locations to meet with almost as much ease as being in the same room, providing benefits of increased productivity, reduced travel time and cost, and increased management visibility.

A generic videoconference system is presented in [Fig 102.10](#). The system consists of a specially designed room, video/audio equipment, transmission equipment, monitor and control computer, and space segment. The video and audio feeds from the meeting room pass through the codec and are compressed. From the codec, the signal passes to the satellite modem for modulation. The radio frequency/terminal (RFT) upconverts the modulated carrier and amplifies it for transmission to the satellite. At the other site, the process is reversed.

A videoconferencing network features point-to-point, broadcast, or point-to-multipoint architectures. In a point-to-point system, two sites are configured for interactive conference with duplex audio and full motion video transmission. Videoconferencing broadcast is appropriate for formal presentations where the presenter

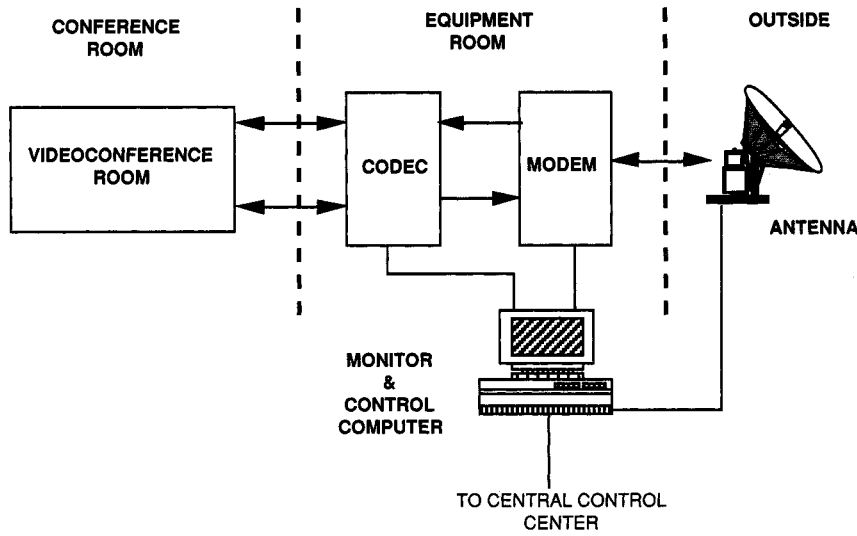


FIGURE 102.10 A generic videoconference system.

does not need to see the audience, such as a speech from a senior corporate executive. In a point-to-multipoint conference, multiple sites can receive a transmitting site. Two of the primary sites are fully interactive with each other. A feature called multipoint switching has been implemented in some commercial systems. This feature allows switching of receive and transmit sites during the conference. The multipoint switching feature can be provided using either a TDMA or SCPC system. A TDMA system allows multiple sites to transmit and receive in a mesh configuration. An economical multipoint switching system is possible with SCPC using only two transmit frequencies. In a “chair” controlled conference, the chair is assigned one of these frequencies for the duration of the conference. Dynamic allocation of the second frequency is controlled by the chair to any of the participating sites at any time during the conference.

Video Broadcast

Video broadcast over satellite is attractive for industry segments such as educational TV, distance learning, business television, and television receive-only (TVRO) applications. Business television allows users to transmit broadcast-quality video programming from a studio to any number of specified locations equipped with TVROs. A video broadcast capability, as an overlay to interactive data networks, is becoming increasingly popular for corporate presentations, education, and training.

A video uplink consists of a video exciter, HPA, antenna, and optionally an encryption system such as B-MAC (multiplexed analog component, version B) encoder, for business video broadcasts. Each remote VSAT must be configured to receive the video transmission. This involves adding a video receiver at each VSAT location that plugs into the VSAT IDU. Audio/video signals from the video receiver can be presented directly or through a B-MAC decoder to a standard TV monitor.

The digital compressed video signal can be used as a replacement for an analog video distribution. Digital coding technology can be used to compress video signals to reduce data rates to 2 Mbps or even lower and reproduce near broadcast-quality video. Distribution of digital video signals at such rates requires less transponder bandwidth and a smaller antenna at remote terminals. Compression techniques used are based on one or a combination of the following: inter/intra-frame prediction, adaptive differential transform, conditional replenishment, discrete cosine transform, adaptive prediction, motion compensation, and vector quantization [Patterson and Delp, 1990].

Satellite News Gathering

Satellite news gathering (SNG) is used for live, on-the-spot coverage and news exchanges with other commercial broadcast stations. This is made possible by the availability of occasional-use space segment and transportable earth stations on news trucks. An SNG system consists of a compact earth station and video/audio transmission

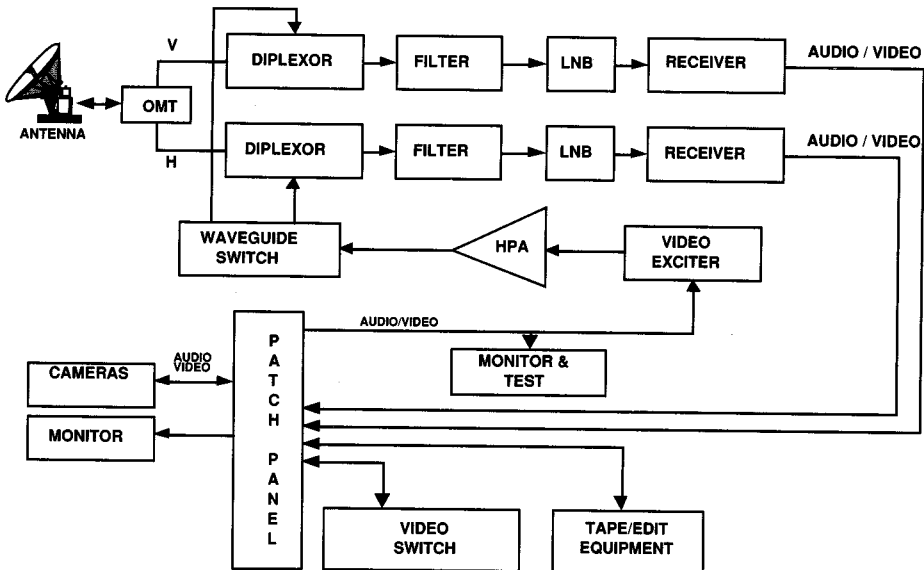


FIGURE 102.11 SNG vehicle video/audio system.

system on a truck. A duplex voice channel is used to coordinate between the space segment provider, studio, and the SNG truck.

Figure 102.11 presents a block diagram of a typical SNG system. The RF subsystem has a transmit path and two independent receive paths. The transmit path consists of an HPA and a frequency agile video exciter which modulates and upconverts the video signal to the satellite's RF frequency. A waveguide switch is used to select transmit polarization. Camera signals go simultaneously to tape for storage and for transmission over the satellite. A receive path is typically provided for both receive polarizations. Each path consists of a transmit reject filter and an LNB which downconverts to L-band. The received L-band signal passes through a video satellite receiver, from which point it can be routed to various monitor or test points or be routed to a tape device for recording and storage.

Audio

The use of commercial broadcast audio transmission via satellite began in the late 1970s with National Public Radio and Mutual Broadcasting using Western Union's WESTAR I satellite. The main application was to send high-quality audio to radio broadcast stations to transmit programming information. This type of system makes use of single channel per carrier (SCPC) satellite transmission, where each satellite channel corresponds to one audio channel. The entire satellite channel is FM modulated. Pre-emphasis is used over the channel to provide additional noise reduction. A variation of this technique, called multiple channel per carrier (MCPC), can be used to transmit multiple channels over a single satellite carrier. Figure 102.12 is a block diagram of the MCPC system.

As the marketplace searched for lower-cost systems, the FM² (or FM/FM) modulation technique evolved, allowing the use of low-cost FM receivers. Through a high-powered FM modulated carrier on the satellite, a low-cost audio and data broadcast receiver can be built. This FM/FM modulation technique is widely used to distribute audio and data on a low-cost basis.

In addition to audio broadcasts, satellite-based voice applications include point-to-point voice, multinode interactive voice, and voice over data VSATs. Point-to-point voice is most prevalently used for high-volume voice trunking for long-distance connectivity or transoceanic connectivity. A multinode, interactive voice architecture is ideal in providing voice connectivity to remote locations that are not serviced by terrestrial voice facilitates. Both mesh and star configurations are used to provide multinode voice connectivity. Automated satellite access control and resource allocation techniques are used to allow for granting requested on-demand

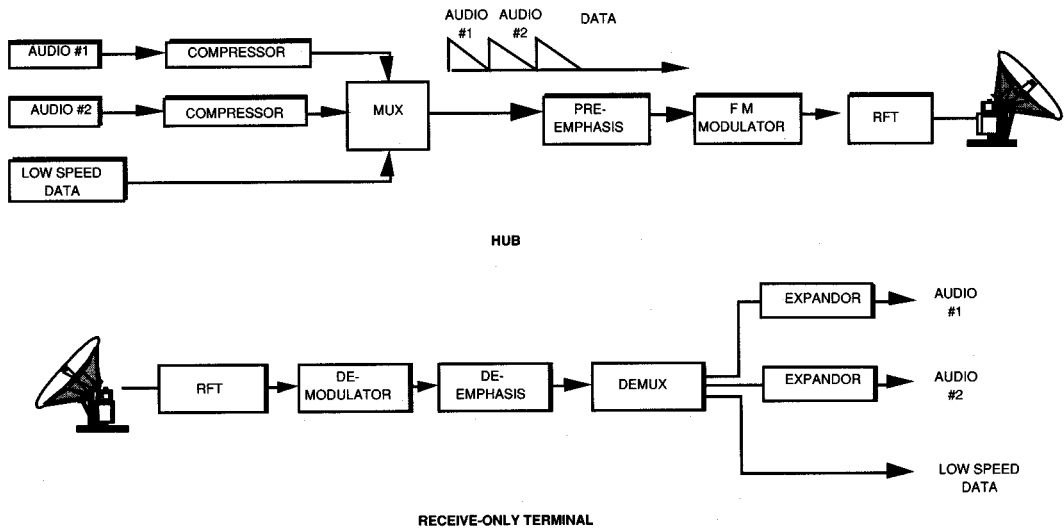


FIGURE 102.12 Block diagram of the MCPC system.

availability of voice connectivity. To support voice over data VSATs, an audio encoder is used to accept an analog voice signal, digitize and packetize it, and format it for transmission through the VSAT data network. A voice port may either be implemented as part of a “baseline” data/voice card or as an add-on stand-alone box.

The integrated data/voice system employs a TDM outbound carrier and shared inbound carriers for data and voice transmission. Two types of voice network communications alternatives may be implemented for voice channel communications: a poll/response access scheme and a reservation TDMA access scheme. With the poll/response access scheme, the hub polls the VSAT voice ports on a cyclic basis. The VSATs return their responses in the form of call requests or status updates. The number of sites in the voice network determines the rate at which VSATs are polled. Thus, this scheme is suitable for a small network. Excessive polling delays will be encountered for a network with a relatively large number of remotes.

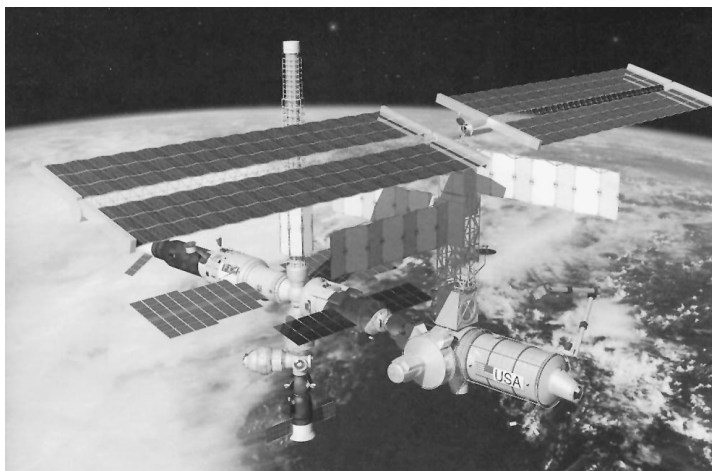
In reservation TDMA, on the other hand, voice call requests are serviced by the assignment (reservation) of a logical channel for inbound voice traffic. Although various means are implemented to avoid collisions on the satellite link, the time needed to reserve capacity on an inbound carrier may be lengthy, depending on traffic conditions. Therefore, call setup times are not as predictable as they are with the poll/response access scheme.

The VSAT design is ideally suited for digital compressed voice. Coding rates of 32, 16, and 9.6 kbps and lower can presently be achieved, depending on the compression technique employed. There are two classes of digitizing voice signals: waveform coding and vocoding. In waveform coding, the analog voice curve is coded and then reproduced by modeling its physical shape. Data rates are relatively high, i.e., higher than 9.6 kbps. Vocoding attempts to reproduce the analog voice curve by abstractly “identifying” the type and shape of the curve. Only a set of parameters is transmitted, describing the nature of the curve. Achieved data rates can be as low as 1.2 kbps.

Second-Generation Systems

The recent wave of satellites have much higher power than their predecessors. The Intelsat K satellite, for example, is equipped with 60-W TWTAs and serves increasing worldwide traffic, video, and VSAT services. Another example is the Telstar 4 satellite which has variable power up to 120 W for Ku-band transmissions and is being promoted to be HDTV compatible in preparation for expected widespread use of HDTV. Other trends in satellite design, i.e., NASA's advanced communication technology satellite (ACTS), include the use of multiple spot beams and onboard IF and/or baseband switching. Onboard switching coupled with electronically hopped spot beams and laser intersatellite links have been proposed. Spot beams provide higher satellite EIRP which permits small, low-cost VSATs to accommodate higher bit rate transmissions. The use of multiple-beam architectures also increases bandwidth availability through frequency reuse. Advances in multibeam satellites

INTERNATIONAL SPACE STATION



The interim International Space Station will look like this. In the right foreground is the U.S. laboratory module and the station's airlock. In the center of the horizontal string of modules is the FGB energy block. The solar power array at the top is one of four that will provide power for the complete station. Below the tower is the Russian-built universal docking module and, at bottom, one of two crew transfer vehicles. (Photo courtesy of National Aeronautics and Space Administration.)

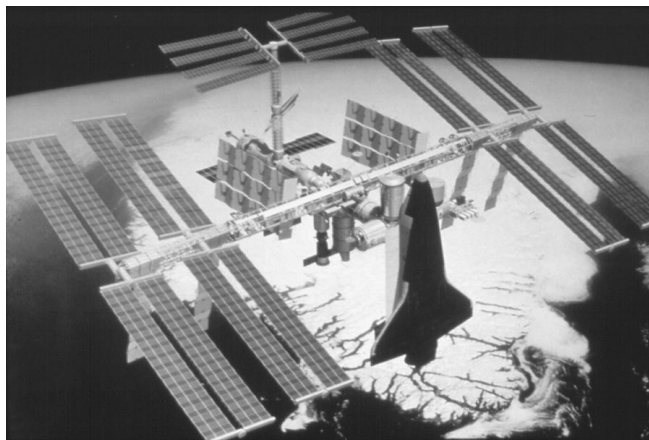
The International Space Station will be a permanent laboratory for human-monitored long term research in the unique environment of Earth-orbital space, an environment that cannot be duplicated on Earth for long duration experiments. This space station program draws upon the resources and scientific and technological expertise of 13 cooperating nations.

This project is being constructed in three phases. Phase I included the 1995 construction of two Boeing-built nodes (Node 1 and Node 2). The nodes will serve as connecting passageways between modules. Phase I was completed in early 1996 with the production of the U.S. laboratory module where astronauts will perform continuous scientific research.

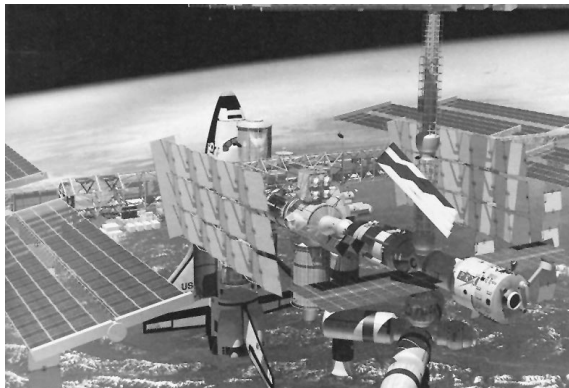
Phase II of the space station program begins in November 1997 with the launch of the FGB functional cargo block on a Russian *Proton* vehicle. The FGB is a 21-ton element that will provide altitude control and propulsion during the early assembly operations, plus solar power and berthing ports for additional modules. In May of 1998, the embryo space station will grow with the addition of the *Proton*-boosted Russian service module, which provides life support and habitation facilities, utilities, and thrusters. Then the crew transfer vehicle, a Russian Soyuz TM capsule, will be joined to the station. By June 1998, the first three-person crew will begin its orbital stay. Phase II will be completed in Spring of 1999.

In Phase III, the International Space Station will progress gradually to its ultimate status as a fully operational permanent orbital research facility. Among key additions to the core configuration are the remaining modules of the U.S.-built solar array; the Japanese experiment module, to be delivered in 2000; and the U.S. habitation module which contains the galley, toilet, shower, sleep stations, and medical facilities. With the delivery of a second Russian crew transfer vehicle in June 2002, the station will be virtually complete.

The completed station will measure 361 feet from tip to tip of the solar arrays. The pressurized living and working space is roughly equivalent to the passenger cabin volume of two Boeing 747 jetliners. The



A concept view of the International Space Station in its final configuration with a space shuttle orbiter docked at the fore port. The cylinder near the orbiter's nose is the U.S. centrifuge accommodation module. Below it, hidden by the orbiter, is the U.S. laboratory module, flanked by the European (left) and Japanese laboratories. (Photo courtesy of National Aeronautics and Space Administration.)



This concept view is of the station from the opposite (aft port) end. In the foreground (lower right) is the Russian service module, with living and working room for three crew members. Next, toward the center of the photo, is the FGB energy block, then (near the orbiter) the U.S. laboratory module. The vertically mounted cylinder below it is the U.S. habituation module. (Photo courtesy of National Aeronautics and Space Administration.)

space station will contain seven laboratories. In addition, the Japanese experiment module has an exposed "back porch" with 10 mounting spaces for experiments that require long duration with the space environment.

Beginning in 1997, there will be a total of 73 assembly and service flights until the station becomes fully operational in midyear 2002. (Courtesy of National Aeronautics and Space Administration.)

with onboard baseband processing allows some of the intelligence in the central hub and VSAT equipment to be moved to the satellite. The result is expected to be improved VSAT-to-VSAT communications and a platform to provide dynamic bandwidth allocation [Naderi and Wu, 1988].

The trend in deploying higher-power satellites has an inverse effect on the size of the earth station antenna. The earth stations are becoming smaller, less complex, and more cost effective. Private hubs are now typically in the range of 3.5 to 7.6 m and are not required to be staffed. Two-way VSATs antennas originally deployed in sizes from 1.2 to 1.8 m are now using elliptical or rectangular-shaped antennas with apertures equivalent to 1.0 m or less. Two-way ultra-small aperture terminals are also emerging. These lower-cost, lower-functionality earth stations are designed for thin route, niche-type applications such as point-of-sale and credit card transaction processing. The advances in DSP technology will continue to enhance the capabilities and performance while at the same time lowering the cost of VSATs. The advances in MMIC technology continue to miniaturize the RF components while increasing reliability.

With advances in digital signal processing and compression techniques, analog video and audio transmission will increasingly be converted to digital transmissions. The advanced compression techniques reduce the bandwidth requirements and allow for smaller and lower-cost VSAT antennas to be used. The continued technological advances in satellite technology and the emerging demand for more flexible communication services will generate new satellite communications applications, such as LAN interconnections and ISDN support [Murthy and Gordon, 1989]. Satellite communications will also play an increasing role in mobile communications on land, air, and on sea. In addition to telephony services, new services such as global distress and safety applications, global positioning, navigation, voice messaging, and data transmissions are now possible.

Defining Terms

Earth station: The interface point for communications to and from a satellite. An earth station (also known as a hub) consists of an antenna and transmit and receive subsystems.

Geosynchronous orbit: An orbit 22,753 miles above the earth in which an object will orbit the earth once every 24 hours above the equator and will appear to be stationary from the earth's surface.

Protocol spoofing: A technique used by VSAT networks to reduce the network delay. The satellite network emulates the host computer front-end processor at the VSAT location and emulates the multiple cluster controllers at the hub location.

Satellite access protocol: A set of rules by which a number of distributed VSATs communicate reliably over a shared satellite channel.

VSAT: Very small aperture terminal. A small earth station suitable for installation at a customer's premises. A VSAT typically consists of an antenna less than 2.4 m, an outdoor unit to receive and transmit signals, and an indoor unit containing the satellite and terrestrial interface units.

Related Topics

74.1 Introduction • 78.1 Introduction

References

- J.C.L. Cannistraro and S. McCarter, "Direct modulation lowers VSAT equipment costs," *Microwaves and RF*, pp. 99–102, August 1990.
- T.T. Ha, *Digital Satellite Communications*, New York: MacMillan, 1986.
- M. Long, *World Satellite Almanac*, 3rd ed., Winter Beach, Fla.: MLE, Inc. 1991.
- K.M. Murthy and K.G. Gordon, "VSAT networking concepts and new applications development," *IEEE Communications Magazine*, pp. 43–49, May 1989.
- F.M. Naderi and W.W. Wu, "Advanced satellite concepts for future generation VSAT networks," *IEEE Communications Magazine*, vol. 26, pp. 13–22, July 1988.
- H.A. Patterson and E.J. Delp, "An overview of digital image bandwidth compression," *Journal of Data and Computer Communications*, pp. 39–49, Winter 1990.

- W. Pritchard and J.A. Sciulli, *Satellite Communication Systems Engineering*, Englewood Cliffs, N.J.: Prentice-Hall, 1986.
- A.H. Rana, J. McCoskey, and W. Check, "VSAT technology, trends, and applications," *IEEE Proc.*, vol. 78, no. 7, pp. 1087-1095, July 1990.
- D. Raychaudhuri and K. Joseph, "Channel access protocols for Ku-band VSAT networks: A comparative evaluation," *IEEE Communications Magazine*, vol. 26, no. 5, pp. 34-44, May 1988.

Further Information

The *World Satellite Almanac* provides a tutorial of the satellite communications industry. It includes the technical characteristics and footprint maps for geosynchronous satellites worldwide. Contact: MLE Inc., P.O. Box 159, Winter Beach, FL 32971.

World Satellite Communications and Earth Station Design is a text which provides an analytical presentation of communication satellites and their applications. Contact: CRC Press, Inc., 2000 Corporate Blvd., N.W., Boca Raton, FL 33431.

The monthly *IEEE Communications Magazine* investigates VSAT communications in a special series spanning several issues between 1988 and 1989. Contact: IEEE Service Center, 445 Hoes Lane, Piscataway, NJ 08854-4150.

Clapp, G., Sworder, D. "Command, Control and Communications (C^3)"
The Electrical Engineering Handbook
Ed. Richard C. Dorf
Boca Raton: CRC Press LLC, 2000

Command, Control, and Communications (C^3)

G. Clapp

*Naval Command, Control and
Ocean Surveillance Center*

D. Sworder

University of California, San Diego

103.1 Scope

103.2 Background

103.3 The Technologies of C^3

103.4 The Dynamics of Encounters

103.5 The Role of the Human Decisionmaker in C^3

103.6 Summary

103.1 Scope

The focus of this chapter is not a detailed profile of a current or planned military C^3 system but it is rather on the issues and the technologies of the C^3 mission. Evolving technology, an evolving world order, and constant programmatic reorderings render such express descriptions to become rapidly outdated. Thus block diagrams of specific military systems (and listings of their acronyms) are de-emphasized. Of paramount interest is not electronics technology in isolation, but rather technology integrated into systems and analysis of these systems operating under complex real world environments that include technologically capable adversaries. The human commander or **decisionmaker**, as the principal action element in a C^3 system, is included explicitly in the system analysis.

103.2 Background

Electronics technology is nowhere more intensively and broadly applied than in military systems. Military systems are effective only through their command and control (C^2) and this is recognized by the fact that C^3 is a critical discipline within the military. Frequently systems will be denoted C^2I or C^3I rather than command and control. This adds to C^2 the essential area of **intelligence** and intelligence products derived from surveillance systems. All variants of these acronyms are to be considered equal, whether or not communications, intelligence, or surveillance have been left implicit or made explicit. Likewise the superscript notation is considered optional and interchangeable. The formal discipline of C^3 within the military has not been matched by focused technical journals or university curricula due to its highly multidisciplinary nature.

Two definitions from a Joint Chiefs of Staff (JCS) publication [JCS, Pub. 1] capture the breadth of C^2 . This reference defines command and control as “The exercise of authority and direction by a properly designated commander over assigned forces in the accomplishment of his mission. Command and control functions are performed through an arrangement of personnel, equipment, communications, facilities, and procedures which are employed by a commander in planning, directing, coordinating and controlling forces and operations in the accomplishment of his mission.”

C^2 systems are defined, with almost equal breadth, as “An integrated system comprised of doctrine, procedures, organizational structure, personnel, equipment, facilities, and communications which provides authorities at all levels with timely and adequate data to plan, direct and control their operations.”

A LOOK TOWARD FUTURE FLIGHT

On March 19, 1996, NASA and McDonnell Douglas Corporation unveiled to the public a new subsonic flight vehicle designated X-36, a remotely piloted tailless research aircraft. The X-36 is designed to demonstrate the feasibility of future tailless military fighters that can achieve agility levels superior to those of today's aircraft.

In the absence of a tail, control of the X-36 is accomplished by a combination of thrust vectoring and innovative aerodynamic control features. Tailless fighter configurations offer reduced weight, increased range, and improvement in survivability. The X-36 is "flown" by a pilot located in a van at the flight test facility; a camera in the X-36 cockpit relays instrument readings and displays to a console in the van. With a wing span of only 10.4 feet and a gross weight under 1,300 pounds, the X-36 is powered by a single turbofan originally designed as a cruise missile power plant.

The X-36 program is intended to establish confidence to incorporate these technologies in future piloted vehicles. This project exemplifies one aspect of a NASA aeronautical research and technology program that seeks to improve the performance, efficiency, and environmental characteristics of all types of planes and, additionally, addresses such infrastructure factors as air traffic control, navigation, and communications. (Courtesy of National Aeronautics and Space Administration.)



Designed jointly by NASA and McDonnell Douglas Corporation, the X-36 is a subscale, remotely piloted tailless vehicle for demonstrating technologies that could lead to lighter, longer-ranging, more survivable, more agile military fighter aircraft. (Photo courtesy of National Aeronautics and Space Administration.)

Though general, two points emerge from these definitions: (1) C³ is multidisciplinary and (2) C³ is a process which, to this point, includes only implicit roles for electronics technology. One military service, however, often refers to C⁴ and C⁴I or has even used C⁴I² where the final C and second I refer to computers and interoperability, respectively, as acknowledgment of the increasing reliance on technology.

A C³ system can be visualized as shown in Fig. 103.1. Within the constraints imposed by organization, **doctrine**, and the skills of the personnel of the military unit, the commander plans and controls his forces. At a basic level, command and control is a resource allocation problem, which often must be solved under much tighter time horizons and subject to greater uncertainty levels than exist in civil applications.

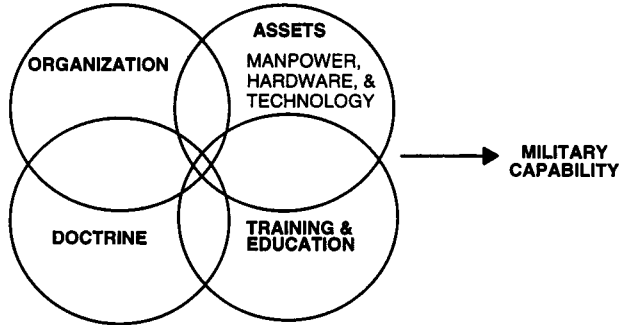


FIGURE 103.1 Components of C³.

The four basic components display overlapped regions to indicate their inseparability. A portion of each category can be designed in isolation; a new antenna or a new radio with decreased size, weight, or power consumption has minimal impact on the other components. However, insertion of a broad new technology (e.g., a radio relay combined with a remotely piloted vehicle (RPV) or the networking of radios) has wide reaching consequences and it may take years to fully integrate into doctrine, training, and organization. The conjunction of the four areas, when specified with some detail, represents or contains an architecture. If the assets, the doctrine, and so on are limited to just one military function, then the aggregation is referred to as a mission architecture. Figure 103.2 depicts two approaches to achieving C3 architectures. The first [Fig. 103.2(a)] is essentially an aggregation and combination of existing assets and is referred to as a “bottom-up” architecture. The “top-down” version of architecture development [Fig. 103.2(b)] begins with earlier and high order perspective (and higher order oversight). Interfaces and interface standards become more important in top-down architectures; instead of numerous custom and unique interfaces, a minimal set of interface standards is desired. When new or updated equipment is designed or acquired it can be integrated without new interface developments, a key property of an “open system” architecture. A developing architecture of this type is entitled, at the Joint Chiefs of Staff level, “C4I for the Warrior.” Service-specific top-down architectures are Copernicus (Navy), AirLand 2000 (Army), MTACCS (Marine Corps Tactical Command and Control System) and a yet unnamed Air Force architecture. Each of these are to be considered as evolving architectures and all reflect the impact and importance of scenarios with highly mobile nodes. The open system or top-down approach promotes interoperability between the developments of each service.

Capital investment constraints limit strict adherence to either architectural approach. MTACCS is a meta-system of seven independently developed systems and is best described as a hybrid architecture. Most communication systems within any of the above architectures existed prior to an architecture and thus have a hybrid nature.

Doctrine is a formalized description of military mission definitions and often includes the procedures to accomplish those missions. Doctrine will also often specify the organizational structure appropriate to the specific missions. Some military establishments adhere to strong doctrinal orientation, even down to strict dictation of technology developments. Other establishments treat doctrine as a loose guideline that can be liberally modified. One foreign military analyst observed that U.S. commanders did not seem to read their own doctrinal publications, and even if they did, would not feel compelled to follow them. A flexible military organization with flexible doctrine, however, can be constrained by inflexible hardware and software. Thus an emerging C3 emphasis is a technical focus on modular equipments, standard interfaces between equipments, “open system” architectures, and (software) programmable equipments.

The best way to understand military C3 is to view it as a set of adaptive control loops. The basic variable is information and most of the effort in C3 synthesis is devoted to information handling and management. The resource allocation problem with feedback found in C3 has obvious similarities to those found in corporate operations and public safety service operations. Each is characterized by multiple priorities, limited resources, timelines, and deadlines for performance. Measures of the consequences of a given action tend to be obscured both by its antecedent actions and by changing external environments. The external environment contains both continuous events (i.e., tracking of targets) and discontinuous events (i.e., an equipment failure or the onset of communications jamming).

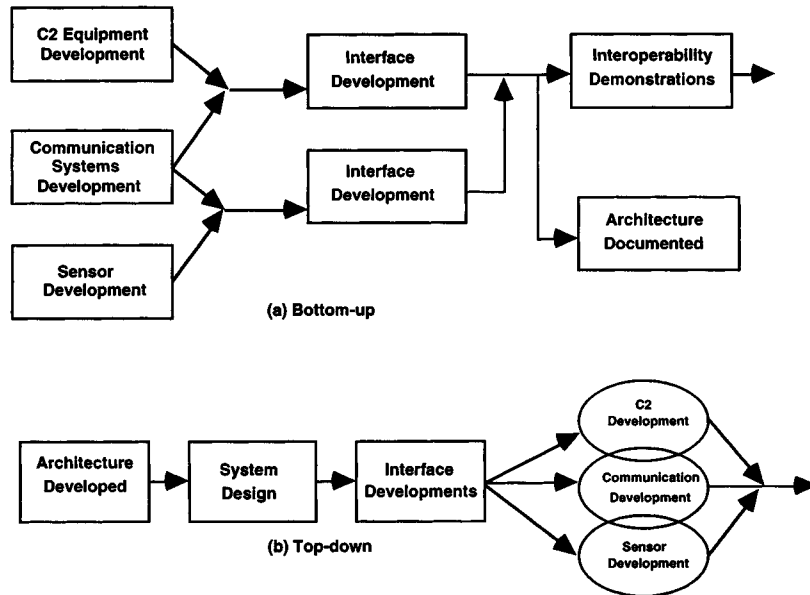


FIGURE 103.2 Architectural processes.

Command and control systems are examples of perhaps the most complex adaptive systems. In its *static* state, C3 assets are aggregates of sensors, processors, databases, humans (with their attributes and organizations), computer hardware/software, mobile platforms, weapons, and communication equipments distributed over wide areas. In the *dynamic* state these assets must be mapped into capabilities in the presence of uncertain or unexpected threats, evolving missions, changing environments, mixed with unreliable communications and possible deception. All can be expected to occur over extended geographic regions and at high tempos. In short, **C³ maps assets into capabilities**. The control processes require rapid and accurate decisionmaking; from this has come the need for heavy reliance on computer-based data systems and high-reliability communications. Despite the existence of fielded weapon systems capable of autonomous operation, the principal action element in the system is still human.

C3 system complexity arises primarily from the magnitude and mobility of the forces involved; forces that can be composed of up to thousands of mobile platforms and hundreds of thousands of personnel. To this is added the large amount of uncertainty present; uncertainty borne of the adversary, of human attributes, dynamics, hostile environments, and communications. Hundreds of radio frequency channels may be in simultaneous use supporting command, surveillance, intelligence, personnel, and logistics functions.

103.3 The Technologies of C³

The general scenario outlined in the previous sections is no longer accommodated by last generation technology of grease pencils, maps, and visual signaling. Technology covered in nearly every other chapter of this handbook is rapidly being incorporated into military C3 systems. Defense departments world wide continue to support technology developments from sub-micron microprocessing devices to global information systems.

Technologies with recent major impact on C3 are

- Digital communications/data links/networking. The newer and critical role of digital (computer-computer) communications initially became possible through satellite communication systems. Tactical data links (short-range digital communications) have been enhanced by error control techniques such as coding, automatic repeat requests, and spread spectrum radios. Networking, a well-established commercial technique, is being developed for tactical applications. Networking offers survivability through alternate

- routing, more efficient (shared) use of channel capacity, and interoperability between interconnected users. Commercial Integrated Services Digital Networks (ISDN) and Asynchronous Transfer Mode (ATM) technology is appearing in both global and nodal military applications. Traditional voice communications remain important; Department of Defense directives require all voice circuits to be secure or encrypted. Digitized voice techniques offer advantage in digital encryption and compression.
- b. Space surveillance, terrestrial surveillance, data fusion. The quantity and quality of surveillance systems continues rapid growth utilizing sensors from ground-based, airborne, and space-based vantages. Remote sensing requirements continue to expand the need for real time digital data communications. Unmanned Airborne Vehicles (UAV) and Unmanned Underwater Vehicles (UUV) platform developments continue as a response to a broad range of C3I needs. Two classes of surveillance are active surveillance systems (radar, sonar, and optical) and passive systems (electronic surveillance measuring (ESM), acoustic, infrared and visual imagery). Passive techniques are preferred as they do not leave a signature that can be exploited by adversaries. A plethora of new sensor systems challenges the currently available communications, processors, and processing systems. Particularly challenging is both the fusion of the outputs of multiple similar sensors and also of dissimilar sensor systems. Fusion protocols and tracking algorithms, software intensive, claim an increasing fraction of available resources. With multiple new sensor systems, a technology challenge is the processing, correlation, and fusing of surveillance data into intelligence products and their distribution in a timely and usable form.
 - c. Computer-based data and information systems. From the communications and surveillance capabilities above, the objective has become formation of a consistent tactical picture throughout the operations theatre. Rapidly evolving processing technology allows vast amounts of data handling and management with corresponding shortening of control decisionmaking times. The ability to match computer processing capability with high data rate, reliable, and survivable computer-grade communications on a global basis to small mobile platforms is an ongoing challenge. Military information systems, in order to retain trusted functioning, require procedures for input data that may have been delayed, omitted, partial, inaccurate, or irrelevant (DOPII). Expanding amounts of software-based systems are needed as a response to increased tempo, data volume, and quality while reducing staff and manpower functions.
 - d. Architectures and architectural thinking. C3 assets, especially communications, are evolving as assets to be shared, controlled, and rapidly reallocated rather than be dedicated to a specific user. Joint and combined operations, requiring improved interoperability, are becoming common as operations become more regionalized. Two functions of focus, Battle Damage Assessment (BDA) and Indicators and Warnings (I&W), are best implemented when surveillance, communications, and intelligence are architecturally integrated. Integrated systems are also best for timely response to deception and false alarms. A current Navy direction is not to inundate the afloat commander with volumes of unsolicited data but rather have him request what is needed. This style, called information pull, represents a significant change from traditional information push. The impact on supporting communications is to give it a more "bursty" character, driven by external events.
 - e. Digital signal processing, programmable systems. Single-function C3 hardware is evolving to multifunction capability. Each node or platform will emerge with new capabilities that permits rapid and flexible reallocation. Current generation tactical military aircraft, as delivered, have virtually no additional space or weight allowance for new equipments. A desire is to evolve from costly retrofitting to a state of software insertion and integration. Traditional single-band radio systems will be replaced with **programmable multiband, multiwaveform systems**. Near real-time management and control of highly flexible, programmable systems will become a growing research and development thrust. Next generation cellular technology involving hybrids of frequency hopping, direct sequence spread, and time division spread spectrum techniques invokes new digital signal processing efforts. Also receiving development is Direct Satellite Broadcast (DSB) to tactical military units.
 - f. Interoperability and standards. C3I systems, with many dispersed nodes, rely heavily on computer-computer communications. Standards are being promoted by industry and government to simplify the development, acquisition, and insertion of new technology as well as to promote interoperability between

independently developed systems. Significantly the Department of Defense has edicted that commercial standards for electronics and telecommunications are to be utilized in preference to military standards in order to promote more rapid and lower cost acquisition of state-of-the-art technology. Two additional motivations for new standards are increased traffic requirements and increased system complexity. C3 applications and users have found significant benefit in increasing communication with programmatically unrelated data sources such as databases and sensors. There is an increase in internal communications as well. Also systems have become more complex, forcing programs to develop modularized architectures. Software is replacing hardware as the most complicated component of communications and C2 systems to design, build, and maintain. Modularized architectures are required to simplify development and enable insertion of new technologies.

The primary computer-to-computer communications architecture has been the Open Systems Interconnection (OSI) Reference Model. The OSI Reference Model has been successful as a layered architecture with well-defined interfaces and specified division of functions. The Department of Defense has committed to adopting an enhanced version of the OSI protocols, called the Government OSI Profile (GOSIP). OSI/GOSIP integration into C3 systems is lagging because of delays in accredited vendor implementations and the cost of upgrading the existing communications infrastructure. NATO is also adopting standards for their joint procurement policies; to a significant degree they overlap commercial standards.

OSI brings to C3 a set of application services that had not been previously available. For example, the OSI electronic mail standards (usually called X.400) provide message forwarding, distribution list creation and distribution, and obsolete message extraction among other services to users. In addition to the security protocols contained in the lower layers of the OSI stack, X.400 has its own security services such as message origin authentication, message flow confidentiality, message content integrity, and nonrepudiation of delivery, services that are highly desirable in C3 environments. OSI also has enhanced file transfer and management capabilities, systems management, directory, and transaction processing, among other application functions, all providing enhanced capability to C3 users.

- g. Precision timing and position location (GPS). Navigation/position location historically is important and becomes more so in high dynamic maneuver warfare. With the introduction of the Global Positioning System (GPS), 3-dimensional positioning is available to the smallest of high-mobility nodes. Even with a less than complete satellite constellation, position accuracies can become less than 100 m.
- h. Displays and workstations. High-resolution displays combined with programmable workstations and software lead to flexible node functions and consequently to flexible architectures. A C3 workstation could, in principle, support any of a number of C3I functions; a relocation of operators may be the only requirement to physically relocate a command node. Numerous decision aids are now being included within workstations and with their more comprehensive capability are now often described as decision support systems (DSS). Man-machine interface (MMI), as a result, grows in importance.
- i. Software techniques. With the growing computational power and memory capability of microprocessor systems, C3 system performance will increasingly be determined by software performance. The cost and complexity of software appears to expand in proportion to host computer capability and is more frequently becoming a system limiting factor. ADA is dictated to be the common programming language of the Defense Department; however, exceptions can be approved. Verification and validation (V&V) of generated software and software maintainence have grown to necessitate organizational changes within the military. Software standards have also increased in importance in new C3 systems. POSIX standards (published as IEEE 1003) govern the software interfaces to operating system services in various computing platforms [NIST, 1990]. As such, they allow application programs written according to the standards to be reused. POSIX standardizes interfaces to security, networking, and diverse system services, including file management, memory and process management, and system administration services. POSIX.5 provides bindings for the ADA programming language.
- j. Simulation and modeling. Both techniques are employed with the objective of designing or analyzing the performance of a C3I system. With the advent of faster computation, complex scenarios can be “gamed” in near real time, and modeling will then be within the decision aid realm.

103.4 The Dynamics of Encounters

Within dynamic systems, and the C3 systems that support them, it is important to identify and clarify time scales involved. Military engagements range from sub-second events such as local missile point defense to the long-term development and implementation of global strategy. Each involves basic aspects of decision and control theory: objectives, observations, and feedback and control. In the military environment, the observation aspect is especially complex, requiring the placement, collection, transmission, and aggregation of data from numerous dispersed sources. Control and decision techniques derived for one echelon level may be inappropriate for others, primarily due to the time available for the assessment and feedback process. Often, the impact of a decision will not be measurable before yet another control decision is required. Thus, the relative roles of automation and humans will be different at different levels. The human may have to project a decisionmaking consequence long before the system hardware/software can obtain measures of it.

As an example of encounter space-time domains, surface Navy echelon levels have order-of-magnitude scales as shown:

Organization Level	Time Scale of Interest	Geographic Extent (km)
Platform	seconds-minutes	10's
Battle Group	minutes-hours	100's
Fleet	hours-days	1000's
Theater	days-weeks	1000's +
Service/National	weeks-years	Global

At the platform level, the time scale range reflects engagement times which may include limited or local amounts of tracking. At the Battle Group level, the time scale corresponds to tasks such as maneuver, coordinated engagement, and track management.

Any of the organizational levels may additionally have planning functions that precede the operational time scales by up to months or years. The planning side includes events such as logistics, maintainence, training, and exercises, all of which contribute toward becoming a more capable combatant. [Figure 103.3](#) portrays the planning and the operational or execution phases as well as portraying the adaptive control loop approach to C3. The lighter shaded feedback path is employed when it is required to compare status with the current plan. It is also available for adjustment when plans or objectives are modified. The execution phases are represented by the Stimulus-Hypothesis-Options-Response (SHOR) Paradigm suggested by Wohl [1981]. The control theoretic implications are apparent in the figure; the Stimulus-Hypothesis is a representation of situation assessment with its implicit uncertainty. Quickness and accuracy with which a military command organization can transverse the execution loop is a general measure of performance (MOP). Qualitatively it is generally accepted that the side with the best ability to transverse the SHOR execution loop will have a significant military advantage. In this light, attributes of the execution loop become a measure of effectiveness (MOE) of the C3 system in terms of operational outcomes. Rules of Engagement (ROE) impact tempo by reducing uncertainty or options available to the decisionmaker. Some scenarios develop with such quickness that the C3 system must react nearly reflexively (e.g., without consideration of possible options). One class of rules is made known to all the participants; if a particular manuever is observed, then a specified response will result.

The SHOR paradigm illustrates why counter-communications and counter-command and control are increasingly important operational and technical areas. Counter-C3 need only delay the process rather than disrupt or destroy it in order to be an effective technique. The Navy, for example, is now incorporating **electronic warfare** (EW) as a warfare area on equal status to the traditional anti-submarine (ASW), anti-aircraft warfare (AAW), and anti-surface warfare (ASUW) areas.

Control of the electromagnetic spectrum is becoming as critical as the control of the physical battlefield. Electronic counter-measures (ECM) such as jamming and deception are technical options available to the commander. Either adversary may elect to respond to the ECM threat by a series of electronic counter-counter measure (ECCM) techniques. Anti-jam (AJ) communications can employ a variety of techniques such as spread spectrum, power control, adaptive coding and feedback, multiple routes, and adaptive antenna arrays. A signal

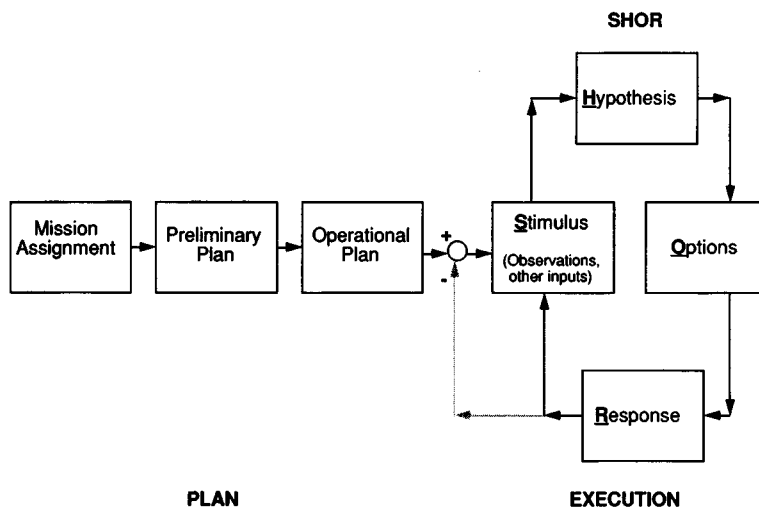


FIGURE 103.3 The planning and execution phases of operations.

may also be protected by making it difficult to intercept; some low probability of intercept (LPI) methods are again spread spectrum, directive antennas, power control, EM propagation strategies, and message brevity.

The SHOR paradigm has important advantages. First, it is generally applicable to all military echelon levels. Second, it represents a control process with its explicit dynamics rather than a relational or physical interconnection of system components. Finally, it puts focus on the roles of controlling and decisionmaking without a pre-bias on whether that function should be performed by humans or computers. The remaining challenge is to be able to describe both human and computer performance with a common type of representational framework.

103.5 The Role of the Human Decisionmaker in C³

Designers of C³ systems often fail to acknowledge the fact that the “central, essential ingredients in any command and control system are not the things which they plan and design; rather they are the commanders and decisionmakers themselves” [Wohl, 1981]. Despite its centrality, designation of human roles is seemingly arbitrary and often controversial. In most system studies, the human decisionmaker is not thought of as an integral part of the system, but is instead given an external position as a “user” of data or an “input” to the rest of the system. Without a means of integrating the behavior of interrelated decisionmakers into a comprehensive description of system response, the proper hominal role is difficult to determine. To justify and support human action, a clear understanding of the benefits and limitations of human intervention is required.

The complexity and unpredictability of a C³ environment prompt the inclusion of hominal blocks. The ability to respond to changing operational conditions requires “intelligence,” and in a C³ system this intelligence is distributed between people and algorithms. The human has a marvelous capacity for coping with vague and confusing data, making sense out of information so fragmentary that it would paralyze a computer. A computer information processing algorithm has, in turn, an unexcelled capability to process and display data at a rate that would bewilder a person. Proper marriage of humans and computers yields a robust system, quick to adapt to changes and capable of handling high data rates. For example, for the various subtasks found in the network management component of a C³ system, the relative roles of people and algorithms might be that shown in Fig. 103.4. With the advent of open system architectures, network management appears as a crucial resource allocation function. High speeds and large databases are best left within the domain of the computer, while those nodes demanding insight appropriately have a corporeal flavor.

A comprehensive C² model is created by bringing together models of subsidiary elements. The form of these submodels should be as compliant as possible within constraints imposed by tractability. In any event, the model should display:

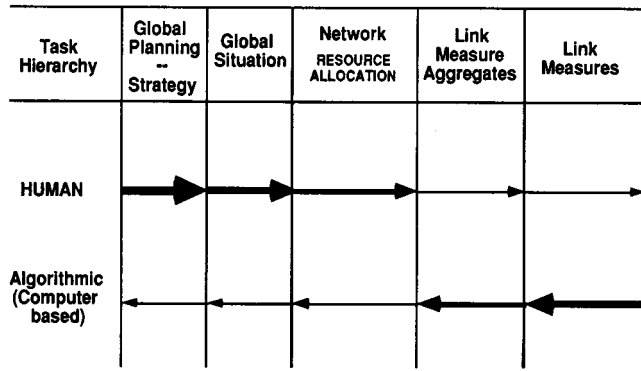


FIGURE 103.4 Control hierarchies.

1. An analytical structure permitting the evaluation of influence functions
2. Explicit communication dependence
3. Amenability to aggregation and disaggregation

Each of these desiderata arises in studies within the field of System Science, and this discipline would appear to provide the natural formalism for quantitative investigations of command and control systems. Athans articulates this view by observing that C3 systems “are characterized by a high degree of complexity, a generic distribution of the decision-making process among several decision making ‘agents,’ the need for reliable operation in the presence of multiple failures, and the inevitable interaction of humans with computer-based decision support systems and decision aids” [Athans, 1987]. It needs to be emphasized, however, that a C2 system differs from those commonly encountered in system theory in at least three primary ways:

1. Because command and control is at its essence a human decisionmaking activity, it is not sufficient to model only the sensors, computers, displays, etc. The hominal dynamics must be integrated with those of the electromechanical elements.
2. Any effective C3 system must have the capacity to evolve over time. Such systems are frequently established with a limited set of elements. Either for a specific operation or during their lifetime a subset of these elements will be modified or replaced, and their roles expanded or constricted as changing demands are placed upon the system. Hence, the system description must be more flexible than those in common use.
3. In contrast to conventional system design problems, there is no single nominal operating condition about which the system is maintained. Indeed, the critical attribute of a C3 system is its ability to respond to major changes in condition or state. In two Middle East naval events (*USS Stark, Vincennes*) the missile defense systems were set for a state that had just immediately changed. Furthermore, the system is often used in environments quite different from those envisioned in its design. Hence, the uncertain circumstances within which the decisionmakers must accomplish their tasks must be properly reflected in any system architecture.

A commander brings special skills to such a system, but some of them are difficult to quantify. For example, people have singular competence in:

1. Decisionmaking in semantically rich problem domains
2. Analogical reasoning and problem structuring
3. Information processing and application of heuristics

To properly identify a specific function for a human decisionmaker, the advantage accruing to his inclusion must be shown. Quantitative models of human responses have been developed in various ways, from ad hoc to purely normative. In the most promising of these, the form of the response dynamics of an individual commander is determined from the solution to an optimization problem. The optimization problem is framed by supposing that the decisionmaker strives to act in the most effective way, but is constrained by both cognitive

limitations and temporal pressures. When the decisionmaker's milieu and motivation are expressed in an analytical framework containing both the exogenous influences of the conflict and the endogenous predispositions generated by training and personal inclination, the input-output relation for the commander is, in principle, expressible as a set of differential equations with logical branching.

This fundamental modeling philosophy has been used successfully by several investigators. Wohl developed the SHOR model of decisionmaker action using the ideas from modern systems theory. The SHOR, in conjunction with planning models (see Fig. 103.3) can be phrased in analytical terms compatible with those of the electromechanical subsystems. With their common form, all of the submodels can be combined to create a comprehensive system description, integrating people with hardware and software algorithms. This model is useful in system architecture studies because it is applicable to all military echelon levels; it represents the fast dynamics of the system explicitly rather than by implicit relational blocks or physical interconnection of subsystem elements, and there is flexibility to allow whether a function is best performed by a human or by an algorithm.

A decisionmaker views a dynamic encounter as a temporally varying, geographically dispersed system subject to unpredictable events, both continuous and discrete. Because critical command decisions have an extended period of influence, the actions taken at different time scales cannot be isolated from each other. This issue of scale interaction comes to the fore particularly when hominal modeling is considered. In contrast to inanimate objects which usually have a single, natural time scale, the demands on a commander transcend the time scale divisions. A trained decisionmaker exhibits a wide spectrum of behaviors as both his tasks and operating environments change; the commander is the truly adaptive block in a command and control architecture. Athans referred to C3 systems as "event driven" because major changes in an engagement occur at isolated times and modulate the more frequent local irregularities [Athans, 1987]. He suggested that the proper model would be a hybrid in which "the state variables are both continuous and discrete." In this metapartitioning of the comprehensive state space, the discrete states represent global (or macro) occurrences that modulate the local (or micro) aspects. This decomposition is useful in formulating the human response model because people react differently in different time scales. The reaction to local phenomena has a reflexive quality. It is in this reaction to the infrequent, but pivotal, macroevents that the idiosyncrasies thought to be particularly human are manifest.

To capture hominal behavior analytically, a framework delineating the intrinsic features of a C3 environment is required. At the macrolevel, the important attributes of a command and control environment are tempo, uncertainty, and complexity. The mission directed decisionmaker model (MDDM) described in Clapp and Sworder [1992] decomposes the C2 model in the hybrid form suggested by Athans. One block in the MDDM, the stimulus-hypothesis evaluation model (SHEM), quantifies relevant features of an engagement while representing the observation and situation assessment tendencies of the decisionmaker in terms of a few natural parameters. Because of its simple structure, the SHEM lends itself to the analysis of systems containing human decisionmakers.

To be more specific, the C2 environmental model must be flexible enough to portray the sudden, large-scale variations in circumstances which occur in operations. It is advantageous to phrase the model in such a way as to make explicit its dependence on events of macroscopic scale as well as the decisionmaker's response. The engagement model used in the MDDM has the form:

$$(d/dt)x_p = f(x_p, u_p, r_t) + g(x_p, u_p, r_t)w_t$$

where x_p is the "global" system state vector representing the external environment to which the decisionmaker seeks to respond. The decisionmaker's action variable is u_p . The process $\{w_t\}$ represents only one portion of the primitive randomness in the encounter—that associated with high-frequency uncertainty and various local disturbances. The supplementary process, $\{r_t\}$, indicates the mode of evolution of the encounter. Transitions in $\{r_t\}$ thus signify extensive events. These macro-events tend to have more temporal structure than that displayed by $\{w_t\}$, but the times of occurrence are typically unpredictable. Different values of r_t (sometimes called supervariables) are identified with different hypotheses delineating the macrostatus of the encounter. It is usually assumed that the number of modal hypotheses is finite.

Even with the aggregation implicit in the engagement model, the encounter dynamics are complex and nonlinear. A decisionmaker mentally converts the engagement dynamics into a hybrid equation with separate descriptions of local and global aspects. The input-output dynamics of the commander are expressed as an ordinary differential equation with updates at observation times. In Sworder et al. [1992], the ability of the SHEM to predict the response of a trained decisionmaker was investigated. An experiment measuring the proficiency of trained air-defense officers in differentiating hostile from friendly targets confirmed the utility of the SHEM.

103.6 Summary

C3I systems, commanders/decisionmakers, and decision aids all have a common performance objective. They must contribute to accurate and timely *situation assessments and responses* in scenarios that have a wide range of tempos, noise, clutter, uncertainty, and complexity.

The C3 system necessarily has the ability to rapidly acquire, process, and transfer large volumes of data over extended regions. Trained, experienced human decisionmakers excel at assessing complex patterns in highly cluttered environments and determining appropriate responses. Decision aids perform as a “smart” interface between these two dissimilar players. Electronics technology provides the means for designing increasingly capable C3 systems and is at its most effective when the system architecture allows flexible and dynamic interoperation of the various hardware “devices” with their trained and motivated decisionmakers.

Defining Terms

Command, control, communications (C³): The process of mapping assets (resources available to the military commander) into capabilities. This control process is impacted by tempo, noise/clutter, and scenario complexity.

Decisionmaking: A commander’s or operator’s action that changes the status of his information or other assets under his control.

Doctrine: A formalized description of military mission definitions to include the procedures to accomplish those missions. Doctrine will also often specify the organizational structure appropriate to the specific mission.

Electronic warfare: Contention for the control of the electromagnetic (EM) spectrum, to allow active and passive EM sensing and communications while denying the same ability to adversaries. Includes deceptive EM techniques.

Environment: A set of objects outside the system, a change in whose attributes affects, and is affected by, the behavior of the system.

Information warfare: The protection, manipulation, degradation, and denial of information to include the traditional electronic warfare.

Intelligence: The aggregated and processed information about the environment, including potential adversaries, available to commanders and their staff.

Open system architecture: A layered architectural design that allows subsystems and/or components to be readily replaced or modified; it is achieved by adherence to standardized interfaces between layers.

Programmable radio system: Radios based on digital waveform synthesis and digital signal processing to allow simultaneous multiband, multiwaveform performance.

System: A set of objects with relations between them and their attributes or properties. It is embedded in an environment containing other interrelated objects.

Related Topics

70.1 Coding • 102.2 Communications Satellite Systems: Applications

References

- M. Athans, "Command and control (C2) theory: A challenge to control science," *IEEE Trans. on Automatic Control*, vol. AC-32, pp. 286–293, April 1987.
- G.A. Clapp and D.D. Swoerer, "Command, control and communications: The human role in military C3 systems," in *Control and Dynamic Systems, Advances in Theory and Applications*, vol. 52, New York: Academic Press, 1992, pp. 513–541.
- S. Johnson and M. Libicki, Eds., *Dominant Battlespace Knowledge: The Winning Edge*, Washington, D.C.: National Defense University Press, U.S. Government Printing Office, 1995.
- Joint Chiefs of Staff (JCS), Publication 1, "Definitions," undated.
- M.C. Libicki, *What is Information Warfare?*, Washington, D.C.: National Defense University Press, 1995.
- National Institute of Standards and Technology [NIST], FIPS 151-1, POSIX: Portable Operating System Interface for Computer Environments (IEEE 1003.1–1988) March 1990.
- D.D. Swoerer, G.A. Clapp, and R. Vojak, "A Dynamic Input-Output Model of the Decisionmaking Process," Proceedings of the 1992 Symposium on Command and Control Research, Monterey, Calif., June 1992.
- J.W. Wohl, "Force management requirements for air force tactical command and control," *IEEE Trans. on Systems, Man and Cybernetics*, vol. SMC-11, pp. 618–639, Sept. 1981.

Further Information

- W. Stallings, *Handbook of Computer-Communications Standards*, vol. 1, The Open Systems Interconnections (OSI) and OSI-Related Standards, New York: Macmillan, 1987.
- W. Stallings, *Handbook of Computer-Communications Standards*, vol. 3, Department of Defense (DOD) Protocol Standards, New York: Macmillan, 1988.
- Information Technology for Command and Control*, S. Andriole and S. Halpern, Eds., IEEE Press, New York, 1991. *SIGNAL*, a monthly (trade) magazine published by the Armed Forces Communications-Electronics Association (AFCEA), Annandale, Va. Contains numerous brief articles on current C3I topics of interest.
- T.P. Coakley, *Command and Control for War and Peace*, National Defense University, U.S. Government Printing Office, Washington, D.C., 1992.
- A.D. Hall, *Metasystems Methodology*, Oxford, England: Pergamon Press, 1989.

Consistency

Consistency is a concept that can be easily understood if we first define the set of all possible models that could have produced the *a posteriori* information \mathbf{y} , in accordance with the class of measurement noise:

$$\mathcal{S}(\mathbf{y}) \triangleq \left\{ g \in \mathcal{S} \mid \mathbf{y} = E(g, \eta), \eta \in \mathcal{N} \right\} \quad (104.40)$$

Therefore, $\mathcal{S}(\mathbf{y}) \subset \mathcal{S}$ is the smallest set of models, according to all the available input data (*a priori* and *a posteriori*), that are indistinguishable from the point of view of the input information. This means that with the knowledge of $(\mathbf{y}, \mathcal{S}, \mathcal{N})$ there is no way to select a smaller set of candidate models. The “size” of set $\mathcal{S}(\mathbf{y})$ places a lower bound on the identification error, which cannot be decreased unless we add some extra information to the problem. This lower bound on the uncertainty error holds for any identification algorithm and represents a type of *uncertainty principle* of identification theory.

The *a priori* and *a posteriori* information are consistent if and only if the set $\mathcal{S}(\mathbf{y})$ is non-empty; otherwise, there is no model in \mathcal{S} that could have possibly generated the experimental output.

Identification Error

The *a priori* knowledge of the real system and measurement noise present in the experiment \mathbf{y} is stated in terms of sets \mathcal{S} and \mathcal{N} . The statement of the problem does not assign probabilities to particular models or noise; therefore, it is deterministic in nature. In addition, the modeling error should be valid no matter which model $g \in \mathcal{S}$ is the real plant (or $\eta \in \mathcal{N}$ the real noise vector) that induces a worst-case approach. In this deterministic worst-case framework, the identification error should “cover” all models $g \in \mathcal{S}$ that combined with all possible noise vectors $\eta \in \mathcal{N}$, are consistent with the experiments, i.e., $\mathcal{S}(\mathbf{y})$. In practice, however, the family of models conservatively covers this “tight” uncertainty set. Hence, it provides an upper bound for the distance from a model to the real plant. In this framework, the worst-case error is defined as follows:

$$d(\mathcal{A}) \triangleq \sup_{\eta \in \mathcal{N}, g \in \mathcal{S}} m\left[g, \mathcal{A}[E(g, \eta), \mathcal{S}, \mathcal{N}] \right] \quad (104.41)$$

where $m(\cdot, \cdot)$ is a specific metric.

The identification algorithm \mathcal{A} maps both *a priori* and *a posteriori* information to a candidate nominal model. In this case, the algorithm is said to be *tuned* to the *a priori* information; otherwise, if it only depends on the experimental data, it is called *untuned*. Almost all classical parameter identification algorithms ([6]) belong to the latter class.

The identification error (Eq. (104.41)) can be considered as *a priori*, in the sense that it takes into account all possible experimental outcomes consistent with the classes \mathcal{N} and \mathcal{S} before the actual experiment is performed. Since it considers all possible experimental data \mathbf{y} , it is called a *global* identification error. A *local* error that applies only to a specific experiment \mathbf{y} can be defined as follows:

$$e(\mathcal{A}, \mathbf{y}) = \sup_{g \in \mathcal{S}(\mathbf{y})} m\left[g, \mathcal{A}(\mathbf{y}, \mathcal{S}, \mathcal{N}) \right] \quad (104.42)$$

Clearly, we always have $e(\mathcal{A}, \mathbf{y}) \leq d(\mathcal{A})$. To decrease the local error more experiments need to be performed, whereas to decrease the global error new *types* of experiments, compatible with new *a priori* classes, should be performed, for example, reducing the experimental noise and changing \mathcal{N} accordingly.

Convergence

Now, what happens with the family of models when the amount of information increases? It is desirable to produce a “smaller” set of models as input data increases, i.e., model uncertainty should decrease. The set of models are expected to tend to the real system when the uncertainty of the input information goes to zero. Hence, an identification algorithm \mathcal{A} is said to be convergent when its worst-case global identification error

$e(\mathcal{A})$ in Eq. (104.41) goes to zero as the input information tends to be “completed.” The latter means that the “partialness” and “corruption” of the available information, both *a priori* and *a posteriori*, tend to zero simultaneously.

Input information is corrupted by measurement noise. Thus, “corruption” tends to zero when the set \mathcal{N} is a singleton $\mathcal{N} = \{0\}$. On the other hand, partialness of information can disappear in two different ways. By *a priori* assumptions when the set \mathcal{S} tends to have only one element (the real system) or *a posterior* measurements when the amount of experimental information is completed by the remaining (usually infinite) data points. This can be unified as follows. The available information (*a priori* and *a posteriori*) is completed when the consistency set $\mathcal{S}(y)$ tends to only one element: the real system. Hence, an identification algorithm \mathcal{A} converges if and only if

$$\lim_{\text{size}[\mathcal{S}(y)] \rightarrow 0} e(\mathcal{A}) = 0 \quad (104.43)$$

Note that as the consistency set $\mathcal{S}(y)$ reduces to a single element, the experiment operator tends to be invertible. Since the identification error is defined in a worst-case sense, its convergence is uniform with respect to the *a priori* sets \mathcal{N} and \mathcal{S} .

Algorithms and Further Research Topics

There are robust identification algorithms that consider frequency domain experiments, called \mathcal{H}_∞ -identification, this being the norm that measures the identification error. The two main ones are the two-stage and the interpolation algorithms. From time-domain measurements, several ℓ_1 -identification procedures are available.

Due to the fact that robust identification is a currently active research area, there are yet many theoretical and computational aspects that have not been fully developed. Among others, there are problems related to identifying unstable plants and nonuniformly spaced experimental samples. Also, sample complexity is a recent research direction, as well as the mixture of time and frequency experiments and parametric and nonparametric models.

A complete description of both frequency (\mathcal{H}_∞) and time (ℓ^1) domain identification algorithms and a discussion of the issues mentioned above can be found, for example in [9].

Defining Terms

BIBO stable: A system is Bounded Input Bounded Output stable if for all bounded inputs and zero initial conditions, the corresponding output is also bounded. In the case of finite-dimensional linear time invariant systems, this definition is equivalent to having all the poles of the system in the open left half plane $Re(s) < 0$.

Control oriented identification: A deterministic identification procedure that starting from experimental data generates a model consistent with both this data and some *a priori* assumptions on the class of systems under consideration.

Robust stability and performance: A given property of a system (such as stability or performance) is *robust* if it holds for a *family of systems* that represents (and contains) the nominal plant.

Robustness margin: A quantitative measure of stability, given by the distance from the nominal model representing the system, to the nearest model lacking the property under consideration. Examples are the classical gain and phase margins.

References

1. Barmish, B.R., *New Tools for Robustness Analysis*, Macmillan, 1994.
2. Bhattacharyya, S.P., Chapellat, H., Keel, L.H., *Robust Control: The Parametric Approach*, Prentice-Hall, 1995.
3. Doyle, J.C., Glover, K., Khargonekar, P., Francis, B., State-space solutions to standard \mathcal{H}_2 and \mathcal{H}_∞ control problems, *IEEE Transactions on Automatic Control*, Vol. 34, 1989.

4. Gahinet, P., Apkarian, P., A linear matrix inequality approach to \mathcal{H}_∞ control, *International Journal on Robust and Nonlinear Control*, 4, 421–448, 1994.
5. Iwasaki, T., Skelton, R., A complete solution to the general \mathcal{H}_∞ control problem: LMI existence conditions and state-space formulas, *Automatica*, 1994.
6. Ljung, L., *System Identification: Theory for the User*, Prentice-Hall, 1987.
7. Mäkilä, P.M., Partington, J.R., Gustafsson, T.K., Worst-case control-relevant identification, *Automatica*, 31, 1799–1819, 1995.
8. Scherer, C., The Riccati Inequality and State-space \mathcal{H}_∞ Optimal Control, Ph.D. Dissertation, Universität Würzburg, Germany, 1990.
9. Sánchez Peña, R., Sznaier, M., *Robust Systems Theory and Applications*, John Wiley & Sons, 1998.
10. Zhou, K., Doyle, J.C., Glover, K., *Robust and Optimal Control*, Prentice-Hall, 1996.

Further Information

Classical Identification:

Ljung, L., *System Identification: Theory for the User*, Prentice-Hall, 1987.
 Söderström, T., Stoica, P., *System Identification*, Prentice-Hall, 1989.

ℓ_1 Optimal Control:

Dahleh, M.A., Díaz-Bobillo, I.J., *Control of Uncertain Systems: A Linear Programming Approach*, Prentice-Hall, 1995.

LQG Optimal Control:

Dorato, P., Abdallah, C., Cerone, V., *Linear-Quadratic Control: An Introduction*, Prentice-Hall, 1995.
 Kwakernaak, H., Sivan, R., *Linear Optimal Control Systems*, Wiley Interscience, 1972.
 Anderson, B.D.O., Moore, J.B., *Optimal Control: Linear Quadratic Methods*, Prentice-Hall, 1990.

Robust Control:

Doyle, J.C., Francis, B., Tannenbaum, A., *Feedback Control Theory*, Maxwell Macmillan, 1992.
 Green, M., Limebeer, D., *Linear Robust Control*, Prentice-Hall, 1995.
 Morari, M., Zafirou, E., *Robust Process Control*, Prentice-Hall, 1989.
 Sánchez Peña, R., Sznaier, M., *Robust Systems Theory and Applications*, John Wiley & Sons, 1998.
 Zhou, K., Doyle, J.C., Glover, K., *Robust and Optimal Control*, Prentice-Hall, 1996.

Parametric Uncertainty:

Ackermann, J., *Robust Control: Systems with Uncertain Physical Parameters*, Springer-Verlag, 1993.
 Barmish, B.R., *New Tools for Robustness Analysis*, Macmillan, 1994.
 Bhattacharyya, S.P., Chapellat, H., Keel, L.H., *Robust Control: The Parametric Approach*, Prentice-Hall, 1995.

Software Packages:

Balas, G., Doyle, J.C., Glover, K., Parkard, A., Smith R., μ -Analysis and Synthesis Toolbox, The MathWorks Inc., Musyn Inc., 1991.
 Gahinet, P., Nemirovski, A., Laub, A., Chilali, M., *LMI Control Toolbox*, The MathWorks Inc., Natick, MA, 1995.
 Safonov, M., Chiang, R., *Robust Control Toolbox*, The MathWorks Inc., 1988.

D. McRuer "Man-Machine Systems"
The Electrical Engineering Handbook
Ed. Richard C. Dorf
Boca Raton: CRC Press LLC, 2000

Man-Machine Systems

- 105.1 [Introduction](#)
 105.2 [Several Natures of Man-Machine Control—A Catalog of Behavioral Complexities](#)
 105.3 [Full-Attention Compensatory Operations—The Crossover Model](#)
- Crossover Frequency for Full-Attention Operations • Remnant •
 Effects of Changes in the Task Variables • Effects of Divided
 Attention

Duane McRuer
Systems Technology, Inc.

105.1 Introduction

In principle the dynamic behavior of the human element in man-machine systems can be described in terms similar to those used to describe other system elements. There are, however, major complications in quantification because of the enormous versatility of the human engaged, simultaneously, as the on-going *architect* and modifier of the man-machine system itself and as an operating entity within that system. In other words, the adaptive and learning capabilities of the human permit both set-up and modification of the effective system structure and the subsequent self-improvement and tuning of the human dynamic characteristics within that structure.

The situations which are simplest to quantify are those in which the *machine* has time-stationary dynamic properties and the human has, after architectural, learning, and adaptation phases, achieved a similar state. Under these circumstances human dynamic operations can be characterized by quasi-linear describing functions and a remnant [Graham and McRuer, 1961] or operator-induced noise. This is the context here.

105.2 Several Natures of Man-Machine Control—A Catalog of Behavioral Complexities

Figure 105.1 [McRuer and Krendel, 1974] shows a general quasi-linear man-machine system with time-stationary properties. This diagram is suitable for the description of human behavior in an interactive man-machine system wherein the human responds to visually sensed inputs and communicates with the machine via a manipulator of some sort (e.g., control stick, wheel, pedal, etc.). This block diagram indicates the minimum needed number of major functional signal pathways internal to the human operator to characterize different behavioral features. The constituent human sensing, data processing, computing, and actuating elements are connected as internal signal processing pathways which can be “reconfigured” as the situation changes. Such reconfiguration is an aspect of human behavior as a system architect. Functional operations on internal signals within a given pathway may also be modified.

The specific internal signal organizational possibilities depicted in Fig. 105.1 have been discovered by manipulating experimental situations (e.g., by changing system inputs and machine dynamics) to isolate different combinations of the specific blocks shown [McRuer and Jex, 1967; McRuer and Krendel 1974; McRuer 1980].

To describe the parts of the figure start at the far right with the *controlled element*. This is the machine being controlled by the human. To its left is the actual interface between the human and the machine—the neuromuscular

HAZARDOUS ENVIRONMENT ROBOTICS

Deneb Robotics, Inc. is an internationally known leader in 3D graphics-based factory simulation, telerobotics, and virtual reality software used widely in the aerospace, automotive, defense, environmental, medical, nuclear, and research communities.

Among the company's broad software product line is TELEGRIP™, which provides 3D graphical interface for previewing, interactive programming, and real-time bilateral control of remote robotic devices. It provides operators a system for safe, quick, and efficient remediation of hazardous environments from a single point of control and input that is isolated from virtually all operator hazards.

Accurate 3D kinematic models of the robot and work space components allow the operator to preplan and optimize robot trajectories before the program is automatically generated. Control commands are monitored when running in autonomous, teleoperational, or shared control modes to assure procedural safety.



A video camera provides a Deneb Robotics engineer with a view of the robot. (Photo courtesy of National Aeronautics and Space Administration.)

actuation system, which is the human's output mechanism. This in itself is a complicated feedback control system capable of operating as an open-loop or combined open-loop/closed-loop system, although that level of complication is not explicit in the simple feedback control system shown here. In the diagram the neuromuscular system comprises limb, muscle, and manipulator dynamics in the forward loop and muscle spindle and tendon organ ensembles as feedback elements. Again, many more biological sensors and other elements are actually involved; this description is intended only to be generally indicative of the minimum level of complexity associated with the *human actuation elements*. All of these elements operate within the human at the level from the spinal cord to the periphery.

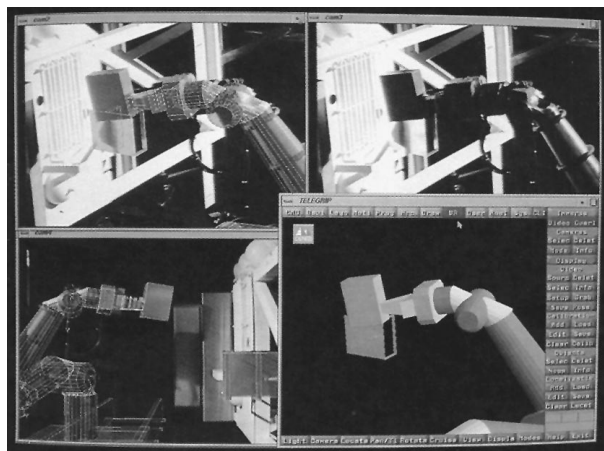
There are other sensor systems, such as joint receptors and peripheral vision, which indicate limb output position. These operate through higher centers and are subsumed in the *proprioceptive* feedback loop incorporating a block at the perceptual level further to the left in the diagram. If motion cues are present, these too can be associated in similar proprioceptive blocks with feedbacks from the controlled element output.

The other three pathways shown at the perceptual level correspond to three different types of control operations on the visually presented system inputs. Depending on which pathway is effectively present, the

A key feature of TELEGRIP is a video overlay option that utilizes video to calibrate 3D computer models with the actual environment. The video overlay technique is especially useful for on-line planning applications or teleoperations in remote, hazardous, or complex environments such as space, undersea, or nuclear sites.

A virtual reality calibration technique was developed for reliable and accurate matching of a graphically simulated environment in 3D geometry with actual video camera views. The system was designed for predictive displays with calibrated graphics that overlay in live video for telerobotics applications. For example, the system allows an operator to designate precise movements of a robot arm before sending the command to execute.

Following successful test of the video overlay techniques, an agreement was concluded with Deneb Robotics that allows the company to integrate video overlay into the commercially available TELEGRIP to expand its use in hazardous environment robotics. (Courtesy of National Aeronautics and Space Administration.)



The operator can view the video image of the real world environment (upper right) and the computer's interpretation of the same scene using TELEGRIP. (Photo courtesy of National Aeronautics and Space Administration.)

control structure of the man-machine system can appear to be *open-loop*, or *combination open-loop/closed-loop*, or totally *closed-loop* with respect to visual stimuli.

When the **compensatory** block is appropriate at the perceptual level, the human controller acts in response to errors or controlled-element output quantities only. Only the Y_{pe} block "exists", with Y_{pi} and the precognitive block both equal to zero. With the compensatory pathway operational, continuous closed-loop control is exerted on the machine so as to minimize system errors in the presence of commands and disturbances. **Compensatory behavior** will characteristically be present when the commands and disturbances are random-appearing and when the only information displayed to the human controller consists of system errors or machine outputs. In the simple case where the describing function Y_{pe} is defined so as to account for the perceptual and neuromuscular components, the system is single-input/single-output, and the operator-induced noise is neglected, the closed-loop system output/input dynamics will be

$$\frac{m}{i} = \frac{Y_{pe} Y_c}{1 + Y_{pe} Y_c} \quad (105.1)$$

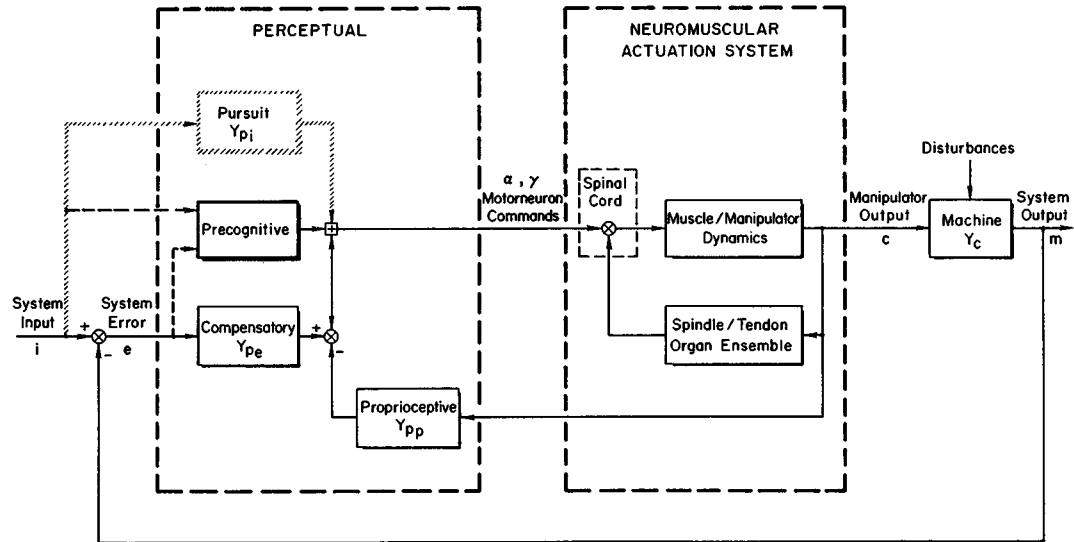


FIGURE 105.1 Major human operator pathways in a man-machine system.

and the error/input

$$\frac{e}{i} = \frac{1}{1 + Y_{pe} Y_c} \quad (105.2)$$

Thus, for compensatory situations, the man-machine system emulates the classic single-input/single-output feedback system. The output can be made to follow the input and the error can be reduced only by making the open-loop describing function large compared to 1 over the operating bandwidth of the system.

When the command inputs can be distinguished from the system outputs by virtue of the display (e.g., i and m are shown or detectable as separate entities relative to a reference) or preview (e.g., as in following a curved course) the *pursuit* block in Fig. 105.1 comes into play and joins the compensatory. The introduction of this new signal pathway provides an open-loop control in conjunction with the compensatory closed-loop error correcting action. The output/input dynamics of the man-machine system will then become

$$\frac{m}{i} = \frac{(Y_{pi} + Y_{pe}) Y_c}{1 + Y_{pe} Y_c} \quad (105.3)$$

and the error/input describing function is

$$\frac{e}{i} = \frac{1 - Y_{pi} Y_c}{1 + Y_{pe} Y_c} \quad (105.4)$$

With the pursuit system organization the error can be reduced by the human's operations in two ways: by making the open-loop describing function large compared with 1 and by generating a pursuit path describing function which tends to be the inverse of the controlled element. This can, of course, only be done over a limited range of frequencies. The quality of the overall control in the pursuit case can, in principle, be much superior to that where only compensatory operations are possible.

An even higher level of control is possible. When complete familiarity with the controlled element dynamics and the entire perceptual field is achieved, the highly skilled human operator can, under certain conditions, generate neuromuscular commands which are deft, discrete, properly timed, scaled, and sequenced so as to result in machine outputs which are almost exactly as desired. These neuromuscular commands are selected

from a repertoire of previously learned control movements. They are conditioned responses which may be triggered by the situation and the command and control quantities, but they are not continuously dependent on these quantities. This pure open-loop programmed-control-like behavior is called **precognitive**. Like the pursuit pathway, it often appears in company with compensatory follow-up or simultaneous operations. This forms a dual-mode form of control in which the human's manual output is initially dominated by the precognitive action, which does most of the job, and is then completed when needed by compensatory error-reduction actions.

The above description of human action pathways available in man-machine systems has emphasized the visual modality. Similar behavior patterns can be exhibited to some extent in other modalities as well. Thus the human's interactions with machines can be even more extraordinarily varied than described here and can range completely over the spectrum from open-loop to closed-loop in character in one or more modalities.

105.3 Full-Attention Compensatory Operations— The Crossover Model

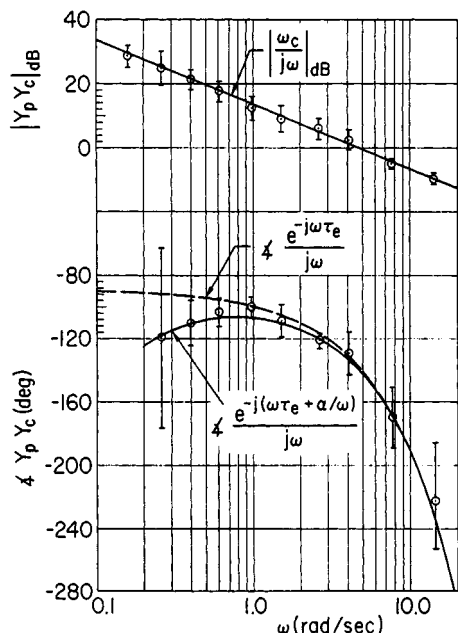
The compensatory pathways with manual control operations using the visual modality have been extensively studied. Thousands of experiments have been performed, and most of the adaptive features of human behavior associated with these kinds of operations are well understood. There are both classical control [e.g., McRuer and Krendel, 1974; and McRuer et al., 1990] and optimal control [e.g., Baron and Kleinman, 1969; Kleinman et al., 1970; Curry et al., 1976; and Thompson, 1990] theoretical formulations available to predict steady-state and dynamic performance.

By far the simplest human behavioral "law" for compensatory systems is the *crossover model*. This states that, for a particular controlled element transfer function, Y_c , the human operator adopts a describing function, Y_{pe} , such that the open-loop man-machine transfer characteristics appear as

$$Y_p Y_c = \frac{\omega_c e^{-\tau j\omega}}{j\omega} \quad (105.5)$$

The two parameters in the crossover model are the crossover frequency, ω_c , and an effective pure time delay, τ . The model applies only in the immediate region of the crossover frequency. The typical data shown in Fig. 105.2 illustrate how well this relationship is obeyed for a variety of subjects and a particular controlled element. The agreement with the amplitude ratio is excellent over a broad range of frequencies. The phase agreement is good in the region of the crossover frequency, ω_c , but departs somewhat at lower frequencies. Figure 105.2 also shows the *extended crossover model*. Here the effects in the crossover region of a potentially large number of low-frequency lags and leads (in the machine and/or the operator) are represented by a phase contribution given by $\exp(-j\alpha/\omega)$. Here the time constant $1/\alpha$ is a lumped-constant representation of myriad low-frequency phase characteristics. It is an appropriate approximation *only* in the general region of crossover and is not intended to extend to extremely low frequencies.

Fundamentally, the crossover model states that the human's transfer characteristics will be different for each set of machine dynamics, but that the form of the composite total open-loop dynamics will be substantially invariant. The effective time delay in Eq. (105.5) is a low-frequency approximation to the combination of all manner of high-frequency pure delays, lags, and leads, including a component representing the effects of



$$[\omega_c = 4.75 \text{ rad/sec}, \tau_e = 0.18 \text{ sec}, \alpha = 0.11 \text{ rad/sec}]$$

FIGURE 105.2 Data and crossover models for a simple rate-control-like controlled element.

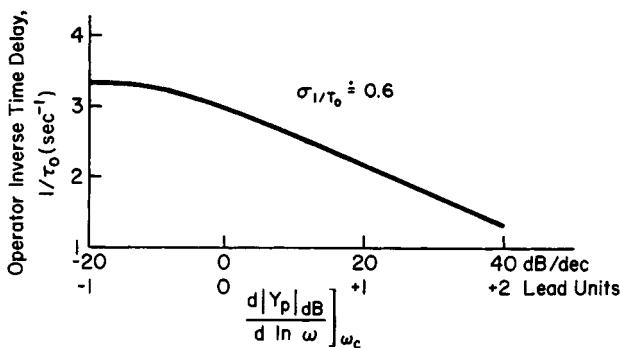


FIGURE 105.3 Variation of crossover model dynamic stimulus-response latency with degree of operator lead equalization.

the neuromuscular actuation system reflected to the crossover region. It follows that the effective time delay, τ , is not a constant. Its two major components are (1) the effective composite time delay of the controlled element (including manipulator effects)—the sum of the machine's lags minus leads at frequencies well above crossover and (2) the high-frequency dynamics of the human operator approximated by a pure delay which has an equivalent phase shift at frequencies within the crossover region. The latter includes a minimum of 0.1 second for the neuromuscular system and an additional increment which depends on the amount of lead generation required of the human to offset the controlled element deficiencies in order to make good the crossover model form. Figure 105.3 [McRuer and Krendel, 1974] shows this variation for a wide range of controlled elements (the neuromuscular delay component is included). More refined estimates are available [e.g., McRuer et al., 1990], but the above description is suitable for first-order estimates of behavior and dynamic performance.

Crossover Frequency for Full-Attention Operations

The crossover frequency tends to be constant for a given set of task variables (controlled-element form, inputs, disturbances, etc.). For example, as a controlled-element gain is changed, the human will change gain to compensate, resulting in the same crossover frequency. The maximum attainable crossover frequency, ω_u , will be

$$\omega_u = \frac{\pi}{2\tau} \quad (105.6)$$

This corresponds to zero phase margin. The nominal crossover frequency and associated pilot gain can be estimated from the condition to provide minimum mean-squared error in the presence of the appropriate form of continuous attention remnant. “Remnant” is operator-induced noise; as described below it depends on the nature of the operator’s equalization and is larger when low-frequency lead is required to make good the crossover model. Thus, the need to generate lead impacts both the effective time delay and the remnant and, accordingly, the crossover frequency for which the minimum mean-squared error is obtained. The nominal crossover frequency for full-attention operations can be estimated [McRuer et al., 1990] using

	ω_c/ω_u
No Operator Lead	0.78
Low-Frequency Operator Lead	0.66

Remnant

The second component of the operator’s response is operator-induced noise or remnant. Remnant can, in principle, result from several sources, but in single-loop systems with ideal linear manipulator characteristics

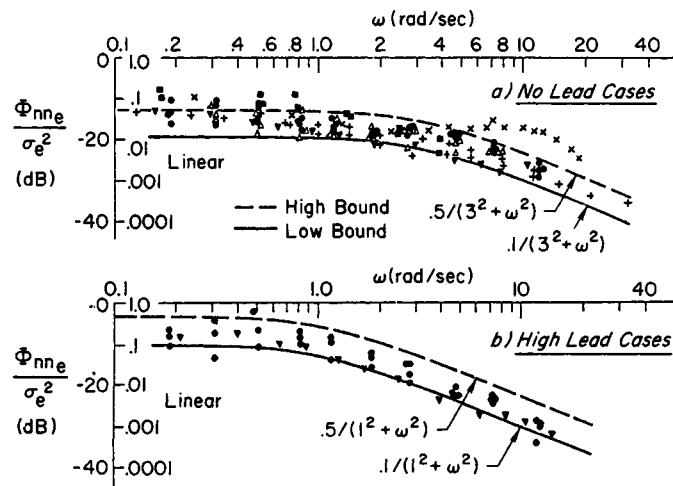


Figure 105.4 Normalized remnant spectra.

and no significant nonlinearities in the controlled element, the basic cause appears to be random time-varying behavior within the operator, which can be thought of as continuous random fluctuations in the effective time delay. The remnant can be described as a continuous, relatively broadband, power spectral density. Fig. 105.4 provides a cross-section of remnant data from several sources. It is very important to note that the magnitude of the power spectral density scales approximately with the mean-squared error.

Effects of Changes in the Task Variables

The task variable which has the most important effect on the trained operator's behavior is the controlled element dynamics. Indeed, the natures of human adaptive changes in adjusting to the controlled element is the main thrust of the crossover model and remnant discussion above. More generally, task variables other than the machine dynamics, as well as environmental and operator-centered variables, can change operator gain, and hence crossover frequency, effective time delay, and remnant. Accordingly, ω_c and τ variations become quantification measures of changes or differences in the task, environmental, and operator-centered variables expressed directly in terms of the operator's control actions.

A common example is the reduction of crossover frequency when the amplitude of the command or disturbance signals are very small. This reflects the human's indifference to small errors and constitutes the principal human behavioral nonlinearity in the crossover model context. Another example occurs in measuring the effects of training, where ω_c increases with trials until stable conditions are obtained for that particular subject and set of constant task and environmental conditions. Similarly, operator gain and remnant can be modified as a consequence of changes in operator-centered variables. A notable example is the decrease in gain and increase in remnant which accompanies alcohol ingestion.

Effects of Divided Attention

Human operators in man-machine systems are, in general, involved in two types of operations—control tasks and a diverse combination of monitoring/supervising/communicating/data-gathering/decision making activities referred to as “managerial tasks.” While the operator's attention is “divided” between the control and managerial tasks, these are often performed nearly simultaneously as parallel processing operations.

By definition, control workload is highest when the operator's full attention is required for control purposes and when this attention is focused on only the most critical input information needed for closed-loop control. For this reason the full-attention crossover model and remnant for compensatory behavior treated above has received the major attention here. Estimates and considerations based on full-attention compensatory assumptions will generally be conservative. For instance, the dynamic performance of the overall man-machine system will typically be improved when additional cues and information provide the basis for the generation of pursuit behavior.

For a given situation the minimum divided attention level should be established by the demands of the control task. When divided attention conditions are present in compensatory situations the major effects on the control performance are reduced crossover frequency and increased system error. To a first order the divided attention effects on average crossover frequency are given in Fig. 105.5. Here the “control dwell fraction,” is η , the proportion of the total time spent on the control task. There are many other complications and considerations [McRuer et al., 1990], but these require more than handbook treatment.

Defining Terms

Compensatory behavior: Human dynamic behavior in which the operator's actions are conditioned primarily by the closed-loop man-machine system errors.

Compensatory display: For the simplest case, a display which shows only the difference between the desired input command and the system output.

Precognitive behavior: Conditioned responses triggered by the total situation; essentially pure open-loop control.

Pursuit behavior: The human operator's outputs depend on system errors, as in compensatory behavior, but may also be direct functions of system inputs and outputs. The human response pathways make the man-machine system a combined open-loop, closed-loop system.

Pursuit display: In the simplest case, a display which shows input command, system output, and the system error as separable entities.

Related Topics

100.3 Frequency Response Methods: Bode Diagram Approach • 100.7 Nonlinear Control Systems

References

- S. Baron, and D.L. Kleinman, “The Human As An Optimal Controller and Information Processor,” NASA CR-1151, 1969.
- R.E. Curry, W.C. Hoffman, and L.R. Young, “Pilot Modeling for Manned Simulation,” AFFDL-TR-76-124, 1976.
- D.Graham and D. McRuer, *Analysis of Nonlinear Control Systems*, New York: John Wiley & Sons, 1961 (also Dover, 1971).
- D.L. Kleinman, S. Baron, and W.H. Levison, “An optimal control model of human response,” *Automatica*, vol. 9, no. 3, 1970.
- D.T. McRuer, “Human dynamics in man-machine systems,” *Automatica*, vol. 16, no. 3, 1980.
- D.T. McRuer, W.E. Clement, P.M. Thompson, and R.E. Magdaleno, “Pilot Modeling for Flying Qualities Applications,” WRDC-TR-89-3125, vol. II, 1990.
- D.T. McRuer, and H.R. Jex, “A review of quasi-linear pilot models,” *IEEE Trans. Human Factors in Electronics*, vol. HFE-8, no. 3, 1967.
- D.T. McRuer, and E.S. Krendel, “Mathematical Models of Human Pilot Behavior,” AGARD-AG-188, 1974.
- P.M. Thompson, “Program CC’s Implementation of the Human Optimal Control Model,” WRDC-TR-89-3125, vol. III, 1990.

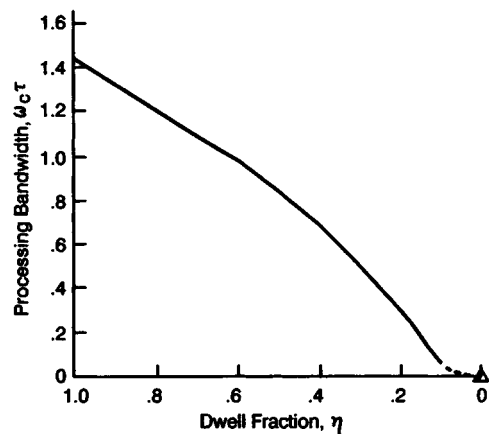


Figure 105.5 Effect of divided attention on processing bandwidth.

Further Information

The references of the chapter, especially Kleinman et al. [1970], McRuer and Krendel [1974], and McRuer et al. [1990], comprise a good cross section of detailed information on modeling aspects of man-machine systems. An excellent general text is T.B. Sheridan and W.R. Farrell, *Man-Machine Systems: Information, Control, and Decision Models of Human Performance*, Cambridge: MIT Press, 1974.

Encyclopedic coverage appears in K.R. Boff, L. Kaufman, and J.P. Thomas, *Handbook of Perception and Human Performance*, New York: Wiley, 1986, and K.R. Boff and J.E. Lincoln, "Engineering Data Compendium: Human Perception and Performance," Harry G. Armstrong Aerospace Medical Research Laboratory, Wright-Patterson Air Force Base, Ohio, 1988.

The aperiodic proceedings of the so-called "Annual Manual" contain a great deal of information about man-machine system developments. Since 1965 these have been published by NASA as SP's (NASA Special Publications) under the general heading of NASA—*University Conference on Manual Control*.

The text article emphasizes the dynamic behavior of the human, not the design of machine dynamics to achieve optimum characteristics in terms of man-machine system dynamic performance and human subjective approval. For these aspects of design, a comprehensive summary of models, references, and applications appears in "Advances in Flying Qualities," *AGARD Lecture Series LS-157*, 1988. Although the applications there are specifically for aerospace vehicle control, the principles illustrated apply to vehicles in general and to other machines subject to continuous control by a human operator.

As with other feedback control systems, system stability is a major consideration. In spite of the extraordinary adaptive properties intrinsic to human controllers, system instability is a rare but often unfavorable event. The nature of such man-machine oscillations and the design steps required to avoid them is treated extensively in Duane McRuer, *Pilot-Induced Oscillations and Human Dynamic Behavior*, NASA Contractor Report 4683, July 1995.

Boehmer, L.S. "Vehicular Systems"
The Electrical Engineering Handbook
Ed. Richard C. Dorf
Boca Raton: CRC Press LLC, 2000

106

Vehicular Systems

- Linda Sue Boehmer
LSB Technology
- 106.1 Introduction
 - 106.2 Design Considerations
 - 106.3 Land Transportation Classifications
 - 106.4 Propulsion
 - 106.5 Microprocessor Controls
 - 106.6 Monitoring and Diagnostics

106.1 Introduction

Vehicular systems have evolved and incorporated advances from many other fields of technology over the past decade. Instrumentation and controls for the various modes (aircraft, marine vessels, cars, trucks, buses, and rail vehicles) resemble each other more every year. Technology from one mode of transportation used to be of little interest to practitioners of any other mode. A technology historian might notice similarities among the functions of airport beacons, lighthouses, traffic lights, and railroad signals, but the specialists in each field had little to say to each other. This is no longer the case. Computers, microprocessor controls, electronics, GPS, and advanced networking and radio technologies are being applied in all forms of passenger and freight transportation, from aviation to marine, highway, and rail transport. The vehicles are now considered in context with an entire system within a particular mode, which is increasingly viewed as part of an overall transportation environment encompassing more than one mode.

Although “multimodal” is a term that was coined by policy makers to facilitate equitable distribution of funding among transportation modes and to facilitate interfaces among them, it applies equally well to the supporting technologies of the original modes. All modes now utilize microprocessor controls in their subsystems. With microprocessor control has come additional diagnostic capability and the use of system level intelligence, linking all intelligent subsystems and analog sensors and controls. Propulsion of vehicles now varies by mode less than it used to. Because of microprocessors, propulsion can be controlled more precisely, allowing vehicles to use non-traditional energy sources and to switch from one source to another easily, even automatically. We do not yet have the ideal multimodal vehicle, capable of navigating, either automatically or by a driver/operator, through air, in water, on roads, and on rails, but technology is no longer a limiting factor. We have not yet achieved the best balance among modes so that the most appropriate mode is utilized for passenger or freight transportation, but the tools exist to make those decisions possible. (This section deals primarily with land transportation. See the index for aviation and maritime applications.)

106.2 Design Considerations

If design could begin with a clean slate, the first step would be to decide which mode of transportation and which power source is best suited for the application, based on geography, priority of the passenger or cargo to be transported, energy efficiency, safety, cost per mile, and other factors. However, this is not really possible because the factors relating to funding sources and existing infrastructure often outweigh any technical considerations.

ROAD ENGINE

George B. Selden

Patented November 5, 1895

#549,160

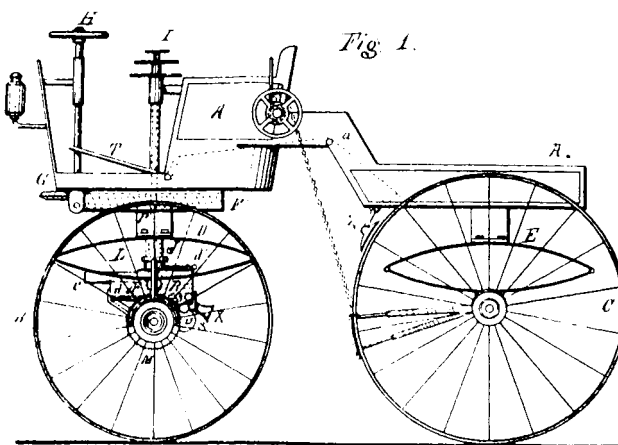
An excerpt from George Selden's patent application:

Be it known that I, George B. Selden, a citizen of the United States, residing in Rochester in the county of Monroe, in the state of New York, have invented an improved Road Engine, of which the following is a specification, reference being had to the accompanying drawings.

The object of my invention is the production of a safe, simple, and cheap road-locomotive light in weight, easy to control and possessed of sufficient power to overcome any ordinary inclination.

Perhaps one of the most famous patent lawsuits surrounded this patent applied for in 1879 by Selden, who was more of a patent attorney than an inventor. He sold the patent to Col. Allen Pope in 1899 who began to enforce the patent and won judgments against several car manufacturers—except one. They were forced to pay royalties on all vehicles they produced.

Henry Ford called the patent preposterous claiming that it didn't cover his vehicles that he had invented first. He refused to pay royalties and won a ruling in his favor in 1911, after millions had been paid out by his competitors. (Copyright © 1995, DewRay Products, Inc. Used with permission.)



Railroads, rail transit, buses, vans, and automobiles each have their own operating environments, although they are increasingly considered part of a system rather than simply as independent vehicles. Many of the underlying technologies are utilized across modal boundaries, but the basics of design remain highly dependent on mode.

Electrical systems are widely used in automobiles and trucks today and electronic systems currently make up about 10% of the value of a car. Electronic systems are currently used to control the engine, transmission, steering, braking, suspension, and traction. Many autos incorporate an integrated computer system for controlling the functions mentioned. In addition, electronic systems are used to display information such as speed and engine conditions.

Air bag inflation units use sensors and electronic controls to insure proper inflation within milliseconds after a collision.

As antilock brakes, **active suspensions**, and other computer-dependent technologies are fully utilized, electronic systems may constitute more than 20% of the value of a car. Much of the added computing power will be used for new technology for smart cars and smart roads, or ITS (intelligent transportation systems). The term refers to a varied assortment of electronics that provide real-time information on accidents, congestion, routing, and roadside services to drivers and traffic controllers. ITS encompass devices that would make vehicles more autonomous: collision-avoidance systems and lane-tracking technology that alert drivers to impending disaster or allow a car to drive itself. ITS also includes interfaces between personal traffic and mass transportation, particularly when rail traffic mixes with cars and at rail crossings, whether or not such crossings are protected by gates. Railroads and mass transit vehicles have many of the same internal subsystems as cars do, and also additional subsystems, for which cars may soon have analogous functions. The electrical and electronic systems and controls account for 15 to 30% of the cost of the vehicle.

The major vehicle subsystems include propulsion, braking, power conditioning, communication, passenger information (audio and visual), heating/air conditioning, door control, speed control, and monitoring and diagnostics. All of these subsystems interact with each other and many also interact with subsystems external to the vehicle.

Some of the initial design considerations for vehicles include:

- Will the vehicle interface with an existing fleet?
- Will the vehicle operate independently or as part of a consist, or both?
- What are the physical requirements, including dimensions, number of passengers (seated vs. standing)? Is the system (or portions of it) elevated, in tunnels, at grade, underground? Will the vehicles mix with or cross other types of traffic? Are ambient conditions exceptionally hot, cold, or dangerous?
- How closely must one vehicle (or consist) follow another and how fast must they be capable of traveling? Where, how often, and for how long will they stop?
- To what degree will the vehicles be automated; how much control will a human operator (and/or other crew) have and under what conditions?
- What kind of power is available, how will it be collected, and can energy generated during electric braking be returned to the power system?
- How will system and subsystem failures be handled, what kind of failures are acceptable, and to what degree (or for how long) will they be tolerated? How often and with what degree of expertise will the vehicles be serviced?

106.3 Land Transportation Classifications

Among land transportation vehicles, there are more subdivisions than the lay person might expect. In general, distinctions are based on vehicle size, weight, speed, and passenger or cargo capacity. Cars, trucks, mini-vans, vans, sport utility vehicles, etc. are familiar terms. There is some variation among them relative to the electronics embedded in the systems and the options available to the driver. The same is true for railroads, rail transit, and mass transit, although the distinctions among classifications are important to the manufacturers and operators of the equipment. The classifications include railroad, commuter rail, heavy rail, light rail, street car, trolley bus, bus, paratransit, and “people mover” or monorail.

106.4 Propulsion

By 1910 electric automobiles were commonplace. Nevertheless, they were replaced by gasoline-fueled automobiles by 1920 because electric cars operated at lower top speeds and over shorter ranges without recharging than gasoline cars could achieve. However, the availability of electric motive power remained a critical factor in the development of cities. Since the mid-1970s, when the electric vehicle reemerged as an appealing transportation option, many have recognized the potential of electric fleet vans. An **electric vehicle** uses electric energy storage, electric controls, and electric propulsion devices. Because the vans use batteries to drive their electric motors, they are well suited

to the short routes and regular schedules followed by vans in a company fleet. One such fleet van, the General Motors Griffon, is produced in England. Because the vans can be recharged regularly at night, they offer electric utilities a new off-peak demand. At the same time, electric vehicles run cleanly and burn no gasoline.

Increasing the distance an electric vehicle can travel on a single charge is the most significant factor in expanding the market for electric vans. The 60-mile (97-km) range of the Griffon makes it a replacement candidate for about 600,000 commercial fleet vehicles now operating in the United States. If advanced batteries doubled the range of a van to 120 miles, the potential market for these vehicles could top 2 million. A variety of electric cars has been introduced over the years, but none have enjoyed general use.

Products of combustion gradually were recognized as major air pollutants and fuels have been acknowledged as non-renewable resources, so alternatives have been sought with increasing diligence.

Today, electric motors are used more widely for rail vehicles than for cars, vans, or buses, although this is slowly changing (see above). Electric motors as a back-up mode for buses are becoming more common in certain areas where air pollution is considered a serious problem and in portions of systems, such as North American tunnels, where fumes from internal combustion can be hazardous.

Power distribution for rail vehicles ranges from three phase ac, at various voltages (usually collected from overhead wires), to several different dc voltages (usually collected from a "third rail"). Until recently (within the past 5 years in the U.S.), most electric traction motors utilized dc power. Today, most traction motors in new vehicles use ac power. Various techniques are used to cool the motors, depending on the operating environment. Collected power is conditioned continuously (see power "converters" and "inverters") to meet the motors' requirements and the power requirements of other vehicle systems, and also is stored to power critical on-board systems if power is lost.

Traction motors also are used for braking, which generates power that can be reconditioned and returned to the power system to power other vehicles or returned to the power grid. Power that cannot be returned or used elsewhere in the system is converted into heat by banks of large braking resistors. Electric braking is supplemented by mechanical braking systems which can be actuated pneumatically, hydraulically, and/or electrically. Coordination of propulsion and braking efforts, especially when traction surfaces are slippery, is an important design point.

Microprocessor controls have allowed optimization of automotive internal combustion processes to economize on fuel and minimize air pollution. Alternative fuels, such as natural gas, are becoming more common because the combustion process can be managed more uniformly, responsively, and safely than ever before.

Diesel electric locomotives have become the propulsion vehicle of choice for long haul freight railroads. Microprocessors control the combustion process which produces electricity to power electric motors when ac power is not available, such as on long sections of rail that are not yet electrified.

Dual mode buses utilize internal combustion when operating on the streets, but switch to electric power in tunnels. Dual mode rail vehicles or streetcars collect power from an overhead catenary or third rail, but can switch to battery power when they are not operating in electrified areas.

Improvements in battery technology (cost, life, power density, weight, and maintenance requirements) and solar power as a supplementary or primary source will improve the acceptance of alternatives to internal combustion and direct electric power.

106.5 Microprocessor Controls

All major vehicle subsystems and many minor ones are now microprocessor-controlled. Embedded microprocessors replace banks of relays and mechanical switches to perform functions on the vehicle and also to control functions that did not exist prior to the advent of microprocessors. Some major vehicle subsystems have several microprocessors handling different functions and coordinating analog and digital input and output signals.

Intelligent subsystems exchange information within a vehicle, among vehicles in a consist, and between the vehicle and its external environment. This information is exchanged through increasingly sophisticated networks, which may or may not use traditional wiring. There may also be a separate network or layers of error-checking to handle safety-critical data.

A human vehicle operator typically has status indicators, alarms, and controls. These have changed dramatically with the advances in microprocessor-controlled subsystems. The "glass cockpit" and "fly by wire" techniques

POWER APPLYING MECHANISM

Otto Zachow and William Besser dich

Patented December 29, 1908

#907,940

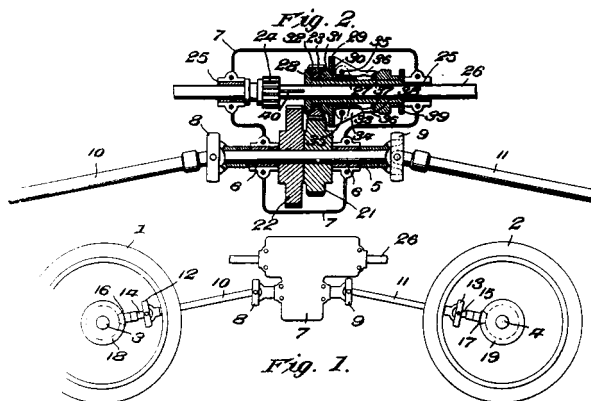
An excerpt from Otto Zachow and William Besserlich's patent application:

A Our invention relates to new and useful improvements in power-applying mechanism and more particularly to that class adapted to be used in connection with motor-propelled vehicles, such as automobiles, or the like, and our object is to provide a mechanism of this class whereby the power may be applied to both the front and rear axles.

Early in this century, Otto Zachow and his friend, William Besserlich, had the idea of making all four wheels of their vehicle turn, when they slid into a ravine and got stuck. Out of frustration the four-wheel drive mechanism was invented.

At the beginning of World War I, they sold about 50 trucks equipped with the mechanism to Great Britain. When the United States entered the war, Zachow and Besserlich sold 3,750 trucks to the U.S. Army.

Today, four-wheel drive is available on a wide range of vehicles from small sport utilities to luxury imports. (Copyright © 1995, DewRay Products, Inc. Used with permission.)



developed for aviation generally transition to cars and trains as they are service-proven and as their cost decreases. A driver or train operator once had a few lights, a gauge or two, a throttle of some sort, and a brake handle or pedal. For vehicles that are not automated but are partially automated or allow manual operation at times, a human operator today is confronted by a dense array of dials, buttons, data and CCTV screens, LCD panels, microphones, and annunciators (audio and visual) of various types. In some cases there is far more information than an operator can use. In others, there is duplication between the old, analog indicators and controls and new, digital or “soft” controls on a touch screen.

There has been some resistance to technology advances, based on the perception that electronics are not as reliable as electromechanical devices (such as relays) and on a concern that they will be more complicated to troubleshoot and maintain than electro-mechanical and analog equipment.

106.6 Monitoring and Diagnostics

A great advantage of microprocessor-controlled systems is the degree to which they can be self-diagnosing. Each intelligent subsystem has internal self-diagnostics which include routines to perform initial tests on power-up, update checks for “hot” startup and continuous checking to assure that inputs and outputs are within expected ranges. Internal self-diagnostics are also capable of performing self-tests on request. When fault conditions are noted, typically there are internal resets to allow for inaccurate data, with faults being logged after a certain number of occurrences or duration of a fault condition.

The basis of any monitoring and diagnostics system is the underlying maintenance philosophy. Microprocessor controls make it possible to capture any combination of information from the intelligent subsystems. Information can then be processed and presented in a variety of ways, along with data from analog sensors which are not part of any intelligent system.

Information of interest includes operating status and existing or historical fault information. “Events” may include faults and also other expected actions that may or may not be considered faults. Historical information can include faults, events, and the status of parameters of interest associated with the fault. The amount of information that can be captured is limited only by the amount of memory provided and the speed at which it can be transferred. Typically, some (or all) of the memory is in a form that will allow the fault data to be preserved after power is lost or vehicles are shut down between operating periods.

Decisions on which information to capture, how often to sample, and how many samples to preserve are ideally based on what will be most valuable for troubleshooting existing faults and predicting future failures. A thorough understanding of each intelligent subsystem is needed in addition to an understanding of the environment in which it operates, including the other subsystems with which it interacts. It is also important to know what level of skill will be applied to interpreting the saved information. If the level of skill will be low, some degree of artificial intelligence can be designed into the diagnostics to guide a maintenance technician through the troubleshooting process.

The information needed to be collected is influenced by the target audience. The most detailed internal subsystem information is primarily used by engineers or specialized technicians to troubleshoot detailed failures or fine tune operation. A subset of less detailed information is used by maintenance staff to determine which components or sub-modules to replace or repair. A further subset of that information is used by a general troubleshooting staff to determine which subsystem is malfunctioning or which higher level modules to replace. An even smaller subset of operating status information and only a few major faults are needed by the operator, with a selection of that data being useful to a central control or maintenance dispatching facility if real time links are available. A variety of techniques are being used to present this information to the target audience(s) in ways and at times that are most appropriate.

“Event recorders” similar to the ones required on passenger airliners, capturing selected parameters, are now required by the FRA for railroads and are under consideration by industry standards groups for other modes.

Defining Terms

Active suspension: An electronically controlled suspension system for maintaining level suspension of a vehicle.

Consist: Two or more vehicles coupled together in a train. The vehicles may be identical or they may each lack a major subsystem (such as propulsion), whose functions may be handled by another vehicle in the consist.

Dual mode: Vehicles that are designed to switch manually or automatically from one type of propulsion to another, for instance from internal combustion to electric.

Electric braking: Use of traction motor to slow the vehicle.

Electric vehicle: Vehicle using electric energy storage, electric controls, and electric propulsion devices.

Traction motor: Electric motor that provides motive power to move vehicles.

Related Topics

66.2 Motors • 82.1 Practical Microprocessors

References

- IEEE *Spectrum*, Technology Issue, January 1996.
R. K. Jurgen, "Putting electronics to work in the 1991 car models," *IEEE Spectrum*, pp. 75-78, December 1990.
Intermodal Surface Transportation Efficiency Act of 1991 (ISTEA): FTA & FHA, Department of Transportation
(see below).

Further Information

The following organizations can provide industry perspectives, applicable standards, and guidelines and technical information.

Vehicular Technology Society, Institute of Electrical and Electronics Engineers, 345 East 47th Street, New York, NY 10017-2394, 1-800-678-IEEE.

American Public Transit Association (APTA), 1201 New York Avenue, NW, Suite 400, Washington, D.C. 20005.

Federal Transit Administration (FTA), Federal Highway Administration (FHA), Federal Railroad Administration (FRA), Department of Transportation, 400 7th Street SW, Washington, D.C. 20590.

Society of Automotive Engineers, 400 Commonwealth Drive, Warrandale, PA 15096.

ITS America, 400 Virginia Avenue, SW, Suite 800, Washington, D.C. 20024-2730.

Chen, K. "Industrial Illuminating Systems"
The Electrical Engineering Handbook
Ed. Richard C. Dorf
Boca Raton: CRC Press LLC, 2000

Industrial Illuminating Systems

-
- | | |
|-------|---|
| 107.1 | New Concepts in Designing an Industrial Illuminating System
Determination of Illuminance Levels • Illumination Computational Methods |
| 107.2 | Factors Affecting Industrial Illumination
Basic Definitions • Factors and Remedies • Daylighting |
| 107.3 | System Components
Light Sources • Ballasts • Luminaires |
| 107.4 | Applications
Types of Industrial Illuminating Systems • Selection of the Equipment |
| 107.5 | System Energy Efficiency Considerations
Energy-Saving Lighting Techniques • Lighting Controls • Lighting and Energy Standards |

Kao Chen
Carlsons Consulting Engineers

107.1 New Concepts in Designing an Industrial Illuminating System

Determination of Illuminance Levels

Among the many new concepts for lighting design, the first to be discussed is the new method of determining **illuminance** levels. In the past when illuminating engineers wanted to find the recommended illuminance level for a given task, they would look in the lighting handbook to find a recommended level and then design an illuminating system for the task using the value as a minimum. This procedure provides very little latitude for fine-tuning an illumination design. In the new method, a more comprehensive investigation of required illuminance is performed according to the following steps:

1. Instead of a single recommended illuminance value, a category letter is assigned. [Table 107.1](#) shows different category letters for a selected group of industries (partial only; for complete list see *IES Lighting Handbook* [1993]).
2. The category letters are used to define a range of illuminance. [Table 107.2](#) details illuminance categories and illuminance values for generic types of activities in interiors.
3. From within the recommended range of illuminance, a specific value of illuminance is selected after consideration is given to the average age of workers, the importance of speed and accuracy, and the reflectance of task background.

The importance of acknowledging the speed and accuracy with which a task must be performed is readily recognized. Less obvious is the need to consider the age of workers and the reflectance of task background.

TABLE 107.1 Illuminance Categories for Selected Group of Industries

Area/Activity	Illuminance Category	Area/Activity	Illuminance Category
Aircraft maintenance	^a	Canning	
Aircraft manufacturing	^a	Continuous-belt canning	E
Assembly		Sink canning	E
Simple	D	Hand packing	D
Moderately difficult	E	Olives	E
Difficult	F	Examination of canned samples	F
Very difficult	G	Container handling	
Exacting	H	Inspection	F
Automobile manufacturing		Can unscramblers	E
Bakeries		Labeling and cartoning	D
Mixing room	D	Casting (see Foundries)	
Face of shelves	D	Central stations (see Electric generating stations)	
Inside of mixing bowl	D	Chemical plants (see Petroleum and chemical plants)	
Fermentation room	D	Clay and concrete products	
Make-up room		Grinding, filter presses, kiln rooms	C
Bread	D	Molding, pressing, cleaning, trimming	D
Sweet yeast-raised products	D	Enameling	E
Proofing room	D	Color and glazing—rough work	E
Oven room	D	Color and glazing—fine work	F
Fillings and other ingredients	D	Cleaning and pressing industry	
Decorating and icing		Checking and sorting	E
Mechanical	D	Dry and wet cleaning and steaming	E
Hand	E	Inspection and spotting	G
Scales and thermometers	D	Pressing	F
Wrapping	D	Repair and alteration	F
Book binding		Cloth products	
Folding, assembling, pasting	D	Cloth inspection	I
Cutting, punching, stitching	E	Cutting	G
Embossing and inspection	F	Sewing	G
Breweries		Pressing	F
Brew house	D	Clothing manufacture (see Sewn Products)	
Boiling and keg washing	D	Receiving opening, storing, shipping	D
Filling (bottles, cans, kegs)	D	Examining (perching)	I
Candy making		Sponging, decanting, winding, measuring	D
Box department	D	Piling up and marking	E
Chocolate department		Cutting	G
Husking, winnowing, fat extraction,	D	Pattern making, preparation of trimming, piping,	E
crushing and refining, feeding		canvas and shoulder pads	
Bean cleaning, sorting, dipping, packing,	D	Filling, bundling, shading, stitching	D
wrapping		Shops	F
Milling	E	Inspection	G
Cream making	D	Pressing	F
Mixing, cooking, molding	D	Sewing	G
Gum drops and jellied forms	D	Control rooms	
Hand decorating	D	(see Electric generating stations—interior)	
Hard candy		Corridors (see Service spaces)	
Mixing, cooking, molding	D	Cotton gin industry	
Die cutting and sorting	E	Overhead equipment—separators, driers, grid	D
Kiss making and wrapping	E	cleaners, slick machines, conveyers, feeders	
Canning and preserving		and catwalks	
Initial grading raw material samples	D	Gin stand	D
Tomatoes	E	Control console	D
Color grading and cutting rooms	F	Lint cleaner	D
Preparation		Bale press	D
Preliminary sorting	D	Dairy farms (see Farms)	
Apricots and peaches	D	Dairy products	
Tomatoes	E	Fluid milk industry	
Olives	F	Boiler room	D
Cutting and pitting	E	Bottle storage	D
Final sorting	E	Bottle sorting	E

^a Industry representatives have established a table of single illuminance values which, in their opinion, can be used. Illuminance values for specific operations can also be determined using illuminance categories of similar tasks and activities found in this table and the application of the appropriate weighting factors.

Source: IES Lighting Handbook, Application Volume.

TABLE 107.2 Illuminance Categories and Illuminance Values for Generic Types of Activities in Interiors

Type of Activity	Illuminance Category	Ranges of Illuminances		Reference Work-Plane
		Lux	Footcandles	
Public spaces with dark surroundings	A	20–30–50	2–3–5	
Simple orientation for short temporary visits	B	50–75–100	5–7.5–10	
Working spaces where visual tasks are only occasionally performed	C	100–150–200	10–15–20	General lighting throughout spaces
Performance of visual tasks of high contrast or large size	D	200–300–500	20–30–50	
Performance of visual tasks of medium contrast or small size	E	500–750–1,000	50–75–100	Illuminance on task
Performance of visual tasks of low contrast or very small size	F	1,000–1,500–2,000	100–150–200	
Performance of visual tasks of low contrast and very small size over a prolonged period	G	2,000–3,000–5,000	200–300–500	Illuminance on task, obtained by a combination of general and local (supplementary lighting)
Performance of very prolonged and exacting visual tasks	H	5,000–7,500–10,000	500–750–1,000	
Performance of very special visual tasks of extremely low contrast and small size	I	10,000–15,000–20,000	1,000–1,500–2,000	

Source: IES Lighting Handbook, Application Volume.

To compensate for reduced visual acuity, more illuminance is needed. Using the average age of workers as the age criterion is a compromise between the need of the young and the older workers and, therefore, a valid criterion.

Task background affects the ability to see because it affects **contrast**, an important aspect of visibility. More illuminance is required to enhance the visibility of tasks with poor contrast. Reflectance is calculated by dividing the reflected value by the incident value. The data given in Tables 107.3 and 107.4 are taken from the *IES Lighting Handbook* [1987] and are applied to provide a single value of illuminance from within the range recommended.

Illuminating system design can begin after the desired value of illuminance for a given task has been determined. Based on the *IES Handbook*, the zonal cavity method of determining the number of luminaires and lamps to yield a specified maintained luminance remains unchanged.

Illumination Computational Methods

Zonal Cavity Method. Introduced in 1964, the zonal cavity method of performing lighting computations has gained rapid acceptance as the preferred way to calculate number and placement of luminaires required to satisfy a specified illuminance level requirement. Zonal cavity provides a higher degree of accuracy than does the old lumen method, because it gives individual consideration to factors that are glossed over empirically in the lumen method.

Definition of Cavities. With the zonal cavity method, the room is considered to contain three vertical zones or cavities. Figure 107.1 defines the various cavities used in this method of computation. Height for luminaire to ceiling is designated as the ceiling cavity (h_{cc}). Distance from luminaire to the work plane is the room cavity (h_r), and the floor cavity (h_f) is measured from the work plane to the floor.

To apply the zonal cavity method, it is necessary to determine a parameter known as the “**cavity ratio**” (CR) for each of the three cavities. Following is the formula for determining the cavity ratio:

$$\text{cavity ratio} = \frac{5h (\text{room length} + \text{room width})}{(\text{room length} \times \text{room width})} \quad (107.1)$$

where h equals h_{cc} for ceiling cavity ratio (CCR), h_r for room cavity ratio (RCR), h_f for floor cavity ratio (FCR).

TABLE 107.3 Weighting Factors for Selecting Specific Illuminance Within Ranges A, B, and C

Occupant and Room Characteristics*	Weighting Factor		
	-1	0	+1
Workers' age (average)	Under 40	40 to 55	Over 55
Average room reflectance ¹	>70%	30 to 70%	<30%

Source: *IES Lighting Handbook, Application Volume*.

Note: This table is used for assessing weighting factors in rooms where a task is not involved.

1. Assign the appropriate weighting factor for each characteristic.
2. Add the two weights; refer to Table 107.2, Categories A through C:
 - a. If the algebraic sum is -1 or -2, use the lowest range value.
 - b. If the algebraic sum is 0, use the middle range value.
 - c. If the algebraic sum is +1 or +2, use the highest range value.

*To obtain average room reflectance: determine the areas of ceiling, walls, and floor; add the three to establish room surface area; determine the proportion of each surface area to the total; multiply each proportion by the pertinent surface reflectance; and add the three numbers obtained.

TABLE 107.4 Weighting Factors for Selecting Specific Illuminance Within Ranges D through I

Task or Worker Characteristics	Weighting Factor		
	-1	0	+1
Workers' age (average)	Under 40	40 to 55	Over 55
Speed or accuracy*	Not important	Important	Critical
Reflectance of task background, %	>70%	30 to 70%	<30%

Source: *IES Lighting Handbook, Application Volume*.

Note: Weighting factors are based upon worker and task information.

1. Assign the appropriate weighting factor for each characteristic.
2. Add the two weights; refer to Table 107.2, Categories D through I:
 - a. If the algebraic sum is -2 or -3, use the lowest range value.
 - b. If the algebraic sum is -1, 0, or +1, use the middle range value.
 - c. If the algebraic sum is +2 or +3, use the highest range value.

*Evaluation of speed and accuracy requires that time limitations, the effect of error on safety, quality, and cost, etc. be considered. For example, leisure reading imposes no restrictions on time, and errors are seldom costly or unsafe. Reading engineering drawings or a micrometer requires accuracy and, sometimes, speed. Properly positioning material in a press or mill can impose demands on safety, accuracy, and time.

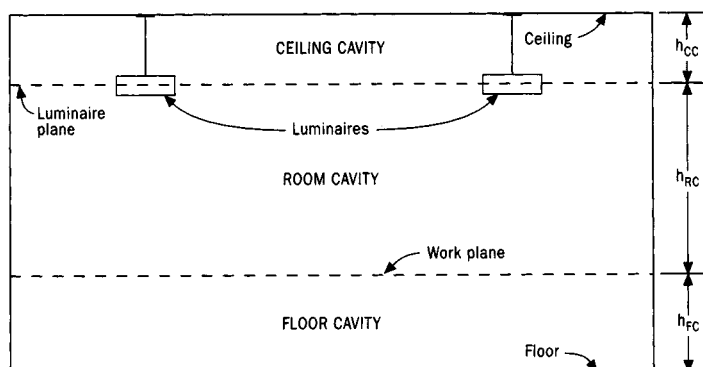


FIGURE 107.1 Basic cavity divisions of space.

Lumen Method Details. Because of the ease of application of the lumen method which yields the average illumination in a room, it is usually employed for larger areas, where the illumination is substantially uniform. The lumen method is based on the definition of a footcandle, which equals one lumen per square foot:

$$\text{footcandle} = \frac{\text{lumen striking an area}}{\text{square feet of area}} \quad (107.2)$$

In order to take into consideration such factors as dirt on the luminaire, general depreciation in lumen output of the lamp, and so on, the above formula is modified as follows:

$$\text{footcandle} = \frac{\text{lamps/luminaire} \times \text{lumens/lp} \times \text{CU} \times \text{LLF}}{\text{area/luminaire}} \quad (107.3)$$

In using the lumen method, the following key steps should be taken:

- a. Determine the required level of illuminance.
- b. Determine the **coefficient of utilization (CU)** which is the ratio of the lumens reaching the working plane to the total lumens generated by the lamps. This is a factor that takes into account the efficiency and the distribution of the luminaire, its mounting height, the room proportions, and the reflectances of the walls, ceiling, and floor. Rooms are classified according to shape by 10 room cavity numbers. The cavity ratio can be calculated using the formula given in Eq. (107.1). The coefficient of utilization is selected from tables prepared for various luminaires by manufacturers.
- c. Determine the **light loss factor (LLF)**. The final light loss factor is the product of all the contributing loss factors. Lamp manufacturers rate filament lamps in accordance with their output when the lamp is new; vapor discharge lamps (fluorescent, mercury, and other types) are rated in accordance with their output after 100 hr of burning.
- d. Calculate the number of lamps and luminaires required:

$$\text{no. of lamps} = \frac{\text{footcandles} \times \text{area}}{\text{lumens/lp} \times \text{CU} \times \text{LLF}} \quad (107.4)$$

$$\text{no. of luminaires} = \frac{\text{no. of lamps}}{\text{lamps/luminaire}} \quad (107.5)$$

- e. Determine the location of the luminaire—luminaire locations depend on the general architecture, size of bays, type of luminaire, position of previous outlets, and so on.

Point-by-Point Method. Although currently light computations emphasize the zonal cavity method, there is still considerable merit in the point-by-point method. This method lends itself especially well to calculating the illumination level at a particular point where total illumination is the sum of general overhead lighting and supplementary lighting. In this method, information from luminaire **candlepower distribution** curves must be applied to the mathematical relationship. The total contribution from all luminaires to the illumination level on the task plane must be summed.

Direct Illumination Component. The angular coordinate system is most applicable to continuous rows of fluorescent luminaires. Two angles are involved: a longitudinal angle α and a lateral angle β . Angle α is the angle between a vertical line passing through the seeing task (point P) and a line from the seeing task to the end of the rows of luminaires. Angle α is easily determined graphically from a chart showing angles α and β

for various combinations of V and H . Angle β is the angle between the vertical plane of the row of luminaires and a tilted plane containing both the seeing task and the luminaire or row of luminaires. [Figure 107.2](#) shows how angles α and β are defined. The direct illumination component for each luminaire or row of luminaires is determined by referring to the table of direct illumination components for the specific luminaire. The direct illumination components are based on the assumption that the luminaire is mounted 6 ft above the seeing task. If this mounting height is other than 6 ft, the direct illumination component shown in [Table 107.5](#) must be multiplied by $6/V$, where V is the mounting height above the task. Thus the total direct illumination component would be the product of $6/V$ and the sum of the individual direct illumination components of each row.

Reflected Illumination Components on the Horizontal Surfaces. This is calculated in exactly the same manner as the average illumination using the lumen method, except that the reflected radiation coefficient (RRC) is substituted for the coefficient of utilization.

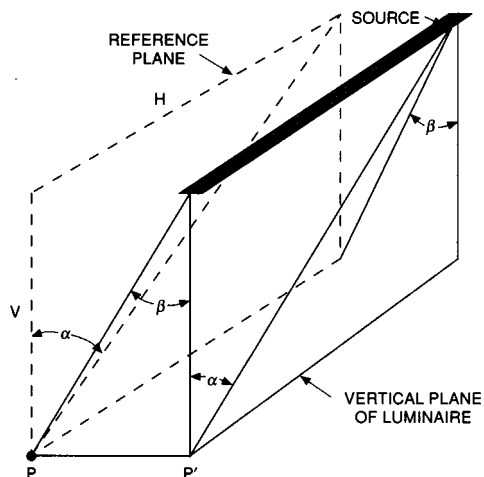


FIGURE 107.2 Definition of angular coordinate systems for direct illumination component.

$$FC_{RH} = \frac{\text{lamps/luminaire} \times \text{lumens/lp} \times RRC \times LLF}{\text{area/luminaire}} \quad (107.6)$$

where $RRC = LC_w + RPM (LC_{CC} - LC_w)$, LC_w = wall luminance coefficient, LC_{CC} = ceiling cavity luminance coefficient, and RPM = room position multiplier.

The wall luminance coefficient and the ceiling cavity luminance coefficient are selected for the appropriate room cavity ratio and proper wall and ceiling cavity reflectances from the table of luminance coefficients in the same manner as the coefficient of utilization. The room position multiplier is a function of the room cavity ratio and of the location in the room of the point where the illumination is desired. [Table 107.6](#) lists the value of the RPM for each possible location of the part in the rooms of all room cavity ratios.

[Figure 107.3](#) shows a grid diagram that illustrates the method of designating the location in the room by a letter and a number.

Reflected Illumination Components on the Vertical Surfaces. To determine illumination reflected to vertical surfaces, the approximate average value is determined using the same general formula, but substituting WRRC (wall reflected radiation coefficient) for the coefficient of utilization:

$$FC_{RV} = \frac{\text{lamps/luminaire} \times \text{lumens/lp} \times WRRC \times LLF}{\text{area/luminaire (on work plane)}} \quad (107.7)$$

where

$$WRRC = \frac{\text{wall luminance coefficient}}{\text{average wall reflectance}} - WDRC \quad (107.8)$$

where WDRC is the wall direct radiation coefficient, which is published for each room cavity ratio together with a table of wall luminance coefficients (see [Table 107.5](#) for a specific type of luminance).

TABLE 107.5 Direct Illumination Components for Category III Luminaire (Based on F40 Lamps Producing 3100 Lumens)

Direct Illumination Components																										
8	5	15	25	35	45	55	65	75	5	15	25	35	45	55	65	75										
∞	Vertical Surface Illumination Footcandles at a Point on a Plane Parallel to Luminaires									Vertical Surface Illumination Footcandles at a Point on a Plane Perpendicular to Luminaires																
0–10	.9	2.6	3.6	3.9	3.3	1.9	.7	.1	.9	.8	.7	.5	.3	.1	—	—										
0–20	1.8	5.0	7.0	7.7	6.6	3.8	1.5	.2	3.6	3.2	2.7	1.9	1.2	.5	.1	—										
0–30	2.6	7.2	10.1	11.3	9.8	5.7	2.3	.3	7.7	7.0	5.8	4.3	2.7	1.1	.3	—										
0–40	3.2	9.0	12.8	14.5	12.9	7.7	3.2	.5	12.6	11.6	9.7	7.5	4.9	2.1	.6	—										
0–50	3.7	10.3	14.9	17.1	15.7	9.6	4.3	.7	17.8	16.6	14.2	11.2	7.7	3.4	1.1	.1										
0–60	4.0	11.2	16.3	18.8	17.6	11.3	5.5	1.0	22.6	21.2	18.4	14.7	10.4	5.1	1.9	.2										
0–70	4.1	11.6	17.0	19.8	18.9	12.7	6.8	1.4	26.2	24.7	21.8	17.8	13.1	7.2	3.2	.3										
0–80	4.1	11.7	17.3	20.2	19.4	13.3	7.4	1.9	28.2	26.7	23.8	19.7	14.9	8.7	4.3	.8										
0–90	4.1	11.7	17.3	20.2	19.4	13.4	7.5	2.0	28.6	27.1	24.2	20.1	15.3	9.1	4.7	1.1										
F.C. at a Point on Work Plane												Category III														
0–10	10.6	9.5	7.6	5.5	3.3	1.3	.3	—	 2 T-12 Lamps—Any Loading For T-10 Lamps—CU × 1.02																	
0–20	20.6	18.5	14.9	10.9	6.6	2.6	.7	—																		
0–30	29.4	26.5	21.6	16.0	9.8	4.0	1.1	—																		
0–40	36.5	33.1	27.4	20.6	12.9	5.4	1.5	—																		
0–50	41.8	38.1	31.9	24.3	15.7	6.7	2.0	.1																		
0–60	45.2	41.3	34.8	26.8	17.6	7.9	2.6	.2																		
0–70	46.9	43.0	36.4	28.3	18.9	8.9	3.2	.3																		
0–80	47.4	43.6	36.9	28.8	19.4	9.3	3.5	.4																		
0–90	47.5	43.7	37.0	28.8	19.4	9.3	3.5	.4																		
Luminance Coefficients for 20% Effective Floor Cavity Reflectance																										
Ceiling Cavity		Reflectances																								
Walls		80			50			10			80			50			10									
WDRC		50			30			50			50			30			30									
		Wall Luminance Coefficients												Ceiling Cavity Luminance Coefficients												
.281	1	.246	.140	.220	.126	.190	.109	.230	.209	.135	.124	.025	.023													
.266	2	.232	.127	.209	.115	.182	.102	.222	.190	.130	.113	.024	.021													
.245	3	.216	.115	.196	.105	.172	.095	.215	.176	.127	.105	.024	.020													
.226	4	.202	.102	.183	.097	.161	.088	.209	.164	.124	.099	.023	.019													
.212	5	.191	.097	.173	.090	.154	.082	.204	.156	.121	.094	.023	.018													
.196	6	.178	.090	.163	.084	.145	.076	.200	.149	.118	.090	.022	.017													
.182	7	.168	.083	.153	.078	.136	.071	.194	.144	.115	.087	.022	.017													
.170	8	.158	.077	.145	.072	.130	.066	.190	.139	.113	.085	.021	.016													
.159	9	.150	.072	.138	.068	.123	.062	.185	.135	.110	.082	.021	.016													
.149	10	.141	.068	.130	.064	.116	.059	.180	.131	.107	.080	.020	.016													

107.2 Factors Affecting Industrial Illumination

Basic Definitions

Illuminance. Illuminance is the density of luminous lux on a surface expressed in either footcandles (lumens/ft²) or lux (lx) (lux = 0.0929 fc).

Luminance (or photometric brightness). Luminance is the luminous intensity of a surface in a given direction per unit of projected area of the surfaces, expressed in candelas per unit area or in lumens per unit area.

Reflectance. Reflectance is the ratio of the light reflected from a surface to that incident upon it. Reflection may be of several types, the most common being specular, diffuse, spread, and mixed.

Glare. Glare is any brightness that causes discomfort, interference with vision, or eye fatigue.

TABLE 107.6 Room Position Multipliers

	A	B	C	D	E	F		A	B	C	D	E	F	
	Room Cavity Ratio = 1							Room Cavity Ratio = 6						
0	.24	.42	.47	.48	.44	.48	0	.20	.23	.26	.28	.29	.30	
1	.42	.74	.81	.83	.84	.84	1	.23	.26	.29	.31	.33	.36	
2	.47	.81	.90	.92	.93	.93	2	.26	.29	.35	.37	.38	.40	
3	.48	.83	.92	.94	.95	.95	3	.28	.31	.37	.39	.41	.43	
4	.48	.84	.93	.95	.96	.97	4	.29	.33	.38	.41	.43	.45	
5	.48	.84	.93	.95	.97	.97	5	.30	.36	.40	.43	.45	.47	
	Room Cavity Ratio = 2							Room Cavity Ratio = 7						
0	.24	.36	.42	.44	.46	.46	0	.18	.21	.23	.25	.26	.27	
1	.36	.51	.60	.63	.66	.68	1	.21	.23	.26	.28	.29	.30	
2	.42	.60	.68	.72	.78	.83	2	.23	.26	.30	.32	.33	.34	
3	.44	.63	.72	.77	.82	.85	3	.25	.28	.32	.34	.35	.36	
4	.46	.66	.78	.82	.85	.86	4	.26	.29	.33	.35	.37	.37	
5	.46	.68	.83	.85	.86	.87	5	.27	.30	.34	.36	.37	.38	
	Room Cavity Ratio = 3							Room Cavity Ratio = 8						
0	.23	.32	.37	.40	.42	.42	0	.17	.18	.21	.22	.22	.23	
1	.32	.40	.48	.51	.53	.57	1	.18	.20	.23	.25	.26	.26	
2	.37	.48	.58	.61	.64	.67	2	.21	.23	.26	.27	.28	.29	
3	.40	.51	.61	.65	.69	.71	3	.22	.25	.27	.29	.30	.30	
4	.42	.53	.64	.69	.73	.75	4	.22	.26	.28	.30	.31	.32	
5	.42	.57	.67	.71	.75	.77	5	.23	.26	.29	.30	.31	.32	
	Room Cavity Ratio = 4							Room Cavity Ratio = 9						
0	.22	.28	.32	.35	.37	.37	0	.15	.17	.18	.19	.20	.20	
1	.28	.33	.40	.42	.44	.48	1	.17	.18	.20	.21	.22	.23	
2	.32	.40	.48	.50	.52	.57	2	.18	.20	.23	.24	.25	.25	
3	.35	.42	.50	.54	.58	.61	3	.19	.21	.24	.25	.26	.26	
4	.37	.44	.52	.58	.62	.64	4	.20	.22	.25	.26	.26	.27	
5	.37	.48	.57	.61	.64	.66	5	.20	.23	.25	.26	.27	.27	
	Room Cavity Ratio = 5							Room Cavity Ratio = 10						
0	.21	.25	.28	.31	.33	.33	0	.14	.16	.16	.17	.18	.18	
1	.25	.29	.33	.36	.38	.42	1	.16	.17	.18	.19	.19	.20	
2	.28	.33	.40	.42	.44	.48	2	.16	.18	.19	.21	.22	.22	
3	.31	.36	.42	.46	.49	.52	3	.17	.19	.21	.22	.23	.23	
4	.33	.38	.44	.49	.52	.54	4	.18	.19	.22	.23	.23	.24	
5	.33	.42	.48	.52	.54	.56	5	.18	.20	.22	.23	.24	.25	

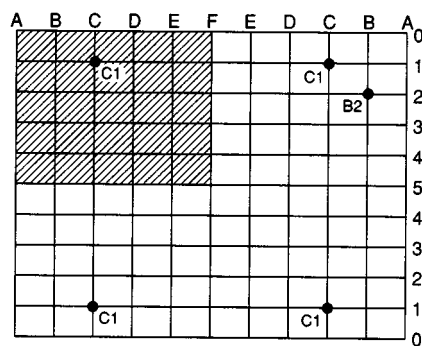


FIGURE 107.3 Grid diagram for locating points on the work plane.

Color Rendering Index (CRI). In 1964 the CIE (Commission Internationale de l'Eclairage) officially adopted the IES procedure for rating lighting sources and developed the current standard by which light sources are rated for their color rendering properties. The CRI is a numerical value for the color comparison of one light source to that of a reference light source.

Color Preference Index (CPI). The CPI is determined by a similar procedure to that used for the CRI. The difference is that CPI recognizes the very real human ingredient of preference. This index is based on individual preference for the coloration of certain identifiable objects, such as complexions, meat, vegetables, fruits, and foliage, to be slightly different than the colors of these objects in daylight. CPI indicates how a source will render color with respect to how we best appreciate and remember that color.

Equivalent Sphere Illumination (ESI). ESI is a means of determining how well a lighting system will provide task visibility in a given situation. ESI may be predicted for many points in a lighting system through the use of any of several available computer programs or measured in an installation with any of several different types of meters.

Visual Comfort Probability (VCP). Discomfort glare is most often produced by direct glare from luminances that are excessively bright. Discomfort glare can also be caused by reflected glare, which should not be confused with **veiling reflections**, which cause a reduction in visual performance rather than discomfort. VCP is based in terms of the percentage of people who will be expected to find the given lighting system acceptable when they are seated in the most undesirable location.

Factors and Remedies

Quality of illumination pertains to the distribution of luminaires in the visual environment. The term is used in a positive sense and implies that all luminaires contribute favorably to visual performance. However, glare, diffusion, reflection, uniformity, color, luminance, and **luminance ratio** all have a significant effect on visibility and the ability to see easily, accurately, and quickly. Industrial installations of poor quality are easily recognized as uncomfortable and possibly hazardous. Some of the factors are discussed in more detail below.

Direct Glare. When glare is caused by the source of lighting within the field of view, whether daylight or electric, it is defined as direct glare. To reduce direct glare, the following suggestions may be useful:

- a. Decrease the brightness of light sources or lighting equipment, or both.
- b. Reduce the area of high luminance causing the glare condition.
- c. Increase the angle between the glare source and the line of vision.
- d. Increase the luminance of the area surrounding the glare source and against which it is seen.

To reduce direct glare, luminaires should be mounted as far above the normal line of sight as possible and should be designed to limit both the luminance and the quality of light emitted in the 45–85 degree zone because such light may interfere with vision. This precaution includes the use of supplementary lighting equipment. There is such a wide divergence of tasks and environmental conditions that it may not be possible to recommend a degree of quality satisfactory to all needs. In production areas, luminaires within the normal field of view should be shielded to at least 25 degrees from the horizontal, preferably to 45 degrees.

Reflected Glare. Reflected glare is caused by the reflection of high-luminance light sources from shiny surfaces. In the manufacturing area, this may be a particularly serious problem where critical seeing is involved with highly polished sheet metal, vernier scales, and machined metal surfaces. There are several ways to minimize or eliminate reflected glare:

- a. Use a light source of low luminance, consistent with the type of work in process and the surroundings.
- b. If the luminance of the light source cannot be reduced to a desirable level, it may be possible to orient the work so that reflections are not directed in the normal line of vision.
- c. Increasing the level of illumination by increasing the number of sources will reduce the effect of reflected glare by reducing the proportion of illumination provided on the task by sources located in positions causing reflections.

TABLE 107.7 Recommended Maximum Luminance Ratios for Industrial Areas

	Environmental Classification		
	A	B	C
(1) Between tasks and adjacent darker surroundings	3 to 1	3 to 1	5 to 1
(2) Between tasks and adjacent lighter surroundings	1 to 3	1 to 3	1 to 5
(3) Between tasks and more remote darker surfaces	10 to 1	20 to 1	*
(4) Between tasks and more remote lighter surfaces	1 to 10	1 to 20	*
(5) Between luminaires (or windows, skylights, etc.) and surfaces adjacent to them	20 to 1	*	*
(6) Anywhere within normal field of view	40 to 1	*	*

*Luminance ratio control not practical.

A—Interior areas where reflectances of entire space can be controlled in line with recommendations for optimum seeing conditions.

B—Areas where reflectances of immediate work area can be controlled, but control of remote surround is limited.

C—Areas (indoor and outdoor) where it is completely impractical to control reflectances and difficult to alter environmental conditions.

Source: IES Lighting Handbook, Application Volume.

- d. In special cases, it may be practical to reduce the specular reflection by changing the specular character of the offending surface.

Distribution, Reflection, and Shadows. Uniform horizontal illuminance (maximum and minimum not more than one-sixth above or below the average level) is usually desirable for industrial interiors to permit flexible arrangements of operations and equipment and to assure more uniform luminance in the entire area.

Reflections of light sources in the task can be useful provided that the reflection does not create reflected glare. In the machining and inspection of small metal parts, reflections can indicate faults in contours, make scribe marks more visible, and so on.

Shadows from the general illumination systems can be desirable for accenting the depth and forms of various objects, but harsh shadows should be avoided. Shadows are softer and less pronounced when large diffusing luminaires are used or the object is illuminated from many sources. Clearly defined shadows are distinct aids in some specialized operations, such as engraving on polished surfaces, some type of bench layout work, or certain textile inspections. This type of shadow effect can best be obtained by supplementary directional lighting combined with ample diffused general illumination.

Luminance and Luminance Ratios. The ability to see details depends on the contrast between the detail and its background. The greater the contrast difference in luminance, the more readily the seeing task is performed. The eye functions most comfortably and efficiently when the luminance within the remainder of the environment is relatively uniform. In manufacturing, there are many areas where it is not practical to achieve the same luminance relationships as easily as in offices. **Table 107.7** is shown as a practical guide to recommended maximum luminance ratios for industrial areas. To achieve the recommended luminance relationships, it is necessary to select the reflectances of all the finishes of the room surfaces and equipment as well as control of the luminance distribution of the lighting equipment. **Table 107.8** lists the recommended reflectance values for industrial interiors and equipment. High-reflectance surfaces are desirable to provide the recommended luminance relationships and high utilization of light.

Color Quality of Light. In general, for seeing tasks industrial areas, there appears to be no effect upon visual acuity by variation in color of light. However, where color discrimination or color matching is a part of the work process, such as in the printing and textile industries, the color of light should be carefully selected. Color always has an effect on the appearance of the workplace and on the complexions of people. The illuminating system and the decorative scheme should be properly coordinated.

TABLE 107.8 Recommended Reflectance Values for Industrial Interiors and Equipment

Surfaces	Reflectance ¹ (%)
Ceiling	80 to 90
Walls	40 to 60
Desk and bench tops, machines and equipment	25 to 45
Floors	not less than 20

¹Reflectance should be maintained as near as practical to recommended values.

Source: IES Lighting Handbook, Application Volume.

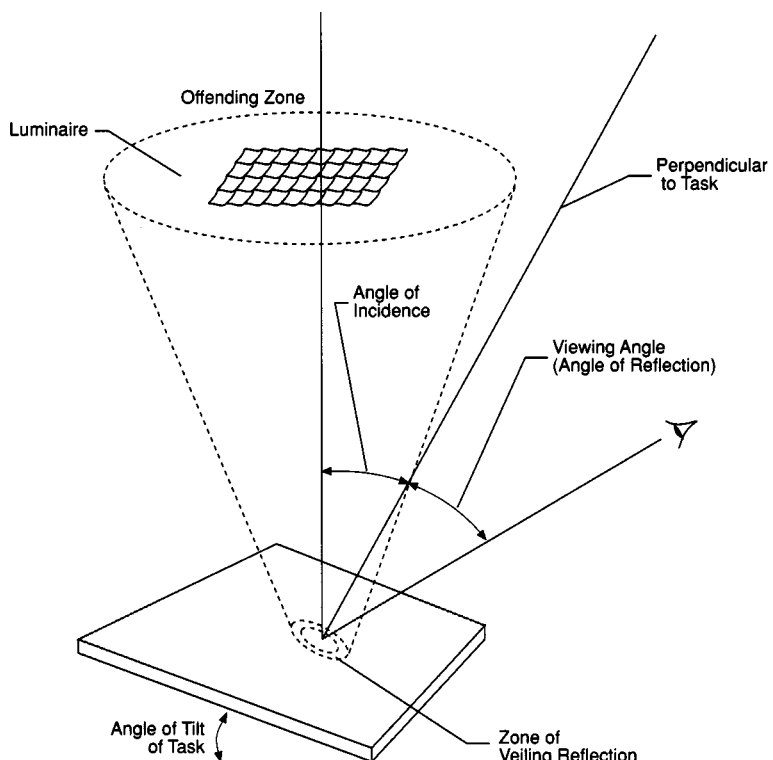


FIGURE 107.4 Diagram showing “offending zone” and zone of veiling reflection.

Veiling Reflections. Figure 107.4 shows that light would reflect into the eyes of the viewer from the “offending zone” and defines the zone of veiling reflection. Veiling reflection would diminish visibility, but the viewer would be unaware of it. The **contrast rendition factor (CRF)** can be applied as a measure of the amount of veiling reflection.

Another important factor is the **lighting effectiveness factor (LEF)**. An overall lighting system efficiency factor considers both the quality of light as reference to equivalent sphere illumination and the effects of veiling reflections. Light patterns such as “batwing” can help solve veiling reflection problems. Figure 107.5 shows the light distribution curve of a typical batwing luminaire.

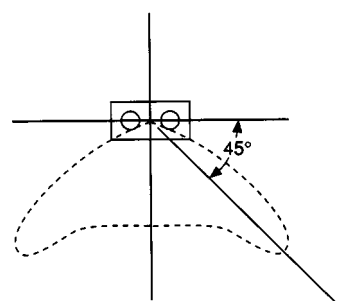


FIGURE 107.5 A typical “batwing” light distribution.

Daylighting

The daylight contribution should be carefully evaluated and should always be coordinated with a planned electric lighting system.

Fenestration. **Fenestration** has at least three useful purposes in industrial buildings:

- a. For the admission, control, and distribution of daylight.
- b. For a distant focus for the eyes, which relaxes the eye muscles.
- c. To eliminate the dissatisfaction many people experience in completely closed-in areas.

An adequate electric lighting system should always be provided because of the wide variation in daylight.

Building Orientation. All fenestration should be equipped with control device appropriate to any luminance problems. Special attention should be given to glare control latitudes where fenestration frequently receives direct sunlight. Diffuse-glaring fixed or adjustable louvers are some of the control means that may be applied.

For an industrial building, windows in the sidewalls admit daylight and natural ventilation and afford occupants a view out. However, their uncontrolled luminance may be a problem. There are many control means to make daylight useful to workers' seeing tasks, resulting in energy savings as the ultimate goal.

107.3 System Components

Light Sources

Incandescent

- a. Recent technology made possible a line of energy-saving incandescent lamps that use the rare gas krypton as a fill gas.
- b. Reflector (R) lamps offer better utilization of the light provided by the lamp compared to a nonreflector type. In this family, there are R lamps, PAR (parabolic aluminized reflector) lamps, and a newer line ER (elliptical reflector) lamps which allow reduction of 50% or more in energy consumption.
- c. Infrared Halogen (IR)—PAR lamps combine both the infrared heat-reflection technology and the regenerative halogen cleaning cycle to provide a dramatic increase in lamp efficacy (4% reduction in energy consumption). Available in 30, 60, and 100 W.

Fluorescent

- a. Energy-efficient lamps are now available in all popular sizes and colors for most applications. Limitations of energy-saving reduced-wattage lamps are:
 - Ambient temperature must be above 60°F.
 - Used on high p.f. fluorescent ballasts only.
 - Not to be used where drafts of cold air are directed onto the lamp.
- b. Typical energy savings are 6 W per lamp for the popular 4-ft 40-W replacement and 15 W per lamp for the 8-ft slimline 75-W replacement.
- c. Compact fluorescent lamps are gaining popularity because they are energy efficient, fit into a small enclosed housing, and can be adapted for incandescent socket use.
- d. Virtually all compact fluorescent lamps use the "rare earth" phosphors for good color rendition and lumen maintenance characteristics.
- e. Utilizing advanced phosphor technology with the optimization of bulb diameter, 40-W lamps are now available that can be retrofitted in a F40 preheat or rapid-start circuit. The new lamp, which could save energy and improve color rendition requirement, has been legislated.
- f. Refer to [Tables 107.9](#) and [107.11](#) for the latest energy efficient lamps.

High-Intensity Discharge (HID)

Today HID lamps include mercury vapor, metal halide, high-pressure sodium, and low-pressure sodium lamps. Metal halide lamps offer the best opportunity from a color acceptability point of view. High-pressure sodium

lamps offer the highest luminous efficacy in an environment where color distinction is not critical. Since HID lamps have had very few problems in application, they are likely to experience further development in the coming years.

Ballasts

Fluorescent. Electronic ballasts are now available for the F40T12, the slimline, the new T8 lamps, and other energy-saving fluorescent lamps on both 120- and 277-V circuits. Using high-frequency ballasts, the efficacy can be raised by nearly 12%. Although electronic ballasts cost more than the standard core-coil ballasts, operating factors should reflect an appreciable reduction in life-cycle cost for a lighting system. There are two types of dimming ballasts: core and electronic. High-frequency ballasts can readily be used to dim fluorescent lamps over a wide range of light level. All external control wiring is low voltage or fiber-optic wiring.

A recent study indicates that 2 F40T12 lamps operated on an electronic ballast will attain an efficacy of 75–80 LPW versus 62 LPW for the same lamps if operated on a standard core-coil type ballast. With the dimmable electronically ballasted system, energy savings can be as high as 40% with respect to a core ballasted system.

High-Intensity Discharge. The choice of a ballast depends on economic considerations versus performance. A mercury lamp will operate from metal halide ballast, but the converse is not always true.

There are several different types of ballasts for high-pressure sodium lamps:

- a. Reactor or lag ballast—Inexpensive, low power losses, and small in size.
- b. Lead ballast —Fairly good regulation for both line and lamp voltage variation.
- c. Magnetic regulated ballast—Provides best voltage regulation with change of either input voltage or lamp voltage. It is the most costly and has the greatest wattage loss.
- d. Electronic ballast—Maintains a steady constant wattage output with changes in the source impedance as well as excellent regulation. During the life of a high-pressure sodium lamp, it can save 20% more energy by maintaining a constant wattage output in addition to the 15% intrinsic energy savings compared to an equivalent core-coil ballast.

Luminaires

Types of Industrial Luminaires. Selection of a specific type for an installation requires consideration of many factors: candlepower distribution, efficiency, shielding and brightness control, mounting height, lumen maintenance characteristics, mechanical construction, and environmental suitability for use in normal, hazardous, or special areas. In general there are five types in accordance with CIE classifications, namely, direct type, semi-direct type, direct-indirect type, semi-indirect type, and indirect type.

Figure 107.6 shows luminaire types with the percentage of total luminaire output emitted above and below horizontal.

Supplementary Luminaire Types. There are five major types based on the candlepower distribution and luminance:

- Type S-I—directional
- Type S-II—spread, high luminance
- Type S-III—spread, moderate luminance
- Type S- IV—uniform luminance
- Type S-V—uniform luminance with pattern

High-Pressure Sodium. Proper luminaire design is the key to lighting efficiency. Newly developed luminaires use prismatic glass reflectors that are especially made for high-pressure sodium lamps. In addition to achieving maximum light utilization, they redirect the intense light source with excellent light cutoff and high-angle brightness control. Luminaire manufacturers recommend aluminum reflectors for all general-purpose industrial applications and glass-coated reflectors where maintenance practice is compatible with servicing glass.

Fluorescent. A new trend for lighting new buildings is the increased use of the reflectorized fixtures. This trend may be traced to an increase in the number of state and national lighting efficiency standards in recent

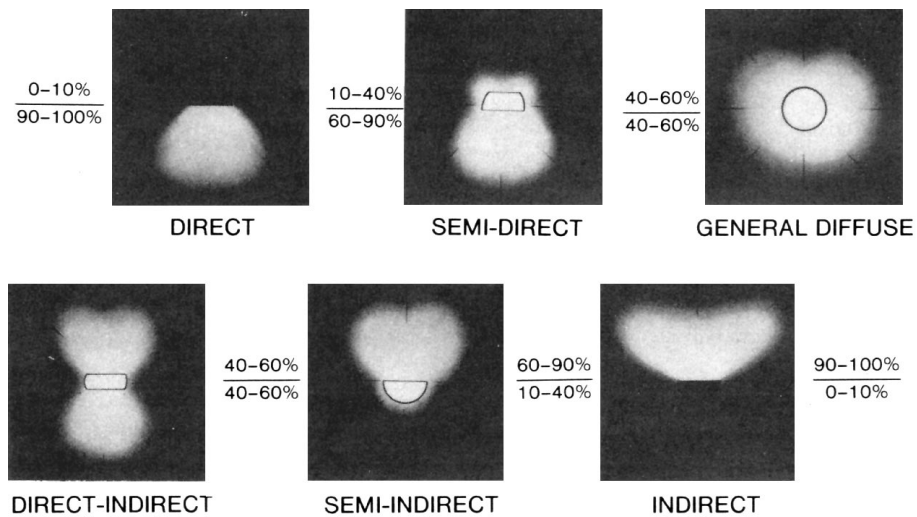


FIGURE 107.6 General lighting luminaire classifications.

years. However, these fixtures can create a “teardrop-like” distribution that may eliminate glare on a computer screen, but also reduces light to other areas.

107.4 Applications

Types of Industrial Illuminating Systems

Factory Illumination for Visual Tasks. The prime requirement for industrial illumination is to facilitate the performance of visual tasks through high-quality illumination. There are three types of lighting used in industrial areas.

- *General Lighting.* It should be designed to provide the desired level of illumination uniformly over the entire area. The variation of light level from point to point within the area should be within 17% of the selected level. A good general lighting system makes it possible to change the location of machinery without rearranging the lighting and also permits full utilization of floor space.
- *Localized General Lighting.* Within a general area there may be a few areas where tasks performed require a greater quantity of light and a different quality of light. When applied, care must be exercised to eliminate direct or reflected glare from the task and from other workers.
- *Supplementary Lighting.* Supplementary lighting is specified for different seeing tasks that require a specific amount or quality of light not readily obtained by standard general lighting methods. Supplementary lighting is a valuable industrial lighting tool. Typical problems arise where work is shielded from the general lighting system by an obstruction or its brightness is otherwise lowered where low contrast, such as scribe marks on steel, may lead to visual errors, and where the product moves too rapidly to be seen clearly by the unaided eye. To attain a good balance, it is important to coordinate the design of supplementary and general lighting with great care.

Security Lighting. Security lighting pertains to the lighting of building exterior and surrounding areas out to and including the boundaries of the property. Security lighting contributes to a sense of personal security and to the protection of property. It may be accomplished through:

- Surveillance lighting to detect and observe intruders.
- Protective lighting to discourage or deter attempts at entrance, vandalism, etc.
- Lighting for safety to permit safe movement of guards and other authorized persons.

Emergency Lighting. Emergency lighting is provided for use when the power supply for the normal lighting fails to ensure that escape routes can be effectively identified and used. Standby lighting is that part of emergency lighting that is sometimes provided to enable normal activities to continue.

The following are recommended minimum illumination requirements for exit signs and egress route:

- *Internally illuminated signs.* An illuminance of 54 lux (5 fc) on the face of the sign is usually specified.
- *Externally illuminated exit sign.* NFPA 101 requires 54 lux (5 fc) on the face of the sign.
- *Egress route.* The horizontal illuminance of any escape route should not be less than 1% of the average provided by the normal lighting, with a minimum average of 5 lux (0.5 fc) at floor level.
- *Location of egress luminaires.* A luminaire should be provided for each exit door and emergency exit door to provide sufficient light to a level of 30 lux (3 fc).

Summaries. In large industrial areas, all these lighting systems may be used. In small areas, localized general lighting may also serve as a substitute for general lighting. In this case, additional supplementary lighting may be required to increase the quantity or improve the quality of the illumination. Many factors must be considered in selecting a lighting system. It is not feasible to recommend one or two systems for all conditions. Because of the relationship of ceiling height to light utilization, most industrial applications call for either direct or semi-direct lighting systems.

Selection of the Equipment

In the selection of equipment, light sources, and luminaires, many variables must be considered. As with any list of variables, it is necessary for purpose of comparison to hold some factors constant. In industrial illumination that factor is usually mounting height and location.

High-Bay Areas. The work generally presents visual tasks that are not difficult because of large machinery and other objects. Illuminance levels for high-bay areas generally range from 50 to 150 fc, although more and more areas are being lighted with 200 and 300 fc. At a high mounting height, it is possible to obtain uniform illumination by using a few high-wattage sources rather than a larger number of low-wattage sources. For luminaires with medium and narrow distribution, greater mounting height or closer spacing is ordinarily required for uniform general illumination.

Regardless of mounting height, wide distribution luminaires are well suited for use in areas that are wide in respect to mounting height. Large machinery and objects tend to cut off light and cast shadows. Since this makes it difficult to see important vertical and angular surfaces, broad light distribution is essential.

High-intensity discharge or fluorescent luminaires for high-bay lighting may be enclosed, ventilated open, or nonventilated open. Enclosed luminaires are usually of a heavy-duty type with a gasketed glass cover to protect the reflector and light source from collection of dirt. The initial luminaire efficiency is lower and the equipment is more costly. Ventilated-open luminaires have largely replaced the nonventilated type.

As far as choices of lamps are concerned, metal halide and HPS are preferred over the mercury type. The use of fluorescent lamps in high-bay areas is limited. Only where the area proportions are such that the room cavity ratios are in the range of 1 to 3 may fluorescent lamps be acceptable. Only high or extra high output fluorescent in 8-ft sizes are recommended.

Medium- and Low-Bay Areas. Seeing tasks in medium- and low-bay areas are usually more difficult than those encountered in the high-bay areas. Increasing the size and reducing the brightness of the luminaires will improve visual comfort and will improve the visibility of specular objects. It may not improve the visibility of diffuse three-dimensional objects.

Luminaires used for general lighting in medium-bay areas are nearly always of the direct or semi-direct type, either fluorescent or wide distribution HID. They may be the ventilated or nonventilated type and the lamps may be shielded by louvers, baffles, or other devices. For lower mounting, the trend is toward the semi-direct type.

Some of the visual tasks involve specular or semi-specular objects, for which optimum lighting might be an indirect system. The quality of fluorescent sources, with their broad distribution of light, makes them a prime selection for medium- and low-bay lighting. When the proper quality control can be attained, low-wattage HID sources are finding an increasing number of low-bay applications.

107.5 System Energy Efficiency Considerations

Energy-Saving Lighting Techniques

Fluorescent Systems Considerations. Fluorescent lamps are sensitive to ambient temperatures. By using reduced wattage lamps or low-loss ballasts, less heat will be generated and the operating temperature point of the lamp will probably change. The critical area is the coldest spot on the bulb surface. Most fluorescent lamps will peak in light output at around a 100°F cold-spot temperature. For enclosed luminaire types that ordinarily operate the lamp at higher temperature, replacing standard lamps with high-efficacy, reduced wattage lamps may result in a net increase in luminaire output even though the reduced wattage lamps are rated for less output than are standard lamps.

Using Daylight. Daylight should be dealt with by first analyzing it and then establishing a design technique to integrate it with the electric lighting system. Daylight may be adequate in quantity and quality to reduce the electric lighting load and result in energy conservation. Poor quality of daylight may lead to discomfort and a loss in visibility that may result in a decrease in human performance and productivity.

Daylighting Design from Windows. The longhand design procedure involves two steps:

- Determine the quantity of illumination coming to the window surface.
- Use that quantity to determine the daylight contribution to the interior part of the space.

Once the contribution of illumination to the window surface has been calculated, two longhand methods are available to determine the illumination contribution to the space. The first method is to follow the point-by-point procedure, which makes two assumptions: (1) interreflected component is ignored and (2) the window is a uniform diffuse emitter. The second method is a lumen method that calculates illumination values at three points defined as the maximum, midway, and minimum. This method includes both the direct and interreflected components of illumination.

Task-Ambient Lighting. This is a particular form of nonuniform illumination that combines task illuminance and ambient illuminance. One advantage is improved energy efficiency. The task component of task-ambient lighting may take two forms: (1) furniture-mounted lighting built into a workstation or (2) floor-mounted fixtures that can be placed adjacent to a desk. The ambient lighting component may be supplied in two ways: (1) conventional luminaires on the ceiling or (2) indirect fixtures utilizing HID or fluorescent lamps with the output directed to the ceiling and adjacent walls. For ceiling-mounted troffers used for ambient lighting, a plug-in system of wiring should be considered so that luminaires can be relocated as task locations change.

Lighting Controls

In order to save energy, it is essential that minimum acceptable lighting levels be used during off-hours, cleaning periods, and for other nonpeak periods as is practical. The ultimate system of control would be to remotely control every fixture and to program the mode of operation, but this is hardly possible. Solid-state dimmers are available, or ballasts can be circuited in separate groupings. Solid-state controls are available for dimming entire areas of ballasted lights, but special ballasts are required and the controls could be expensive.

Manual control of a lighting system is often the least expensive, but also the least effective alternative. Automatic controls vary from a simple timer to a sophisticated computer system. [Figure 107.7](#) shows a typical programmable lighting control scheme. A price versus benefit cost analysis will be required for each installation. The system should be programmed for normal operation and have a local manual override. A good convenient practice is to have lights switched in distributed groups so that areas can be lighted or darkened as conditions change.

Lighting and Energy Standards

In 1976, the Energy Research and Development Association (ERDA) contracted with the National Conference of States on Building Codes and Standards (NCSBCS) to codify ASHRAE 90-75. The resulting document was

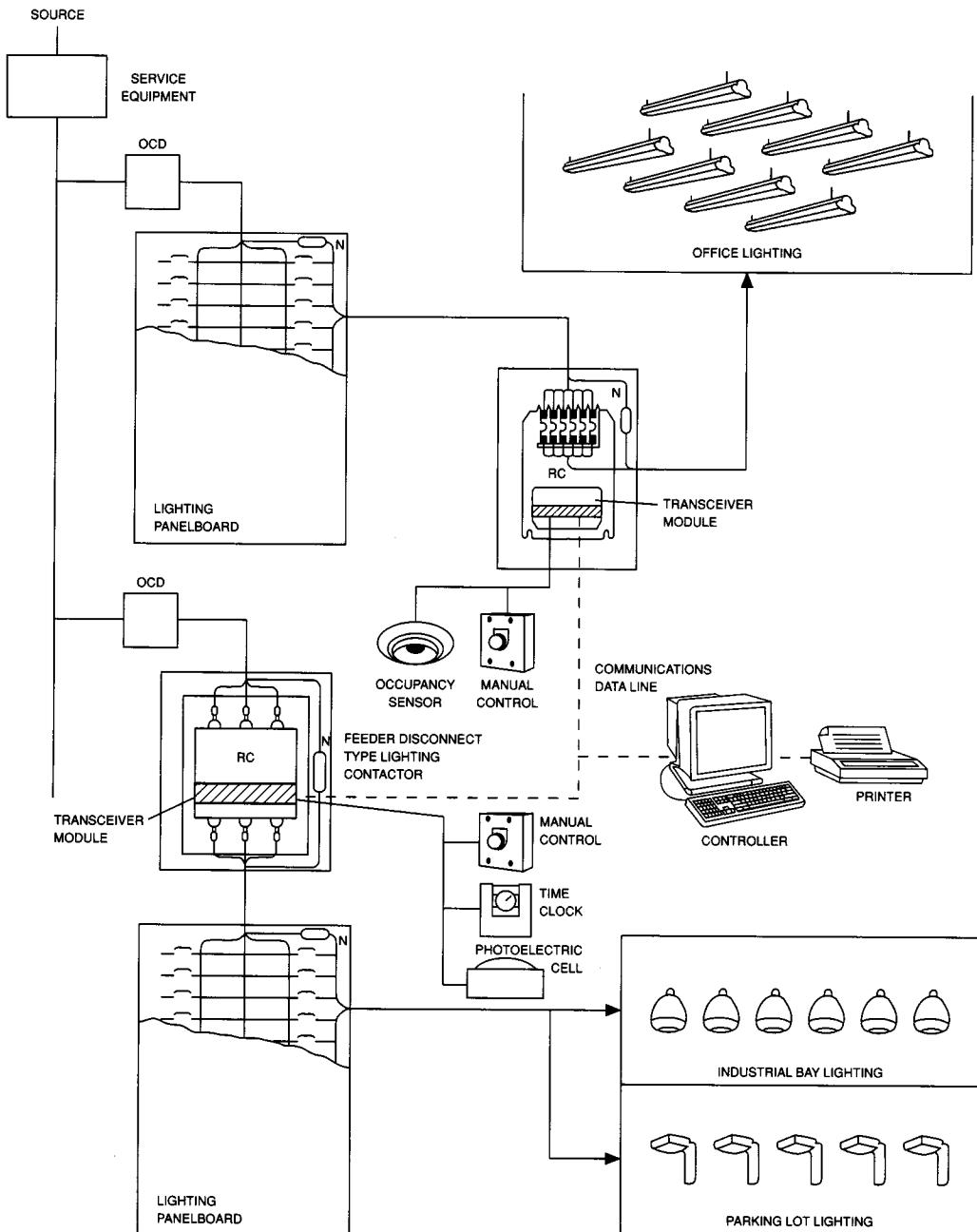


FIGURE 107.7 Programmable lighting control scheme.

called "The Model Code for Energy Conservation in New Buildings." The model code has been adopted by a number of states to satisfy the requirements of Public Laws 94-163 and 94-385.

There have been several revisions on the ANSI/ASHRAE/IES 90-75 since 1976. All were included in the lighting portion of ANSI/ASHRAE/IES 90A-1980, "Energy Conservation in New Building Design," and in EMS-1981, "IES Recommended Lighting Power Budget Determination Procedure."

ASHRAE/IES 90.1-1989, "Energy Efficient Design of New Buildings Except New Low-Rise Residential Buildings," is the third generation document on building energy efficiency since the first publication in 1975. This standard is intended to be a voluntary standard which can be adopted by building officials for state and local codes.

LIGHTING: THE NEXT 10 YEARS

Many exciting developments are occurring in the lighting industry. However, one of the greatest challenges is the development of a replacement light source for the common cathode ray tube (CRT) found in televisions and other applications.

CRTs have gradually expanded from our primary information sources, televisions and computers, into scientific instrumentation, cars, and automatic teller machines. However, the inherent shortcomings of this technology are limiting the further development of existing and new applications that require display technology.

CRTs produce few lumens for the power they consume and are inherently large and heavy. Their many weaknesses are compounded in the area of big screen displays. The desire to view ever larger and higher resolution images is pushing the CRT beyond its practical limits. New lighting technologies applied to flat panel displays and projection systems could change the consumer television market if certain barriers are overcome.

One approach has been to adopt large area LCDs (which pose a significant engineering challenge) as the primary imaging device. However, these devices do not inherently emit light and would be useless in the dark without backlights. The light source of choice for this approach has been cold cathode fluorescent lamps, which are commonly applied in today's laptop computers.

We can expect to see unique lamp shapes and ingenious reflector systems developed to illuminate the LCD uniformly, without adding significantly to the overall depth of the display system. There is also a lot of work in the development of electroluminescent panels as an alternative to fluorescent lamps, although these devices present color difficulties as well as comparatively low efficacies.

Large-area LED image displays have already been fabricated since blue LEDs emerged in the marketplace. An array of red, green, and blue LEDs are mounted on a panel and individually addressed to generate all colors, including white. This approach will be redefined in the coming decade, but faces a number of challenges.

TABLE 107.9 The Proposed Efficiency Standards for Fluorescent Lamps

Lamp Type	Nominal Lamp Wattage	Minimum Average CRI	Minimum Average Lamp Efficacy
F40	>35 W	69	75
F40	≤35 W	45	75
F40/U	>35 W	69	68
F40/U	≤35 W	45	64
F96T12	>65 W	69	80
F96T12	≤65 W	45	80
F96T12/HO	>100 W	69	80
F96T12/HO	≤100 W	45	80

Note: The above excludes lamps designed for plant growth, cold temperature service, reflectorized/aperture, impact resistance, reprographic service, colored lighting, ultraviolet, and lamps with CRI of more than 82.

Another approach involves large-area plasma panels that are self-luminescent due to gas discharges. With this technology, the brightness improves considerably over that available from a CRT. Brilliant, high-resolution images have been achieved in medium screen sizes, but cost remains a problem and there is still the challenge of expanding the technology to even larger screen sizes.

The approach that is most likely to succeed during the next decade is the use of projection technology. These systems are fundamentally similar to slide or movie projectors where the film has been replaced by either a transmissive or reflective imaging device that provides a continuously variable image illuminated and projected onto a screen. The image can be front projected or rear projected.

The most pressing challenge remains: development of an illumination source that can provide a brighter image with better colors than CRT technology. If this can be achieved, other benefits will flow from the technology, with the potential to drastically reduce power consumption as well as cabinet size, weight, and cost. Furthermore, the inherent digital nature of the imaging panels would make the resulting product data compatible for the much touted merging of the Internet and television programming.

High-resolution rear projection televisions using lamps as the illumination source are already available in Japan from Sony and Sharp. We can expect to see this type of product in the U.S. market this year. However, the overall product cost, lamp life, and screen brightness all need improvement before this technology moves into the mainstream.

The technical challenge for the lighting industry is to produce a miniature point source that delivers high efficacy, high color temperature, and long lifetime. The challenge for the immediate future is to push the arc gap even smaller while extending the lamp life to be comparable to today's CRTs and maintaining lumen output and good color temperature. Furthermore, all these requirements have to be met at a very low cost.

The rewards for the successful manufacturer are immense, considering the size of the market, not to mention the spin-off markets that could pick up on this technology. During the next decade, we are sure to see a lot of exciting developments in this area, which will ultimately affect our daily activities. (Adapted from Ian Edwards, "Fundamentals of Lighting", *Optics & Photonics News*, Optical Society of America, 7(11), 20, 1996. With permission.)

Energy Policy Act

On October 25, 1992, the Energy Policy Act was signed into law by the President.

Among the many provisions, the act establishes energy efficiency standards for HVAC, lighting, and motor equipment; encourages establishment of a national window energy-efficiency rating system; and encourages state regulators to pursue demand-side-management (DSM) programs.

Under the bill, lighting manufacturers will have 3 years to stop making F96T12 and F96T12/HO 8 ft fluorescent lamps and some types of incandescent reflectors. Standard F40 lamps except in the SP and SPX or equivalent types of high color rendering lamps would also fade away. General service incandescent lamps to be axed would include those from 30 to 100 W, in 115 to 130 V ratings, having medium screw bases, of both reflector and PAR types, having a diameter larger than 2^{3/4} in.

There are no immediate regulations impacting HID lamps. Within 18 months of the legislation's enactment, the Department of Energy (DOE) will determine the HID types for which standards could possibly save energy and publish testing requirements for these lamps.

As far as the general service lamps are concerned, the most common incandescent lamps — 40, 60, 75, 100, and 150 W — are not covered by an efficiency standard because there is no suitable method to ensure energy savings. These types, however, are covered by another provision of the law, namely the energy efficiency labeling standards.

TABLE 107.10 The Proposed Efficiency Standards for Incandescent Reflector Lamps

Nominal Lamp Wattage	Minimum Average Lamp Efficacy (LPW)
40–50	10.5
51–66	11.0
67–85	12.5
86–115	14.0
116–155	14.5

Note: The above excludes miniature, decorative, traffic signal, marine, mine, stage/studio, railway, colored lamps, and other special application types.

TABLE 107.11 1992 Energy Policy Act — Replacement Lamps

Present Type	W	Acceptable W	W	Improved Type	W	Max. Savings	W
F96T12/CW	75	F96T12/CW/SS	60	F96T12/D41/SS	60	F096T8/741	59
F96T12/WW	75	F96T12/WW/SS	60	F96T12/D30/SS	60	F096T8/730	59

Effective April 28, 1994, the Federal Trade Commission (FTC) must provide manufacturers with labeling requirements for all lamps covered: fluorescent, incandescent, and reflector incandescent. Though not yet defined, the proposals include: an energy rating for the lamps, probably LPW (lumens per watt), and energy cost per year to operate the lamp. The energy efficiency label will then allow side-by-side comparison of two different lamp types, thus enabling consumers to make a more intelligent choice of lamps; taking into account not just the purchase price, but also the operating cost. Manufacturers must begin applying labels by April 28, 1995. [Table 107.9](#) shows the proposed efficiency standards for the fluorescent lamps, and [Table 107.10](#) shows the proposed efficiency standards for incandescent reflector lamps.

There is no requirement to replace all existing lamps in any installation. However, as these lamps burn out, the replacement must meet the new standards.

Replacement for popular fluorescent types includes reduced-wattage energy saving types. These lamps will meet the color and efficiency standards, as will the full wattage triphosphor lamps having a CRI over 69. [Table 107.11](#) shows some types of replacement lamps. On the incandescent side, replacements for the standard incandescent spot and flood lamps will be lower wattage halogen type reflector lamps which do meet the LPW requirements. The halogen and halogen/infrared types of reflector lamps will remain the only type of such lamps on the market. ER and BR types, those intended for rough and vibration service will also be excluded here.

There is also a provision for lighting fixture manufacturers to come up with voluntary luminaire efficiency standards. If these standards are found to be inadequate, the DOE will come up with the mandatory efficiency standards.

The new Energy Policy Act is all-encompassing. It promises to change forever the way industries produce, distribute, and utilize the valued energy resources. The end result should be increased energy security, decreased environmental emissions, and cleaner air and water for all humankind.

Defining Terms

Candlepower distribution: A curve, generally polar, representing the variation of luminous intensity of a lamp or luminaire in a plane through the light center.

Cavity ratio (CR): A number indicating cavity proportions calculated from length, width, and height. It is further defined into ceiling cavity ratio, floor cavity ratio, and room cavity ratio.

Coefficient of utilization (CU): The ratio of the lumens reaching the working plane to the total lumens generated by the lamp. This factor takes into account the efficiency and distribution of the luminaire, its mounting height, the room proportions, and the reflectances of the walls, ceiling, and floor.

Color preference index (CPI): Measure appraising a light source for appreciative viewing of colored objects or for promoting an optimistic viewpoint by flattery.

Color rendering index (CRI): Measure of the degree of color shift objects undergo when illuminated by the light source as compared with the color of those same objects when illuminated by a reference source of comparable color temperature.

Contrast: The relationship between the luminances of an object and its immediate background. It is equal to $(L_1 - L_2)/L_1$ where L_1 and L_2 are the luminances of the background and object. The ratio $\Delta L/L_1$ is also known as Weber's fraction where $\Delta L = L_1 - L_2$.

Contrast rendition factor (CRF): The ratio of visual task contrast with a given lighting environment to the contrast with sphere illumination.

Equivalent sphere illumination (ESI): The level of sphere illumination which would produce task visibility equivalent to that produced by a specific lighting environment.

Fenestration: Any opening or arrangement of opening (normally filled with media for control) for the admission of daylight.

Footcandle: The unit of illuminance when the foot is taken as the unit of length. It is the illuminance on a surface one square foot in area on which there is a uniformly distributed flux of one lumen.

Illuminance: The density of luminous flux on a surface expressed in either footcandles (lumens/ft²) or lux (lx). (lux = 0.0929 fc)

Lighting effectiveness factor (LEF): The ratio of equivalent sphere illumination to ordinary measured or calculated illumination.

Light loss factor (LLF): The ratio of the illumination when it reaches its lowest level at the task just before corrective action is taken, to the initial level if none of the contributing loss factors were considered.

Luminance ratio: The ratio between the luminance of two areas in the visual field.

Veiling reflection: Regular reflections superimposed upon diffuse reflections from an object that partially or total obscure the details to be seen by reducing the contrast.

Visual comfort probability (VCP): This rating is based in terms of the percentage of people who will be expected to find the given lighting system acceptable when they are seated in most undesirable locations.

Related Topics

3.1 Voltage and Current Laws • 3.4 Power and Energy

References

- ANSI/IES, "Recommended Practices for Industrial Lighting," Illuminating Engineering Society, New York, 1991.
- K. Chen, *Energy Effective Industrial Illuminating Systems*, Lilburn, Ga.: The Fairmont Press, 1994.
- K. Chen, *Industrial Power Distribution and Illuminating Systems*, New York: Marcel Dekker, 1990.
- K. Chen, "New concepts in interior lighting design," *IEEE Trans. Industry Applications*, Sept./ Oct. 1984.
- IES Lighting Handbook, Application Volume*, Illuminating Engineering Society, New York, 1993.
- Lighting Handbook*, Westinghouse Electric Corporation, Bloomfield, N.J., 1976.

Further Information

L. Watson, *Lighting Design Handbook*, New York.: McGraw-Hill, 1991. It focuses on the art and process of lighting design and provides invaluable, up-to-date technical details on equipment, color use, scenic projection, lasers, holograms, fiber-optics, computers, and energy conservation.

C.L. Robbins, *Daylighting—Design and Analysis*, New York: Van Nostrand Reinhold, 1986. Organized to correspond to the building design process, the book contains data for calculation of annual cost and energy savings as well as many case studies.

Software—Lighting Calculations by Zonal Cavity Method, Orloff Computer Services, 1820 E. Garry Ave., Santa Ana, CA 92705.

Schmalzel, J.L.. "Instruments"
The Electrical Engineering Handbook
Ed. Richard C. Dorf
Boca Raton: CRC Press LLC, 2000

108

Instruments

- 108.1 Introduction
- 108.2 Physical Variables
- 108.3 Transducers
- 108.4 Instrument Elements
- 108.5 Instrumentation System
- 108.6 Modeling Elements of an Instrumentation System
- 108.7 Summary of Noise Reduction Techniques
- 108.8 Personal Computer-Based Instruments
- 108.9 Modeling PC-Based Instruments
- 108.10 The Effects of Sampling
- 108.11 Other Factors

John L. Schmalzel
Rowan University

108.1 Introduction

Instruments are the means for monitoring or measuring physical variables. The basic elements of an instrumentation application are shown in Fig. 108.1. A physical system produces a *measurand*, $m(t)$, shown as time-varying, which is transformed by a **transducer** into an electrical signal, $s(t)$, that is then processed by an instrument to yield the desired output information variable, $i(t)$. Producing meaningful information from physical variables requires conversion and processing. Electronic instruments require that physical variables be converted to electrical signals through a process of *transduction*, followed by signal *conditioning* and signal *processing* to obtain useful results.

108.2 Physical Variables

The measurand can be one of many physical variables; the type depends on the application. For example, in process control, typical measurands can include pressure, temperature, and flow. Representative physical variables with corresponding units are summarized in Table 108.1.

108.3 Transducers

Transducers convert one form of energy to another. To be useful for an electronic instrument, a transducer must produce an electrical output such as voltage or current to allow required signal conditioning and signal processing steps to be completed. A variety of transducers are available to meet a measurement requirement; some common examples are listed in Table 108.2. Transducers can be compared based on their operating principles, the measurand range, interface design, and reliability. Khazan [1994] gives a complete summary of transducer schemes.

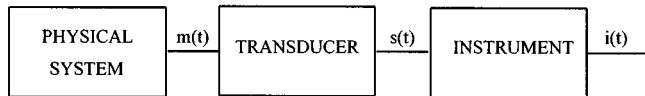


FIGURE 108.1 Generalized block diagram of an instrument applied to a physical measurement.

TABLE 108.1 Representative Physical Variables, Symbols, and Units

Physical Variable	Symbol	SI Units, Abbreviations
Current	I	ampere, A
Energy	E	joule, J
Force	F	newton, N
Flow	Q	volume flow rate, m^3/s
Frequency	f	hertz, Hz
Length	L	meter, m
Mass	m	kilogram, kg
Pressure	P	N/m^2
Power	P	Watt, W
Resistance	R	ohm, Ω
Temperature	T	Kelvin, K
Time	t	second, s
Velocity	V	m/s
Voltage	V	volt, V

TABLE 108.2 Representative Transducers

Measurand	Transducer	Operating Principles
Displacement (Length)	Resistive	Change in resistance, capacitance, or inductance caused by linear or angular displacement of transducer element
	Capacitive	
	Inductive	
Force	Strain gage	Resistance, piezoresistivity
	Thermistor	Resistance
Temperature	Thermocouple	Peltier, seebeck effect
	Diaphragm	Diaphragm motion sensed by a displacement technique.
Pressure	Differential pressure	Pressure drop across restriction
	Turbine	Angular velocity proportional to flow rate
Flow		

108.4 Instrument Elements

Signal conditioning consists of amplification, filtering, limiting, and other operations that prepare the raw instrument input signal for further operations. The signal may be the output of a transducer or it may be an electrical signal obtained directly from an electronic device or circuit. Signal processing applies some algorithm to the basic signal in order to obtain meaningful information. Signal conditioning and processing operations may be performed using *analog* or *digital* circuit techniques, or using a combination of methods. There are a variety of trade-offs between them. For example, analog methods offer bandwidth advantages, whereas digital techniques offer advanced algorithm support and long-term stability. The use of microprocessors within an instrument makes it possible to perform many useful functions including calibration, linearization, conversion, storage, display, and transmission. A block diagram of a representative microprocessor-based instrument is shown in Fig. 108.2.

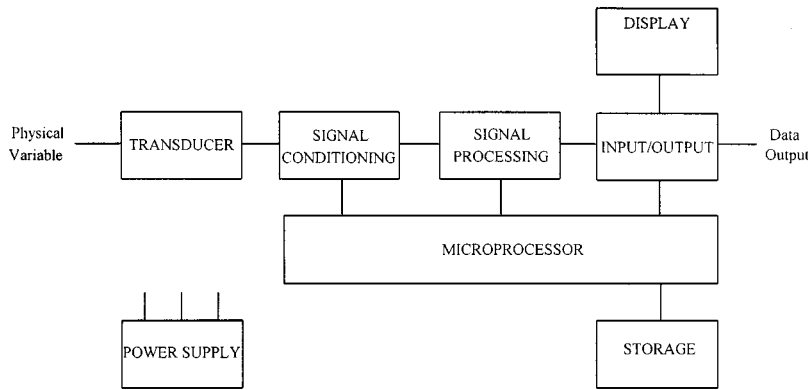


FIGURE 108.2 Block diagram of generalized, microprocessor-based instrument.

108.5 Instrumentation System

An instrument is never used in isolation. The instrumentation components contribute to an overall system response in a number of ways that are based on the **measurement system** elements present. These elements include: (1) sources, (2) interconnect, (3) device or system under test, (4) response measuring equipment, and (5) environmental variables. Figure 108.3 shows the elements of a typical instrumentation system.

108.6 Modeling Elements of an Instrumentation System

Best results are achieved when the instrumentation system is clearly understood, and its effects compensated for when practical. Lumped parameter modeling of the elements shown in Fig. 108.3 provides a means for determining the contribution each element makes to the overall system behavior. Of particular importance are the input and output impedances of each element. In addition, the effects of interconnect and environmental variables can also be modeled to determine their influence on the system. The relative dimensions of the measurement system with respect to the highest frequencies encountered—whether signal or noise—determine whether simplified circuit theory models, or generalized solutions to Maxwell's equations must be used. Generally, if measurement system dimensions are on the order of 1/20 of the shortest wavelength, simple circuit theory models can be used. Operation in this regime also allows impedance matching to be largely ignored; e.g., not requiring mandatory use of $50\ \Omega$ sources, $50\ \Omega$ transmission lines, and $50\ \Omega$ terminations which is commonly encountered in high-frequency systems. Table 108.3 summarizes several common instruments and input or output impedance models corresponding to Fig. 108.4. At low frequencies, interconnect can be modeled by ignoring the very low series resistance and inductance (Z_{s1} , Z_{s2}) terms, and considering only the shunt

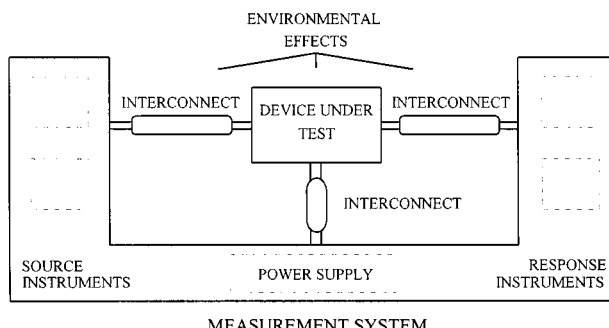


FIGURE 108.3 Fundamental elements of an instrumentation system.

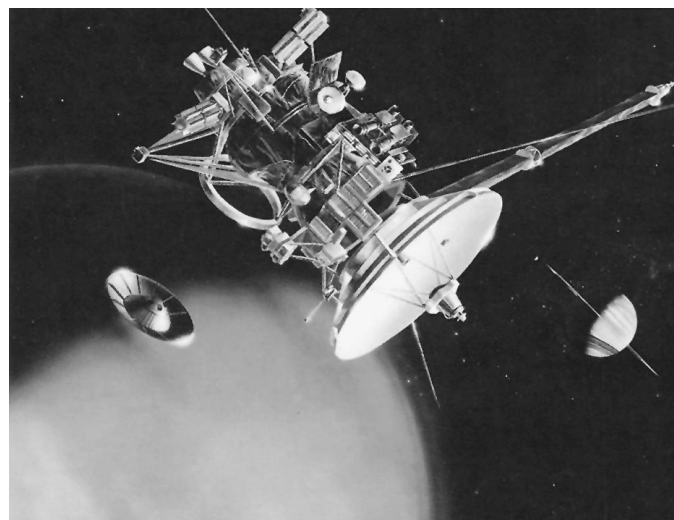
CASSINI SPACECRAFT

One of NASA's latest planetary systems research segments is called the Discovery Program. This program is an effort to develop frequent, small planetary missions that perform high quality scientific investigations. Discovery missions planned for 1997 include the sending of a Mars lander to the planet and launching the Lunar Prospector to map the moon's surface composition.

The principle planetary mission of NASA's Discovery Program is the 1997 launch of Cassini. Cassini is a joint project of NASA, the European Space Agency (ESA), and the Italian Space Agency, and is managed by the Jet Propulsion Laboratory (JPL).

The flight vehicle consists of the main Cassini spacecraft and the ESA-built Huygens Probe, a 750-pound, six instrument package that will descend into the atmosphere of Saturn's moon Titan, which is believed to be chemically similar to the atmosphere of early Earth.

Launched towards the end of 1997, Cassini will make flybys of Venus and Jupiter en route to a rendezvous with Saturn in July 2004. Cassini will release the Huygens Probe during its first orbit, then make approximately 40 revolutions over a span of four years, while the spacecraft's 12 instruments conduct a detailed exploration of the whole Saturnian system, including Titan and the planet's other icy moons. (Courtesy of National Aeronautics and Space Administration.)



This artist's concept shows the Cassini spacecraft orbiting around Saturn, just after deploying a probe that will descend into the atmosphere of Saturn's moon Titan. Launched October 1997, Cassini will reach Saturn in July 2004 and orbit the planet for four years thereafter. (Photo courtesy of National Aeronautics and Space Administration.)

capacitance (Z_p) which is in the range of 50 to 150 pF/m for different types of cable. At high frequencies, the characteristic impedance of the interconnect is used; e.g., 50Ω or 75Ω for commonly used coaxial cables; 120Ω for twisted pair.

The response of an entire instrumentation system can be modeled by interconnecting the individual model elements. [Figure 108.5](#) shows an example that was obtained by substituting models for an operational amplifier

TABLE 108.3 Summary of Common Instruments and Their Lumped-Parameter Models

Instrument Description, Model, Manufacturer	Input Impedance, Z_i	Output Impedance, Z_o
Function generator, FG501A, Tektronix		50Ω
Multimeter, DM501A, Tektronix	$10 M\Omega$ (Volts mode)	
Oscilloscope, 54601A, Hewlett Packard	$1 M\Omega \parallel 13 pF$	

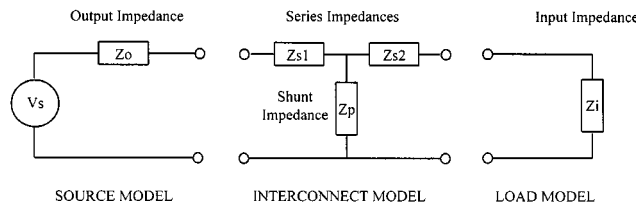


FIGURE 108.4 Simplified output and input models for instrument elements.

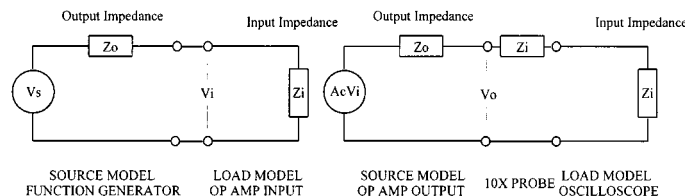


FIGURE 108.5 Model of representative instrumentation system. Each variable would be substituted as required. For example, $V_s = 1.0\sin 2\pi 1000t$ for a 0.707 Vrms, 1 kHz sine wave; $Z_o = 50 \Omega$ for the FG501A; $Z_i = 1 k\Omega$ for an op amp configured as an inverting amplifier with $R_i = 1 k\Omega$; and gain of 10; $A_c V_i = -10.0\sin 2\pi 1000t$; $Z_o = 1 \Omega$ for low current output; $Z_i = 9 M\Omega \parallel 1.4 pF$ for a compensated 10X probe; and with $Z_i = 1 M\Omega \parallel 13 pF$ for the input model of the HP54601A oscilloscope.

(op amp) circuit (corresponds to the device under test in Fig. 108.3) that was driven by a function generator for the source, and that measured the response with an oscilloscope connected to the output of the op amp using a 10X probe. In this application, the impedance of the interconnect between the source and op amp can be neglected since the frequencies are low and the input impedance of the op amp is much greater than that of the cable. The circuit model of the compensated 10X probe contains a very high series impedance ($9 M\Omega \parallel 1.4 pF$) relative to the oscilloscope ($1 M\Omega \parallel 13 pF$) so it cannot be ignored.

The models can be used to determine the *frequency response* of the complete system which describes the magnitude and phase response of the system to sinusoidal, steady-state inputs. This can reveal the contribution of each element to the overall response and helps indicate which elements produce the dominant response. The graphical results of the frequency response analysis is termed a *Bode plot*. If each of N elements has an individual transfer function, $H_i(j\omega)$, $i = 1$ to N , then a composite transfer function can be found for the total system, $T(j\omega)$, which is generally not the simple product of each transfer function, $H_1(j\omega) \cdot H_2(j\omega) \cdot \dots \cdot H_N(j\omega)$ due to loading effects between elements. The use of a circuit simulation program such as PSpice (MicroSim Corp.) simplifies the investigation into instrument behavior. A library of subcircuit models can be developed for each instrumentation and interconnect element to support measurement system loading effects analysis. For example, a PSpice subcircuit definition for the HP54601A oscilloscope is:

```
.SUBCKT HP54601A 1 2
Cin 1 2 13p
Rin 1 2 1MEG
.ENDS
```

TABLE 108.4 Noise Reduction Checklist

Source	Interconnect	Response
Shield enclosures	Shield leads	Shield enclosures
Filter inputs and outputs	Minimize loop area (twist leads)	Filter inputs and outputs
Limit bandwidth	Keep signal leads near ground	Limit bandwidth
Minimize loop areas	Separate low-, high-level signals Keep signal and ground leads short Low f: Use single ground High f: Use multiple grounds	Minimize loop areas

Source: H.W. Ott, *Noise Reduction Techniques in Electronic Systems*, 2nd ed., New York: John Wiley & Sons, 1988. With permission.

This network model would be added as a load to the output of the device under test in order to predict its loaded behavior.

108.7 Summary of Noise Reduction Techniques

Elimination of undesired measurement errors benefits from a systematic approach to identifying and solving noise problems. Source, interconnect, and response elements of a measurement system can be treated individually. Some techniques, such as shielding, are applicable to all three. Various combinations of techniques should be tried to achieve best results. There are many choices of grounding techniques that vary depending on whether elements are floating or ground-referred, and based on bandwidth. In general, multiple ground connections that create *ground loops* should be avoided. Difficult ground loop problems may require isolation or other techniques to interrupt the ground connection between elements. Table 108.4 summarizes a checklist of noise reduction techniques.

108.8 Personal Computer-Based Instruments

Many instrument functions are available for interface to personal computer (PC) systems. These range from plug-in cards that reside on the PC backplane to standalone instruments that communicate with the PC over standard interfaces such as RS-232 or IEEE-488. Software to control *data acquisition*, analysis, and display completes the computer-based instrument. Examples of such software include *Lab Windows* or *Lab View* (National Instruments), *HP VEE* (Hewlett-Packard), and *Testpoint* (Keithley-Metabyte). Figure 108.6 shows a block diagram of an output screen developed using *Lab Windows* for an acoustic measurement application. A

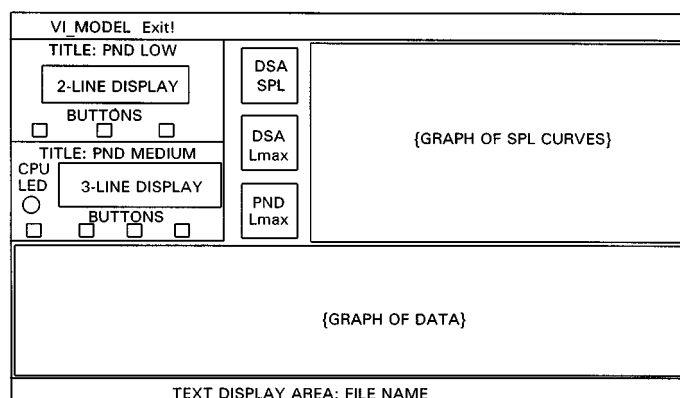


FIGURE 108.6 Example block diagram of a virtual instrument user interface.

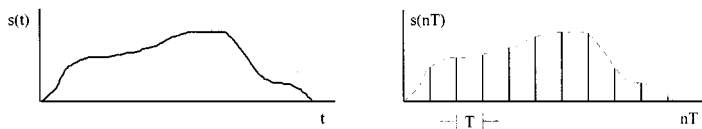


FIGURE 108.7 Sampling a continuous-time signal yields a discrete-time signal.

menu bar provides pull-down options. Several windows simultaneously display selection options and present results graphically and with text.

108.9 Modeling PC-Based Instruments

The approach outlined previously for modeling conventional measurement systems can be extended to PC-based instruments with one major difference: PC-based instruments by their nature are digital machines and perform functions in discrete time. Best performance of PC-based instrument systems must therefore consider *sampled data* effects. Figure 108.7 shows a data acquisition system modeled using an ideal sampler which instantaneously samples a continuous signal, $s(t)$, every T seconds. This yields a sequence, $s(nT)$, of discrete values that represent the value of the continuous signal at integer multiples of T seconds.

108.10 The Effects of Sampling

The Fourier transform of a sampled signal yields a frequency domain function that is periodic in frequency, with a period that is $1/f_s$. The *sampling theorem* states that in order to unambiguously preserve information, the sampling frequency, $f_s = 1/T$, must be at least twice the highest frequency present in the continuous-time signal. If f_s is less than twice the highest frequency, *aliasing* will occur. Aliased frequencies are indistinguishable from one another. A useful method for visualizing this result is through the use of an *aliasing diagram*. An example is shown in Fig. 108.8. Note that the *Nyquist frequency* is defined to be $f_s/2$.

108.11 Other Factors

Other important factors that should be considered when using PC-based instruments over manual counterparts are summarized in Table 108.5. Perhaps the most important choice is the selection of a minimum sampling rate for the data acquisition process. It must be chosen to meet the requirements of the Nyquist frequency. However, in order to ensure that no higher frequencies are present, an *anti-aliasing* low pass filter that eliminates energy above the Nyquist frequency should be employed. In order to provide sufficient transition bandwidth for the filter, a slightly higher sampling rate should generally be employed. A factor of 1.25 to 5 times the minimum f_s is a good compromise. Automated equipment may introduce substantial transients into the measurement system. Sufficient time must be provided for the resulting transients to settle to an acceptable error bound; for example, 1%.

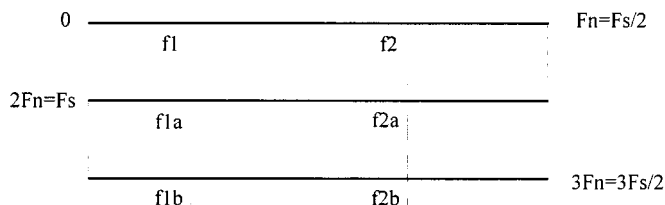


FIGURE 108.8 Aliasing diagram. The two baseband frequencies, f_1 and f_2 , have aliases at frequencies that intersect the vertical dashed lines. For example, using a sampling frequency of 10 kHz ($F_n = 5$ kHz) with $f_1 = 1$ kHz and $f_2 = 3.5$ kHz, signals at 9 kHz (f_{1a}) and 11 kHz (f_{1b}) would be aliased to 1 kHz (f_1), while signals at 6.5 kHz (f_{2a}) and 13.5 kHz (f_{2b}) would be aliased to 3.5 kHz (f_2).

TABLE 108.5 Automated Measurement Factors

Factor	Consideration
Leveling	Frequency response measurements require use of a leveled generator. Alternatively, store a calibration curve.
Multiplexing	Measurements from multiple nodes require lead switching to shared instruments; consider these effects.
Sampling frequency	Must exceed the Nyquist frequency. Include an anti-aliasing filter. Manual instruments typically use integrating (dual-slope) analog-to-digital converters which give good noise rejection over integer numbers of line cycles. Faster sampling rates for ATE are achieved using successive-approximation or other techniques. User may have to perform averaging as a post-processing step in order to achieve acceptable signal-to-noise ratios.
Settling time	Allow sufficient time for transients to settle for both stimulus/response instruments and device under test.
Storage	Automatic measurements can produce large arrays of data at high speeds. Actual throughput to a hard disk may be much less than the maximum sampling rate of a data acquisition element (plug-in board, external instrument).
Triggering	Choices between free-running, external, and internal.

Defining Terms

Instrument: The means for monitoring or measuring physical variables. Usually includes transducers, signal conditioning, signal processing, and display.

Measurement system: The sum of all stimulus and response instrumentation, device under test, interconnect, environmental variables, and the interaction among the elements.

Transducer: A device that transforms one form of energy to an electrical output that can be processed by an instrument.

Virtual instrument: An instrument created through computer control of instrumentation resources with analysis and display of the data collected.

Related Topics

3.1 Voltage and Current Laws • 8.5 Sampled Data • 73.2 Noise • 112.1 Introduction

References

- N. Ahmed and T. Natarajan, *Discrete-Time Signals and Systems*, Reston, Vir.: Reston Publishing, 1983.
E.O. Doebelin, *Measurement Systems: Application and Design*, 4th ed., New York: McGraw-Hill, 1990.
J.P. Holman, *Experimental Methods for Engineers*, 6th ed., New York: McGraw-Hill, 1994.
A.D. Khazan, *Transducers and Their Elements: Design and Application*, Englewood Cliffs, N.J.: Prentice-Hall, 1994.
H.W. Ott, *Noise Reduction Techniques in Electronic Systems*, 2nd ed., New York: John Wiley & Sons, 1988.
W.J. Tompkins and J.G. Webster, Eds., *Interfacing Sensors to the IBM PC*, Englewood Cliffs, N.J.: Prentice-Hall, 1988.

Further Information

The monthly journals, *IEEE Transactions on Instrumentation and Measurement*, and *IEEE Transactions on Biomedical Instrumentation*, report advances in instrumentation. For subscription information, contact: IEEE Service Center, 445 Hoes Lane, PO Box 1331, Piscataway, NJ 08855-1331. (800) 678-IEEE.

Information about automatic test equipment and software for data acquisition, analysis, and display, can be obtained from several vendors; for example, Hewlett-Packard, Englewood, CO, (800)-829-4444; Keithley-Metabyte, Taunton, MA, (800) 348-0033; and National Instruments, Austin, TX, (512) 794-0100. Information about transducers can be obtained from Omega International, Stamford, CT, (203) 359-1660.

Kayton, M. "Navigation Systems"
The Electrical Engineering Handbook
Ed. Richard C. Dorf
Boca Raton: CRC Press LLC, 2000

109

Navigation Systems

- 109.1 Introduction
- 109.2 Coordinate Frames
- 109.3 Categories of Navigation
- 109.4 Dead Reckoning
- 109.5 Radio Navigation
- 109.6 Celestial Navigation
- 109.7 Map Matching Navigation
- 109.8 Navigation Software
- 109.9 Design Trade-Offs

Myron Kayton
Kayton Engineering Co.

109.1 Introduction

Navigation is the determination of the position and velocity of a moving vehicle on land, at sea, in the air, or in space. The three components of position and the three components of velocity make up a six-component **state vector** that fully describes the translational motion of the vehicle because the differential equations of motion are of second order. Surveyors are beginning to use the same sensors as navigators but are achieving higher accuracy as a result of longer periods of observation, a fixed location, and more complex, non-real-time data reduction.

In the usual navigation system, the state vector is derived on-board, displayed to the crew, recorded on-board, or transmitted to the ground. Navigation information is usually sent to other on-board subsystems; for example, to the waypoint steering, engine control, communication control, and weapon-control computers. Some navigation systems, called *position-location systems*, measure a vehicle's state vector using sensors on the ground or in another vehicle (Section 109.5). The external sensors usually track passive radar returns or a transponder. Position-location systems usually supply information to a dispatch or control center.

Traditionally, *ship navigation* included the art of pilotage—entering and leaving port, making use of wind and tides, and knowing the coasts and sea conditions. However, in modern usage, navigation is confined to the measurement of the state vector. The handling of the vehicle is called *conning* for ships, *flight control* for aircraft, and *attitude control* for spacecraft.

The term *guidance* has two meanings, both of which are different than *navigation*:

1. Steering toward a destination of known position from the vehicle's present position, as measured by a navigation system. The steering equations on a planet are derived from a plane triangle for nearby destinations and from a spherical triangle for distant destinations.
2. Steering toward a destination without calculating the state vector explicitly. A guided vehicle homes on radio, infrared, or visual emissions. Guidance toward a *moving* target is usually of interest to military tactical missiles in which a steering algorithm assures impact within the maneuver and fuel constraints of the interceptor. Guidance toward a *fixed* target involves beam riding, as in the Instrument Landing System, Section 109.5.

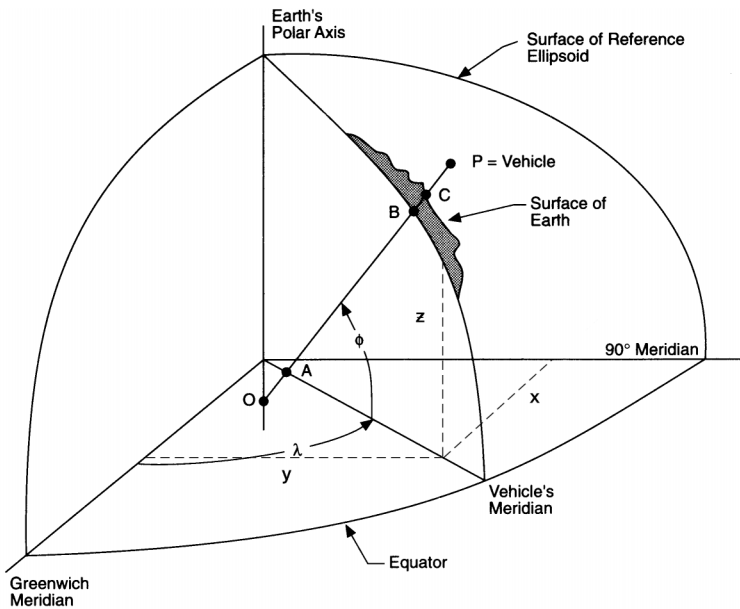


FIGURE 109.1 Latitude-longitude-altitude coordinate frame. ϕ = geodetic latitude; OP is normal to the ellipsoid at B; λ = geodetic longitude; $h = \overline{BP}$ = altitude above the reference ellipsoid = altitude above mean sea level.

109.2 Coordinate Frames

Navigation is with respect to a coordinate frame of the designer's choice. Short-range robots navigate with respect to the local terrain or a building's walls. For navigation over hundreds of kilometers (e.g., automobiles and trucks), various map grids exist whose coordinates can be calculated from latitude-longitude (Fig. 109.1). NATO land vehicles use a Universal Transverse Mercator grid. Long-range aircraft and ships navigate relative to an earth-bound coordinate frame, the most common of which are latitude-longitude-altitude and rectangular x, y, z (Fig. 109.1). The most accurate world-wide reference ellipsoid is described in [WGS-84, 1991]. Spacecraft in orbit around the earth navigate with respect to an earth-centered, inertially nonrotating coordinate frame whose z axis coincides with the polar axis of the earth and whose x axis lies along the equator. Interplanetary spacecraft navigate with respect to a sun-centered, inertially nonrotating coordinate frame whose z axis is perpendicular to the **ecliptic** and whose x axis points to a convenient star [Battin, 1987].

109.3 Categories of Navigation

Navigation systems can be categorized as:

1. *Absolute navigation systems* that measure the state vector without regard to the path traveled by the vehicle in the past. These are of two kinds:
 - Radio systems (Section 109.5). They consist of a network of transmitters (sometimes also receivers) on the ground or in satellites. A vehicle detects the transmissions and computes its position relative to the known positions of the stations in the navigation coordinate frame. The vehicle's velocity is measured from the Doppler shift of the transmissions or from a sequence of position measurements.
 - Celestial systems (Section 109.6). They measure the elevation and azimuth of celestial bodies relative to the land level and North. Electronic star sensors are used in special-purpose high-altitude aircraft and in spacecraft. Manual celestial navigation was practiced at sea for millennia (see Bowditch).
2. *Dead-reckoning navigation systems* that derive their state vector from a continuous series of measurements beginning at a known initial position. There are two kinds, those that measure vehicle heading and either

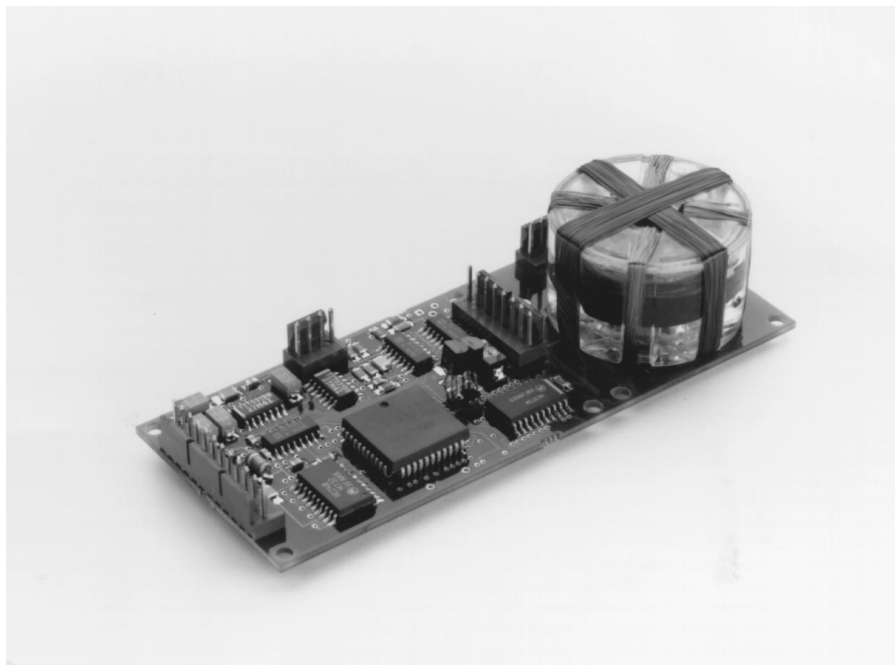


FIGURE 109.2 Saturated core (“flux-gate”) magnetometer, mounted on a “compass engine” board. The two orthogonal sensing coils (visible) and the drive coil, wound on the toroidal core, measure two components of the magnetic field in the plane of the toroid. (Courtesy of KVH Industries, Inc.)

speed or acceleration (Section 109.4) and those that measure emissions from continuous-wave radio stations whose signals create ambiguous “*lanes*” (Section 109.5).

Dead reckoning systems must be reinitialized as errors accumulate and if power is lost.

3. *Mapping navigation systems* that observe and recognize images of the ground, profiles of altitude, sequences of turns, or external features (Section 109.7). They compare their observations to a stored database, often on compact disc.

109.4 Dead Reckoning

The simplest dead-reckoning systems measure vehicle heading and speed, resolve speed into the navigation coordinates, then integrate to obtain position (Fig. 109.3). The oldest heading sensor is the magnetic compass, a magnetized needle or electrically excited toroidal core (called a *flux gate*), as shown in Fig. 109.2. It measures the direction of the earth’s magnetic field to an accuracy of 2 degrees at a steady velocity below 60-degrees magnetic latitude. The horizontal component of the magnetic field points toward *magnetic north*. The angle from true to magnetic north is called *magnetic variation* and is stored in the computers of modern vehicles as a function of position over the region of anticipated travel [Quinn, 1996]. *Magnetic deviations* caused by iron in the vehicle can exceed 30 degrees and must be compensated in the navigation computer or, in older ships, by placing compensating magnets near the sensor.

A more complex heading sensor is the *gyrocompass*, consisting of a spinning wheel whose axle is constrained to the horizontal plane (often by a pendulum). The ships’ version points north, when properly compensated for vehicle motion, and exhibits errors less than a degree. The aircraft version (more properly called a *directional gyroscope*) holds any preset heading relative to earth and drifts at 50 deg/hr or more. Inexpensive gyroscopes (some built on silicon chips as vibrating beams with on-chip signal conditioning) are often coupled to magnetic compasses to reduce maneuver-induced errors.

The simplest speed-sensor is a wheel odometer that generates electrical pulses. Ships use a dynamic-pressure probe or an electric-field sensor that measures the speed of the hull through the conductive water. Aircraft

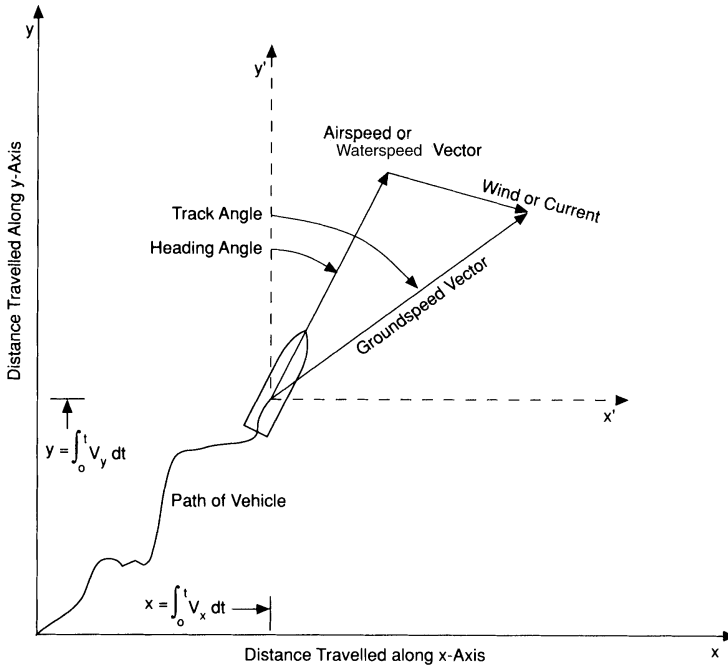


FIGURE 109.3 Geometry of dead reckoning.

measure the dynamic pressure of the air stream from which they derive airspeed in an *air-data* computer. The velocity of the wind or sea current must be vectorially added to that of the vehicle, as measured by a dynamic-pressure sensor (Fig. 109.3). Hence, unpredicted wind or current will introduce an error into the dead-reckoning computation. Most sensors are insensitive to the component of airspeed or waterspeed normal to their axis (*leeway* in a ship, *drift* in an aircraft). A Doppler radar measures the frequency shift in radar returns from the ground or water below the aircraft, from which speed is inferred. A Doppler sonar measures a ship's speed relative to the water layer or ocean floor from which the beam reflects. Multibeam Doppler radars or sonars can measure all the components of the vehicle's velocity. Doppler radars are widely used on military helicopters.

The most complex dead-reckoning system is an *inertial navigator* in which accelerometers measure the vehicle's acceleration while gyroscopes measure the orientation of the accelerometers. An on-board computer resolves the accelerations into navigation coordinates and integrates them to obtain velocity and position. The gyroscopes and accelerometers are mounted in either of two ways:

1. In servoed gimbals that angularly isolate them from rotations of the vehicle.
2. Fastened directly to the vehicle ("strap-down"), whereupon the sensors are exposed to the maximum angular rates and accelerations of the vehicle (Fig. 109.4).

Inertial-quality gyroscopes measure vehicle orientation within 0.1 degree for steering and pointing. Most accelerometers consist of a gram-sized proof-mass mounted on flexure pivots. The newest accelerometers, not yet of inertial grade, are etched into silicon chips. Older gyroscopes contained metal wheels rotating in ball bearings or gas bearings. The newest gyroscopes are evacuated cavities or optical fibers in which counter-rotating laser beams are compared in phase to measure the sensor's angular velocity relative to **inertial space** about an axis normal to the plane of the beams. Vibrating hemispheres and rotating vibrating tines are the basis of some navigation-quality gyroscopes (drift rates less than 0.1 deg/h).

Fault-tolerant configurations of cleverly oriented redundant gyroscopes and accelerometers (typically four to six) detect and correct sensor failures. Inertial navigators are used aboard naval ships, in airliners, in most military fixed-wing aircraft, in space boosters and entry vehicles, in manned spacecraft, in tanks, and on large mobile artillery pieces.

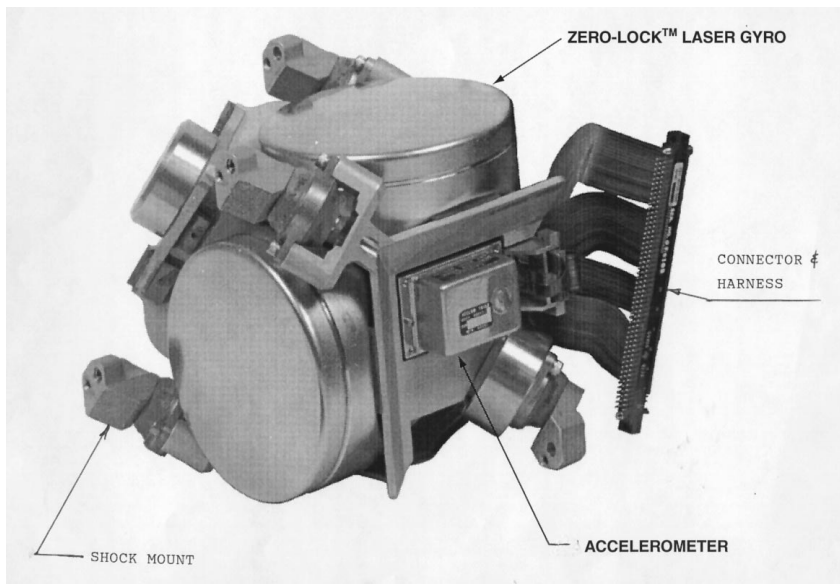


FIGURE 109.4 Inertial reference unit. Two laser gyroscopes (flat discs), an accelerometer, an electrical connector, and three shock mounts are visible. This unit is used in Airbuses and many military aircraft such as the F-18 and Comanche helicopter. (Courtesy of Litton Guidance and Control Systems.)

109.5 Radio Navigation

Scores of radio navigation aids have been invented and many of them have been widely deployed, as summarized in [Table 109.1](#).

The most precise is the global positioning system (GPS), a network of 24 satellites and a half-dozen ground stations for monitoring and control. A vehicle derives its three-dimensional position and velocity from ranging signals at 1.575 GHz received from four or more satellites (military users also receive 1.227 GHz). The former Soviet Union deployed a similar system, called GLONASS. GPS offers better than 100-m ranging errors to civil users and 15-m ranging errors to military users. Simple receivers were available for less than \$300 in 1997. They are used on highways, in low-rise cities, at sea, in aircraft, and in low-orbit spacecraft. GPS provides continuous worldwide navigation for the first time in history. It will make dead reckoning unnecessary on many vehicles and will reduce the cost of most navigation systems. [Figure 109.5](#) is an artist's drawing of a GPS Block 2F spacecraft, scheduled for launch in the year 2002.

Differential GPS (DGPS) employs one or more ground stations at known locations, that receive GPS signals and transmit measured errors on a radio link to nearby ships and aircraft. DGPS improves accuracy (centimeters for fixed observers) and detects faults in GPS satellites. In 1997, the U.S. was conducting experiments with a nationwide DGPS system of about 25 stations. This *Wide Area Augmentation System* (WAAS) could eventually replace VORTAC and Category I ILS. A denser network of DGPS stations and GPS-emulating pseudolites, whose stations are located at airports, might replace ILS and MLS (below). In 1997, the cost, accuracy, and reliability of such a *Local Area Augmentation System* (LAAS) were still being compared to existing landing aids but marine LAAS were in operation for navigation into harbors in North America, the North Sea, and the Baltic Sea.

The most widely used marine radio aid in 1997 was Loran-C (see [Table 109.1](#)). The 100-kHz signals are usable within 1000 **nautical miles (nmi)** of a “chain” consisting of three or four stations. Chains cover the United States, parts of western Europe, Japan, Saudi Arabia, and a few other areas. The former Soviet Union has a compatible system called Chaika. The vehicle-borne receiver measures the difference in time of arrival of pulses emitted by two stations, thus locating the vehicle on one branch of a hyperbola. Two or more station pairs give a two-dimensional position fix whose typical accuracy is 0.25 nmi, limited by propagation uncertainties over the terrain between the transmitting station and the user. The measurement of 100-microsecond

TABLE 109.1 Worldwide Radio Navigation Aids

System	Frequency		Number of Stations	Number of Users in 1996			
	Hz	Band		Air	Marine	Space	Land
Omega	10–13 kHz	VLF	8	15,000	10,000	0	0
Loran-C/Chaika	100 kHz	LF	50	120,000	550,000	0	25,000
Decca	70–130 kHz	LF	150	2,000	20,000	0	0
Beacons*	200–1600 kHz	MF	4000	130,000	500,000	0	0
Instrument Landing System (ILS)*	{ 108–112 MHz 329–335 MHz	{ VHF UHF	1500	150,000	0	0	0
VOR*	108–118 MHz	VHF	1500	180,000	0	0	0
SARSAT/COSPAS	{ 121.5 MHz 243,406 MHz	{ VHF UHF	5 satellites	200,000	200,000	0	100,000
Transit	150, 400 MHz	VHF	7 satellites	0	0	0	0
PLRS	420–450 MHz	UHF	None	0	0	0	2,000
JTIDS	960–1213 MHz	L	None	500	0	0	0
DME*	962–1213 MHz	L	1500	90,000	0	4	0
Tacan*	962–1213 MHz	L	850	15,000	0	4	0
Secondary Surveillance Radar (SSR)*	1030, 1090 MHz	L	800	250,000	0	0	0
Identification Friend or Foe (IFF)							
GPS-GLONASS	1227, 1575 MHz	L	24 + 24 satellites	120,000	275,000	4	125,000
Satellite Control Network (SCN)	{ 1760–1850 MHz 2200–2300 MHz	{ S S	10	0	0	200	0
Spaceflight Tracking and Data Network (STDN)	{ 2025–2150 MHz 2200–2300 MHz	{ S 10 ground	3 satellites	0	0	50	0
Radar Altimeter	4200 MHz	C	None	20,000	0	0	0
MLS*	5031–5091 MHz	C	30	100	0	0	0
FPQ-6, FPQ-16 radar	5.4–5.9 GHz	C	10	0	0	0	0
Weather/map radar	10 GHz	X	None	10,000	0	0	0
Shuttle rendezvous radar	13.9 GHz	Ku	None	0	0	4	0
Airborne Doppler radar	13–16 GHz	Ku	None	20,000	0	0	0
SPN-41 carrier-landing monitor	15 GHz	Ku	25	1600	0	0	0
SPN-42/46 carrier-landing radar	33 GHz	Ka	25	1600	0	0	0

*Standardized by International Civil Aviation Organization.

time difference is possible with low-quality clocks in the vehicles. Loran is also used by general aviation aircraft for en-route navigation and for nonprecision approaches to airports (in which the cloud bottoms are more than 200 feet above the runway). Loran service will probably be discontinued at the beginning of the 21st century.

The most widely used aircraft radio aid is VORTAC, whose stations offer three services:

1. Analog bearing measurements at 108 to 118 MHz (called VOR). The vehicle compares the phases of a rotating cardioid pattern and an omnidirectional sinusoid emitted by the ground station.
2. Pulse distance measurements (DME) at 1 GHz by measuring the time delay for an aircraft to interrogate a VORTAC station and receive a reply,
3. Tacan bearing information conveyed in the amplitude modulation of the DME replies from the VORTAC stations.

Omega is a worldwide radio aid consisting of eight radio stations that emit continuous sine waves at 10 to 13 kHz. Vehicles with precise clocks measure their range to a station by observing the absolute time of reception. Other vehicles measure the range differences between two stations in the form of phase differences between the received sinusoids. Differential Omega creates hyperbolic “lanes” that are 10 to 150 nmi wide. The lanes are indistinguishable from each other by measuring phase; hence the vehicle must count lanes from a point of known position. Errors are about 2 nmi due to radio propagation irregularities. Omega is used by submarines,



FIGURE 109.5 Global positioning satellite, Block 2F. (Courtesy of Rockwell.)

over-ocean general-aviation aircraft, and a few international air carriers. It was scheduled to be decommissioned in 1997.

Landing guidance throughout the western world, and increasingly in China, India, and the former Soviet Union, is with the Instrument Landing System (ILS). Transmitters adjacent to the runway create a horizontal guidance signal near 110 MHz and a vertical guidance signal near 330 MHz. Both signals are modulated such that the nulls intersect along a line in space that leads an aircraft from a distance of about 10 nmi to within 50 ft above the runway. ILS gives no information about where the aircraft is located along the beam except at two or three vertical *marker beacons*. Most ILS installations are certified to the International Civil Aviation Organization's (ICAO) *Category I*, where the pilot must abort the landing if the runway is not visible at an altitude of 200 ft. One hundred ILSs (in 1996) were certified to *Category II*, which allows the aircraft to descend to 100 ft before aborting for lack of visibility. *Category III* allows an aircraft to land at still lower weather ceilings. Category III landing aids are of special interest in Western Europe, which has the worst flying weather in the developed world. Category III ILS detects its own failures and switches to a redundant channel within one second to protect aircraft that are flaring-out (within 50 ft of the runway) and can no longer execute a missed approach. Once above the runway, the aircraft's bottom-mounted radar altimeter measures altitude and either the electronics or the pilot guides the flare maneuver. Landing aids are described by Kayton and Fried [1997].

Throughout the western world, civil aircraft use VOR/DME whereas military aircraft use Tacan/DME for en-route navigation. In the 1990s, China and the successor states to the Soviet Union were installing ICAO-standard navigation aids (VOR, DME, ILS) at their international airports and along the corridors that lead to them from the borders. Overflying western aircraft navigate inertially, with Omega, or with GPS. Domestic flights within the Soviet Union depended on radar tracking, non-directional beacons, and an L-band range-angle system called "RSBN". They will eventually upgrade to a satellite-based enroute and landing system.

U.S. Navy aircraft use a microwave scanning system at 15.6 GHz to land on aircraft carriers; NASA's space shuttle uses the Navy system to land at its spaceports. Another microwave landing system (MLS) at 5 GHz was supposed to replace the ILS in civil operations, especially for Categories II and III. However, experiments from

1990 to 1997 showed that differential GPS could achieve an accuracy better than 1 m as a landing aid. Hence, it is likely that a LAAS will replace or supplement ILS, which has been guaranteed to remain in service at least until the year 2010 (Federal Radionavigation Plan). NATO may use MLS or a LAAS as a portable landing aid for tactical airstrips.

All the space-faring nations operate worldwide radio networks that track spacecraft, compute their state vectors, and predict future state vectors using complex models of gravity, atmospheric drag, and lunisolar perturbations. NASA operates three tracking and data relay satellites (TDRS) that track spacecraft in low earth orbit with accuracies of 10 to 50 m and 0.3 m/s. Specialized ground-based tracking stations monitor and reposition the world's many communication satellites [Berlin, 1988]. Other specialized stations track and communicate with deep space probes. They achieve accuracies of 30 m and a few centimeters per second, even at enormous interplanetary distances, due to long periods of observation and precise orbit equations (see [Yuan, 1983]).

Position-location and position-reporting systems monitor the state vectors of many vehicles and usually display the data in a control room or dispatch center. Some vehicles derive their state vector from the ranging modulations; others merely report an independently derived position. Table 109.1 lists *Secondary Surveillance Radars* that receive coded replies from aircraft so they can be identified by human controllers and by collision-avoidance algorithms. The table also lists the U.S. NASA and military spacecraft-tracking networks (STDN and SCN). Tracking and reporting systems have long been in use at marine ports, for airplane traffic control and for space vehicles. They are increasingly being installed in fire trucks, police cars, ambulances, and delivery-truck fleets that report to a control center. The aeronautical bureaucracy calls them *Automatic Dependent Surveillance* (ADS) systems. The continuous broadcast of on-board-derived position (probably GPS-based) may become the basis of the worldwide air traffic control system of the early 21st century.

Several commercial communication satellites plan to offer digital-ranging services worldwide. The intermittent nature of commercial fixes would require that vehicles dead-reckon between fixes, perhaps using solid-state inertial instruments. Thus, if taxpayers insist on collecting fees for service, private comm-nav networks may replace the government-funded GPS and air-traffic communication network in the next century. Worldwide traffic control over oceans and undeveloped land areas would become possible.

Military communication-navigation systems measure the position of air, land, and naval vehicles on battlefields and report to headquarters; examples are the American Joint Tactical Information Distribution System (JTIDS) and the Position Location Reporting System (PLRS).

A worldwide network of SARSAT-COSPAS stations monitors signals from satellite-based transponders listening on 121.5, 243, and 406 MHz, the three international distress frequencies. Software at the listening stations calculates the position of Emergency Location Transmitters within 20 kilometers, based on the observed Doppler-shift history, so that rescue vehicles can be dispatched. Thousands of lives have been saved worldwide, from arctic bush-pilots to tropical fishermen.

109.6 Celestial Navigation

Human navigators use sextants to measure the elevation angle of celestial bodies above the visible horizon. The peak elevation angle occurs at local noon or midnight:

$$\text{elev angle (degrees)} = 90 - \text{latitude} + \text{declination}$$

Thus at local noon or midnight, latitude can be calculated by simple arithmetic. Tables of declination, the angle of the sun or star above the earth's equatorial plane, were part of the ancient navigator's proprietary lore. The declination of the sun was first publicly tabulated in the fifteenth century in Spain. When time became measurable at sea, with a chronometer in the nineteenth century and by radio in the twentieth century, off-meridian observations of the elevation of two or more celestial bodies were possible at any known time of night (cloud cover permitting). These fixes were hand-calculated using logarithms, then plotted on charts. In the 1930s, hand-held sextants were built that measured the elevation of celestial bodies from an aircraft using a bubble-level reference instead of the horizon. The accuracy of celestial fixes was 3–10 miles at sea and 5–20 miles in the air, limited by the uncertainty in the horizon and the inability to make precise angular measurements on a pitching, rolling vehicle. Kayton (1990) reviews the history of celestial navigation at sea and in the air.

The first automatic star trackers were built in the late 1950s. They measured the azimuth and elevation of stars relative to a gyroscopically stabilized platform. Approximate position measurements by dead reckoning allowed the telescope to point within a fraction of a degree of the desired star. Thus, a narrow field-of-view was possible, permitting the telescope and photodetector to track stars in the daytime. An on-board computer stored the right ascension and declination of 20–100 stars and computed the vehicle's position. Automatic star trackers are used in long-range military aircraft and on space shuttles in conjunction with inertial navigators. Clever design of the optics and of stellar-inertial signal-processing filters achieves accuracies better than 500 ft [Kayton and Fried, 1997].

Spacecraft use the line-of-sight to the sun and stars to measure orientation (for *attitude control*). Earth-pointing spacecraft usually carry horizon scanners that locate the center of the earth's carbon-dioxide disc. All spacecraft navigate by radio tracking from earth. When interplanetary spacecraft approach the target planet, the navigation computers (on earth) transform from sun-centered to planet-centered coordinates by observing star occultations and transmitting the images to earth for human interpretation. During the Apollo translunar missions, crews experimentally measured the angle between celestial bodies and the earth or moon with a specially designed manual sextant coupled to a digital computer which calculated the state vector. Other experiments have been made in which American and Soviet crews used manual sextants to observe the angle between celestial bodies and landmarks on earth, from which state vectors were calculated. Autonomous land vehicles on other planets and certain military spacecraft may need celestial navigation.

109.7 Map-Matching Navigation

As computer power grows, map-matching navigation is becoming more important. On aircraft, mapping radars and optical sensors present a visual image of the terrain to the crew. Automatic map-matchers have been built, since the 1960s, that correlate the observed image to stored images, choosing the closest match to update the dead-reckoned state vector. More commonly, aircraft and cruise missiles measure the vertical profile of the terrain below the vehicle and match it to a stored profile. Matching profiles, perhaps hourly, reduces the long-term drift of their inertial navigators. The profile of the terrain is measured by subtracting the readings of a baro-inertial altimeter (calibrated for altitude above sea level) and a radar altimeter (measuring terrain clearance). An on-board computer calculates the autocorrelation function between the measured profile and each of many stored profiles on possible parallel paths of the vehicle. The on-board inertial navigator usually contains a digital filter that corrects the drift of the azimuth gyroscope as a sequence of fixes is obtained. Hence the direction of flight through the stored map is known, saving the considerable computation time that would be needed to correlate for an unknown azimuth of the flight path. Marine versions profile the seafloor with a sonar and compare the measured profile to stored bottom maps.

GPS is adequate for automotive navigation except in high-rise cities, in tunnels, and on streets with heavy foliage. To fill coverage gaps, map-matching software can take advantage of the fact that the vehicle remains on roads. On the highway, dead-reckoning or GPS errors can be rectified to the nearest road. In cities, turns can be correlated with the nearest intersection of matching geometry. An accuracy of several meters is possible if all streets are included on the stored map (e.g., alleys, driveways, and parking garages).

The most complex mapping systems observe their surroundings, usually by digitized video, and create their own map of the surrounding terrain. Guidance software then steers the vehicle. In 1997, such systems were in development for hazardous sites such as nuclear plants, waste-disposal facilities, and battlefields, and for unmanned planetary exploration.

Delivery robots in buildings are furnished with a map and need only find their successive destinations while avoiding obstacles. They navigate by following stripes on the floor, by observing infrared beacons, or by observing the returns from on-board ultrasonic sonar or laser radar.

109.8 Navigation Software

Navigation software is sometimes embedded in a central processor with other avionic-system software, sometimes confined to one or more navigation computers. The navigation software contains algorithms and data

GPS POSITIONING SYSTEM DELIVERS HIGH ACCURACY

A system for real-time differential GPS (DGPS) positioning will deliver submeter accuracy to Earth satellites and ground-based users worldwide. Developed at NASA's Jet Propulsion Laboratory, the system could improve real-time position accuracy to a few decimeters for single-frequency users and 10 cm or better for dual frequency users. In addition to high accuracy, the system provides nearly complete separation of GPS orbit and clock corrections and continuous determination of inter-frequency delay biases for all GPS satellites and reference receivers.

Key features include: the use of dynamic orbit estimation, which depends on high-accuracy satellite force models, signal models, geophysical models, and geometric models, in a Kalman filter formulation; use of real-time stochastic estimation to minimize orbit and clock errors arising from quasi-random variations in atmospheric propagation relays and solar radiation pressure; simultaneous processing of smoothed pseudorange and continuous carrier phase data; and use of the stable solar-magnetic reference frame, rather than an Earth-fixed frame, in computing the ionosphere corrections.

System operation began in January 1997. Early tests show approximate user differential range errors of less than 20 cm throughout the coverage area, with a North American reference network only. More comprehensive tests with additional global reference sites will be conducted. (Reprinted with permission of *NASA Tech Briefs*, 20(10), 30, 1996).

that process the measurements made by each sensor (e.g., inertial or air data). It contains calibration constants, initialization sequences, self-test algorithms, reasonability tests, and alternative algorithms for periods when sensors have failed or are not receiving information. In the simplest systems, the state vector is calculated independently from each sensor; most often, the navigation software contains multisensor algorithms that calculate the best estimate of position and velocity from several sensors. Prior to 1970, the best estimate was calculated from a least squares algorithm with constant weighting functions or from a frequency-domain filter with constant coefficients. Now, a *Kalman filter* calculates the best estimate from mathematical models of the dynamics of each sensor.

Digital maps, often stored on compact disc, are carried on some aircraft and land vehicles so position can be visually displayed to the crew. Military aircraft superimpose their navigated position on a stored map of terrain and cultural features to aid in the penetration of and escape from enemy territory. Civil operators had not invested in digital data bases as of 1996. Algorithms for waypoint steering and for control of the vehicle's attitude are contained in the software of the *flight management* and *flight control* subsystems.

Specially equipped aircraft (sometimes ships) are often used for the routine calibration of radio navigation aids, speed and velocity sensors, heading sensors, and new algorithms.

109.9 Design Trade-Offs

The designers of a navigation system conduct trade-offs for each vehicle to determine which navigation systems to use. Tradeoffs consider the following attributes:

- *Cost*, including the construction and maintenance of transmitter stations and the purchase of on-board electronics and software. Users are concerned only with the costs of on-board hardware and software.
- *Accuracy* of position and velocity, which is specified as a circular error probable (CEP, in meters or nautical miles). The maximum allowable CEP is often based on the calculated risk of collision on a typical mission.

- *Autonomy*, the extent to which the vehicle determines its own position and velocity without external aids. Autonomy is important to certain military vehicles and to civil vehicles operating in areas of inadequate radio-navigation coverage.
- *Time delay* in calculating position and velocity, caused by computational and sensor delays.
- *Geographic coverage*. Radio systems operating below 100 kHz can be received beyond line of sight on earth; those operating above 100 MHz are confined to line of sight. On other planets, new navigation aids—perhaps navigation satellites or ground stations—will be installed.
- *Automation*. The vehicle's operator (on-board crew or ground controller) receives a direct reading of position, velocity, and equipment status, usually without human intervention. The navigator's crew station disappeared in aircraft in the 1970s. Human navigators are becoming scarce, even on ships, in the 1990s, because electronic equipment automatically selects stations, calculates waypoint steering, and accommodates failures.

Defining Terms

Circular Error Probable (CEP): Radius of a circle, centered at the destination, that contains 50% of the navigation measurements from a large sample.

Ecliptic: Plane of earth's orbit around the sun.

Inertial Space: Any coordinate frame whose origin is on a freely falling (orbiting) body and whose axes are nonrotating relative to the fixed stars. It is definable within 10^{-7} degree/h.

Lanes: Hyperbolic bands on the earth's surface in which continuous-wave radio signals repeat in phase.

Nautical Mile (nmi): 1852 m, exactly. Approximately 1 min of arc on the earth's surface.

State vector: Six-component vector, three of whose elements are position and three of whose elements are velocity.

Update: The intermittent resetting of the dead-reckoned state vector based on absolute navigation measurements (see Section 109.3).

Related Topic

102.2 Communications Satellite Systems: Applications

References

- R.H. Battin, *An Introduction to the Mathematics and Methods of Astrodynamics*, Washington: AIAA Press, 1987, 796 pp.
- P. Berlin, *The Geostationary Applications Satellite*, Cambridge: Cambridge University Press, 1988, 214 pp.
- N. Bowditch, *The American Practical Navigator*, Washington, D.C.: U.S. Government Printing Office, 1995, 873 pp.
- M. Kayton, *Navigation: Land, Sea, Air, and Space*, New York: IEEE Press, 1990, 461 pp.
- M. Kayton and W.R. Fried, *Avionics Navigation Systems*, 2nd ed., New York: Wiley, 1997, 773 pp.
- R.A. Minzner, *The U.S. Standard Atmosphere 1976*, NOAA Report 76-1562, NASA SP-390, 1976 or latest edition, 227 pp.
- NASA, *Space Network Users Guide*, Greenbelt, Md.: Goddard Space Flight Center, 1988 or latest edition, 500 pp.
- B.W. Parkinson and J.J. Spilker, Eds., *Global Positioning System, Theory and Applications*, American Institute of Aeronautics and Astronautics, 1996, 1300 pp., 2 vols.
- J. Quinn, "1995 revision of joint U.S./U.K. geomagnetic field models," *J. Geomagnetism and Geo-Electricity*, 1996.
- U.S. Air Force, *NAVSTAR-GPS Interface Control Document*, Annapolis, Md.: ARINC Research, 1991, 115 pp.
- U.S. Government, *Federal Radionavigation Plan*, Department of Transportation, 1996, 229 pp., issued biennially WGS-84, U.S. Defense Mapping Agency, *World Geodetic System 1984*, Washington, D.C.: 1991.
- J. Yuen, *Deep Space Telecommunication Systems Engineering*, New York: Plenum Press, 1983, 603 pp.
- Y. Zhao, *Vehicle Location and Navigation Systems*, Massachusetts: Artech House, 1997, 345 pp.

Further Information

IEEE Transactions on Aerospace and Electronic Systems, bimonthly through 1991, now quarterly.
Proceedings of the IEEE Position Location and Navigation Symposium (PLANS), biennially.
Navigation, journal of the U.S. Institute of Navigation, quarterly.
Journal of Navigation, Royal Institute of Navigation (UK), quarterly.
AIAA Journal of Guidance and Control, bimonthly.
Commercial aeronautical standards produced by International Civil Aviation Organization (ICAO, Montreal),
Aeronautical Radio, Inc. (ARINC, Annapolis, Md.), Radio Technical Commission for Aeronautics (RTCA,
Inc., Washington) and European Organization for Civil Aviation Equipment (EUROCAE, Paris).

Ramakumar, R. "Reliability Engineering"
The Electrical Engineering Handbook
Ed. Richard C. Dorf
Boca Raton: CRC Press LLC, 2000

110

Reliability Engineering¹

- 110.1 Introduction
- 110.2 Catastrophic Failure Models
- 110.3 The Bathtub Curve
- 110.4 Mean Time To Failure (MTTF)
- 110.5 Average Failure Rate
- 110.6 *A Posteriori* Failure Probability
- 110.7 Units for Failure Rates
- 110.8 Application of the Binomial Distribution
- 110.9 Application of the Poisson Distribution
- 110.10 The Exponential Distribution
- 110.11 The Weibull Distribution
- 110.12 Combinatorial Aspects
- 110.13 Modeling Maintenance
- 110.14 Markov Models
- 110.15 Binary Model for a Repairable Component
- 110.16 Two Dissimilar Repairable Components
- 110.17 Two Identical Repairable Components
- 110.18 Frequency and Duration Techniques
- 110.19 Applications of Markov Process
- 110.20 Some Useful Approximations
- 110.21 Application Aspects
- 110.22 Reliability and Economics

R. Ramakumar

Oklahoma State University

110.1 Introduction

Reliability engineering is a vast field and it has grown significantly during the past five decades (since World War II). The two major approaches to reliability assessment and prediction are (1) traditional methods based on probabilistic assessment of field data and (2) methods based on the analysis of failure mechanisms and physics of failure. The latter is more accurate, but is difficult and time consuming to implement. The first one, in spite of its many flaws, continues to be in use. Some of the many areas encompassing reliability engineering are reliability allocation and optimization, reliability growth and modeling, reliability testing including accelerated testing, data analysis and graphical techniques, quality control and acceptance sampling, maintenance engineering, repairable system modeling and analysis, software reliability, system safety analysis, Bayesian analysis, reliability management, simulation and Monte Carlo techniques, Failure Modes, Effects and Criticality Analysis (FMECA), and economic aspects of reliability, to mention a few.

Application of reliability techniques is gaining importance in all branches of engineering because of its effectiveness in the detection, prevention, and correction of failures in the design, manufacturing, and operational

¹Some of the material in this chapter was previously published by CRC Press in *The Engineering Handbook*, R. C. Dorf, Ed., 1996.

INFORMATION MANAGEMENT SYSTEM FOR MANUFACTURING EFFICIENCY

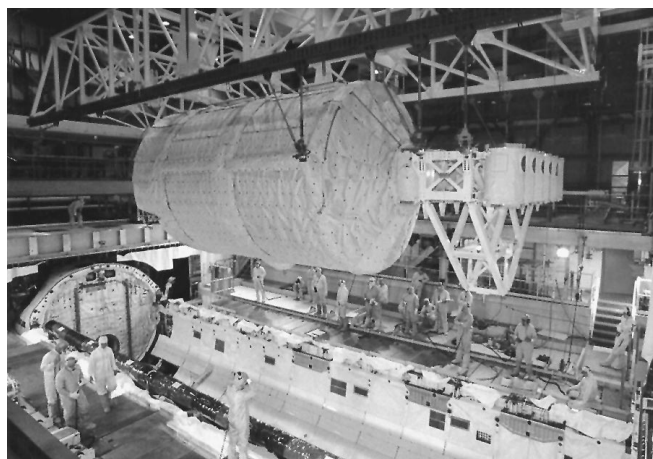
At current schedules, each of NASA's four Space Shuttle Orbiters must fly two or three times a year. Preparing an orbiter for its next mission is an incredibly complex process and much of the work is accomplished in the Orbiter Processing Facility (OPF) at Kennedy Space Center.

The average "flow"—the complete cycle of refurbishing an orbiter—requires the integration of approximately 10,000 work events, takes 65 days, and some 40,000 technician labor hours. Under the best conditions, scheduling each of the 10,000 work events in a single flow would be a task of monumental proportions. But the job is further complicated by the fact that only half the work is standard and predictable; the other half is composed of problem-generated tasks and jobs specific to the next mission, which creates a highly dynamic processing environment and requires frequent rescheduling.

For all the difficulties, Kennedy Space Center and its prime contractor for shuttle processing—Lockheed Space Operations Company (LSOC)—are doing an outstanding job of managing OPF operations with the help of a number of processing innovations in recent years. One of the most important is the Ground Processing Scheduling System, or GPSS. The GPSS is a software system for enhancing efficiency by providing an automated scheduling tool that predicts conflicts between scheduled tasks, helps human schedulers resolve those conflicts, and searches for near-optimal schedules.

GPSS is a cooperative development of Ames Research Center, Kennedy Space Center, LSOC, and a related company, Lockheed Missiles and Space Company. It originated at Ames, where a group of computer scientists conducted basic research on the use of artificial intelligence techniques to automate the scheduling process. A product of the work was a software system for complex, multifaceted operations known as the Gerry scheduling engine.

Kennedy Space Center brought Ames and Lockheed together and the group formed an inter-center/NASA contractor partnership to transfer the technology of the Gerry scheduling engine to the Space Shuttle program. The transfer was successfully accomplished and GPSS has become the accepted general purpose scheduling tool for OPF operations. (Courtesy of National Aeronautics and Space Administration.)



Kennedy Space Center technicians are preparing a Space Shuttle Orbiter for its next mission, an intricate task that requires scheduling 10,000 separate events over 65 days. A NASA-developed computer program automated this extremely complex scheduling job. (Photo courtesy of National Aeronautics and Space Administration.)

phases of products and systems. Increasing emphasis being placed on quality of components and systems, coupled with pressures to minimize cost and increase value, further emphasize the need to study, understand, quantify, and predict reliability and arrive at innovative designs and operational and maintenance procedures.

From the electrical engineering point of view, two (among several) areas that have received significant attention are electronic equipment (including computer hardware) and electric power systems. Other major areas include communication systems and software engineering. As the complexity of electronic equipment grew during and after World War II and as the consequences of failures in the field became more and more apparent, the U.S. military became seriously involved, promoted the formation of groups, and became instrumental in the development of the earliest handbooks and specifications. The great northeast blackout in the U.S. in November 1965 triggered the serious application of reliability concepts in the power systems area.

The objectives of this chapter are to introduce the reader to the fundamentals and applications of classical reliability concepts and bring out the important benefits of reliability considerations. Brief summaries of application aspects of reliability for electronic systems and power systems are also included.

110.2 Catastrophic Failure Models

Catastrophic failure refers to the case in which repair of the component is either not possible or available or of no value to the successful completion of the mission originally planned. Modeling such failures is typically based on life test results. We can consider the “lifetime” or “time to failure” T as a continuous random variable. Then,

$$P(\text{survival up to time } t) = P(T > t) \equiv R(t) \quad (110.1)$$

where $R(t)$ is the **reliability** function. Obviously, as $t \rightarrow \infty$, $R(t) \rightarrow 0$ since the probability of failure increases with time of operation. Moreover,

$$P(\text{failure at } t) = P(T \leq t) \equiv Q(t) \quad (110.2)$$

where $Q(t)$ is the unreliability function. From the definition of the distribution function of a continuous random variable, it is clear that $Q(t)$ is indeed the distribution function for T . Therefore, the failure density function $f(t)$ can be obtained as

$$f(t) = \frac{d}{dt} Q(t) \quad (110.3)$$

The **hazard rate function** $\lambda(t)$ is defined as

$$\lambda(t) \equiv \lim_{\Delta t \rightarrow 0} \frac{1}{\Delta t} \left[\begin{array}{l} \text{probability of failure in } (t, t + \Delta t), \\ \text{given survival up to } t \end{array} \right] \quad (110.4)$$

It can be shown that

$$\lambda(t) = \frac{f(t)}{R(t)} \quad (110.5)$$

The four functions, $f(t)$, $Q(t)$, $R(t)$, and $\lambda(t)$ constitute the set of functions used in basic reliability analysis. The relationships between these functions are given in [Table 110.1](#).

TABLE 110.1 Relationships Between Different Reliability Functions

$f(t)$	$\lambda(t)$	$Q(t)$	$R(t)$
$f(t) = f(t)$	$\lambda(t) \exp\left[-\int_0^t \lambda(\xi)d\xi\right]$	$\frac{d}{dt} Q(t)$	$-\frac{d}{dt} R(t)$
$\lambda(t) = \frac{f(t)}{1 - \int_0^t f(\xi)d\xi}$	$\lambda(t)$	$\frac{1}{1 - Q(t)} \frac{d}{dt} (Q(t))$	$-\frac{d}{dt} [\ln R(t)]$
$Q(t) = \int_0^t f(\xi)d\xi$	$1 - \exp\left[-\int_0^t \lambda(\xi)d\xi\right]$	$Q(t)$	$1 - R(t)$
$R(t) = 1 - \int_0^t f(\xi)d\xi$	$\exp\left[-\int_0^t \lambda(\xi)d\xi\right]$	$1 - Q(t)$	$R(t)$

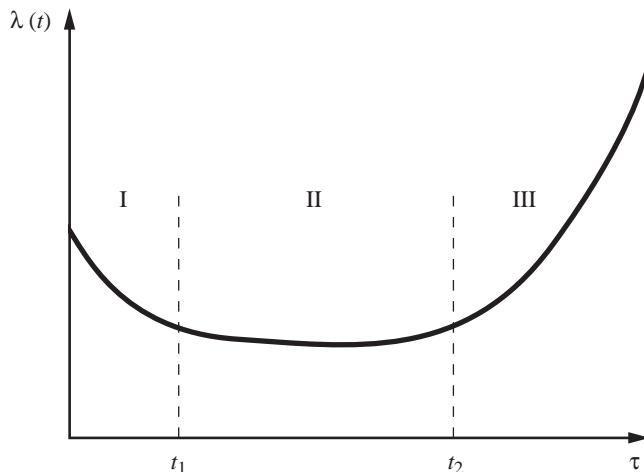


FIGURE 110.1 Bathtub-shaped hazard function

110.3 The Bathtub Curve

Of the four functions discussed, the hazard rate function $\lambda(t)$ displays the different stages during the lifetime of a component most clearly. In fact, typical $\lambda(t)$ plots have the general shape of a bathtub as shown in Fig. 110.1. The first region corresponds to wearin (infant mortality) or early failures during debugging. The hazard rate goes down as debugging continues. The second region corresponds to an essentially constant and low failure rate and failures can be considered to be nearly random. This is the useful lifetime of the component. The third region corresponds to wearout or fatigue phase with a sharply increasing hazard rate.

“Burn-in” refers to the practice of subjecting components to an initial operating period of t_1 (see Fig. 110.1) before delivering them to the customer. This eliminates all the initial failures from occurring after delivery to customers requiring high-reliability components. Moreover, it is prudent to replace a component as it approaches the wearout region, i.e., after an operating period of $(t_2 - t_1)$. Electronic components tend to have a long useful life (constant hazard) period. Wearout region tends to dominate in the case of mechanical components.

110.4 Mean Time To Failure (MTTF)

The mean or expected value of the continuous random variable “time-to-failure” is the *MTTF*. This is a very useful parameter and is often enough to assess the suitability of components. It can be obtained using either the failure density function $f(t)$ or the reliability function $R(t)$ as follows:

$$MTTF = \int_0^\infty t f(t) dt \quad \text{or} \quad \int_0^\infty R(t) dt \quad (110.6)$$

In the case of repairable components, the repair time can also be considered as a continuous random variable with an expected value of *MTTR*. The mean time between failures, *MTBF*, is the sum of *MTTF* and *MTTR*. Since for well-designed components $MTTR \ll MTTF$, *MTBF* and *MTTF* are often used interchangably.

110.5 Average Failure Rate

The average failure rate over the time interval 0 to T is defined as

$$AFR(0, T) \equiv AFR(T) = -\frac{\ln R(T)}{T} \quad (110.7)$$

110.6 A Posteriori Failure Probability

When components are subjected to a burn-in (or wearin) period of duration T , and if the component survives during $(0, T)$, the probability of failure during $(T, T+t)$ is called the *a posteriori* failure probability $Q_c(t)$. It can be found using

$$Q_c(t) = \frac{\int_T^{T+t} f(\xi) d\xi}{\int_T^\infty f(\xi) d\xi} \quad (110.8)$$

The probability of survival during $(T, T+t)$ is

$$R(t|T) = 1 - Q_c(t) = \frac{\int_{T+t}^\infty f(\xi) d\xi}{\int_T^\infty f(\xi) d\xi} = \frac{R(T + t)}{R(T)} = \exp\left[-\int_T^{T+t} \lambda(\xi) d\xi\right] \quad (110.9)$$

110.7 Units for Failure Rates

Several units are used to express failure rates. In addition to $\lambda(t)$ which is usually in number per hour, $\%/K$ is used to denote failure rate in percent per thousand hours and *PPM/K* is used to express failure rate in parts per million per thousand hours. The last unit is also known as *FIT* for “fails in time”. The relationships between these units are given in [Table 110.2](#).

TABLE 110.2 Relationships Between Different Failure Rate Units

	$\lambda(\#/hr)$	%K	PPM/K (FIT)
$\lambda =$	λ	$10^{-5} (\%/\text{K})$	$10^{-9} (\text{PPM}/\text{K})$
$\%/\text{K} =$	$10^5 \lambda$	$\%/\text{K}$	$10^{-4} (\text{PPM}/\text{K})$
PPM/K (FIT) =	$10^9 \lambda$	$10^4 (\%/\text{K})$	PPM/K

110.8 Application of the Binomial Distribution

In an experiment consisting of n identical independent trials, with each trial resulting in success or failure with probabilities of p and q , the probability P_r of r successes and $(n-r)$ failures is

$$P_r = {}_n C_r p^r (1-p)^{n-r} \quad (110.10)$$

If X denotes the number of successes in n trials, then it is a discrete random variable with a mean value of (np) and a variance of (npq) .

In a system consisting of a collection of n identical components with a probability p that a component is defective, the probability of finding r defects out of n is given by the P_r in Eq. (110.10). If p is the probability of success of one component and if at least r of them must be good for system success, then the system reliability (probability of system success) is given by

$$R = \sum_{k=r}^n {}_n C_k p^k (1-p)^{n-k} \quad (110.11)$$

For systems with **redundancy**, $r < n$.

110.9 Application of the Poisson Distribution

For events that occur “in-time” at an average rate of λ occurrences per unit of time, the probability $P_x(t)$ of exactly x occurrences during the time interval $(0, t)$ is given by

$$P_x(t) = \frac{(\lambda t)^x e^{-\lambda t}}{x!} \quad (110.12)$$

The number of occurrences X in $(0, t)$ is a discrete random variable with a mean value μ of (λt) and a standard deviation σ of $\sqrt{\lambda t}$. By setting $X = 0$ in Eq. (110.12), we obtain the probability of no occurrence in $(0, t)$ as $e^{-\lambda t}$. If the event is failure, then no occurrence means success and $e^{-\lambda t}$ is the probability of success or system reliability. This is the well-known and often-used exponential distribution, also known as the constant-hazard model.

110.10 The Exponential Distribution

A constant hazard rate (constant λ) corresponding to the useful lifetime of components leads to the single-parameter exponential distribution. The functions of interest associated with a constant λ are:

$$f(t) = \lambda e^{-\lambda t}, \quad t > 0 \quad (110.13)$$

$$R(t) = e^{-\lambda t} \quad (110.14)$$

$$Q(t) = Q_c(t) = 1 - e^{-\lambda t} \quad (110.15)$$

The *a posteriori* failure probability $Q_c(t)$ is independent of the prior operating time T , indicating that the component does not degrade no matter how long it operates. Obviously, such a scenario is valid only during the useful lifetime (horizontal portion of the bathtub curve) of the component.

The mean and standard deviation of the random variable “lifetime” are

$$\mu \equiv MTTF = \frac{1}{\lambda} \quad \text{and} \quad \sigma = \frac{1}{\lambda} \quad (110.16)$$

110.11 The Weibull Distribution

The Weibull distribution has two parameters, a scale parameter α and a shape parameter β . By adjusting these two parameters, a wide range of experimental data can be modeled in system reliability studies.

The associated functions are

$$\lambda(t) = \frac{\beta t^{\beta-1}}{\alpha^\beta}; \alpha > 0, \beta > 0, t \geq 0 \quad (110.17)$$

$$f(t) = \frac{\beta t^{\beta-1}}{\alpha^\beta} \exp\left[-\left(\frac{t}{\alpha}\right)^\beta\right] \quad (110.18)$$

$$R(t) = \exp\left[-\left(\frac{t}{\alpha}\right)^\beta\right] \quad (110.19)$$

With $\beta = 1$, the Weibull distribution reduces to the constant hazard model with $\lambda = (1/\alpha)$. With $\beta = 2$, the Weibull distribution reduces to the Rayleigh distribution.

The associated *MTTF* is

$$MTTF = \mu = \alpha \Gamma\left(1 + \frac{1}{\beta}\right) \quad (110.20)$$

where Γ denotes the gamma function.

110.12 Combinatorial Aspects

Analysis of complex systems is facilitated by decomposition into functional entities consisting of subsystems or units and by the application of combinatorial considerations and network modeling techniques.

A **series** or **chain structure** consisting of n units is shown in Fig. 110.2. From the reliability point of view, the system will succeed only if all the units succeed. The units may or may not be physically in series. If R_i is the probability of success of the i th unit, then the series system reliability R_s is given as

$$R_s = \prod_{i=1}^n R_i \quad (110.21)$$

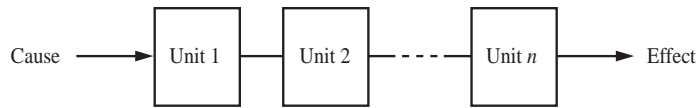


FIGURE 110.2 Series or chain structure.

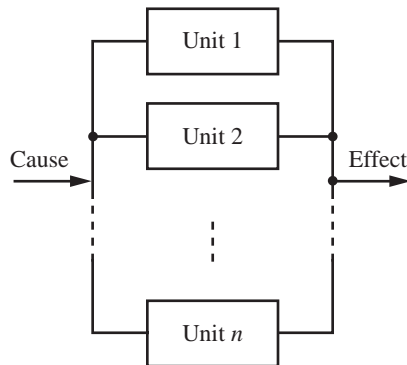


FIGURE 110.3 Parallel structure.

if the units do not interact with each other. If they do, then the conditional probabilities must be carefully evaluated.

If each of the units has a constant hazard, then

$$R_s(t) = \prod_{i=1}^n \exp(-\lambda_i t) \quad (110.22)$$

where λ_i is the constant failure rate for the i th unit or component. This enables us to replace the n components in series by an equivalent component with a constant hazard λ_s where

$$\lambda_s = \sum_{i=1}^n \lambda_i \quad (110.23)$$

If the components are identical, then $\lambda_s = n\lambda$ and the MTTF for the equivalent component is $(1/n)$ of the MTTF of one component.

A **parallel structure** consisting of n units is shown in Fig. 110.3. From the reliability point of view, the system will succeed if any one of the n units succeeds. Once again, the units may or may not be physically or topologically in parallel. If Q_i is the probability of failure of the i th unit, then the parallel system reliability R_p is given as

$$R_p = 1 - \prod_{i=1}^n Q_i \quad (110.24)$$

if the units do not interact with each other (meaning independent).

If each of the units has a constant hazard, then

$$R_p(t) = 1 - \prod_{i=1}^n [1 - \exp(-\lambda_i t)] \quad (110.25)$$

and we do not have the luxury of being able to replace the parallel system by an equivalent component with a constant hazard. The parallel system does not exhibit constant-hazard behavior even though each of the units has constant-hazard.

The *MTTF* of the parallel system can be obtained by using Eq. (110.25) in (110.6). The results for the case of components with identical hazards λ are: $(1.5/\lambda)$, $(1.833/\lambda)$, and $(2.083/\lambda)$ for $n = 2, 3$, and 4 respectively. The largest gain in *MTTF* is obtained by going from one component to two components in parallel. It is uncommon to have more than two or three components in a truly parallel configuration because of the cost involved. For two non-identical components in parallel with hazard rates of λ_1 and λ_2 , the *MTTF* is given as

$$MTTF = \frac{1}{\lambda_1} + \frac{1}{\lambda_2} - \frac{1}{\lambda_1 + \lambda_2} \quad (110.26)$$

An r -out-of- n structure, also known as a partially redundant system, can be evaluated using Eq. (110.11). If all the components are identical, independent, and have a constant hazard of λ , then the system reliability can be expressed as

$$R(t) = \sum_{k=r}^n {}_nC_k e^{-k\lambda t} (1 - e^{-\lambda t})^{n-k} \quad (110.27)$$

For $r = 1$, the structure becomes a parallel system and for $r = n$, it becomes a series system.

Series-parallel systems are evaluated by repeated application of the expressions derived for series and parallel configurations by employing the well-known network reduction techniques.

Several general techniques are available for evaluating the reliability of complex structures that do not come under purely series or parallel or series parallel. They range from inspection to cutset and tieset methods and connection matrix techniques that are amenable for computer programming.

110.13 Modeling Maintenance

Maintenance of a component could be a scheduled (or preventive) one or a forced (corrective) one. The latter follows in-service failures and can be handled using Markov models discussed later. Scheduled maintenance is conducted at fixed intervals of time, irrespective of the system continuing to operate satisfactorily.

Scheduled maintenance, under ideal conditions, takes very little time (compared to the time between maintenances) and the component is restored to an “as new” condition. Even if the component is not repairable, scheduled maintenance postpones failure and prolongs the life of the component. Scheduled maintenance makes sense only for those components with increasing hazard rates. Most mechanical systems come under this category. It can be shown that the density function $f_T^*(t)$ with scheduled maintenance included can be expressed as

$$f_T^*(t) = \sum_{k=0}^{\infty} f_1(t - kT_M) R^k(T_M) \quad (110.28)$$

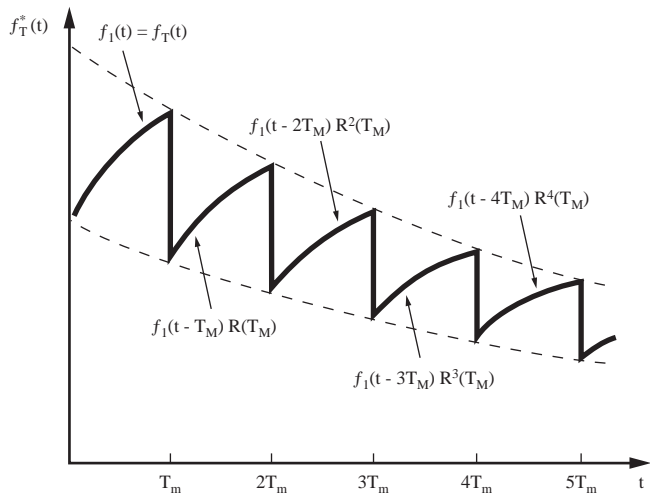


FIGURE 110.4 Density function with ideal scheduled maintenance incorporated.

$$\text{where } f_1(t) = \begin{cases} f_T(t) & \text{for } 0 < t \leq T_M \\ 0 & \text{otherwise} \end{cases} \quad (110.29)$$

$R(t)$ = component reliability function

T_M = time between maintenances, constant

and $f_T(t)$ = original failure density function

In Eq. (110.28), $k = 0$ is used only between $t = 0$ and $t = T_M$; $k = 1$ is used only between $t = T_M$ and $t = 2T_M$ and so on.

A typical $f_T^*(t)$ is shown in Fig. 110.4. The time scale is divided into equal intervals of T_M each. The function in each segment is a scaled-down version of the one in the previous segment, the scaling factor being equal to $R(T_M)$. Irrespective of the nature of the original failure density function, scheduled maintenance gives it an exponential tendency. This is another justification for the widespread use of exponential distribution in system reliability evaluations.

110.14 Markov Models

Of the different Markov models available, the discrete-state continuous-time Markov process has found many applications in system reliability evaluation, including the modeling of repairable systems. The model consists of a set of discrete states, called the state space, in which the system can reside and a set of transition rates between appropriate states. Using these, a set of first order differential equations are derived in the standard vector-matrix form for the time-dependent probabilities of the various states. Solution of these equations incorporating proper initial conditions gives the probabilities of the system residing in different states as functions of time. Several useful results can be gleaned from these functions.

110.15 Binary Model for a Repairable Component

The binary model for a repairable component assumes that the component can exist in one of two states—the UP state or the DOWN state. The transition rates between these two states, S_0 and S_1 , are assumed to be constant

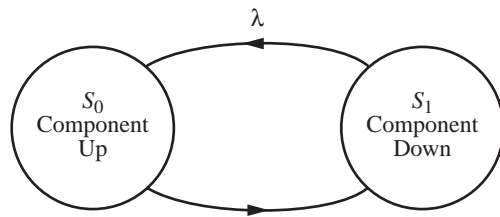


FIGURE 110.5 State space diagram for a single reparable component.

and equal to λ and μ . These transition rates are the constant failure and repair rates implied in the modeling process and their reciprocals are the MTTF and MTTR, respectively. [Figure 110.5](#) illustrates the binary model.

The associated Markov differential equations are

$$\begin{bmatrix} P'_0(t) \\ P'_1(t) \end{bmatrix} = \begin{bmatrix} -\lambda & \mu \\ \lambda & -\mu \end{bmatrix} \begin{bmatrix} P_0(t) \\ P_1(t) \end{bmatrix} \quad (110.30)$$

with the initial conditions

$$\begin{bmatrix} P_0(0) \\ P_1(0) \end{bmatrix} = \begin{bmatrix} 1 \\ 0 \end{bmatrix} \quad (110.31)$$

The coefficient matrix of Markov differential equations, namely $\begin{bmatrix} -\lambda & \mu \\ \lambda & -\mu \end{bmatrix}$

is obtained by transposing the matrix of rates of departures $\begin{bmatrix} 0 & \lambda \\ \mu & 0 \end{bmatrix}$

and replacing the diagonal entries by the negative of the sum of all the other entries in their respective columns. Solution of (110.30) with initial conditions as given by (110.31) yields:

$$P_0(t) = \frac{\mu}{\lambda + \mu} + \frac{\lambda}{\lambda + \mu} e^{-(\lambda+\mu)t} \quad (110.32)$$

$$P_1(t) = \frac{\lambda}{\lambda + \mu} \left[1 - e^{-(\lambda+\mu)t} \right] \quad (110.33)$$

The limiting, or steady-state, probabilities are found by letting $t \rightarrow \infty$. They are also known as limiting **availability** A and limiting unavailability U and they are

$$P_0 \equiv \frac{\mu}{\lambda + \mu} \equiv A \quad \text{and} \quad P_1 = \frac{\lambda}{\lambda + \mu} \equiv U \quad (110.34)$$

The time-dependent $A(t)$ and $U(t)$ are simply $P_0(t)$, and $P_1(t)$ respectively.

Referring back to Eq. (110.14) for a constant hazard component and comparing it with Eq. (110.32) which incorporates repair, the difference between $R(t)$ and $A(t)$ becomes obvious. Availability $A(t)$ is the probability

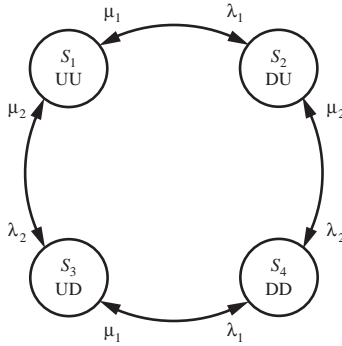


FIGURE 110.6 State space diagram for two dissimilar repairable components.

that the component is up at time t and reliability $R(t)$ is the probability that the system has continuously operated from 0 to t . Thus, $R(t)$ is much more stringent than $A(t)$. While both $R(0)$ and $A(0)$ are unity, $R(t)$ drops off rapidly as compared to $A(t)$ as time progresses. With a small value of $MTTR$ (or large value of μ), it is possible to realize a very high availability for a repairable component.

110.16 Two Dissimilar Repairable Components

Irrespective of whether the two components are in series or in parallel, the state space consists of four possible states. They are: S_1 (1 up, 2 up), S_2 (1 down, 2 up), S_3 (1 up, 2 down), and S_4 (1 down, 2 down). The actual system configuration will determine which of these four states corresponds to system success and failure. The associated state-space diagram is shown in Fig. 110.6. Analysis of this system results in the following steady-state probabilities:

$$P_1 = \frac{\mu_1 \mu_2}{\text{Denom}} ; P_2 = \frac{\lambda_1 \mu_2}{\text{Denom}} ; P_3 = \frac{\lambda_2 \mu_1}{\text{Denom}} ; P_4 = \frac{\lambda_1 \lambda_2}{\text{Denom}} \quad (110.35)$$

$$\text{where Denom} \equiv (\lambda_1 + \mu_1)(\lambda_2 + \mu_2) \quad (110.36)$$

For components in series, $A = P_1$ and $U = (P_2 + P_3 + P_4)$ and the two components can be replaced by an equivalent component with a failure rate of $\lambda_s = (\lambda_1 + \lambda_2)$ and a mean repair duration of r_s where

$$r_s \equiv \frac{\lambda_1 r_1 + \lambda_2 r_2}{\lambda_s} \quad (110.37)$$

Extending this to n components in series, the equivalent system will have

$$\lambda_s = \sum_{i=1}^n \lambda_i \quad \text{and} \quad r_s \equiv \frac{1}{\lambda_s} \sum_{i=1}^n \lambda_i r_i \quad (110.38)$$

$$\text{and system unavailability} = U_s \equiv \lambda_s r_s = \sum_{i=1}^n \lambda_i r_i \quad (110.39)$$

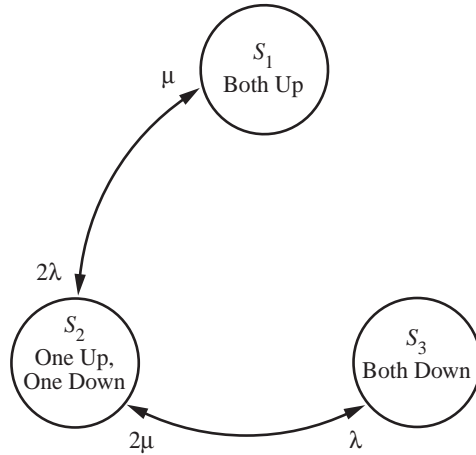


FIGURE 110.7 State space diagram for two identical repairable components.

For components in parallel, $A = (P_1 + P_2 + P_3)$ and $U = P_4$ and the two components can be replaced by an equivalent component with

$$\lambda_p \equiv \lambda_1(\lambda_2 r_1) + \lambda_2(\lambda_1 r_2) \text{ and } \mu_p = \mu_1 + \mu_2 \quad (110.40)$$

$$\text{and system unavailability} = U_p = \lambda_p(1/\mu_p) \quad (110.41)$$

Extension to more than two components in parallel follows similar lines. For three components in parallel,

$$\mu_p = (\mu_1 + \mu_2 + \mu_3) \text{ and } U_p = \lambda_1\lambda_2\lambda_3 r_1 r_2 r_3 \quad (110.42)$$

110.17 Two Identical Repairable Components

In this case, only three states are needed to complete the state space. They are: S_1 : Both UP; S_2 : One UP and One DOWN; and S_3 : Both DOWN. The corresponding state space diagram is shown in Fig. 110.7. Analysis of this system results in the following steady-state probabilities:

$$P_1 = \left(\frac{\mu}{\lambda + \mu} \right)^2; P_2 = \frac{2\lambda}{\mu} \left(\frac{\mu}{\lambda + \mu} \right)^2; P_3 = \left(\frac{\lambda}{\lambda + \mu} \right)^2 \quad (110.43)$$

110.18 Frequency and Duration Techniques

The expected residence time in a state is the mean value of the passage time from the state in question to any other state. Cycle time is the time required to complete an “in” and “not-in” cycle for that state. Frequency of occurrence (or encounter) for a state is the reciprocal of its cycle time. It can be shown that the frequency of occurrence of a state is equal to the steady-state probability of being in that state times the total rate of departure from it. Also, the expected value of the residence time is equal to the reciprocal of the total rate of departure from that state.

Under steady-state conditions, the expected frequency of entering a state must be equal to the expected frequency of leaving that state (this assumes that the system is “ergodic”, which will not be elaborated for lack

of space). Using this principle, frequency balance equations can be easily written (one for each state) and solved in conjunction with the fact that the sum of the steady-state probabilities of all the states must be equal to unity to obtain the steady state probabilities. This procedure is much simpler than solving the Markov differential equations and letting $t \rightarrow \infty$.

110.19 Applications of Markov Process

Once the different states are identified and a state-space diagram is developed, Markov analysis can proceed systematically (probably with the help of a computer in the case of large systems) to yield a wealth of results useful in system reliability evaluation. Inclusion of installation time after repair, maintenance, spare, standby systems, and limitations imposed by restricted repair facilities are some of the many problems that can be studied.

110.20 Some Useful Approximations

- For an r-out-of-n structure with failure and repair rates of λ and μ for each, the equivalent MTTR and MTTF can be approximated as

$$MTTR_{eq} = \frac{MTTR \text{ of one component}}{n - r + 1} \quad (110.44)$$

$$MTTF_{eq} = \left(\begin{array}{c} MTTF \\ \text{of one} \\ \text{component} \end{array} \right) \left(\frac{MTTF}{MTTR} \right)^{n-r} \left\{ \frac{(n-r)! (r-1)!}{n!} \right\} \quad (110.45)$$

- Influence of weather must be considered for components operating in an outdoor environment. If λ and λ' are the normal weather and stormy weather failure rates, λ' will be much greater than λ and the average failure rate λ_f can be approximated as

$$\lambda_f \equiv \left(\frac{N}{N + S} \right) \lambda + \left(\frac{S}{N + S} \right) \lambda' \quad (110.46)$$

where N and S are the expected durations of normal and stormy weather.

- For well-designed high-reliability components, the failure rate λ will be very small and $\lambda t \ll 1$. Then, for a single component,

$$R(t) \equiv 1 - \lambda t \quad \text{and} \quad Q(t) \equiv \lambda t \quad (110.47)$$

and for n dissimilar components in series,

$$R(t) \equiv 1 - \sum_{i=1}^n \lambda_i t \quad \text{and} \quad Q(t) \equiv \sum_{i=1}^n \lambda_i t \quad (110.48)$$

For the case of n identical components in parallel,

$$R(t) \equiv 1 - (\lambda t)^n \quad \text{and} \quad Q(t) \equiv (\lambda t)^n \quad (110.49)$$

For the case of an r-out-of-n configuration,

$$Q(t) \equiv {}_n C_{(n-r+1)} (\lambda t)^{n-r+1} \quad (110.50)$$

The approximations detailed in (3) are called rare-event approximations.

110.21 Application Aspects

Electronic systems utilize large numbers of similar components over which the designer has very little control. Quality control methods can be used in the procurement and manufacturing phases. However, the circuit designer has no control over the design reliability of the devices except in cases such as custom-designed integrated circuits. In addition, electronic components cannot be inspected easily because of encapsulation. Although gross defects can be easily detected by suitable testing processes, defects that are not immediately effective (for example, weak mechanical bond of a lead-in conductor, material flaws in semiconductors, defective sealing, etc.) primarily contribute to unreliability. Temperature and voltage are the predominant failure-accelerating stresses for the majority of electronic components. As weaker components fail and are replaced by better ones, the percentage of defects in a population is reduced, resulting in a decreasing hazard rate. Wearout is rarely of significance in the failure of electronic components and systems. The designer should be careful to ensure that the loads (voltage, current, temperature) are within rated values and strive for a design that minimizes hot spots and temperature rises. Parameter drifts and accidental short circuits at connections can also lead to system failures. The circuit designer can follow a few basic rules to significantly improve electronic system reliability: reduce the number of adjustable components; avoid selection of components on the basis of parameter values obtained by testing; assemble components such that adjustments are easily accessible; and partition circuits into subassemblies for easy testing and diagnosis of problems.

Power systems are expected to provide all customers a reliable supply of electric power upon which much of modern life depends. Power systems are also very large, consisting of scores of large generators, hundreds of miles of high-voltage transmission lines, thousands of miles of distribution lines, along with the necessary transformers, switchgear, and substations interconnecting them. Reliability at the customer level can be improved by additional investment; the challenge is to balance reliability and the associated investment cost against the cost of energy charged to customers. This should be done in the presence of a number of random inputs and events: generator outages, line outages (which are highly weather dependent), random component outages, and uncertainties in the load demand (which is also weather dependent). Probabilistic techniques to evaluate power system reliability have been used effectively to resolve this problem satisfactorily. The system is divided into a number of subsystems and each one is analyzed separately. Then, composite system reliability evaluation techniques are employed to combine the results and arrive at a number of quantifiable reliability indices as inputs to managerial decisions. The major subsystems involved are generation, transmission, distribution, substations, and protection systems. Care should be taken to ensure that reliabilities of different parts of the system conform to each other and that no part of the system is unusually strong or weak. Obviously, different levels of reliability will be required for different parts of the system depending on the impacts of failures at different points on the interconnected power system.

110.22 Reliability and Economics

Reliability and economics are very closely related. Issues such as the level of reliability required, the amount of additional expenditures justified, where to invest the additional resources to maximize reliability, how to achieve a certain level of overall reliability at minimum cost, and how to assess the cost of failures and monetary equivalent of non-monetary items are all quite complex and not purely technical. However, once managerial decisions are made and reliability goals are set, certain well-proven techniques such as incorporating redundancy, improving maintenance procedures, selecting better quality components, etc. can be employed by the designer to achieve the goals.

Defining Terms

Availability: The availability $A(t)$ is the probability that a system is performing its required function successfully at time t . The steady-state availability A is the fraction of time that an item, system, or component is able to perform its specified or required function.

Bathtub curve: For most physical components and living entities, the plot of failure (or hazard) rate vs. time has the shape of the longitudinal cross-section of a bathtub and hence its name.

Hazard rate function: The plot of instantaneous failure rate vs. time is called the hazard function. It clearly and distinctly exhibits the different life cycles of the component.

MTTF: The mean time to failure is the mean or expected value of “time to failure”.

Parallel structure: Also known as a completely redundant system, it describes a system that can succeed when at least one of two or more components succeeds.

Redundancy: Refers to the existence of more than one means, identical or otherwise, for accomplishing a task or mission.

Reliability: The reliability $R(t)$ of an item or system is the probability that it has performed successfully over the time interval from 0 to t . In the case of non-repairable systems, $R(t) = A(t)$. With repair, $R(t) \leq A(t)$.

Series structure: Also known as a chain structure or non-redundant system, it describes a system whose success depends on the success of all of its components.

Related Topics

23.2 Testing • 98.5 Mean Time to Failure • 98.10 Markov Modeling • 98.12 Reliability Calculations for Real Time Systems

References

- R. Billinton and R.N. Allan, *Reliability Evaluation of Engineering Systems: Concepts and Techniques*, 2nd ed., New York: Plenum, 1992.
- E.E. Lewis, *Introduction to Reliability Engineering*, New York: John Wiley & Sons, 1987.
- M.G. Pecht and F.R. Nash, “Predicting the reliability of electronic equipment”, Proc. IEEE, 82(7), 992–1004, 1994.
- R. Ramakumar, *Engineering Reliability: Fundamentals and Applications*, Englewood Cliffs, N.J.: Prentice-Hall, 1993.
- M.L. Shooman, *Probabilistic Reliability: An Engineering Approach*, 2nd ed., Malabar, Fla.: R.E. Krieger Publishing Company, 1990.

For Further Information

- R. Billinton and R.N. Allan, *Reliability Evaluation of Power Systems*, London, England: Pitman Advanced Publishing Program, 1984.
- A.E. Green and A.J. Bourne, *Reliability Technology*, New York: Wiley-Interscience, 1972.
- E.J. Henley and H. Kumamoto, *Probabilistic Risk Assessment—Reliability Engineering, Design, and Analysis*, New York: IEEE Press, 1991.
- IEEE Transactions on Reliability*, New York: Institute of Electrical and Electronics Engineers.
- P.D.T. O'Connor, *Practical Reliability Engineering*, 3rd ed. New York: John Wiley & Sons, 1985.
- Proceedings: Annual Reliability and Maintainability Symposium*, New York: Institute of Electrical and Electronics Engineers.
- D.P. Siewiorek, and R.S. Swarz, *The Theory and Practice of Reliable System Design*, Bedford, Mass.: Digital Press, 1982.
- K.S. Trivedi, *Probability and Statistics with Reliability, Queuing, and Computer Science Applications*, Englewood Cliffs, N.J.: Prentice-Hall, 1982.
- A. Villemeur, *Reliability, Availability, Maintainability and Safety Assessment, Volumes I and II*, New York: John Wiley & Sons, 1992.

Blades, K., Allenby, B. "Environmental Effects"
The Electrical Engineering Handbook
Ed. Richard C. Dorf
Boca Raton: CRC Press LLC, 2000

111

Environmental Effects

Karen Blades and
Braden Allenby

*Lawrence Livermore
National Laboratory*

- 111.1 Introduction
- 111.2 Industrial Ecology
- 111.3 Design for Environment
- 111.4 Environmental Implications for the Electronics Industry
- 111.5 Emerging Technology
 - Integrated Circuits • Printed Wiring Boards
- 111.6 Tools and Strategies for Environmental Design
 - Design Tools • Design Strategies • Conclusion • Acknowledgements • Disclaimer

111.1 Introduction

The importance of electronics technology for consumers, and the electronics sector for the global economy, is already substantial and continues to grow rapidly. Such growth and innovation coupled with the global concerns for the environment and the need to better manage the resources of the earth pose many challenges for the electronics industry. While thought of as a “clean” industry, the technological advances made by the industry creates a significant demand on the earth’s resources. As an example, the amount of water required in the production of semiconductors, the engines that motor most of today’s electronic gadgets, is enormous—about 2000 gallons to process a single silicon wafer. Building silicon chips requires the use of highly toxic materials, albeit in relatively low volumes. Similarly, printed wiring boards present in most electronic products and produced in high volume use large amounts of solvents or gases which are either health hazards, ozone depleting, or contribute to the greenhouse effect and contain lead solder. The challenge for the industry is to continue the innovation that delivers the products and services that people want yet find creative solutions to minimize the environmental impact, enhance competitiveness, and address regulatory issues without impacting quality, productivity, or cost; in other words, to become an industry that is more “eco-efficient”. Eco-efficiency is reached by the delivery of competitively priced goods and services that satisfy human needs and support a high quality of life, while progressively reducing ecological impacts and resource intensity, to a level at least in line with the earth’s estimated carrying capacity.

Like sustainable development, a concept popularized by the Brundtland Report, *Our Common Future*, the notion of eco-efficiency requires a fundamental shift in the way environment is considered in industrial activity. Sustainable development—“development that meets the needs of the present without compromising the ability of future generations to meet their own needs” [World Commission on Environment and Development, 1987]—contemplates the integration of environmental, economic, and technological considerations to achieve continued human and economic development within the biological and physical constraints of the planet. Both eco-efficiency and sustainable development provide a useful direction, yet they prove difficult to operationalize and cannot guide technology development. Thus, the theoretical foundations for integrating technology and environment throughout the global economy are being provided by a new, multidisciplinary field known as “**industrial ecology**”.

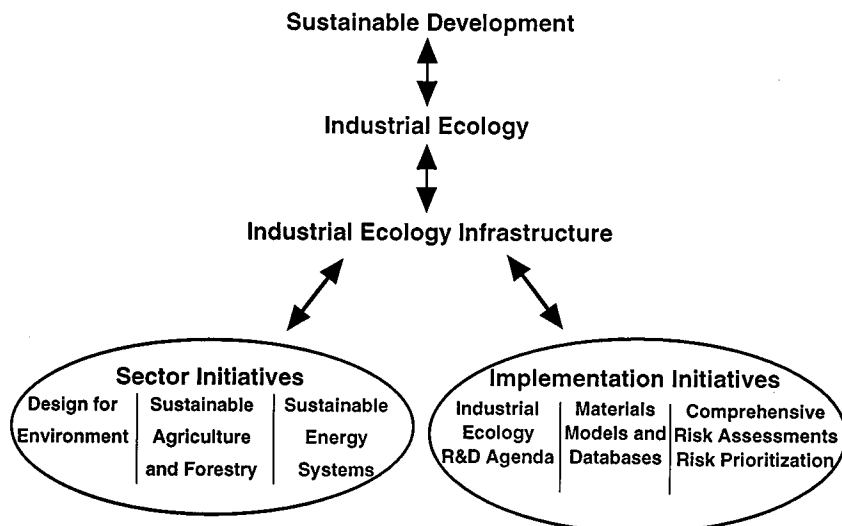


FIGURE 111.1 Industrial ecology framework.

The ideas of industrial ecology, which have begun to take root in the engineering community, have helped to establish a framework within which the industry can move toward realizing sustainable development. The electrical, electronics, and telecommunications sectors are enablers of sustainability because they allow the provision of increasing quality-of-life using less material and energy, respectively, “**dematerialization**” and “**decarbonization**”. This chapter will provide an introduction into industrial ecology and its implications for the electronics industry. Current activities, initiatives, and opportunities will also be explored, illustrating that the concomitant achievement of greater economic and environmental efficiency is indeed feasible in many cases.

111.2 Industrial Ecology

Industrial ecology is an emerging field that views manufacturing and other industrial activity including forestry, agriculture, mining, and other extractive sectors, as an integral component of global natural systems. In doing so, it takes a systems view of design and manufacturing activities so as to reduce or, more desirably, eliminate the environmental impacts of materials, manufacturing processes, technologies, and products across their life cycles, including use and disposal. It incorporates, among other things, research involving energy supply and use, new materials, new technologies and technological systems, basic sciences, economics, law, management, and social sciences.

The study of industrial ecology will, in the long run, provide the means by which the human species can deliberately and rationally approach a desirable long-term global carrying capacity. Oversimplifying, it can be thought of as “the science of sustainability”. The approach is “deliberate” and “rational”, to differentiate it from other, unplanned paths that might result, for example, in global pandemics, or economic and cultural collapse. The endpoint is “desirable”, to differentiate it from other conceivable states such as a Malthusian subsistence world, which could involve much lower population levels, or oscillating population levels that depend on death rates to maintain a balance between resources and population levels. Figure 111.1 illustrates how industrial ecology provides a framework for operationalizing the vision of sustainable development.

As the term implies, industrial ecology is concerned with the evolution of technology and economic systems such that human economic activity mimics a mature biological system from the standpoint of being self-contained in its material and resource use. In such a system, little if any virgin material input is required, and little if any waste that must be disposed of outside of the economic system is generated. Energetically, the system can be open, just as biological systems are, although it is likely that overall energy consumption and intensity will be limited.

Although it is still a nascent field, a few fundamental principles are already apparent. Most importantly, the evolution of environmentally appropriate technology is seen as critical to reaching and maintaining a sustainable state. Unlike earlier approaches to environmental issues, which tended to regard technology as neutral at best, industrial ecology focuses on development of economically and environmentally efficient technology as key to any desirable, sustainable global state.

Also, environmental considerations must be integrated into all aspects of economic behavior, especially product and process design, and the design of economic and social systems within which those products are used and disposed. Environmental concerns must be internalized into technological systems and economic factors. It is not sufficient to design an energy efficient computer, for example; it is also necessary to ensure that the product, its components, or its constituent materials can be refurbished or recycled after the customer is through with it—all of this in a highly competitive and rapidly evolving market. This consideration implies a comprehensive and systems-based approach that is far more fundamental than any we have yet developed.

Industrial ecology requires an approach that is truly multidisciplinary. It is important to emphasize that industrial ecology is an objective field of study based on existing scientific and technological disciplines, not a form of industrial policy. It is profoundly a systems oriented and comprehensive approach which poses problems for most institutions—the government, riddled with fiefdoms; academia, with rigid departmental lines; and private firms, with job slots defined by occupation. Nonetheless, it is all too frequent that industrial ecology is seen as an economic program by economists, a legal program by lawyers, a technical program by engineers, and a scientific program by scientists. It is in part each of these; more importantly, it is all of these.

Industrial ecology has an important implication, however, of special interest to electronics and telecommunications engineers, and thus deserving of emphasis. The achievement of sustainability will, in part, require the substitution of intellectual and information capital for traditional physical capital, energy, and material inputs. Environmentally appropriate electronics, information management, and telecommunications technologies and services—and the manufacturing base that supports them—are therefore enabling technologies to achieve sustainable development. This offers unique opportunities for professional satisfaction, but also places a unique responsibility on the community of electrical and electronics engineers. We in particular cannot simply wait for the theory of industrial ecology to be fully developed before taking action.

111.3 Design for Environment

Design for Environment (DFE) is the means by which the precepts of industrial ecology, as currently understood, can in fact begin to be implemented in the real world today. DFE requires that environmental objectives and constraints be driven into process and product design, and materials and technology choices.

The focus is on the design stage because, for many articles, that is where most, if not all, of their life cycle environmental impacts are explicitly or implicitly established. Traditionally, electronics design has been based on a correct-by-verification approach, in which the environmental ramifications of a product (from manufacturing through disposition) are not considered until the product design is completed. DFE, by contrast, takes place early in a product's design phase as part of the concurrent engineering process to ensure that the environmental consequences of a product's life cycle are understood before manufacturing decisions are committed.

It is estimated that some 80 to 90% of the environmental impacts generated by product manufacture, use, and disposal are “locked-in” by the initial design. Materials choices, for example, ripple backwards towards environmental impacts associated with the extractive, smelting, and chemical industries. The design of a product and component selection control many environmental impacts associated with manufacturing, enabling, for example, substitution of no-clean or aqueous cleaning of printed wiring boards for processes that release ozone depleting substances, air toxics, or volatile organic compounds that are precursors of photochemical smog. The design of products controls many aspects of environmental impacts during use—energy efficient design is one example. Product design also controls the ease with which a product may be refurbished, or disassembled for parts or materials reclamation, after consumer use. DFE tools and methodologies offer a means to address such concerns at the design stage.

Obviously, DFE is not a panacea. It cannot, for example, compensate for failures of the current price structure to account for external factors, such as the real (i.e., social) cost of energy. It cannot compensate for deficiencies

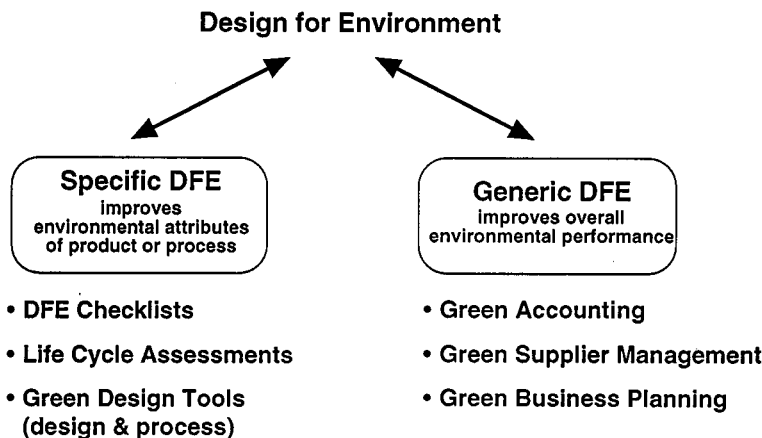


FIGURE 111.2 Examples of DFE activities within the firm.

in sectors outside electronics, such as a poorly coordinated, polluting, or even non-existent disposal and material recycling system in some areas of the world. Moreover, it is important to realize that DFE recognizes environmental considerations as on par with other objective and constraints—such as economic, technological, and market structure—not as superseding or dominating them. Nonetheless, if properly implemented, DFE programs represent a quantum leap forward in the way private firms integrate environmental concerns into their operations and technology.

It is useful to think of DFE within the firm as encompassing two different groups of activities as shown in Fig. 111.2. In all cases, DFE activities require inclusion of life-cycle considerations in the analytical process. The first, which might be styled “generic DFE”, involves the implementation of broad programs that make the company’s operations more environmentally preferable across the board. This might include, for example, development and implementation of “green accounting” practices, which ensure that relevant environmental costs are broken out by product line and process, so that they can be managed down. The “standard components” lists maintained by many companies can be reviewed to ensure that they direct the use of environmentally appropriate components and products wherever possible. Thus, for example, open relays might be deleted from such lists, on the grounds that they “can’t swim”, and thus might implicitly establish a need for chlorinated solvent, as opposed to aqueous, cleaning systems.

Contract provisions can be reviewed to ensure that suppliers are being directed to use environmentally preferable technologies and materials where possible. For example, are virgin materials being required where they are unnecessary? Do contracts, standards, and specifications clearly call for the use of recycled materials where they meet relevant performance requirements? Likewise, customer and internal standards and specifications can be reviewed with the same goal in mind.

The second group of DFE activities can be thought of as “specific DFE”. Here, DFE is considered as a module of existing product realization processes, specifically the “Design for X”, or DFX, systems used by many electronics manufacturers. The method involves creation of software tools and checklists, similar to those used in Design for Manufacturability, Design for Testability, or Design for Safety modules that ensure relevant environmental considerations are also included in the design process from the beginning. The challenge is to create modules which, in keeping with industrial ecology theory, are broad, comprehensive, and systems-based, yet can be defined well enough to be integrated into current design activities.

The successful application of DFE to the design of electronic systems requires the coordination of several design and data-based activities, such as environmental impact metrics; data and data management; design optimization, including cost assessments; and others. Failure to address any of these aspects can limit the effectiveness and usefulness of DFE efforts. Data and methodological deficiencies abound, and the challenge is great, yet experience at world class companies such as AT&T, Digital, IBM, Motorola, Siemens Nixdorf, Volvo, and Xerox indicate that it can be done. AT&T, for example, is testing a draft DFE practice; baselining the environmental attributes of a telephone at different life cycle stages to determine where meaningful environmental

improvements in design can be achieved; and developing software tools that can inform environmentally preferable design decisions [Seifert, 1995]. In Sweden, the government and Volvo have developed a relatively simple Environment Priority Strategies for Environmental Design, or EPS, system which uses Environmental Load Units, or ELUs, to inform materials choices during the design process. In Germany, Siemens Nixdorf has developed an “Eco-balance” system to help it make design choices that reflect both environmental and economic requirements. Xerox is a world leader in designing their products for refurbishment using a product life extension approach.

More broadly, the American Electronics Association (AEA) Design for Environment Task Force has created a series of White Papers discussing various aspects of Design for Environment and its implementation. The Microelectronics and Computer Technology Corporation (MCC) has published a comprehensive study [Lipp *et al.*, 1993] of the environmental impacts of a computer workstation, which is valuable not only for its technical findings, but for the substantial data and methodological gaps the study process identified. The Society of Environmental Toxicology and Chemistry (SETAC) and others, especially in Europe, are working on a number of comprehensive life-cycle assessment (LCA) methodologies designed to identify and prioritize environmental impacts of substances throughout their life cycle. The International Organization for Standards (ISO) is in the process of creating an international LCA standard. The IEEE Environment, Health and Safety Committee, formed in July, 1992, to support the integration of environmental, health, and safety considerations into electronics products and processes from design and manufacturing, to use, to recycling, refurbishing, or disposal has held a series of annual symposium on electronics and the environment. The proceedings from these symposia are valuable resources to the practitioners of DFE.

111.4 Environmental Implications for the Electronics Industry

Global concerns and regulations associated with environmental issues are increasingly affecting the manufacturing and design of electronic products, their technology development, and marketing strategies. No point illustrates this better than the German Blue Angel **Eco-Labeling** scheme for personal computers (the Blue Angel is a quasi-governmental, multi-attribute eco-labeling program). The Blue Angel requirements are numerous and span the complete life-cycle of the computers. Examples of some the requirements include: modular design of the entire system, customer-replaceable subassemblies and modules, use of non-halogenated flame retardants, and take back by manufacturers at the end of the product life. Market requirements such as these, focused on products and integrating as they do environmental and technology considerations, cannot possibly be met by continuing to treat environmental impact as an unavoidable result of industrial activity, i.e., as overhead. These requirements make environmental concerns truly strategic for the firm.

Perhaps the most familiar example of “a new generation of environmental management” requirements which will have enormous effects on electronics design is **“product take back”**. These programs, such as the one mentioned in the Blue Angel labeling scheme, are being introduced in Germany and other countries for electronics manufacturers. They generally require that the firm take its products back once the consumer is through with them, recycle or refurbish the product, and assume responsibility for any remaining waste generated by the product. Other members of the European Union and Japan are among others considering such “take back” requirements. Similarly, the emergence of the international standard, **ISO 14000**, which includes requirements for environmental management systems, methodologies for **life cycle assessment** and environmental product specifications will have vast implications for the electronics industry. Though technically voluntary, in practice these standards in fact become requirements for firms wishing to engage in global commerce. These examples represent a global trend towards proactive management of business and products in the name of the environment.

111.5 Emerging Technology

New tools and technologies are emerging which will influence the environmental performance of electronic products and help the industry respond to the regulatory “push” and the market “pull” for environmentally responsible products. In the electronics industry, technology developments are important not only for the end-products, but

for components, recycling, and materials technology as well. Below is a brief summary of technology developments and their associated environment impacts as well as tools to address the many environmental concerns facing the industry.

The electronics industry has taken active steps toward environmental stewardship, evidenced by the formulation of the IEEE Environment, Safety and Health Committee, the 1996 Electronics Industry Environmental Roadmap published by MCC, and chapters focused on environment in The National Technology Roadmap for Semiconductors. Moves such as this, taken together with the technical sophistication of control systems used in manufacturing processes, have allowed the electronics industry to maintain low emission levels relative to some other industries. Despite the industry's environmental actions, the projected growth in electronics over the next 10 to 20 years is dramatic and continued technological innovation will be required to maintain historically low environmental impacts. Moreover, the rapid pace of technological change generates concomitantly high rates of product obsolescence and disposal, a factor that has led countries such as Germany and the Netherlands to focus on electronics products for environmental management.

Environmental considerations are not, of course, the only forces driving the technological evolution in the electronics industry. Major driving forces, as always, also include price, cost, performance, and market/regulatory requirements. However, to the extent that the trend is toward smaller devices, fewer processing steps, increased automation, and higher performance per device, such evolution will likely have a positive environmental impact at the unit production level, i.e., less materials, less chemicals, less waste related to each unit produced. Technology advances that have environmental implications at the upstream processing stage may well have significant benefits in the later stages of systems development and production. For example, material substitution in early production stages may decrease waste implications throughout the entire process. Since both semiconductors and printed wiring boards are produced in high volume and are present in virtually all electronic products ranging from electronic appliances, to computers, automotive, aerospace, and military applications, we will briefly examine the impact of these two areas of the electronic industry.

Integrated Circuits

The complex process of manufacturing semiconductor integrated circuits (IC) often consists of over a hundred steps during which many copies of an individual IC are formed on a single wafer. Each of the major process steps used in IC manufacturing involves some combination of energy use, material consumption, and material waste. Water usage is high due to the many cleaning and rinsing process steps. Absent process innovation, this trend will continue as wafer sizes increase, driving up the cost of water and waste water fees, and increasing mandated water conservation.

Environmental issues that also require attention include the constituent materials for encapsulants, the metals used for connection and attachment, the energy consumed in high-temperature processes, and the chemicals and solvents used in the packaging process. Here, emerging packaging technologies will have the effect of reducing the quantity of materials used in the packaging process by shrinking IC package sizes. Increasing predominance of plastic packaging will reduce energy consumption associated with hermetic ceramic packaging.

Printed Wiring Boards

Printed wiring boards represent the dominant interconnect technology on which chips will be attached and represents another key opportunity for making significant environmental advances. PWB manufacturing is a complicated process and uses large amounts of materials and energy (e.g., 1 MegaW of heat and 220 kW of energy is consumed during fabrication of prepeg for PWBs). On average, the waste streams constitutes 92%—and the final product just 8%—of the total weight of the materials used in PWB production process. Approximately 80% of the waste produced is hazardous and most of the waste is aqueous, including a range of hazardous chemicals. Printed wiring boards are not recycled because the removal of soldered sub-assemblies is costly and advanced chip designs require new printed wiring boards to be competitive. As a result, the boards are incinerated and the residual ash buried in hazardous waste landfills due to the lead content (from lead solder).

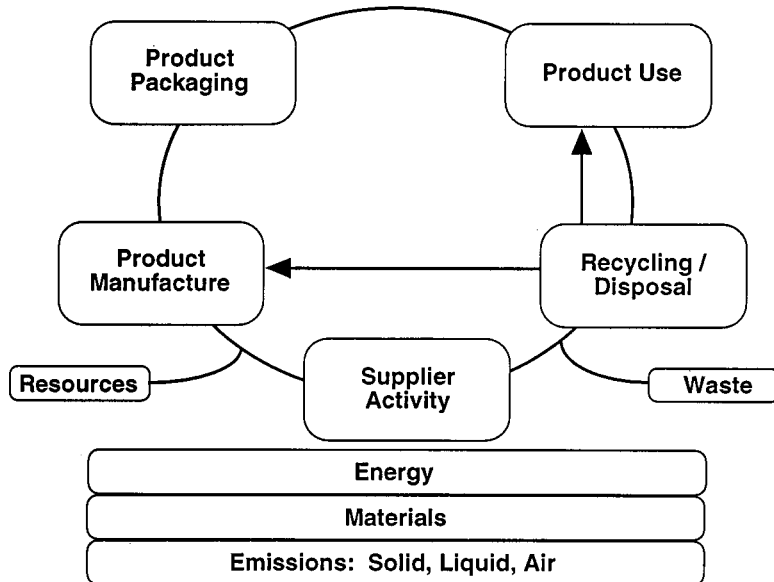


FIGURE 111.3 Design for environment: systems-based, life cycle approach.

111.6 Tools and Strategies for Environmental Design

The key to reducing the environmental impact of electronic products will be the application of DFE tools and methodologies. Development of CAD/CAM tools based on environmental impact metrics, materials selection data, cost, and product data management are examples of available or clearly foreseeable tools to assist firms in adopting DFE practices.

These tools will need to be based on life cycle assessment, the objective process used to evaluate the environmental impacts associated with a product and identify opportunities for improvement. Life cycle assessment seeks to minimize the environmental impact of the manufacture, use, and eventual disposal of products without compromising essential product functions. Figure 111.3 shows the life stages that would be considered for electronic products (i.e., the life cycle considered has been bounded by product design activities). The ability of the electronics industry to operate in a more environmentally and economically efficient mode, use less chemicals and materials, and reduce energy consumption will require support tools that can be used to evaluate both product and process designs. To date, many firms are making immediate gains by incorporating basic tools like DFE checklists, design standards and internal databases on chemicals and materials, while other firms are developing sophisticated software tools that give products environmental scores based on the product's compliance with a set of predetermined environmental attributes. These software tools rely heavily on environmental metrics (typically internal to the firm) to assess the environmental impact and then assign a score to the associated impact.

Other types of tools that will be necessary to implement DFE will include tools to characterize environmental risk, define and build flexible processes to reduce waste, and support dematerialization of processes and products. The following sections provide a brief review of design tools or strategies that can be employed

Design Tools

Environmental design tools vary widely in the evaluation procedures offered in terms of the type of data used, method of analysis, and the results provided to the electronic designer. The tool strategies range in scope from assessment of the entire product life cycle to the evaluation of a single aspect of its fabrication, use, or disposal. Today's DFE tools can be generally characterized as either life cycle analysis, recyclability analysis, manufacturing analysis, or process flow analysis tools.

The effectiveness of these design tools is based both on the tool's functionality as well as its corresponding support data. One of the biggest challenges designers face with regards to DFE is a lack of reliable data on materials, parts, and components needed to adequately convey the impact and trade-offs of their design decisions. To account for these data deficiencies, a number of environmental design tools attempt to use innovative, analytical methods to estimate environmental impacts: while necessary, this indicates they must be used with care and an understanding of their assumptions.

Although DFE provides a systems-based, life cycle approach, its true value to the system designer is lost unless the impact of DFE decisions on other relevant economic and performance measures (i.e., cost, electrical performance, reliability, etc.) can be quickly and accurately assessed. Trade-off analysis tools that have DFE embedded can perform process flow-based environmental analysis (energy/mass balance, waste stream analysis, etc.) concurrently with non-environmental cost and performance analysis so that system designers can accurately evaluate the impact of critical design decisions early.

Design Strategies

Design strategies such as lead minimization through component selection, and the reduction of waste resulting from rapid technological evolution through modular design, help to minimize the environmental impact of electronic products. Although at this time no suitable lead-free alternatives exist for electronic interconnections, designers can still minimize the lead content of electronic designs. Surface mount technology requires less solder than through-hole technology. New interconnection technologies, such as microball grid array and direct chip attachment, also require less solder. The environmental benefits increase with the use of these advanced interconnection technologies.

The rapid advancement of the electronics industry has created a time when many products become obsolete in less than five years' time. Electronic products must be built to last, but only until it is time to take them apart for rebuilding or for reuse of material. This means employing modular design strategies to facilitate disassembly for recycle or upgrade of the product rather than replacement. Designers must extend their views to consider the full utilization of materials and the environmental impact of the material life cycle as well as the product life cycle.

Conclusion

The diverse product variety of the electronics industry offers numerous opportunities to curtail the environmental impact of the industry. These opportunities are multidimensional. Services made possible through telecommunications technology enable people to work from home reducing emissions that would be generated by traveling to work. Smaller, faster computers and the Internet require less material usage, reducing the energy demand during processing and waste generated during fabrication. All these represent examples of how the electronics industry provides enablers of sustainability.

Global concerns and regulations associated with environmental issues are increasingly affecting the manufacturing and design of the electronics industry. Environmental management standards, "take back" programs, ISO 14000 standards development activity, and eco-label requirements represent a sample of the initiatives driving the industries move to more environmentally efficient practices. While the industry has initiated some activities to address environmental concerns, the future competitiveness of the industry will depend on improvements in environmental technology in manufacturing, accurate assessment of the environmental impact of products and process, and design products that employ design for environment, reuse, and recyclability. Industrial ecology offers a framework for analyzing the environmental effects of the electronics industry which is complicated by the rapid pace of change.

Acknowledgements

This work was performed under the auspices of the U.S. Department of Energy by Lawrence Livermore National Laboratory under Contract W-7405-Eng-48.

Disclaimer

This document was prepared as an account of work sponsored by an agency of the United States Government. Neither the United States Government nor the University of California nor any of their employees, makes any warranty, express or implied, or assumes any legal liability or responsibility for the accuracy, completeness, or usefulness of any information, apparatus, product, or process disclosed, or represents that its use would not infringe privately owned rights. Reference herein to any specific commercial product, process, or service by trade name, trademark, manufacturer, or otherwise, does not necessarily constitute or imply its endorsement, recommendation, or favoring by the United States Government or the University of California. The views and opinions of authors expressed herein do not necessarily state or reflect those of the United States Government or the University of California, and shall not be used for advertising or product endorsement purposes.

Defining Terms

Decarbonization: The reduction, over time, of carbon content per unit energy produced. Natural gas, for example, produces more energy per unit carbon than coal; equivalently, more CO₂ is produced from coal than from natural gas per unit energy produced.

Dematerialization: The decline, over time, in weight of materials used in industrial end products, or in the embedded energy of the products. Dematerialization is an extremely important concept for the environment because the use of less material translates into smaller quantities of waste generated in both production and consumption.

Design for environment (DFE): The systematic consideration of design performance with respect to environment over the full product and process life cycle from design through manufacturing, packaging, distribution, installation, use, and end of life. It is proactive to reduce environmental impact by addressing environmental concerns in the product or process design stage.

Eco-label: Label or certificate awarded to a product that has met specific environmental performance requirements. Some of the most widely known eco-labels include Germany's Blue Angel, Nordic White Swan, and U.S. Green Seal.

Industrial ecology: The objective, multidisciplinary study of industrial and economic systems and their linkages with fundamental natural systems.

ISO 14000: Series of international standards fashioned from the ISO 9000 standard which includes requirements for environmental management systems, environmental auditing and labeling guidelines, life cycle analysis guidelines, and environmental product standards.

Life cycle assessment (LCA): The method for systematically assessing the material use, energy use, waste emissions, services, processes, and technologies associated with a product.

Product take back: Program in which manufacturer agrees to take back product at the end-of-life (typically at no cost to the consumer) and disposal of product in an environmentally responsible manner.

Related Topic

25.3 Application-Specific Integrated Circuits

References

- B.F. Dambach and B.A. Allenby, "Implementing design for environment at AT&T," *Total Quality Environmental Management*, 4, 51–62, 1995.
- T.E. Graedel and B.R. Allenby, *Industrial Ecology*, Englewood Cliffs, N.J.: Prentice-Hall, 1995.
- S. Lipp, G. Pitts, and F. Cassidy, Eds. "A life cycle environmental assessment of a computer workstation," *Environmental Consciousness: A Strategic Competitiveness Issue for the Electronics and Computer Industry*, Austin, Tex.: Microelectronics and Computer Technology Corporation.
- S. Pederson, C. Wilson, G. Pitts, and B. Stotesbery, Eds. *Electronics Industry Roadmap*, Austin, Tex.: Microelectronics and Computer Technology Corporation, 1996.

L. Seifert, "AT&T technology and the environment," *AT&T Tech. J.*, 74, 4–7, 1995.
World Commission on Environment and Development, *Our Common Future*, Oxford: Oxford University Press, 1987.

Further Information

The IEEE Environment, Health and Safety Committee annually sponsors and publishes the proceeding of the *International Symposium on Electronics and the Environment*. These proceedings are a valuable resource for practitioners of DFE.

The National Technology Roadmap for Semiconductors, published by the Semiconductor Industry Association contains information on the environmental impacts of semiconductor fabrication as well as initiatives begun to address these concerns.

The *AT&T Technical Journal* has a dedicated issue on Industrial Ecology and DFE entitled AT&T Technology and the Environment, volume 74, no. 6, November/December 1995.

Other suggested reading:

American Electronics Association, "The hows and whys of design for the environment," 1993.

B.R. Allenby and D.J. Richards, Eds., *The Greening of Industrial Ecosystems*, Washington, D.C.: National Academy Press, 1994.

P. Eisenberger, Ed., *Basic Research Needs for Environmentally Responsive Technologies of the Future*, Princeton, N.J.: Princeton Materials Institute, 1996.

T.E. Graedel and B.R. Allenby, *Design for Environment*, Englewood Cliffs, N.J.: Prentice-Hall, 1996.

Rimvall, C.M, Jobling, C.P. "Computer-Aided Control Systems Design"
The Electrical Engineering Handbook
Ed. Richard C. Dorf
Boca Raton: CRC Press LLC, 2000

112

Computer-Aided Control Systems Design¹

112.1 Introduction

112.2 A Brief History of CACSD

Technological Developments • User Interfaces • CACSD Packages of Note

112.3 The State of the Art in CACSD

Consolidation of CACSD • A critique of Matrix Environments for CACSD • “Open Systems” • Other Desirable Features

112.4 CACSD Block-Diagram Tools

Basic Block-Diagram System Representations • Architectures of Block-Diagram Systems • Open-Architectures of Block-Diagram Editors

C. Magnus Rimvall

F. L. Smith & Co. A/S

Christopher P. Jobling

University of Wales

112.1 Introduction

The use of computers in the design of control systems has a long and fairly distinguished history. It begins before the dawn of the modern information age with the analog computing devices that were used to create tables of ballistic data for artillery and anti-aircraft gunners and continues to the present day in which modern desktop machines have computing power undreamed of when the classical and modern control theories were laid down in the middle years of the twentieth century.

Modern computer-aided control system design (CACSD) has been made possible by the synthesis of several key developments in computing. The development and continued dominance of high-level procedural languages such as FORTRAN enabled the development and distribution of standard mathematical software. The emergence of fully interactive operating systems such as UNIX and its user “shells” influenced the development of CACSD packages which have been constructed along similar lines. The ready availability and cheapness of raster-graphic displays has provided the on-screen display of data from control systems analysis, the creation of tools for modeling control systems using familiar block diagrams and have the potential to make order-of-magnitude improvements in the ease-of-use, ease-of-manipulation, and efficiency of the interaction between the control designer, his model, analysis tools, and end-product—software for embedded controllers. The driving force of all these developments is the seemingly continual increase in computing power year-on-year and the result has been to make computers accessible to large numbers of people while at the same time making them easier to use.

A control engineer often describes systems through the use of block diagrams. This is not only the traditional graphical representation of a control system, it is also an almost discipline-independent, and thus universally understandable, representation for dynamic systems. The diagrams may also constitute a complete documentation

¹Originally published as “Computer-Aided Control Systems Design”, Chapter 23, pp 429–442, in Levine, W. S. (Ed.), *The Control Handbook*, CRC Press, 1995.

of the designed system. Block diagrams are self-documenting and, when appropriately annotated, may form complete and consistent specifications of control systems. It is, therefore, not surprising that a number of tools for modeling (control) systems through block diagrams have emerged on the market over the last 5 to 10 years.

In addition to serving as a documentation aid, the overall cost and cycle time for developing complex controllers is radically reduced if analysis/simulation code and/or real-time code is automatically generated from the block-diagrams. This eliminates time-consuming manual coding, and avoids the introduction of coding bugs.

In this chapter, we explore the state-of-the-art in CACSD. We begin with a brief survey of the tools that have been developed over the years. We then focus on the matrix environments that provide the current standard and attempt to explain why they are important. We also examine modern block-diagram editors, simulation and code generation tools, and finally allow ourselves to speculate on the future.

112.2 A Brief History of CACSD

The term computer-aided control system design may be defined as:

The use of digital computers as a primary tool during the modeling, identification, analysis, and design phases of control engineering.

CACSD tools and packages typically provide well-integrated support for the analysis and design of linear plant and controllers although many modern packages also provide support for the modeling, simulation, and linearization of nonlinear systems and some have the capability of implementing a control law in software.

Figure 112.1 (adapted and updated from Rimvall [1987,1988]) illustrates the development of CACSD packages over the last four decades. In order to put events into proper context, other key influencing factors, chiefly hardware and software developments, are also shown. In this section we describe the background to the emergence of CACSD tools in more detail, starting with technological developments and then moving on to user interface aspects. The aim is to understand the current state-of-the-art by examining the historical context in which these tools have been developed.

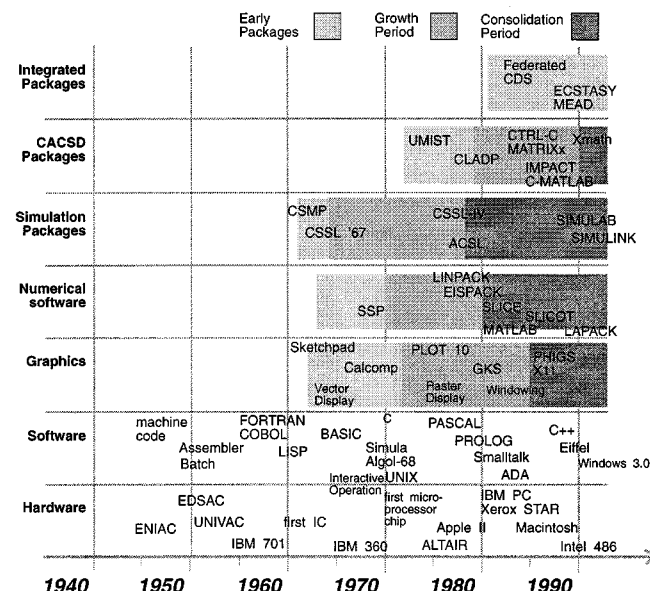


FIGURE 112.1 The historical development of interactive CACSD tools showing the availability of related hardware and software. Some actual products are included to indicate the state-of-the-art.

Technological Developments

Computing Hardware

Since 1953, there has been a phenomenal growth in the capabilities and power of computing hardware. Observers estimate that the power of computing devices (in terms of both execution speed and memory availability) has doubled every second to third year, whereas the size and cost (per computational unit) of the hardware has halved at approximately the same rate.

In terms of CACSD, the chief effect of these developments has been to widen the range of applications for computing and at the same time to make computers, and therefore the applications, widely available to practitioners in all branches of the subject. For example control engineers, control theorists, and control implementors all benefit as described below.

- Desk-top machines which are orders of magnitude more powerful than mainframe machines of two decades ago provide the means by which CACSD can be brought to the data analysis, model building, simulation, performance analysis and modification, control law synthesis, and documentation that is the day-to-day work of the control engineer.
- Without powerful computing hardware, many of the complex algorithms developed by control theorists for both analysis and implementation would otherwise be impractical.
- Embedded computer systems, which implement controllers, smart actuators, and smart sensors, are routinely used to implement the control laws developed by control engineers and control theorists.

System Software

The development of system software, such as operating systems, programming languages and program execution environments, has been slower than that of hardware, but is nonetheless impressive. Less impressive is the steadily increasing cost of application software, estimated at about 80% of the total installation cost of a computing system, which developments in computer science have been largely unable to reduce. We are, in fact, in the midst of a software crisis, dating from about 1968, which is the result of ever increasing improvements in hardware. Such improvements increase the possibilities for software, raise the expectations of users, and therefore raise the stakes in software production faster than improvements in software development technology has been made.

High Level Languages

The invention of FORTRAN was a major breakthrough in engineering computing. A high-level language, FORTRAN and the *compilers* that convert it into machine code, allowed engineers to write programs in a language that was sufficiently close to mathematical notation so as to be quite natural. Since its invention, numerous other high-level languages have been created, although FORTRAN continues to dominate engineering “number-crunching”. For the implementation of control algorithms, assembly languages are still popular although high(er) level languages such as C, which is the predominant systems programming language, MODULA, and ADA are gaining acceptance in the market place.

Graphical Displays

Engineers are, in general, more comfortable with pictures than with text as a means of communicating their ideas. Hence, the wide availability of graphical displays is of prime importance to many areas of engineering computing. Indeed, the development of computer graphics has been the means by which certain control systems design techniques, such as multivariable control systems analysis, have been made practicable. Computer graphics have also been instrumental in providing improvements in human-machine interfaces such as schematic systems input and direct manipulation interfaces with windows, icons, pull-down menus, and pop-up dialog boxes. Further improvements in user interfacing techniques such as *hypermedia* will continue to rely on developments in display technology.

For modern CACSD, the most significant development in display technology has been the development of cheap, high-resolution *raster graphics displays*, although, historically, great strides were made with less well

known and more expensive *vector refresh* and *vector storage* display technology. The prime feature of raster-scan technology is that an area of the image may be made to appear to move on the screen by the application of simple logical operations. Raster graphics displays are, therefore, ideal for building direct manipulation graphics applications such as block diagram editors, which will be discussed later. They are not so well suited to the direct display and manipulation of vector images, which are a key part of many engineering graphics applications. For example, it is difficult to move part of a vector image such as a bode-plot without destroying the rest of the picture or to display sloping lines that look smooth at low resolutions. However, the dominance of the technology has been a factor in ensuring that the deficiencies in the technology can be overcome by clever software.

Quality Numerical Software

Following the invention of FORTRAN there was a gradual development of useful general purpose subroutines that could be archived into libraries, distributed, and shared. This lead eventually to the development of standard subroutine libraries such as EIS-PACK [Smith et al., 1977], LINPACK [Dongarra et al., 1979], and LAPACK [Anderson et al., 19789] (for solving eigenvalue problems and sets of linear equations) which have had a direct influence on the development of CACSD.

Simulation Languages

For many years before the predominance of digital computers, dynamic system behavior was simulated using analog and hybrid computers. *Digital simulation* began to take over from analog and hybrid simulation during the mid-1960s. Digital simulation programs can be used to model a wider range of nonlinear phenomena more reliably than analog or hybrid computers, at the cost of losing real-time and introducing quantization problems. However, the disadvantages of the technology are more than outweighed by improvements in modeling possibilities and increases in productivity. Digital simulation has superseded analog computation in all but a few specialized areas.

The first digital simulation systems were FORTRAN programs. Eventually, special purpose languages emerged which allowed statements written in a form close to state equation notation to be translated into FORTRAN which enabled the engineer to concentrate on the problem description. In 1967, a standard language called CSSL (Continuous Systems Simulation Language) [Augustin et al., 1967] was proposed by the U.S. Simulation Council and this forms the basis of most simulation languages in use today.

User Interfaces

Over the years, user interaction with computers has become progressively more direct. In the very early days, the user interface was another human being. These “operators” were gradually replaced by *operating systems* which provided communication first through the medium of punch-card and paper tape, then later by teletype machines, text-based visual display units, and, most recently, by windowed graphical user interfaces. Along with this change, there has been a corresponding change in style for CACSD tools. Batch mode programs were collected into “packages” and provided with question and answer or menued interfaces. These, in turn, have been largely superceded by command driven interfaces and direct-manipulation graphical user interfaces, currently used only for specialized tasks such as block-diagram input, will have a wider role in future CACSD packages.

CACSD Packages of Note

As the supporting technology has developed, control engineers mainly working in academia have been actively engaged in developing tools to support developments in control theory and in combining these tools into packages. Early pioneering work was carried out in Europe where the emphasis was on frequency response methods for multivariable control systems analysis and design. Some of the first CACSD packages were developed in the mid-1970s. In the U.S., control theory was concentrated in the time domain and made use of

state-space models. Several packages of tools for state-space design were created and reached maturity in the late 1970s. These packages were usually written in FORTRAN and made use of a question-and-answer interface. Some of the better packages made use of standard numerical libraries such as EISPACK and LINPACK, but many made use of home-grown algorithms with sometimes dubious numerical properties.

One of the earliest standardization efforts was concerned with algorithms and there have been several attempts to create standard CACSD libraries. One of these, SLICOT [van den Boom et al., 1991], is still ongoing. But it has to be admitted that such efforts have had little success in the marketplace. The real break-through came with the development of the “matrix environments”, which are discussed in the next section. Currently, although many research groups continue to develop specialist tools and packages in conventional languages such as FORTRAN, most CACSD tool-makers now use these matrix environments as a high-level language for creating “toolboxes” of tools.

112.3 The State of the Art in CACSD

In this section we shall describe the matrix environments that have come to dominate CACSD, that is, the analysis, synthesis, and design of linear controllers for linear plants. We shall then move on to examine some of the requirements of CACSD which are less well served by the current generation of tools.

Consolidation of CACSD

As can be seen in Fig. 112.1, the 1980s was a decade of consolidation during which CACSD technology matured. Menu driven and Q&A dialogs were superseded by command languages. The matrix environment has become the *de facto* standard for CACSD.

The reasons for this are due to the simplicity of the data structures and the interface model and the *flexibility* of the package. We illustrate these properties using MATLAB (MATrix LABoratory) [Moler, 1980], the original matrix environment. Originally designed as a teaching program for graduate students, giving interactive access to the linear algebra routines EISPACK and LINPACK, MATLAB was released into the public domain in around 1980.

In MATLAB, matrices and matrix operations are entered into the computer in the straightforward fashion illustrated in Fig. 112.2.

This elegant treatment of linear algebra readily appealed to control scientists who realized that it was equally applicable to the solution of “modern control” problems based on linear state-space models (Fig. 112.3).

```

>> a = [1 3 5
        7 6 5; 0 0 5];
>> [vec, val] = eig(a)
vec =
      -0.7408    -0.3622    -0.1633
       0.6717    -0.9321    -0.8981
         0          0        0.4082

val =
      -1.7202            0            0
         0        8.7202            0
         0            0        5.0000

```

FIGURE 112.2 Entering and manipulating matrices in MATLAB. In this example, a matrix is defined and its eigenvectors and eigenvalues are determined.

```

>> A = [0,1,0;0,0,1;-2,-3,4];
>> B = [0, 0, 1];
>> C = [1, 0, 0];
>> poles = eig(A)

poles =
-0.4142
2.0000
2.4142

>> stable = all(poles < 0)

stable =
0
>>

```

FIGURE 112.3 Using state-space matrices. A simple stability test showing the power of the matrix functions built-in to MATLAB. The Boolean function ‘all’ returns the value TRUE (or 1) if all the elements of the argument are non-zero. The argument is itself a vector of Boolean values (that is, those values of the vector of the poles of the A matrix that are negative). By treating matrices as “first-class objects”, MATLAB provides many such opportunities for avoiding loops and other control structures required to do similar tasks in conventional languages.

```

function qs = control(a, b)
% Returns the controllability matrix [b, ab, a^2b, ...]
% used as: qs = control(a, b)
[ma, na] = size(a); [mb, nb] = size(b);
if ma != na
    error('Non-square A matrix')
elseif ma != mb
    error('Unequal number of rows in A and B')
else
    qs = b; k = b;
    for i = 2:ma;
        k = a*k; qs = [qs, k];
    end
end

```

FIGURE 112.4 The extension of MATLAB by means of “macro” or M-files. Here is a routine for determining the controllability of a state-space model.

However, powerful though the basic “matrix calculator” capabilities of MATLAB are, its real flexibility is due to its support of *macro files*. A macro file (M-file), in its simplest form, is just a collection of ordinary MATLAB commands which are stored in a file. When called, such a “script” of commands is executed just as if it had been typed by the user. MATLAB’s real strength lies in its ability to use M-files to create new functions. Such a function is defined in Fig. 112.4. Once defined in this way, the new function can be executed as if it was a part of the language (Fig. 112.5).

By creating a set of functions in this way, it is relatively easy to build up a “toolbox” of useful functions for a particular application domain. This is exactly what happened shortly after the release of the original MATLAB. Entrepreneurs quickly realized that if they cleaned up the code, added control oriented data types and functions and some graphics capability, MATLAB could be resold as a proprietary CACSD package. So, based mainly on the state-space methods in vogue in the U.S., several packages, such as MATRIXx and Ctrl-C, emerged and were a great success.

```

>> qs=control(A,B)

qs =
0     0     1
0     1     4
1     4    13
>>

```

FIGURE 112.5 Using a user-defined function as an extension to MATLAB.

MATLAB itself underwent further development. It was rewritten in C for efficiency and enhanced portability and released as a commercial product in 1985. Like its competitors, the main market was initially the CACSD market, where, supported by two sets of toolbox extensions called the Control and Signal Processing Toolboxes, MATLAB made rapid inroads into academia and industry. A recent development has been the provision of add-on graphical input of system models, in the form of block diagrams, support for “point-and-click” nonlinear simulation, and enhanced graphical functionality. At least one package, MATRIXx, has evolved further by the addition of data structures and more sophisticated support for macro development. The result is the package X-Math described by Floyd et al. [1991].

A Critique of Matrix Environments for CACSD

MATLAB and similar matrix environments are far from completely ideal. Rimvall [1987] gave the following requirements for a CACSD environment which are largely still valid today.

- Software packages must support the same entities used by human specialists in the field.
- The basic commands of an interactive environment must be fast yet flexible.
- CACSD packages should support an algorithmic interface.
- The transition from basic use to advanced use must be gradual.
- The system must be transparent.
- Small and large systems should be equally treated by the user interface.
- The system must be able to communicate with the outside world.

Matrix environments do not meet all of these requirements. The following sections give a critical review of the state-of-the-art.

Support of Control Entities

For a control engineer, the entities of interest are

- numerical descriptions of systems (state-space models, transfer functions, etc.)
- symbolic elements for general system equations
- graphical elements for the definition of system topologies
- support of large-scale data management, e.g., in the form of a relational database
- support of small-scale data management, e.g., in the form of spreadsheets
- graphical displays of numerical computations, possibly together with graphical interaction for requirement specifications, etc.

MATLAB was developed by a numerical analyst for numerical analysts. Such people need, and MATLAB provides, only one data structure, the complex matrix. It is a credit to its flexibility that the package can be adapted to a control engineer’s needs by the careful use of convention and toolbox extensions ([Fig. 112.6](#)), but the price paid is increased complexity.

Take, as a simple example, single-input single-output control systems design. For each element in the system model, i.e., plant, controller, feedback network, the user has to look after four matrices for a state-space model or two polynomials for a transfer function. He cannot simply refer to the “transfer function G ”, but must refer instead to the numerator and the denominator polynomials (see [Fig. 112.7](#)) that stand for G . These polynomials can, in turn, only be distinguished from row vectors by convention and context.

In MATRIXx, this problem was avoided by using packing techniques and a special data-structure so that, for example, the state-space model in [Fig. 112.3](#), would have been stored as shown in [Fig. 112.8](#) and additional data would be stored in the workspace of the program so that the A, B, C, D matrices could be later extracted when needed.

Such packing schemes are quite widely used by toolbox writers to overcome the limitations imposed by the two-dimensional matrix. One is usually advised, but not required, to manipulate such structures only through

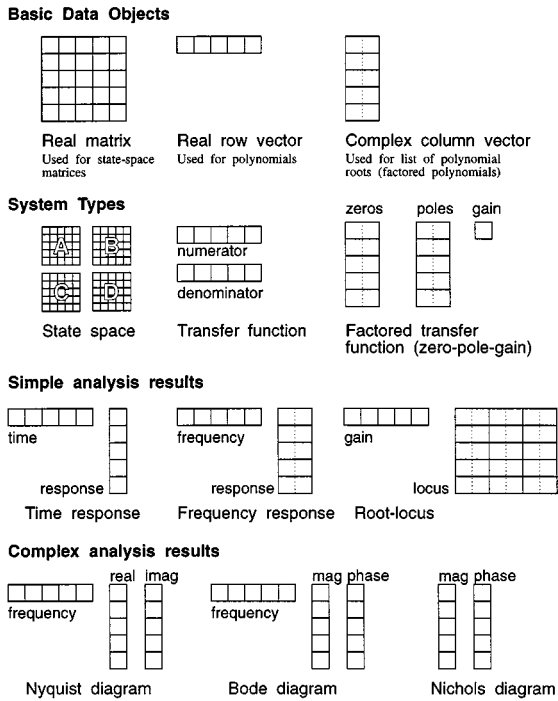


FIGURE 112.6 Some of the MATLAB conventions used to support control engineering data types.

```
>> % Plant: G(s) = 5/s(s^2 + 2s + 1)
>> num_G = 5; den_G = conv([1 0],[1 2 1]);
>> % Controller: Gc(s) = 15(s + 1)/(s + 2)
>> K_Gc = 15; Z_Gc = -1; P_Gc = -2;
>> [num_Gc,den_Gc] = zp2tf(K_Gc,Z_Gc,P_Gc);
>> % Feedback: H(s) = 1/(s + 10)
>> num_H = 1; den_H = [1 10];
```

FIGURE 112.7 Defining a control system in MATLAB.

```
>> G = [ 0, 1, 0, 0
         0, 0, 0, 0
        -2, -3, 4, 1
         1, 0, 0, 0]
>> % size(A) = [3,3], size(B) = [3,1], size(C) = [1,3]
```

FIGURE 112.8 A packed “system matrix”, additional values would have to be included to store the sizes of the relevant elements but these are not shown for clarity.

the packing and unpacking routines that usually accompany the toolbox code. For example, the packed state-space model might have a function `sstosys` to pack the data and `systoss` to unpack it into separate components as shown in Fig. 112.9. The advantage is that once packed, the state-space model G can be used in processing as if it was the single system object it represents. To see this, compare the code for simulation and analysis of a system given in Fig. 112.10(a) with the MATLAB Control System Toolbox code given in Fig. 112.10(b).

However, aside from the problem that packed data structures may be accidentally used as ordinary matrices, there is a more severe problem that results from a lack of standardization. There are now a number of toolboxes

```

>> G = ssstosys(A,B,C,D);
>> [a,b,c,d] = ssstosys(G)

A =    1   0   0
      0   0   1
      -2  -3   4

B =    0
      0
      1

C =  1 0 0

D =  0
>>

```

FIGURE 112.9 Packing and unpacking system models.

```

>> Go = series(Gc,G)
>> rlocus(Go)

a) Using packed data

>> [Go_A,Go_B,Go_C,Go_D] = ...
     series(Gc_A,Gc_B,Gc_C,Gc_D,G_A,G_B,G_C,G_D)
>> rlocus(Go_A,Go_B,Go_C,Go_D)

b) Using non-packed data, the MATLAB control systems toolbox

```

FIGURE 112.10 Use of a packed datastructure to simplify interaction.

that are used in CACSD, and none of them takes a standard approach to packing data structures. Thus, the data structures used in the Multivariable Control Systems Toolbox are completely incompatible with those used in the Systems Identification Toolbox, which itself is incompatible with the standard Control Systems Toolbox. The consequence is that each toolbox must supply conversion tools and the situation is similar to the problems faced with integrating data from two different packages.

There is, therefore, an identified need for matrix environments to provide a wider range of data types, preferably user definable. These would be used in the same way as record datatypes are used in conventional programming systems and would be considerably safer to use since the types expected and returned by functions could be specified in advance and the scope for misuse would be much reduced. In addition, the need to invent new types for each application would be somewhat reduced. This approach has been taken in the matrix environment X-Math and similar features are planned for a future release of MATLAB. Some of the other requirements listed above, such as graphical systems input, graphical display of results, and spreadsheet data manipulation, are covered to a greater or lesser extent by the current generation of matrix environments. The others, namely symbolic data processing and database support, are not but are considered to be outside the scope of this article.

Fast Yet Flexible Command Language

MATLAB clearly satisfies this criterion as is evidenced by the natural interaction shown in Fig. 112.3. For CACSD use, it is debatable whether the principle still holds, mainly because of the way that the package entities needed for control have to be constructed and managed by the user. Nonetheless, no-one could complain that matrix environments are not flexible: the growing number of new control applications for them provides ample evidence of that.

Algorithmic Interface

The support of an algorithmic interface is simply a recognition of the fact that no package developer can anticipate the requirements of every user. So, the package must be extensible by provision of user-defined

macros and functions. MATLAB has these, and their provision is clearly important to the users of the package and developers of toolbox extensions. However, there is a limit to the software robustness of the mechanisms that MATLAB provides. MATLAB is an un-typed language, all data structures used in extensions to MATLAB are implemented in terms of collections of matrices and vectors. It is therefore up to the programmer to develop conventions for using these data items such that the algorithms work properly. A strongly typed language, in which the user must specify the nature of each data object before it is used, is a much safer basis on which to provide extensions that are to be used by many other people.

Transition From Basic to Advanced Use

The user of a CACSD package is faced with two different types of complexity: the complexity of the user interface and the complexity of the underlying theory and algorithms. In both cases extra guidance is needed for novice users. Typically, the designers of CACSD packages do not wish to stand in the way of the expert users, so they provide direct access to the whole package and interfere in the use of the package as little as possible. This creates problems for novice or infrequent users of the package—novices because they are coming to the package without any knowledge of it, infrequent users because they have probably forgotten most of what they learned the last time they used the package.

In MATLAB, the user interface is deceptively simple. One can take a short tutorial and learn the basic concepts and underlying principles in perhaps one hour. But what happens when one is finished with the tutorial and wants to do some actual work? The sheer number of commands in the system can be overwhelming. In basic MATLAB there are some two hundred commands, add a few toolboxes and the number quickly increases. The only way to find out how to use a command is to know its name. If you don't know the name you can list all the commands available, but since each command name is limited to eight characters, there is not necessarily going to be any relationship between command name and command function. Having found a command the next step is to learn how to use it. In a research prototype CACSD package called IMPACT, Rimvall and Bomholt [1985] provided a latent question and answer mode feature which switches from normal command entry to step by step elicitation of parameters when requested by the user. Other ways of overcoming some of these difficulties [Rimvall, 1988] include providing a means of loading toolboxes only when they are needed, thereby reducing the instantaneous “name-space”, and providing operator overloading so that the same named procedure in X-Math [Floyd et al., 1991] and enables, for example, the multiplication operator ‘*’ to mean matrix multiplication, series combination of systems, polynomial convolution, or time response evaluation depending on the types of the operands.

Transparency

This is a fundamental principle of software engineering that simply means that there should be no hidden processing or reliance on side effects on which the package depends for its correct operation. Everything the package does and the package itself should, at all times, be under the complete control of the user.

Scalability

This simply means that account should always be taken of the limitations of numerical algorithms. The package should warn the user when limits are reached and the algorithms should thereafter ‘degrade gracefully’. It is surprising how many applications have been programmed with artificial limits set on various arrays which is fine so long as the user never presents the package with a problem that its designer never believed would ever be tackled (an inevitable event). Most matrix environments are limited only by the available memory.

“Open Systems”

The need to transfer data to other systems is simply a recognition that no one package can do all things equally well. In many applications, it makes sense to pass a processing task onto an expert. The ability of a package to be able to exchange data (both import and export) is the main feature of so-called open systems. At the very least it must be possible to save data in a form that can be retrieved by an external program. MATLAB and its

cousins provide basic file transfer capabilities, but the ideal CACSD package would have some link to a much more convenient data sharing mechanism such as could be provided by a database.

Other Desirable Features

- *Form or menu drive input* is often more useful than a functional command driven interface for certain type of data entry. A good example is the plotting of results where the selection of options and parameters for axis scaling, tick marks, etc. are more conveniently specified by means of a dialog box than by a series of function calls. Such a facility is provided in X-Math's graphics.
- *Graphical input* is useful for defining systems to be analyzed. Today, most of the major packages provide block diagram input, usually tied to nonlinear simulation. What is rarer is graphical input of more application-specific system representations such as circuit diagrams.
- *Strong data typing*, as already discussed, is useful for toolbox developers since it provides a robust means of developing extra algorithms within the context of the CACSD package. On the other hand, there is a fine balance between the needs of the algorithm developer and the algorithm implementor. The former is probably best served by a type-less environment in which it is easy and quick to try out new ideas (such an environment is often called a *rapid-prototyping environment*). The latter, who needs to ensure that the algorithms will work properly under all conditions, needs strong typing to ensure that this can be guaranteed. A similar dichotomy between inventors and implementors can be observed in software engineering.
- *Data persistence*. Unless explicitly saved, CACSD data is not maintained between sessions. Neither can data easily be shared between users. The evolution of models and results over time cannot be recorded. Hence, CACSD packages need database support.
- *Matrix environments only support numerical computation*. It is often useful to be able to manipulate a symbolic representation of a control system. Delaying the replacement of symbolic parameters for numerical values for as long as possible can often yield great insight into such properties as stability, sensitivity, and robustness.

112.4 CACSD Block-Diagram Tools

As we have discussed in the previous sections, the 1980s was an important decade for control engineering. Apart from new theories, better design methods, and more accurate numerical algorithms, this was the decade when powerful and easy-to-use interactive CACSD tools were put on the average control engineer's desk. Through the use of interactive and extendible programs, new methods and algorithms could be easily implemented and quickly brought to bear on real control engineering problems. Yet despite this tremendous improvement in the availability of good control design environments, the total cost and cycle time for a complex control design was still perceived by many groups and companies as being too high. One of the major remaining bottlenecks was the manual conversion of a control design into testable simulation code and, at a later stage, the conversion of the eventual design into the actual embedded real-time controller code.

A control engineer often describes a system through the use of block diagrams of different kinds. To bypass the bottleneck between theoretical design and actual real-time implementation, systems which took engineering block diagrams and automatically converted them into simulation and/or real-time code started to emerge in the middle of the 1980s. As an early example, already in 1984 General Electric decided to develop a block-diagram-based tool with automatic code generation capabilities. This program allowed draftspersons to enter control block diagrams and automatically convert the functionality of these diagrams into real-time code. Although it used limited graphics, this GE-Internal "Autocode" program successfully produced code at 50% of the cost of traditionally generated code, primarily due to error reduction of not hand coding. This reduction of costs provided the evidence that automatic translation of block diagrams is both feasible and desirable. However, due to advances in both computer graphics and code-generation techniques, the first tool was obsolete by the late 1980s. In recent years, several commercial block-diagram-based tools have become available. These

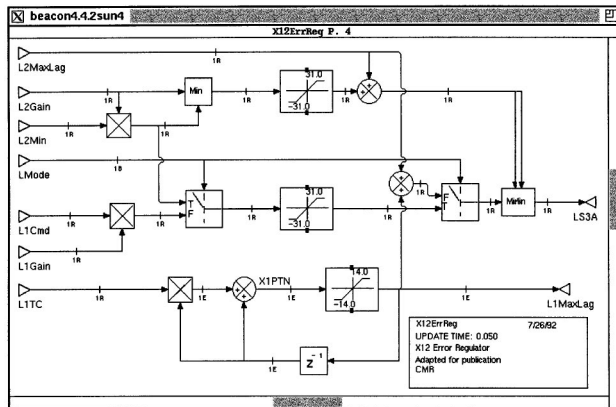


FIGURE 112.11 A signal-flow diagram in the BEACON system.

tools include System Build from Integrated Systems Incorporated, ModelC from Systems Control Technology, the PC-Based XAnalog from Xanalog, Simulab/Simulink from the Mathworks, and BEACON from General Electric. Some of these tools primarily serve as interfaces to analysis packages such as MATRIXx (System-Build), CTRL-C (Model-C), and MATLAB (Simulink). In some cases they can also be used to directly generate a computer language such as FORTRAN, ADA, or C. A summary of an early 1989 evaluation of the suitability of using System Build, CTRL-C, and Grumman's Protoblock for engine control is given in [Spang et al., 1993].

Basic Block-Diagram System Representations

Some basic user requirements fulfilled by most modern block-diagram oriented CACSD packages are

1. A simple-to-use graphical user-interface that can be used with little or no training. The graphical interface is usually based on the Macintosh, MS-Windows, and/or the X-Window System standard.
2. A set of rules for drawing controls-oriented diagrams, sometimes adhering to a standard diagram representations such as IEC-1331 or Petri Nets.
3. An object-based representation of the diagram entities and their graphical behavior. The underlying package must retain a semantical understanding of the diagram so that, for example, pertinent information such as signal types, dimensions, and ranges are propagated through the diagram, or connecting lines are retained when objects are moved.
4. Hierarchical structure which allows individual blocks to reference either other block diagrams or external modules (e.g., pre-coded system primitives).
5. Efficient internal simulation capabilities and/or real time code generation capabilities including optimization of execution speed and/or memory allocation.

As a consequence of the last two points, the block-diagram tools must have an open architecture so that the created modules can be associated with external code in a modular fashion. There are two main reasons for this:

- When the block-diagrams are used to simulate a physical system, the resulting models must frequently be interfaced with already existing submodels (e.g., from various FORTRAN libraries).
- When real-time controllers are implemented, the auto-generated code must be interfaced with operating system code and other “foreign” software.

All of today's block-diagram CACSD tools use hierarchical *signal-flow diagrams* as their main system representation. As illustrated in Fig. 112.11, a signal-flow diagram is a directed graph with the nodes representing standard arithmetic, dynamic and logic control blocks such as adders, delays, various filters, nonlinear blocks, and Boolean logic blocks. The connections between the blocks represent “signal” information which is

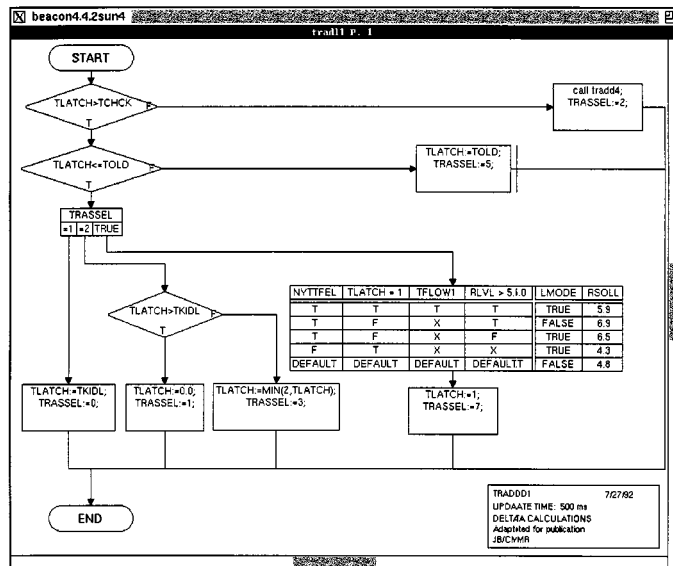


FIGURE 112.12 A BEACON control-flow block diagram.

transmitted from one block to another. The connections also indicate the order of execution of the various blocks. Signal flow diagrams are ideal for describing the dynamics of a system or controller.

Some CACSD packages also support some alternate system representation better suited for the logic and sequencing portion of a controller. Possible representations include *ladder-logic*, *dynamic truth-tables*, *flowcharts*, *Petri-nets*, or *state-transition diagrams*.

Figure 112.12 shows a typical control flow diagram or flowchart. The connections in this case represent the order of execution. The triangular blocks are decision blocks while the square blocks are variable assignment blocks written in a PASCAL-like language. Also shown are a multiway branch and a truth table. BEACON requires that the control flow diagrams produce structured code which equivalently means that a diagram can be implemented as a sequence of if-then-else statements without go-to's.

Hierarchies greatly facilitate the drawing and organization of diagrams. They provide appropriate levels of abstraction so that individual diagrams can be understood without clutter from details. Hierarchies simplify individual diagrams, making the resulting code easier to test. One can build up a set of subdiagram libraries which can be linked into possibly several higher level diagrams. Some block-diagram editors also allow the mixing of various diagram types in a hierarchical fashion (e.g., to call a low-level signal-flow diagram implementing a control-law scheme from a decision-making flow-chart diagram).

The graphical modeling environments cannot be viewed as replacements for the matrix environments described in the previous sections, as most of the block-diagram environments have very limited analytical capabilities (usually only simulation and linearization). However, many of today's block diagram tools have been developed as companion packages by the same commercial vendors that also sell matrix environments. Through linearization, it thus becomes possible to transform a non-linear block diagram to a linear representation which can then be analyzed and used for design in the matrix environment. Unfortunately, such automatic transformations are only available between tools from the same vendor, cross-translations between arbitrary tools are not possible.

Architectures of Block-Diagram Systems

To illustrate typical features and capabilities of a block-diagram oriented simulation or code-generation package, examples will be drawn from BEACON, a CACSD environment developed at GE between 1989 and 1995. There

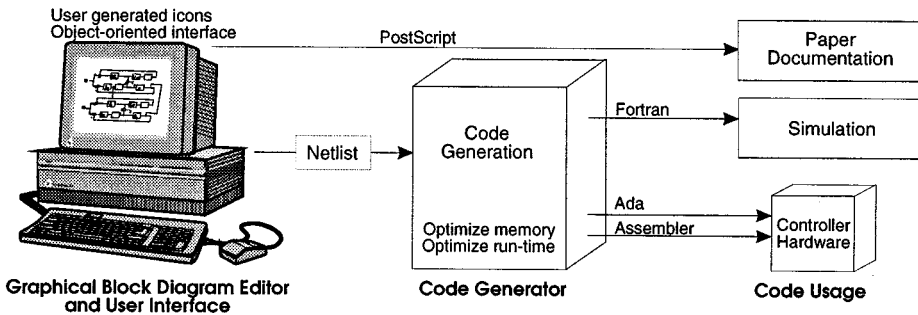


FIGURE 112.13 The BEACON architecture.

are, of course, many other block diagram systems, but being commercial products, the essential features are difficult to describe in detail. That said, another system that is well documented and worthy of study is the BlockEdit tool which was part of ECSTASY, a CACSD package developed in the UK in the late 1980s [Munro and Jobling, 1994]. BEACON has been in production use within GE since the first quarter of 1992. Through the use of BEACON, the company has been able to substantially reduce the overall cost and cycle time for developing complex controllers. The automatic generation of code not only eliminates the time-consuming manual coding, but also avoids the manual introduction of bugs into the code.

BEACON allows the user to graphically design a complete real-time controller as a series of hierarchical block diagrams. These diagrams can thereafter be automatically converted into a variety of computer languages for either control analysis, simulation, or real-time computer code, as illustrated in Fig. 112.13.

As shown in this figure, the BEACON system consists of three major components:

1. A graphical block-diagram editor with which the engineer designs the system to be simulated/coded [Spang et al., 1993]. Within this editor, the user may also create new graphical icons representing various numerical or logical blocks.
2. A netlist generated from the diagram and containing a full description of that diagram. The netlist format is keyword-oriented, it has a syntax resembling that of a higher-level language such as Pascal or Ada. To allow a variety of code generators and other uses such as the generation of I/O or termination lists or the automatic generation of test cases, all of the information except graphical location contained in the block diagram is written to the ASCII nestlist file.
3. An automatic code generator which translates the block diagrams into simulation and/or real-time computer code [Rimvall et al., 1993].

The BEACON architecture is one of the most open and extendible in the industry, allowing for straightforward extensions to the capability of the system and easy interfacing to other systems. Therefore, the architecture of other block diagram environments is often variants of that of BEACON. Some of the most common differences found in other systems are:

- *Built-in simulation capabilities.* Many of today's commercial systems have a non-linear simulation engine directly built into the system, avoiding BEACON's explicit translation step. Simulation results may then also be directly displayed on or accessed from the original diagram (e.g., in the form of time histories). This allows the user to see immediately the effects of any changes made to the diagram. One drawback of this approach is that these non-compiled approaches all have some kind of threaded-code or interpretative model execution, leading to much slower simulations than explicitly compiled simulation models such as those coming out of BEACON. Some systems allow for either of the two approaches.
- *The avoidance of an explicit netlist.* Many systems have a monolithic architecture with no direct access to the information in a modeled system. This prevents users from directly interfacing the block-diagram editor to other tools or filters (as often performed on a quite *ad-hoc* basis by the users within GE).
- *No code-generation.* Some older systems have built-in simulation capabilities only, with no generation of real-time or explicit simulation code.

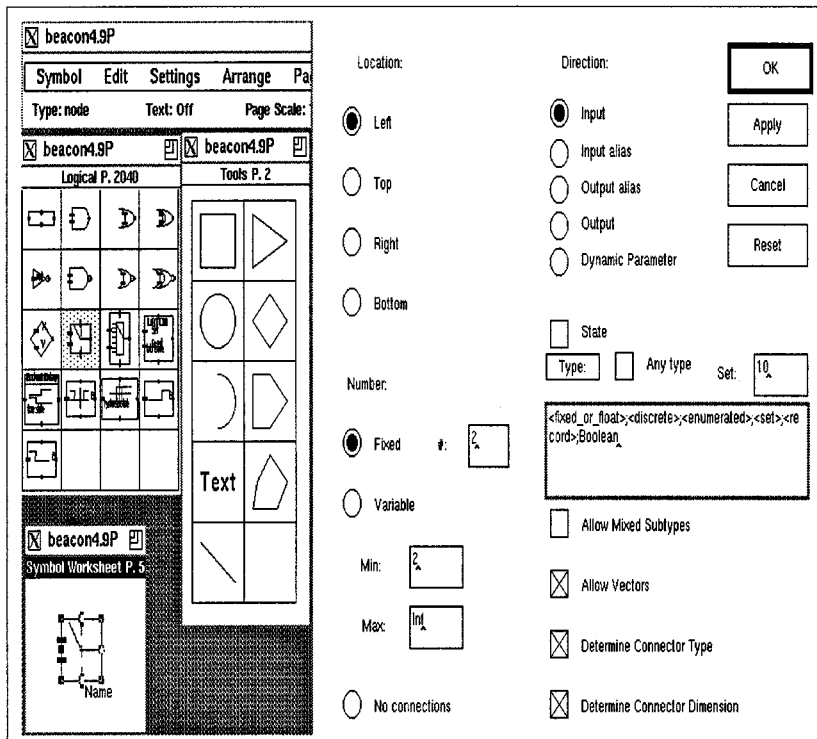


FIGURE 112.14 The BEACON symbol editor.

Open-Architectures of Block-Diagram Editors

Flexible block-diagrams have the capability of allowing users to develop or modify the graphical representation of symbols to meet the needs of various applications. In addition, it must be possible to add or modify the semantical meaning of the new or changed graphical symbols for simulation- or code-generation purposes.

The Editing of Block-Diagram Symbols

In BEACON, all symbols were developed using a Symbol Editor as shown in Figs. 112.14 and 112.15. This graphical editor is similar to most other object-oriented graphical editors, with the additional ability to describe diagram connectivity and the display of changing parameter values on the symbol itself. Each symbol is made up of a variety of separate objects (shapes) that are grouped together.

In Fig. 112.14, we see a Symbol Editor session, with the edited Switch symbol in the lower left window. The drawing primitives with its graphical shapes is the one in the middle. The large window to the right is an example of a block attributes window. In this case, it is the connectivity definition attributes for the left edge of the switch block; these attributes are used to define the sides and vertices which allow inputs or outputs, the allowed number of connections, vector dimension, and types.

Associated with most BEACON block symbols is a parameter form. These forms are unique for each individual block, allowing the user to define the parameters of the block and the specific function. For example, the integrator allows specification of the type of integration to be implemented as well as rate limits and initial conditions.

The forms are constructed during palette design using the Forms Editor shown in Fig. 112.15. To the left of the screen we see the actual parameter form of the Integrator block. In the middle we have the palette from which the primitive form elements may be picked. Each primitive forms object, such as text/value boxes and action buttons, have definable characteristics that will vary from element to element. To the right of Fig. 112.15 we see the characteristics of the data-input box for the parameter “lower limit”.

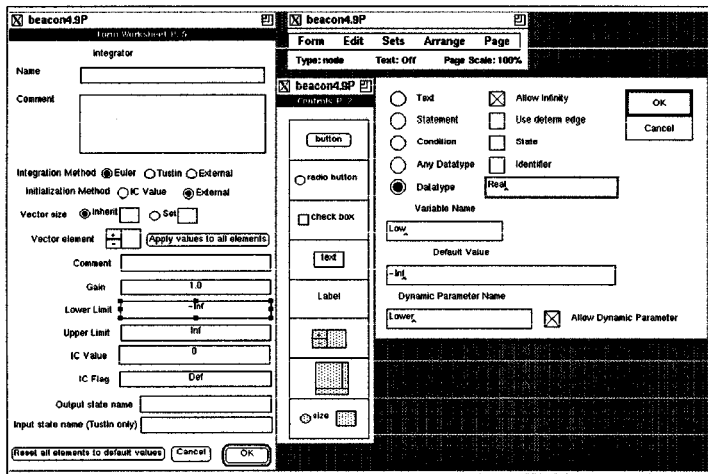


FIGURE 112.15 Examples of block parameter forms.

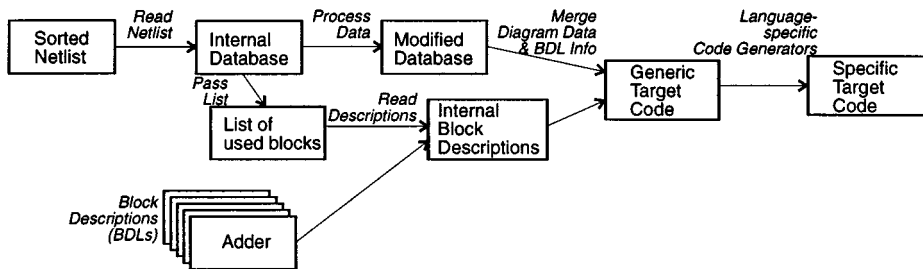


FIGURE 112.16 General principle of the workstation-based code generator.

The Functional Description of Symbols

The BEACON code generator will process a netlist into FORTRAN, Ada, C, or 68000 code. It accomplishes this by merging the block ordering information, the connectivity information, and the block-specific parameter values found in the netlist with block-specific functional descriptions of each block type. These block descriptions are stored separately from the netlist. This process is illustrated in Fig. 112.16.

Each block type supported by BEACON (e.g., adder, integrator, switch) will have a single block definition describing the functionality of the block. Whenever a new block symbol is added using the graphical Symbol Editor, a corresponding block definition file must be added to the system too. This block definition is written in “BEACON Block-Definition Language” (BDL), a special-purpose structured language that contains all the necessary elements for describing block connectivity, block parameters, and algorithms, as well as implementational detail such as fixed-point scaling.

Code From Signal-Flow Diagrams

The code resulting from a signal-flow diagram is a well-structured and yet locally optimized implementation of the diagram. It has the following characteristics:

- Through processing the sorted netlist, each block on the diagram is individually mapped onto the target language. Named blocks, e.g., LIMAXLAG in Fig. 112.11, are preceded by a comment stating that name in the code.

- Each connection on the diagram corresponds to a memory location in the code. To ensure readable code, each labeled connection, e.g., X1PTN in Fig. 112.11, is explicitly declared as a variable in the code. Unlabeled connections are mapped into reusable temporary variables or, in the case of assembler code, temporarily used registers. This ensures a locally optimized and yet fully readable code.
- States and other variables explicitly named on the diagram retain their name in the code. Unnamed states are automatically assigned unique names.
- Each numerical value is directly inserted into the code using the appropriate format of the target language and arithmetic type/precision used.

Code From Control-Flow Diagrams

Control-flow diagrams are processed in a similar manner to signal-flow diagrams. The main difference is that while a signal flow diagram uses a fixed set of blocks with well-defined semantics (the block interconnections and block parameters being the only variants between two blocks of the same type), the blocks in control-flow diagrams may contain arbitrary expressions, assignment statements, and/or procedure calls (as shown in Fig. 112.12). These BEACON language constructs must be translated into the primitives of each target language.

The BEACON graphical editor ensures that control-flow diagrams are well structured, i.e., that the diagram can be mapped into structured code. The automatic translation of large truth-tables into complex structured code is particularly time-saving.

Conclusions

In this chapter we have reviewed the tools available for the computer-aided design of control systems. The main features of the current state-of-the-art are analysis tools built around a “matrix environment” and modeling, simulation, and code generation tools constructed around the block diagram representation. For the most part, control systems analysis and design is done from a textual interface and modeling, simulation, and code generation rely on a graphical user interface. There are links between the two “environments”, usually provided by some form of linearization.

Future CACSD environments will have to give equal emphasis to “control data objects” as they now do for matrices. This is becoming urgent as the number of specialist toolboxes being written for MATLAB and similar packages increases. Only by having a set of commonly approved data-types can the further development of incompatible data formats *within a single package* be prevented. Rimvall has defined an extended MATLAB-compatible command language to overcome such problems and the issues are discussed in [Rimvall and Wette, 1993].

As graphical user interfaces become more popular on computing devices, the possibilities for interactive manipulation of systems will have to be explored. We expect that graphical tools for control systems analysis and design will become common-place over the next few years and may eventually replace textual interfaces for most users.

A final important area for development of CACSD will be driven by the need to embed control systems design into information systems for enterprise integration. To some extent this is already happening with the need for multidisciplinary teams of engineers to work on common problems. The computer-based support of such projects requires facilities for the development and exchange of models, the storage of design data, version control, configuration management, project management, and computer-supported cooperative work. It is likely that CACSD will have to develop into a much more open set of tools supported by databases, networks, and distributed computation. The implications of some of these developments are discussed in [Barker et al., 1993].

Related Topics

100.1 Models • 100.2 Dynamic Response • 100.3 Frequency Response Methods: Bode Diagram Approach

References

- E. Anderson, Z. Bai, C. Bischof, J. Demmel, J. Dongarra, J. DuCroz, A. Greenbaum, S. Hammarling, A. McKenney, and D. Soresen, "LAPACK: A portable liner algebra library for supercomputers," technical report, Argonne National Laboratory, 1989.
- D. Augustin, J. C. Strauss, M. S. Fineberg, B. B. Johnson, R. N. Linebarger, and F. J. Samson, "The SCi continuous system simulation language (CSSL)," *Simulation*, 9(6), 281–304, 1967.
- H. A. Barker, M. Chen, P. W. Grant, C. P. Jobling, and P. Townsend, "Open architecture for computer-aided control engineering," *IEEE Control Systems Magazine*, 12(3), 17–27, 1993.
- J. J. Dongarra, J. R. Bunch, C. B. Moler, and G. W. Stewart, "LINPACK users' guide," *Lecture Notes in Computer Science*, 1979.
- M. A. Floyd, P. J. Dawes, and U. Milletti, "X-Math: a new generation of object-oriented CACSD tools," in *Proceedings European Control Conference*, 3, 2232–2237, 1991.
- C. Moler, "MATLAB—user's guide," technical report, Albuquerque, N.M.: University of New Mexico, 1980.
- N. Munro and C. P. Jobling, "ECSTASY: A control system CAD environment," in *CAD for Control Systems*, D. A. Linkens, Ed., New York: Marcel Dekker, pp. 449–467.
- C. M. Rimvall, "CACSD software and man-machine interfaces of modern control environments," *Transactions of the Institute of Measurement and Control*, 9(2), 1987.
- C. M. Rimvall, "Interactive environments for CACSD software," in *Preprints of 4th IFAC Symp. on Computer Aided Design in Control Systems CADCS '88*, pp. 17–26, Beijing, PRC, 1988.
- C. M. Rimvall and L. Bomholt, "A flexible man-machine interface for CACSD applications," in *Proc. 3rd IFAC Symp. on Computer Aided Design in Control and Engineering*, Pergamon Press, 1985.
- C. M. Rimvall, M. Radecki, A. Komar, A. Wadhwa, H. A. Spang III, R. Knopf, and M. Idelchik, "Automatic generation of real-time code using the BEACON CAE environment," in *Proceedings of the 12th IFAC World Congress on Automatic Control*, 6, 99–104, 1993.
- C. M. Rimvall and M. Wette, "Towards standards for CACE command syntax and graphical interfaces," in *Proceedings of the 12th IFAC World Congress on Automatic Control*, 8, 87–390, 1993.
- B. T. Smith, J. M. Boyle, J. J. Dongarra, B. S. Garbow, and Y. Ikebe, "Matrix eigensystem routines—EISPACK guide extension," *Lecture Notes in Computer Science*, 51, 1977.
- H. A. Spang III, C. M. Rimvall, H. A. Sutherland, and W. Dixon, "An evaluation of block diagram CAE tools," in *Proceedings of the 11th IFAC World Congress on Automatic Control*, 9, 79–84, 1990.
- H. A. Spang III, A. Wadhwa, C. M. Rimvall, R. Knopf, M. Radecki, and M. Idelchik, "The BEACON block-diagram environment," in *Proceedings of the 12th IFAC World Congress on Automatic Control*, 6, 105–110, 1993.
- A. van den Boom, A. Brown, F. Dumortier, A. Geurts, S. Hammarling, R. Kool, M. Vanbegin, P. van Dooren, and S. van Huffel, "SLICOT: A subroutine library in control and systems theory," in *Proceedings 5th IFAC Symposium on Computer Aided Design in Control Systems—CADCS'91*, pages 1–76, Swansea, UK, 1991.

Further Information

Keeping up to date with developments in CACSD is not always easy but the proceedings of the triennial IFAC symposium on Computer-Aided Design in Control Systems (CADCS) and the IEEE biennial workshop on CACSD are useful indicators of the latest trends. The proceedings of the last three of these meetings are given below. The other items give useful snapshots of the state-of-the-art at various points in the last 10 years or so. In addition to these sources, the *IEEE Control Systems Magazine* regularly publishes articles on CACSD and is a good place to look for other information.

- M. Jamshidi and C. J. Herget, Eds., *Computer-Aided Control Systems Engineering*, North-Holland, 1985.
- CADCS, *Proceedings of the 5th IFAC Symposium on Computer Aided Design in Control Systems*, Swansea, UK: Pergamon Press, 1991.
- M. Jamshidi, M. Tarokh, and B. Shafai, *Computer-Aided Analysis and Design of Control Systems*, Englewood Cliffs, N.J.: Prentice-Hall, 1991.
- CACSD, *Proceedings of the IEEE Control Systems Society Symposium on CACSD*, Napa, Calif.: IEEE, 1992.

- M. Jamshidi and C. J. Herget, Eds., *Recent Advances in Computer-Aided Control Systems Engineering. Studies in Automation and Control*, Amsterdam: Elsevier Science Publishers, 1992.
- CACSD, *Proceedings of the IEEE/IFAC Joint Symposium on Computer-Aided Control System Design*, Tucson, Az., Pergamon Press, 1994.
- D. A. Linkens, Ed., *CAD for Control Systems*, New York: Marcel Dekker, 1994.
- CACSD, *Proceedings of the IEEE Symposium on Computer-Aided Control System Design*, Deerborn: IEEE, 1996.
- IFAC CACSD, *Proceedings of the 1997 IFAC Symposium on Computer-Aided Control System Design*, Ghent, Belgium: IFAC, 1997.